

A Methodology to Assess and Rank the Effects of Hidden Failures in Protection
Schemes based on Regions of Vulnerability and Index of Severity.

David C. Elizondo

Dissertation submitted to the Faculty of the
Virginia Polytechnic Institute and State University
in partial fulfillment of the requirements for the degree of

Doctor of Philosophy

In

Electrical Engineering

Jaime De La Ree, Chair

Arun G. Phadke

Yilu Liu

William T. Baumann

Antonio A. Trani

Reynaldo Nuqui

April 16, 2003

Blacksburg, Virginia

Keywords: Hidden Failures, Regions of Vulnerability, Index of Severity, Wide-Area Disturbances, Power System Protection.

A Methodology to Assess and Rank the Effects of Hidden Failures in Protection Schemes based on Regions of Vulnerability and Index of Severity

David C. Elizondo

Abstract

Wide-area disturbances are power outages occurring over large geographical regions that dramatically affect the power system reliability, causing interruptions of the electric supply to residential, commercial, and industrial users. Historically, wide-area disturbances have greatly affected societies.

Virginia Tech directed a research project related to the causes of the major disturbances in electric power systems. Research results showed that the role of the power system's protection schemes in the wide-area disturbances is critical. Incorrect operations of power system's protection schemes have contributed to a spread of the disturbances. This research defined hidden failures of protection schemes and showed that these kinds of failures have contributed in the degradation of 70-80 percent of the wide-area disturbances. During a wide-area disturbance analysis, it was found that hidden failures in protection schemes caused the disconnection of power system elements in an incorrect and undesirable manner contributing to the disturbance degradation.

This dissertation presents a methodology to assess and rank the effects of unwanted disconnections caused by hidden failures based on Regions of Vulnerability and index of severity in the protection schemes.

The developed methodology for the evaluation of the Region of Vulnerability found that the indicator that most accurately reflects the relationship of the Region of Vulnerability with the single line diagram is kilometers. For the representation of the Region of Vulnerability in the power system, we found segments in the transmission line in which the occurrence of faults do make the relay to operate, producing the unwanted disconnection caused by hidden failure. The

results in the test system show that the infeed currents restrain the Region of Vulnerability from spreading along power system elements.

Finally the methodology to compute the index of severity is developed. The index of severity has the objective of ranking the protection schemes, considers the dynamics of the protection schemes, and evaluates the overall disturbance consequence under the static and dynamic perspectives.

Acknowledgments

To describe five years full of learning experiences and valuable input from a number of people in this section of the dissertation is complicated, but here is my attempt.

First of all I would like to thank my Lord, because now the second part of my dream has come to reality.

The guidance, patience, and always vigorous talks with my advisor, Dr. Jaime De La Ree, were an important factor in the achievement of this dissertation. I thank him for his contributions in my integral growth as a person. Special thanks to the committee members: Dr. Phadke, Dr. Yilu Liu, Dr. Antonio Trani, and Dr. William Baumann for their valuable feedback. Dr. Virgilio Centeno and Dr. Antonio Nieto recommendations helped me to conceive my plans in the appropriate perspective.

The Power Engineering staff, Carolyn Guynn and Glenda Caldwell helped in many ways during these five years; they made me feel like home. The Power Engineering graduate students with whom I had long discussions in our attempts to “find the truth” will always be in my memory. The words included in Reynaldo Nuqui’s dissertation are precise: we could develop a competitive but healthy academic environment in the Power Lab; efforts exist towards the unification of the group after graduation. Special thanks to: Abdel Khatib, Reynaldo Nuqui, Bin Qiu, Sebastian Rosado, Arturo Bretas, Dr. Aysen Arsoy, Juancarlo Depablos, Marcos Donolo, Q Qiu, Liling Huang, Dr. Dong, and Ling Chen. The enthusiastic members of the “Aztec Night” deserve to be mentioned; those meetings provided the escape from the routine and after enjoying them we came back with a fresh mind, ready to reexamine the problems to solve.

This research work was made possible in part thanks to the National Council for Science and Technology, CONACYT, Mexico, and a grant from EPRI-DoD.

Finally I would like to thank my family that provided support from my foreign country. Special thanks to my wife: Leticia Alvarez. I thank you for all your patience and great help during these five years; thanks for being part of this journey and take care of the two wonderful sons that were born during our graduate studies. I am sure I could not have completed this project without you.

For my wife: Leticia Alvarez

Table of Contents

Abstract	ii
Acknowledgments.....	iv
Table of Contents.....	vi
List of Figures	viii
List of Tables	xi
Chapter 1. Introduction.....	1
Chapter 2. Qualitative Evaluation of Regions of Vulnerability	5
2.1 Definition of Region of Vulnerability.....	5
2.2 Development of Regions of Vulnerability	8
2.3 Catalogue of Regions of Vulnerability	19
Chapter 3. Protection System Design.....	24
3.1 Protection System Design: Scope and Limitations	24
3.2 Protection Schemes for Power System Components	27
3.2.1. Protection Schemes for Generators, Buses, and Transformers	28
3.2.2. Protection Schemes for Transmission Lines	30
3.3 Wide Area Protection.....	39
3.3.1. Under Frequency Load Shedding	39
3.3.2. Under Voltage Load Shedding and Generation Rejection.....	45
Chapter 4. Quantitative Evaluation of Regions of Vulnerability	46
4.1 Refinement of the Methodology: Dimension of the Region of Vulnerability	46
4.1.1. Evaluation of the Region of Vulnerability in Per Unit	46
4.1.2. Evaluation of the Region of Vulnerability in Electrical Quantities	53

4.1.3.	Evaluation of the Region of Vulnerability in Physical Quantities.....	60
4.1.4.	Comparison of the Regions of Vulnerability in Different Dimensions	62
4.2	Refinement of the Methodology: Physical Representation of the RV in the System...	67
4.2.1.	Region of Vulnerability distributed along Power System Elements	67
4.2.2.	Region of Vulnerability that overreaches Transmission lines	72
4.2.3.	Region of Vulnerability that overreaches Transformers.....	81
4.2.4.	Final Procedure to Compute the Regions of Vulnerability.....	85
Chapter 5.	Areas of Consequence and Index of Severity.....	89
5.1	Definition of Areas of Consequence and Index of Severity Development.....	89
5.1.1.	Definition of Areas of Consequence	89
5.1.2.	Index of Severity for Static and Dynamic Security Assessment	91
5.1.3.	Index of Severity for this Dissertation.....	96
5.2	Simulation Cases of the effects of Hidden Failures in a Power System.....	104
5.2.1.	Procedure for the Simulation Cases.....	104
5.2.2.	Simulation Cases.....	112
5.2.3.	Critical Protection Schemes: The Ranking of the Index of Severity	146
Chapter 6.	Conclusions and Future Work	148
References	152
Appendices	154
Appendix A	127-Bus Sample System Data.....	154
Appendix B	ETMSP Relay Settings Information	168
Appendix C	IEEE-39 Bus Sample System Data	194
Appendix D	Transmission Line Overload Factors	198
Appendix E	ETMSP: A Brief Description of the Program.....	204
Curriculum Vitae	221

List of Figures

Figure 1: A logic schematic section with two relays connected in series.....	6
Figure 2: Conditions for a correct trip for the Figure 1 logic schematic.	7
Figure 3: One-line Diagram for the Directional Comparison Blocking.....	9
Figure 4: Logic Schematic for the Directional Comparison Blocking, A and B line sides.....	9
Figure 5: Region of Vulnerability for Hidden Failure Mode of Table 1, Row 1.....	12
Figure 6: One-line Diagram for the Directional Comparison Unblocking.....	12
Figure 7: Logic Schematic for the Directional Comparison Unblocking, A and B line sides.....	13
Figure 8: Region of Vulnerability for Hidden Failure Mode of Table 1, Row 3.....	15
Figure 9: One-line Diagram for the Permissive Underreaching Transfer-Trip.....	16
Figure 10: Logic Schematic for the Permissive Underreaching Transfer-Trip, A and B line sides.....	16
Figure 11: Region of Vulnerability for Hidden Failure Mode of Table 1, Row 5.....	18
Figure 12: Region of Vulnerability for Hidden Failure Modes of Table 1, Rows 1,2,3,4, and 5.....	19
Figure 13: Region of Vulnerability Type 1, Reverse Local Bus.....	21
Figure 14: Region of Vulnerability Type 2, Reverse Remote Bus.....	22
Figure 15: Region of Vulnerability Type 3, Zone 2.....	22
Figure 16: Region of Vulnerability Type 4, Zone 3.....	23
Figure 17: Single Line Diagram of the 127 Bus Sample System.....	26
Figure 18: Part of Our Test System used to Describe the Infeed Effect.....	31
Figure 19: Directional Comparison Blocking, Single Line Diagram.....	33
Figure 20: Miss-coordination Problems of Z2 Relays due to Network Characteristics.....	37
Figure 21: UFLS Relays Localization in the Test System.....	44
Figure 22: Single Line Diagram of the IEEE-39 Bus System.....	47
Figure 23: The term Bus Density applied in a segment of the power system for the Directional Comparison Blocking and the Z2 distance relay.....	48
Figure 24: The Restriction applied in a simple transmission system.....	49
Figure 25: Transmission Lines and Their Respective Region of Vulnerability.....	51
Figure 26: Ratio of Region of Vulnerability Over Transmission Line Impedance.....	51
Figure 27: Single Line Diagram of the 127 Sample System.....	54
Figure 28: Representation of the Region of Vulnerability, Case Line 73.....	62
Figure 29: Representation of the Region of Vulnerability, Case Line 81.....	63
Figure 30: Representation of the Region of Vulnerability, Case Line 65.....	64
Figure 31: Representation of Regions of Vulnerability that are confined within the Nearby Power System Elements. None of the cases presented violate the restriction equation.....	69

Figure 32: Representation of Regions of Vulnerability that are distributed along the Power System Elements. Four of the Five Cases presented do violate the Restriction Equation.....	71
Figure 33: Representation of Cases 27, 31, 49 and 50.....	76
Figure 34: Process in the Calculation of the Region of Vulnerability.....	77
Figure 35: Reference for the Fault Placement during the Validation of the Region of Vulnerability for Cases in Table 36.....	78
Figure 36: “Valid Cases”, Cases that do not present Infeed Currents due to Network Topology.....	80
Figure 37: “Valid: Case,” that have Specific Network Characteristic: Parallel Lines.....	80
Figure 38: Overreached Transformer and the Faults Located in the Downstream Transmission Lines.....	83
Figure 39: The Mapping of the R-X diagram with the Single Line Diagram in order to determine the Valid Region of Vulnerability for a Single line Case.....	86
Figure 40: The Mapping of the R-X Diagram with the Single Line Diagram in order to Determine the Valid Region of Vulnerability for a Multiple Line Case.....	87
Figure 41: Power System Security Stages for Unwanted Disconnections Caused by Hidden Failures.....	100
Figure 42: Solution Proposed to the Unwanted Disconnections Caused by Hidden Failures: HFMCS.....	101
Figure 43: First Part of the Algorithm for the Simulation Cases.....	104
Figure 44: A Sample of the Representation of the Fault Location, HF Relay, and the Region of Vulnerability.....	105
Figure 45: Monitoring the operation of the Relay and the Validation of the Region of Vulnerability.....	106
Figure 46: The limit in the Search for a Valid Region of Vulnerability, 1% around the bus in question.....	107
Figure 47: Second Part of the Algorithm for the Simulation Cases.....	107
Figure 48: Sequence of Events of the Double Contingency.....	109
Figure 49: A Sample of the Monitoring of a Distance Relay Operation.....	110
Figure 50: Protection Scheme 101-97, its Region of Vulnerability, and the Fault Location.....	112
Figure 51: Apparent Impedance seen by the Relay 101-97 during the fault period.....	113
Figure 52: Generators Frequency Response for the Relay 101-97 Case.....	114
Figure 53: Generator Relative Angles Response for the Relay 101-97 Case.....	115
Figure 54: More Affected Bus Magnitudes for the Relay 101-97 Case.....	115
Figure 55: Less Affected Bus Magnitudes for the Relay 101-97 Case.....	116
Figure 56: Protection Scheme 84-90, its Region of Vulnerability, and the Fault Location.....	117
Figure 57: Apparent Impedance seen by the Relay 84-90 during the fault period.....	118
Figure 58: Localization of the Distance Relays that operated in the Sample System for Relay 84-90 Case.....	119
Figure 59: Apparent Impedance as seen by the distance relays that operated due to the excursion of the power system parameters.....	120
Figure 60: Real Power of the Line 48-45 that was switched open due to the operation of the relay 48-45.....	120
Figure 61: Real Power of the Lines that were switched open due to the operation of Distance Relays.....	121
Figure 62: Generators Frequency Response for the Relay 84-90 Case.....	121
Figure 63: Localization of buses in which the Under Frequency Relays Operated for case 84-90.....	124

Figure 64: Generator Relative Angles Response for the Relay 84-90 Case.....	125
Figure 65: Power System Elements affected by the re-distribution of power flows after the second contingency..	126
Figure 66: Voltage Magnitude of the Buses 36 to 73, Relay 84-90 Case.....	126
Figure 67: Voltage Profile in the Bus 40 and 41 and its relationship with Real Power through the line 37-40, for the Relay 84-90 Case.....	127
Figure 68: Real and Reactive Power Profile in the Line 37-40 for the Relay 84-90 Case.	128
Figure 69: Real Power Profile in the Line 11, see Figure 65, number “5,” Relay 84-90 Case.	129
Figure 70: Protection Scheme 89-85, its Region of Vulnerability, and the Fault Location.....	130
Figure 71: Apparent Impedance seen by the Relay 89-85 during the fault period.....	131
Figure 72: Generators Frequency Response for the Relay 89-85 Case.....	132
Figure 73: Generator Relative Angles Response for the Relay 89-85 Case.....	132
Figure 74: More Affected Bus Magnitudes for the Relay 89-85 Case.....	133
Figure 75: Zoom at the Voltage profiles of Buses 85 and 86, Case Relay 89-85.....	133
Figure 76: Less Affected Bus Magnitudes for the Relay 89-85 Case.	134
Figure 77: Protection Scheme 74-73, its Region of Vulnerability, and the Fault Location. In this case the relay setting overreaches the transformer and it expands over the lines 106, 107 and 104.....	135
Figure 78: Apparent Impedance seen by the Relay 74-73 during the fault period.....	137
Figure 79: Generators Frequency Response for the Relay 74-73 Case.....	137
Figure 80: Localization of the Buses in which the Under Frequency Relays Operated, Case 74-73.	138
Figure 81: Generator Relative Angles Response for the Relay 74-73 Case.....	139
Figure 82: More Affected Bus Magnitudes for the Relay 74-73 Case.....	139
Figure 83: Less Affected Bus Magnitudes for the Relay 74-73 Case.	140
Figure 84: Protection Scheme 63-104, its Region of Vulnerability, and the Fault Location.	141
Figure 85: Apparent Impedance seen by the Relay 63-104 during the fault period.	142
Figure 86: Generators Frequency Response for the Relay 63-104 Case.....	143
Figure 87: Localization of the buses in which the under frequency relays operated, Case 63-104.	143
Figure 88: Generator Relative Angles Response for the Relay 63-104 Case.....	144
Figure 89: More Affected Bus Magnitudes for the Relay 63-104 Case.....	144
Figure 90: Less Affected Bus Magnitudes for the Relay 63-104 Case.	145

List of Tables

Table 1: Region of Vulnerability Development, an Example.	9
Table 2: Sequence of Events for an Unwanted Disconnection Caused by a Hidden Failure; Table 1, Row 1.	10
Table 3: Sequence of Events for an Unwanted Disconnection Caused by a Hidden Failure; Table 1, Row 3.	13
Table 4: Sequence of Events for an Unwanted Disconnection Caused by a Hidden Failure; Table 1, Row 5.	17
Table 5: List of Hidden Failures Modes sorted by Power System Element.	20
Table 6: Basic Information of the 127 Bus Sample System.	27
Table 7 : Relay Models available in ETMSP.....	27
Table 8 : Remote Operation Commands available in ETMSP	28
Table 9: General Protection Requirements for Generators.....	28
Table 10: ETMSP Card for Relay Model “DIST”	35
Table 11: Filled in Sample of ETMSP Card for Relay Model “DIST”	35
Table 12: Fixed Entries of ETMSP Card for Relay Model “DIST”	36
Table 13: Variable Entries of ETMSP Card for Relay Model “DIST”	36
Table 14 : Lines coordinated with additional time delay.....	38
Table 15 : Characteristics of the Under Frequency Load Shedding Program.....	40
Table 16 : Classification of the Load According to its Representation.....	41
Table 17 : ETMSP Card for Relay Model “UFLT.”.....	41
Table 18 : Filled in Sample of ETMSP Card for Relay Model “UFLT”	42
Table 19 : Fixed Entries of ETMSP Card for Relay Model “UFLT.”	42
Table 20 : Variable Entries of ETMSP Card for Relay Model “UFLT.”	43
Table 21 : Remote Command Entries of ETMSP Card for Relay Model “UFLT”	43
Table 22 : Factors $(kV_{Base}^2 / MVA_{Base})$ for the different Voltage Levels of the Sample Power System.	56
Table 23: Transmission Lines with the Twenty Greatest Impedances in <i>Per Unit</i>	57
Table 24: Classification of the Twenty Greatest Transmission Lines According to its Voltage level; Impedances in <i>Per Unit</i>	57
Table 25: Transmission Lines with the Twenty Greatest Impedances in <i>Ohms</i>	58
Table 26: Classification of the Twenty Greatest Transmission Lines According to its Voltage level; Impedances in <i>Ohms</i>	58
Table 27: Typical Values for Resistance and Reactance in Ohms/Km for Different Voltage Levels	60
Table 28 : Magnitude of the Region of Vulnerability, Case Line 73, in Per Unit, Ohms, and Kilometers.	63
Table 29: Magnitude of the Region of Vulnerability, Case Line 81, in Per Unit, Ohms, and Kilometers.	64
Table 30 : Magnitude of the Region of Vulnerability, Case Line 65, in Per Unit, Ohms, and Kilometers.	65
Table 31: Comparison of the Region of Vulnerability in Different Dimensions.....	65
Table 32: Region of Vulnerability in Per Unit for Cases 81, 65, and 73	66

Table 33: Region of Vulnerability in Ohms and Kilometers for Cases 81, 65, and 73.....	66
Table 34: 63 Cases in which the Setting of a Transmission Line Relay Overreaches at Least one Power System Element.....	72
Table 35: 31 Cases in which the Setting of a Transmission Line Relay overreaches only Transmission Lines.....	74
Table 36: Validation of the Region of Vulnerability, Simulation Results for Transmission lines: Valid and Not Valid Cases.....	79
Table 37: Cases in which the Setting of a Transmission Line overreaches Transformers.....	81
Table 38: Network Transformers that are overreached by Relay Settings.....	84
Table 39: Cases in which the Setting of a Transmission Line Overreaches Network Transformers.....	85
Table 40: Stages in the procedure for the Evaluation of the Region of Vulnerability.....	88
Table 41: Calculation of the Regions of Vulnerability for the cases presented in Chapter Chapter 5.....	88
Table 42: Characteristics and Differences of the Index of Severity in Static and Dynamic Security Analysis compared with the Index of Severity developed in this Dissertation.....	96
Table 43: Individual Indices that Conform the Composite Index of Severity.....	101
Table 44: A number of Base Case Transmission Line Loading Factors	103
Table 45: A sample of the Contingency Description to be presented in the Cases.....	109
Table 46: Selected Output Variables in the Time Domain Simulation	110
Table 47: Representation of the Region of Vulnerability and Location of the Fault, Relay 101-97.....	113
Table 48: Contingency Description for the Relay 101-97.	113
Table 49: Distance Relays Operated during the Relay 101-97 Case.....	114
Table 50: Under Frequency Relays Operated during the Relay 101-97 Case.....	114
Table 51: Overload Assessment for the Relay 101-97 Case.....	116
Table 52: Overall evaluation for the Relay 101-97 Case.....	116
Table 53: Representation of the Region of Vulnerability and Location of the Fault, Relay 84-90.....	117
Table 54: Contingency Description for the Relay 84-90.	118
Table 55: Distance Relays Operated during the Relay 84-90 Case.	118
Table 56: Identification of the Generator Clusters for Relay Case 84-90.....	122
Table 57: Under Frequency Relays that operated for the Relay 84-90 Case.	122
Table 58: Overall evaluation for the Relay 84-90 Case.....	129
Table 59: Representation of the Region of Vulnerability and Location of the Fault, Relay 89-85.....	130
Table 60: Contingency Description for the Relay 89-85.....	130
Table 61: Distance Relays Operated during the Relay 89-85 Case.	131
Table 62: Under Frequency Relays Operated during the Relay 89-85 Case.....	132
Table 63: Overload Assessment for the Relay 89-85 Case.	134
Table 64: Overall evaluation for the Relay 89-85 Case.....	135
Table 65: Representation of the Region of Vulnerability and Location of the Fault, Relay 74-73.....	136
Table 66: Contingency Description for the Relay 74-73.....	136

Table 67: Distance Relays Operated during the Relay 74-73 Case	137
Table 68: Under Frequency Relays Operated during the Relay 74-73 Case.....	138
Table 69: Overload Assessment for the Relay 74-73 Case.	140
Table 70: Overall evaluation for the Relay 74-73 Case.....	140
Table 71: Representation of the Region of Vulnerability and Location of the Fault, Relay 63-104.....	141
Table 72: Contingency Description for the Relay 63-104.	142
Table 73: Distance Relays Operated during the Relay 63-104 Case.....	142
Table 74: Under Frequency Relays Operated during the Relay 63-104 Case.....	143
Table 75: Overload Assessment for the Relay 63-104 Case.....	145
Table 76: Overall evaluation for the Relay 63-104 Case.....	146
Table 77: Individual Indexes for the Five Cases Presented.....	146
Table 78: Maximum Value for each Individual Index for the Five Cases Presented.....	147
Table 79: Normalized Individual Indexes for the Five Cases Presented.....	147
Table 80: Index of Severity for the Five Cases Presented, Sorted By Descending Order.	147

Chapter 1. Introduction

In developed countries, most of the infrastructures such as transportation, telecommunications, and finance depend on their electric power systems [1]. In those countries, the reliability of the electric service has been a concern to the electric power industry, government agencies, and universities. Wide-area disturbances are power outages occurring over large geographical regions that dramatically affect the power system reliability, causing interruptions of the electric supply to residential, commercial, and industrial users. Historically, wide-area disturbances have greatly affected societies. One of the most famous wide-area disturbances happened in New York City in 1977 [2]. The absence of electricity in downtown New York City left streets without lights and deactivated electronic alarms—contributing conditions for the robberies and vandalism that took place. Another wide-area disturbance occurred during the summer of 1996. The western coast of the United States suffered an electric service interruption that spanned from Washington to California. Four million people were affected, and 6 million gallons of raw sewage was dumped in California’s Santa Monica Bay [3-4].

Virginia Tech directed a research project related to the causes of the major disturbances in electric power systems [5]. Research results showed that the role of the power system’s protection schemes in the wide-area disturbances is critical. Incorrect operations of power system’s protection schemes have contributed to a spread of the disturbances. This research defined hidden failures of protection schemes and showed that these kinds of failures have contributed in the degradation of 70-80 percent of the wide-area disturbances. During a wide-area disturbance analysis, it was found that hidden failures in protection schemes caused the disconnection of power system elements in an incorrect and undesirable manner contributing to the disturbance degradation [6].

This dissertation presents a methodology to assess and rank the effects of unwanted disconnections caused by hidden failures based on Regions of Vulnerability and index of severity in the protection schemes.

The main objectives of this dissertation include:

a) Evaluate and improve the methodology to compute the Region of Vulnerability. To continue with the research related to the Region of Vulnerability and find out its significance, how can it be computed, and how can it be represented into the power system.

b) Develop a quantitative indicator to rank the criticality of protection schemes which considers the impact of the unwanted disconnections in the power system. This indicator must include the dynamics of the protection schemes and evaluate the overall disturbance consequence under the static and dynamic perspectives.

The main contributions of this dissertation include:

1. Analysis and explanation of the process in which the Regions of Vulnerability evolve from the Hidden Failure Modes.

2. Refinement of the Methodology: the Region of Vulnerability in a new dimension. Firstly, the Region of Vulnerability dimension is modified from per unit to ohms. Secondly, from the ohms dimension the Region of Vulnerability is modified and computed in kilometers. The benefits from the changes in dimension are demonstrated.

3. Refinement of the Methodology: the representation of the Region of Vulnerability in the power system. The novel concept of *Validation of the Region of Vulnerability* is introduced. A “valid” Region of Vulnerability is defined as the part of transmission line in which the occurrence of faults do make the relay to operate, producing the unwanted disconnection caused by hidden failure. The assurance of the operation of the relay is a fundamental issue in this validation. The results in this system showed that the infeed currents restrain the Region of Vulnerability from spreading along power system elements. The final procedure related to the Re-Calculation of the Region of Vulnerability is developed.

4. Development of the Index of Severity. A methodology to compute the index of severity is developed. The index considers the dynamics of the protection schemes and is computed based on the magnitude of the Region of Vulnerability, the lost load, the lost generation, and the static overload assessment.

The dissertation's outline is as follows:

Chapter 2 includes the concept of Region of Vulnerability, describes the process in which the Regions of Vulnerability evolve from the Hidden Failure Modes, and presents a catalogue of Regions of Vulnerability for a number of protection schemes.

Chapter 3 analyzes and implements protection schemes for power system elements and wide area protection schemes using the relay models available in a transient stability program (ETMSP).

Chapter 4 refines the methodology for the evaluation of the Region of Vulnerability. The modifications in the dimension of the Region of Vulnerability have “per unit” as the reference. The first change is to bring the Region of Vulnerability from per unit to ohms; subsequently, the dimension of the Region of Vulnerability is modified from ohms to kilometers. The benefits obtained from these changes in dimension are demonstrated. The representation of the Region of Vulnerability in the power system is analyzed and refined. The novel concept of *Validation of the Region of Vulnerability* is introduced and the assurance of the operation of the relay is a fundamental issue in this validation. The strong impact of the infeed currents is highlighted. The Regions of Vulnerability for the five simulation cases to be presented in Chapter 5 are evaluated based on the refined methodology.

Chapter 5 defines the terms Areas of Consequence and Index of Severity. It includes a literature review of the index of severity and its use in power system security, specifically for static and dynamic security assessment. The differences of the index of severity found in the literature review and the developed index of severity are described. The effects of the unwanted disconnections caused by Hidden Failures in a Power System are simulated and assessed through

the cases that are run in a transient stability program. Five simulations are developed and detailed explained. The index of severity for the five simulation cases is computed.

Chapter 6 summarizes on the main contributions of this dissertation and presents the directions for future research.

Five appendices are included in this dissertation. Appendix 1 contains the data of the 127-bus sample power system. Appendix 2 includes the distance and under frequency relay settings information. Appendix 3 contains the data of the 39-bus sample power system. Appendix 4 presents the base case loading factors for the static overload assessment. Finally, Appendix 5 presents a brief explanation of the procedure to develop the simulation cases and a number of files related to the ETMSP program.

Chapter 2. Qualitative Evaluation of Regions of Vulnerability

This chapter develops the Regions of Vulnerability for different protection schemes based on their hidden failure modes [5]. A generic protection scheme and a number of transmission lines protection schemes are presented in order to explain the Region of Vulnerability concept. A catalogue of Regions of Vulnerability is developed for the different relays and protection schemes (see section 2.3).

2.1 Definition of Region of Vulnerability

Previous research has shown that a number of hidden failure modes are based on a protection element functionality defect [6]. In general, a protection element functionality defect (PEFD) takes place when the protection devices are unable to perform their designed and expected actions. This defect can be present on any of the protection scheme elements, and may take the form of hardware failures, outdated relay's settings, and human negligence or errors. Examples of PEFD's are a relay's contact that is always open or closed, a timer that operates regardless of its pre-assigned time delay, an outdated setting in a relay, and a human error in the coordination of relays.

The occurrence of a PEFD in a protection scheme may result in an unwanted disconnection of a power system element, such as a transmission line. This switching action is related to the PEFD and is called an unwanted disconnection caused by a hidden failure. The consequences of unwanted disconnections caused by hidden failures in the power system may be quite severe. Unwanted disconnections caused by hidden failures take place when the power system is stressed—such as during electrical faults—and may add stress to the already stressed power system. This combination of events may cause a cascading effect. Most of the wide-area disturbances include a cascading effect, which is an uncontrolled disconnection of the power system elements caused by a degradation of the power system parameters (voltage, current, frequency) and power system instability.

The unwanted disconnections caused by hidden failures can occur in any of the power system elements: generators, buses, transformers, and transmission lines. These unwanted disconnections are the result of a combination of two events: a PEFD in the protection scheme, and the occurrence of “another condition” in the power system. A particular PEFD may produce a change in the requirements to be met for a power element disconnection. When a protection scheme has a PEFD, the occurrence of “another condition” may result in an unwanted disconnection caused by a hidden failure. This other condition may take the form of an electrical fault or a power system parameter change, such as deviations from nominal values in current, voltage, or frequency. It is important to further analyze this other condition as the triggering issue for the unwanted disconnection caused by a hidden failure.

A number of the hidden failure modes that have been identified have a section in their logic schematic where two relay contacts are connected in series [6]. Figure 1 shows this arrangement. As mentioned earlier, the sequence of events in an unwanted disconnection caused by a hidden failure starts with a PEFD on one relay, such as R2. Considering that R2 has a PEFD and its contacts are always closed; Figure 1 shows that the operation of relay R1 contacts would trigger a control action and, in this case, would close the direct current path to the circuit breaker trip coil. This last event sends a control signal to the circuit breaker, incorrectly disconnecting a power system element.

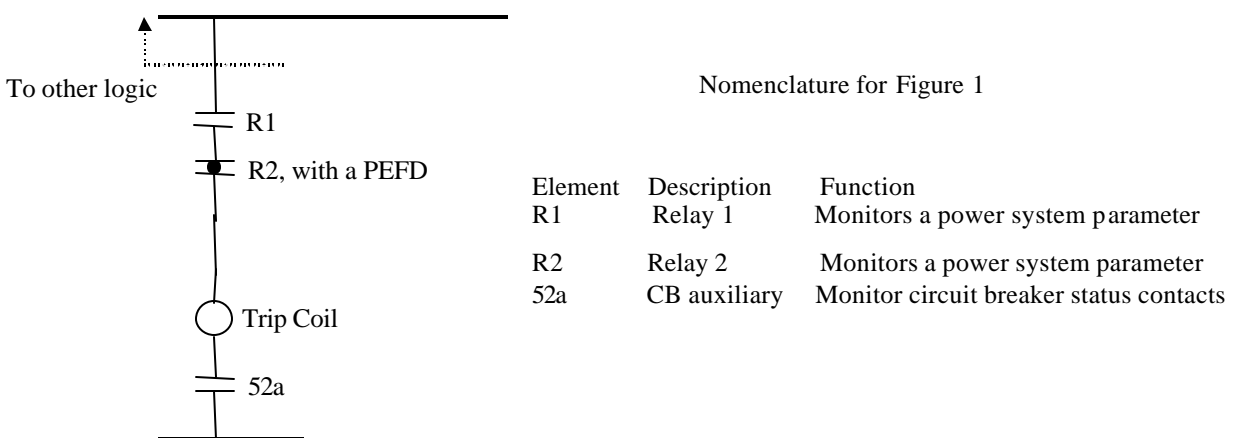


Figure 1: A logic schematic section with two relays connected in series.

Figure 1 deserves to be analyzed in more detail, since it describes the sequence of events for an unwanted disconnection caused by a hidden failure. Generally, the conditions required to be present for R1 operation are different from the ones needed to operate R2. The problems arise after R2 has a PEFD and its contacts are closed. The conditions required for R1 operation are not the same as those that have to be present to correctly operate the circuit breaker. These conditions result from the R1 and the R2 requirements, as shown in Figure 2. Since in Figure 1 the relays R1 and R2 are connected in series, then in order to correctly operate the circuit breaker, R1 and R2 relays must *both* close their contacts. In other words, the conditions required to operate R1 *and* to operate R2 must *both* be present. Figure 2 shows the intersection of these conditions: R1 and R2 requirements.

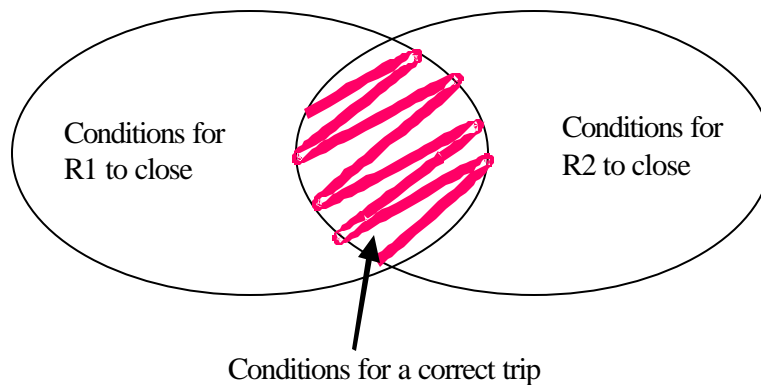


Figure 2: Conditions for a correct trip for the Figure 1 logic schematic.

The PEFD in R2, which makes its contacts to be closed, provides *one* of the conditions required to trip the circuit breaker regardless of the condition existence in the power system. The PEFD in R2 allows tripping the circuit breaker when the conditions required to operate *R1 only* are satisfied. If the power system conditions change in such a way that cause R1 to operate closing its contacts, then this switching action is an unwanted disconnection caused by a hidden failure. Because of the PEFD in R2, there is the need to identify all conditions for which R1 will close its contacts, since these represent the triggering issue for the unwanted disconnection caused by a hidden failure. The identification of all conditions causing the operation of relay R1 would depend on several factors. The first one is the relay type, which would provide the kind of inputs that the relay will receive, such as current, voltage, and frequency. These inputs are compared with setting values, and the relay may or may not change its contact's status. Another issue is to

consider other relays on which R1 depends. R1 may be a simple over-current relay depending on the system current magnitude only. R1 may also take the form of a receiver relay that depends on a transmitter and a number of other relays. The role of R1 in the protection scheme must be identified regarding what kind of events will be observable to the relay.

The occurrence of the previously discussed “another condition” in the power system—the condition for which R1 would close its contacts, for the Figure 1 example—becomes the triggering issue for an unwanted disconnection caused by a hidden failure. This other condition can be represented in a physical area in the power system—a Region of Vulnerability.

Surachet Tamronglak [5] developed the Region of Vulnerability concept as: “a physical region in the network such that any fault within that region will trigger the system hidden failure to produce an unwanted and undesirable operation.” In theory, the Region of Vulnerability would be referred to as a zone in which the triggering issues for an unwanted disconnection caused by a hidden failure are located. In reality, we cannot talk about a Region of Vulnerability in a general form. The Regions of Vulnerability acquire particular shapes, dimensions, and magnitudes depending on the hidden failure modes of the protection scheme being analyzed. The example that follows applies the ideas discussed in this section to particular relays and protection schemes to show how the Regions of Vulnerability are developed.

2.2 Development of Regions of Vulnerability

In order to explain how the Regions of Vulnerability are developed based on the hidden failure modes, an example related to protection schemes for a transmission line is presented next. The protection schemes and their respective hidden failure modes to be considered in the example are listed in Table 1. A complete description of the protection schemes for transmission lines, and the hidden failure modes associated with those schemes can be found in [7] and [6], respectively. The nomenclature for the hidden failure modes included in Table 1 will be described in the subsection where the logic schematic of the protection scheme is presented.

Table 1: Region of Vulnerability Development, an Example.

Protection Scheme	Power System Element	Hidden Failure Mode (HFM)
Directional comparison blocking.	Transmission lines	FD_A can not pick up
Directional comparison blocking.	Transmission lines	T_A can not transmit
Directional comparison un-blocking.	Transmission lines	D_A is always picked up
Permissive overreaching transfer-trip	Transmission lines	D_A is always picked up
Permissive underreaching transfer-trip	Transmission lines	T_A is always picked up

Directional Comparison Blocking Scheme. Figure 3 shows the one-line diagram of the directional comparison blocking scheme. In this one-line diagram the Region of Vulnerability will be developed. Figure 4 shows the logic schematic for the directional comparison blocking with two hidden failure modes as described in Table 1, rows 1 and 2. The nomenclature for Figure 3 and Figure 4 is included below.

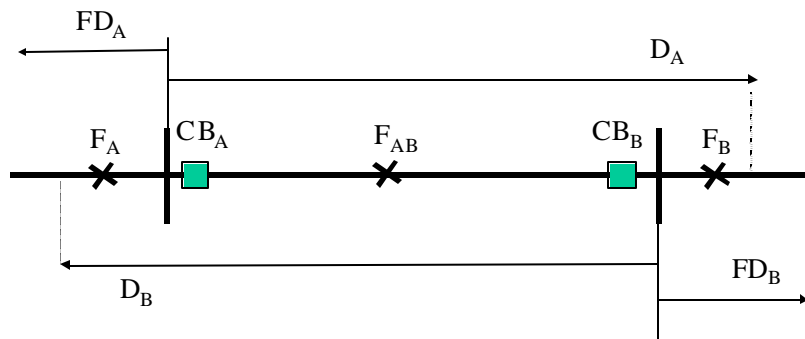


Figure 3: One-line Diagram for the Directional Comparison Blocking.

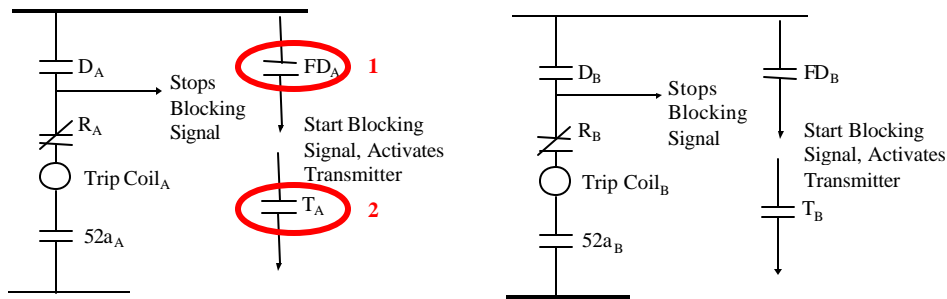


Figure 4: Logic Schematic for the Directional Comparison Blocking, A and B line sides.

Nomenclature and Protection Scheme Elements for Figure 3 and Figure 4 *.

Element	Description	Function
FD _A	Fault detector	Detect external faults and start transmitter
D _A	Directional relay	Detects faults and stops transmitter
R _A	Receiver	Receives remote/local signal
T _A	Transmitter	Transmits communication signal
CB _A	Circuit Breaker	Disconnect one line side
52a _A	CB auxiliary contacts	Monitor breaker status
F _A	Fault behind bus A, under D _B reach	
F _B	Fault behind bus B, under D _A reach	
F _{AB}	Fault between A and B	

* The same elements apply also for line side B.

Table 2 shows the sequence of events for an unwanted disconnection caused by a hidden failure. The circuit breaker that is opened incorrectly is CB_B. The sequence of events described in Table 2 is related to the PEFD in the logic schematic shown in Figure 4, number 1, and the electrical fault located at “F_A.” See Figure 3.

Table 2: Sequence of Events for an Unwanted Disconnection Caused by a Hidden Failure; Table 1, Row 1.

Case for F _A PEFD:FD _A can not pick up			
Operated Relays	Consequences at side A logic schematic	Consequences at side B logic schematic	Final Result
FD _A	FD _A cannot close, T _A is not activated, no BS _A . R _A remains closed.	No BS _A , so R _B remains closed.	
D _B		D _B closes its contacts.	Unwanted trip at B side, since BS _A was not received, R _B remained closed and D _B was activated.
Nomenclature: BS _A : Blocking signal of side A			

The first event in the unwanted disconnection caused by a hidden failure is the PEFD shown in Figure 4, number 1. The FD_A relay has its contacts normally open, and the PEFD will not allow the relay to change its contacts status. Therefore, the relay contacts will be always open regardless on the power system conditions that make the relay to react. Since the FD_A is a distance relay, the relay reacts to the apparent impedance seen by its terminals. The power system condition required to operate this relay is an electrical fault within the relay protective zone.

In the directional comparison blocking scheme, the receiver relays R_A and R_B take input signals from both fault locator relays: FD_A and FD_B . This means that the receiver relays, R_A and R_B , change its contacts status (open its normally-closed contacts) if the blocking signal coming from either FD_A or FD_B is received. When either FD_A or FD_B signal is received on a transmission line side, the receiver on that side opens its contacts, and no circuit breaker trip occurs. The PEFD on FD_A makes the relay unable to react to the power system conditions for which it was designed. In other words, the relay cannot close its contacts even though there is a power system condition that is observable to it. This FD_A inability to close its contacts has the consequence of not sending a blocking signal to the receiver relays. Since the receiver relays (R_A and R_B) react to the blocking signal coming from either FD_A or FD_B , there is a case in which the inability of a fault detector to close its contacts leaves a flaw in the logic—a vulnerable logic.

The vulnerable logic that results from the PEFD in the FD_A relay reveal itself until another condition occurs in the power system. This other condition has particular characteristics and it becomes observable to one of the relays in the directional comparison blocking scheme. This other condition produces a relay reaction and because of this relay operation only, an unwanted disconnection caused by a hidden failure takes place. Under this vulnerable logic scenario, in which the receiver R_B can only receive input signals from FD_B (FD_A has a PEFD), the occurrence of “ F_A ” makes the D_B relay to operate resulting in an unwanted disconnection caused by a hidden failure: CB_B is opened incorrectly. The second event in the unwanted disconnection caused by a hidden failure, the power system other condition, is the electrical fault: “ F_A .” See Figure 3 and Figure 4.

The operation of relay D_B defines the initial point of the concept of Region of Vulnerability and the Region of Vulnerability characteristics. Figure 5 shows the representation of a Region of Vulnerability for the hidden failure mode included in Table 1, row 1. The Region of Vulnerability is located in the reverse part with respect to the protection scheme element with the hidden failure mode: FD_A . The size of this Region of Vulnerability depends on the D_B relay settings, which is the relay that reacts to the power system other condition: “ F_A .” The dimension of this Region of Vulnerability also depends on the D_B relay. Since D_B reacts to certain impedance seen by its terminals, the dimension of this Region of Vulnerability is ohms.

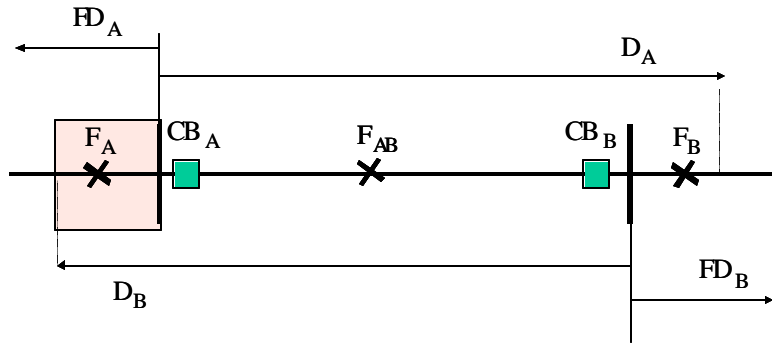


Figure 5: Region of Vulnerability for Hidden Failure Mode of Table 1, Row 1.

Directional Comparison Blocking Scheme. The hidden failure mode shown in Table 1, row 2, T_A cannot transmit is a failure in the communication equipment. By observing the logic in Figure 4, it can be seen that T_A and FD_A are connected in series. Therefore, the consequences are that PEFD FD_A cannot pick-up, and PEFD T_A cannot transmit result in the same Region of Vulnerability as shown in Figure 5.

Directional Comparison Unblocking Scheme. Figure 6 shows the one-line diagram of the directional comparison unblocking scheme. In this one-line diagram the Region of Vulnerability will be developed. Figure 7 shows the logic schematic for the directional comparison unblocking with the hidden failure mode as described in Table 1, row 3. The nomenclature for Figure 6 and Figure 7 is included below.

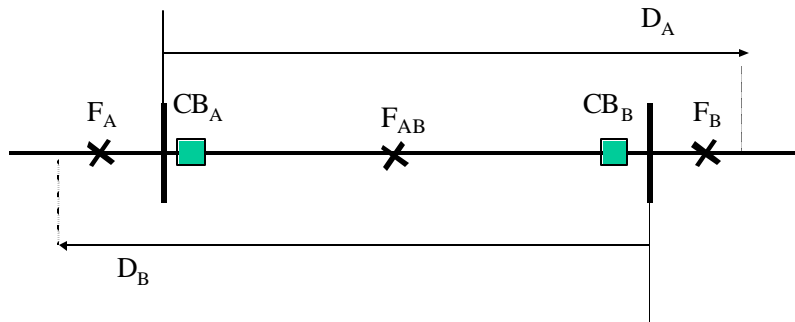


Figure 6: One-line Diagram for the Directional Comparison Unblocking.

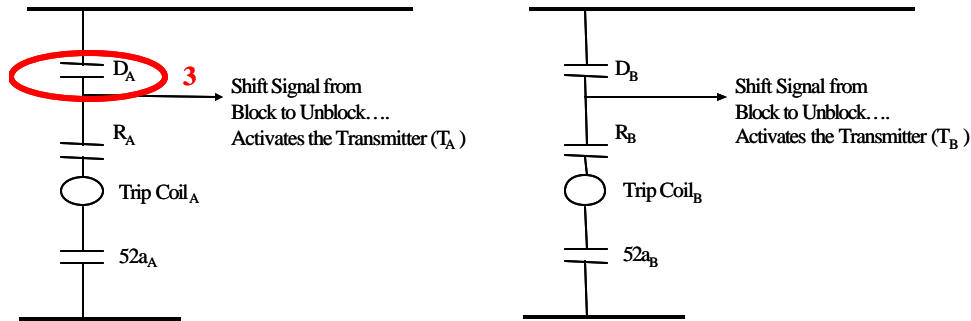


Figure 7: Logic Schematic for the Directional Comparison Unblocking, A and B line sides.

Nomenclature and Protection Scheme Elements for Figure 6 and Figure 7 *.

Element	Description	Function
D_A	Directional relay	Detects faults and shifts transmitter signal to unblocking
R_A	Receiver	Receives remote signal
T_A	Transmitter	Transmits communication signal
CB_A	Circuit Breaker	Disconnect one line side
$52a_A$	CB auxiliary contacts	Monitor breaker status
F_A	Fault behind bus A, under D_B reach	
F_B	Fault behind bus B, under D_A reach	
F_{AB}	Fault between A and B	

* The same elements apply also for line side B.

Table 3 shows the sequence of events for an unwanted disconnection caused by a hidden failure. The circuit breakers that are opened incorrectly are CB_A and CB_B . The sequence of events described in Table 3 is related to the PEFD in the logic schematic shown in Figure 7, number 3, and the electrical fault located at “ F_A .” See Figure 6.

Table 3: Sequence of Events for an Unwanted Disconnection Caused by a Hidden Failure; Table 1, Row 3.

Case for F_A , PEFD: D_A is always picked up			
Operated Relays	Consequences at side A logic schematic	Consequences at side B logic schematic	Final Result
D_B	D_A contacts are always closed, they activate T_A to shift frequency to unblocking signal, UBS_A .	R_B receives UBS_A and closes it's normally open contacts.	Unwanted trip at A, since D_A was always closed and R_A closed its contacts.
	R_A receives UBS_B and closes it's normally open contacts.	D_B contact closes, activates T_B to shift frequency to unblocking signal, UBS_B	Unwanted trip at B, since D_B was activated and R_B closed its contacts.
Nomenclature: UBS_A : Un-Blocking signal of side A UBS_B : Un-Blocking signal of side B			

The first event in the unwanted disconnection caused by a hidden failure is the PEFD shown in Figure 7, number 3. The D_A relay has its contacts normally open, but because of the PEFD, its contacts are closed. In other words, the relay contacts will be always closed regardless on the power system conditions that make the relay to react. Since D_A is a distance relay, the relay reacts to the apparent impedance seen by its terminals. The power system condition required to operate this relay is an electrical fault within the relay protective zone.

In the directional comparison unblocking scheme, the receiver relay R_A take input signals from the distance relay D_B only, as R_B take input signals from the distance relay D_A only. Once a receiver gets the remote signal, it closes its contacts. The PEFD on D_A makes the relay to be in the closed position. In other words, D_A relay contacts are always closed regardless of the power system condition that is observable to the relay. Having relay D_A always closed has the consequence of sending the unblocking signal to the remote end; therefore, R_B closes its contacts. Since each receiver relay (R_A and R_B) depends on the remote end distance relay (D_B and D_A), there is a case in which the inability of a distance relay to remain open when it should leaves a flaw in the logic—a vulnerable logic.

The vulnerable logic that results from the PEFD in the D_A relay reveal itself until another condition occurs in the power system. This other condition has particular characteristics and it becomes observable to one of the relays in the directional comparison unblocking scheme. This other condition produces a relay reaction and because of this relay operation only, an unwanted disconnection caused by a hidden failure takes place. Under this vulnerable logic scenario, in which R_B is closed (D_A has a PEFD), the occurrence of “ F_A ” makes the D_B relay to operate resulting in an unwanted disconnection caused by a hidden failure: CB_B and CB_A are opened incorrectly. The second event in the unwanted disconnection caused by a hidden failure, the power system other condition, is the electrical fault: “ F_A .” See Figure 6 and Figure 7.

The operation of the relay D_B defines the Region of Vulnerability characteristics. Figure 8 shows the representation of a Region of Vulnerability for the hidden failure mode included in Table 1, row 3. The Region of Vulnerability is located in the reverse part with respect to the protection scheme element with the hidden failure mode: D_A . The size of this Region of Vulnerability

depends on the D_B relay settings, which is the relay that reacts to the power system other condition: “ F_A .” The dimension of this Region of Vulnerability also depends on the D_B relay. Since D_B reacts to certain impedance seen by its terminals, the dimension of this Region of Vulnerability is ohms.

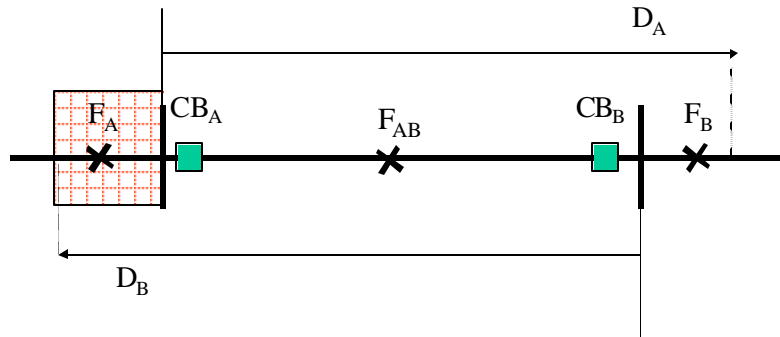


Figure 8: Region of Vulnerability for Hidden Failure Mode of Table 1, Row 3.

Permissive Overreaching Transfer-Trip Scheme. In Table 1, row 4 shows the hidden failure mode: D_A is always picked up. This hidden failure mode takes place in the logic schematic of the permissive overreaching transfer-trip scheme. The one-line diagram and the logic schematic for this scheme are identical to the ones related to the directional comparison unblocking shown in Figure 6 and Figure 7, respectively. This fact makes the hidden failure mode in question, D_A is always picked up, to be the same for both schemes. The resulting Region of Vulnerability and its characteristics is the same than the one described in Figure 8.

Permissive Underreaching Transfer-Trip Scheme. Figure 9 shows the one-line diagram of the permissive underreaching transfer-trip scheme. In this one-line diagram the Region of Vulnerability will be developed. Figure 10 shows the logic schematic for the permissive underreaching transfer-trip with the hidden failure mode as described in Table 1, row 5. The nomenclature for Figure 9 and Figure 10 is included below.

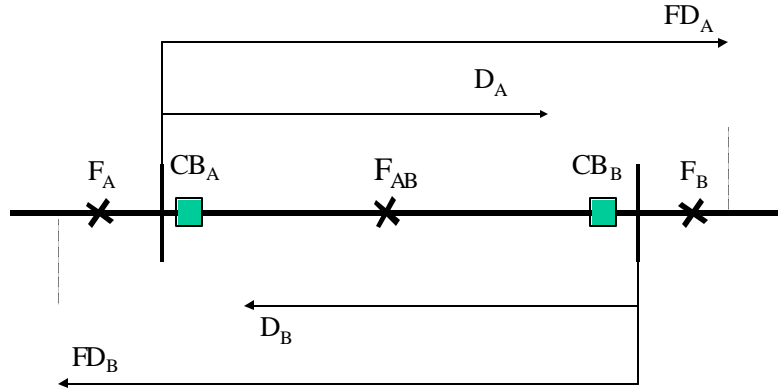


Figure 9: One-line Diagram for the Permissive Underreaching Transfer-Trip.

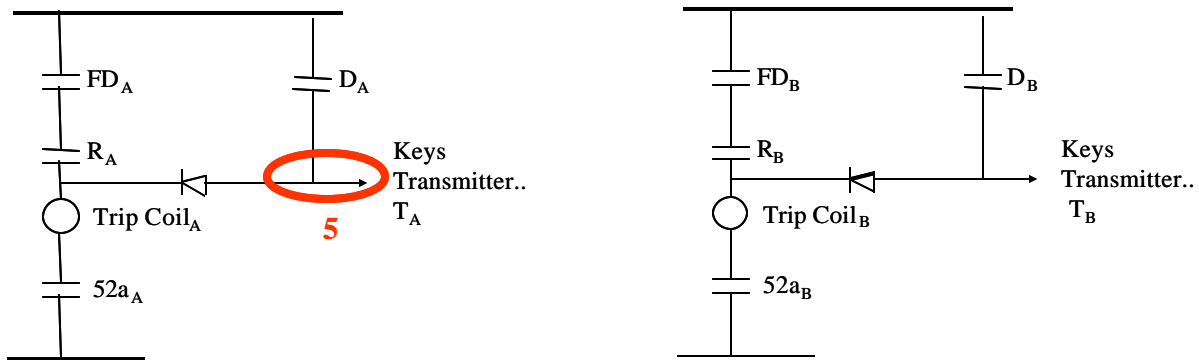


Figure 10: Logic Schematic for the Permissive Underreaching Transfer-Trip, A and B line sides.

Nomenclature and Protection Scheme Elements for Figure 9 and Figure 10 *.

Element	Description	Function
FD _A	Fault detector	Detect faults
D _A	Directional relay	Detects faults and shifts transmitter signal to tripping mode
R _A	Receiver	Receives remote signal
T _A	Transmitter	Transmits communication signal
CB _A	Circuit Breaker	Disconnect one line side
52a _A	CB auxiliary contacts	Monitor breaker status
F _A	Fault behind bus A, under FD _B reach	
F _B	Fault behind bus B, under FD _A reach	
F _{AB}	Fault between A and B	

* The same elements apply also for line side B.

Table 4 shows the sequence of events for an unwanted disconnection caused by a hidden failure. The circuit breaker that is opened incorrectly is CB_B. The sequence of events described in Table

4 is related to the PEFD in the logic schematic shown in Figure 10, number 5, and the electrical fault located at “F_A.” See Figure 9.

Table 4: Sequence of Events for an Unwanted Disconnection Caused by a Hidden Failure; Table 1, Row 5.

Case for F _A PEFD-A:T _A is always picked up			
Operated Relays	Consequences at side A logic schematic	Consequences at side B logic schematic	Final Result
FD _B	T _A is always picked up, transmits a TS _A	R _B receives TS _A and closes it's normally open contacts FD _B contact closes.	Unwanted trip at B, R _B and FD _B closed.
Nomenclature: TS _A : Transfer-Trip signal of side A			

The first event in the unwanted disconnection caused by a hidden failure is the PEFD shown in Figure 10, number 5. Because of the PEFD, the transmitter (T_A) is always picked up; therefore, the transmitter shifts the frequency, and a transfer-trip signal is always being transmitted.

In the permissive underreaching transfer scheme, the receiver relay R_A takes input signals from the transmitter T_B only, as R_B takes input signals from the transmitter T_A only. Once a receiver gets the remote signal, it closes its contacts. The PEFD on T_A makes the transmitter to be always sending the transfer-trip signal. Having T_A in continuous transmission has the consequence of sending the transfer-trip signal to the remote end; therefore, R_B closes its contacts. Since each receiver relay (R_A and R_B) depends on the remote end transmitter (T_B and T_A), there is a case in which the inability of a transmitter to remain on the blocking-signal frequency when it should leaves a flaw in the logic—a vulnerable logic.

The vulnerable logic that results from the PEFD on the T_A reveal itself until another condition occurs in the power system. This other condition has particular characteristics and it becomes observable to one of the relays in the permissive underreaching transfer scheme. This other condition produces a relay reaction and because of this relay operation only, an unwanted disconnection caused by a hidden failure takes place. Under this vulnerable logic scenario, in which R_B is closed (T_A has a PEFD), the occurrence of “F_A” makes the FD_B relay to operate resulting in an unwanted disconnection caused by a hidden failure: CB_B is opened incorrectly.

The second event in the unwanted disconnection caused by a hidden failure, the power system other condition, is the electrical fault: “ F_A .” See Figure 9 and Figure 10.

The operation of the relay FD_B defines the Region of Vulnerability characteristics. Figure 11 shows the representation of a Region of Vulnerability for the hidden failure mode included in Table 1, row 5. The Region of Vulnerability is located in the reverse part with respect to the protection scheme element with the hidden failure mode: T_A . The size of this Region of Vulnerability depends on the FD_B relay settings, which is the relay that reacts to the power system other condition: “ F_A .” The dimension of this Region of Vulnerability also depends on the FD_B relay. Since FD_B reacts to certain impedance seen by its terminals, the dimension of this Region of Vulnerability is ohms.

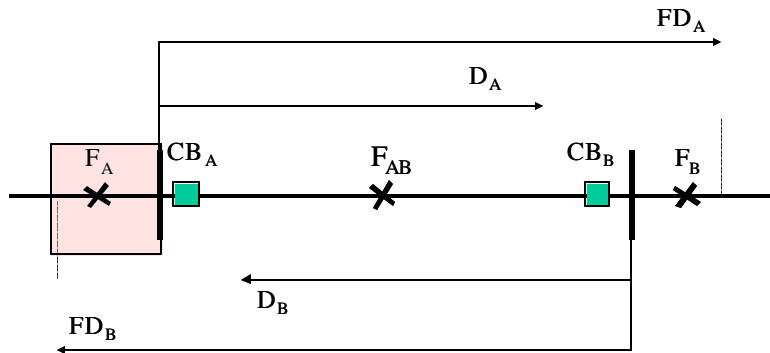


Figure 11: Region of Vulnerability for Hidden Failure Mode of Table 1, Row 5.

The Regions of Vulnerability are classified depending on their representation in the power network, their shape, size, and location with respect to the protection scheme element with the hidden failure mode. Figure 12 shows the five Regions of Vulnerability developed for the five hidden failure modes. As it can be seen in the figure, the five Regions of Vulnerability are represented in the power system with a similar shape and location; therefore, it makes sense to group them to form the Region of Vulnerability type 1: reverse local bus.

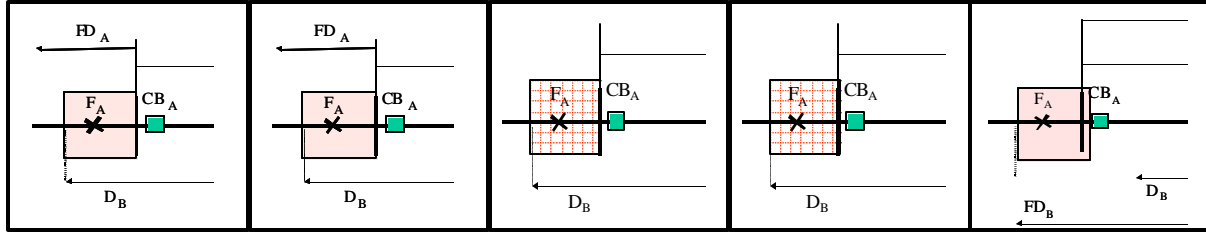


Figure 12: Region of Vulnerability for Hidden Failure Modes of Table 1, Rows 1,2,3,4, and 5.

The examples presented in this section showed the procedure in which the Regions of Vulnerability are developed. For the five hidden failure modes analyzed in Table 1, the PEFD and the triggering issue for the unwanted disconnection caused by a hidden failure were identified. Next section presents a number of the Regions of Vulnerability that were developed following a similar procedure to the one presented in these examples.

2.3 Catalogue of Regions of Vulnerability

Table 5 shows the list of the hidden failure modes that were developed in [6]. Table 5 presents: a number for each hidden failure mode, the specific hidden failure mode, the relay or relay system in question within the protection scheme, and the power system element in which the protection scheme is applied. The terminology of a number of hidden failure modes was defined in section 2.2. For the remaining hidden failure modes shown in Table 5, the terminology is included in reference [6]. Particular details of the protection schemes operations and their respective hidden failure modes are included in [6].

Table 5: List of Hidden Failures Modes sorted by Power System Element.

Ref	Hidden Failure Mode	Relay / Relay System	Power System Element
1	FDA is unable to pickup	Directional Comparison Blocking	Transmission Lines
2	TA is unable to transmit	Directional Comparison Blocking	Transmission Lines
3	RA is unable to pickup	Directional Comparison Blocking	Transmission Lines
4	DA is always picked up	Directional Comparison Unblocking	Transmission Lines
5	RA is always picked up	Directional Comparison Unblocking	Transmission Lines
6	DA is always picked up	Permissive Overreaching Transfer- Trip	Transmission Lines
7	RA is always picked up	Permissive Overreaching Transfer- Trip	Transmission Lines
8	TA is always picked up	Permissive Underreaching Transfer- Trip	Transmission Lines
9	RA is always picked up	Permissive Underreaching Transfer- Trip	Transmission Lines
10	Loss of signal	Single Phase Comparison Blocking	Transmission Lines
11	FDLA is always picked up	Single Phase Comparison Blocking	Transmission Lines
12	FDLA can not pick up	Single Phase Comparison Blocking	Transmission Lines
13	Loss of signal	Dual Phase Comparison Blocking	Transmission Lines
14	FDLA is always picked up	Dual Phase Comparison Blocking	Transmission Lines
15	FDLA can not pick up	Dual Phase Comparison Blocking	Transmission Lines
16	T2 contacts are always closed.	Distance Relay, Zone 2	Back-up Transmission Lines
17	Directional unit contacts always closed	Directional Over-current Relays	Back-up Transmission Lines
18	Over-current unit contacts always closed	Directional Over-current Relays	Back-up Transmission Lines
19	T3 contacts are always closed.	Distance Relay, Zone 3	Back-up Transmission Lines
20	Directional unit contacts always closed	Directional Over-current Relay	Back-up Transformer
21	Over-current unit contacts always closed	Directional Over-current Relay	Back-up Transformer
22	Directional unit contacts always closed	Directional Over-current Relay	Transformer
23	Directional unit contacts always closed	Directional Over-current Relay	Transformer
24	Restraint coils shorted	Percentage differential relay	Transformer
25	Restraint coils shorted	Percentage differential relay	Bus
26	T3 contacts are always closed.	Breaker Failure Relay	Circuit Breaker
27	Restraint coils shorted	Percentage differential relay	Generator
28	Undervoltage normally closed contacts can not picked-up	Loss of Field Relay	Generator
29	Overcurrent relay contacts are always closed	Inadvertent Energization	Generator

Regions of Vulnerability for Transmission Lines

Figure 13 shows the type of Region of Vulnerability presented in section 2.2: reverse local bus. In this case the unwanted disconnection caused by a hidden failure takes place in a transmission line. In the presence of a particular PEFD and an electrical fault occurring inside the shaded area, the circuit breaker CB_{BC} will trip the B-side of the transmission line BC incorrectly. From Table 5, the hidden failure modes associated to this Region of Vulnerability type 1 are rows: 1, 2, 4, 6, and 8.

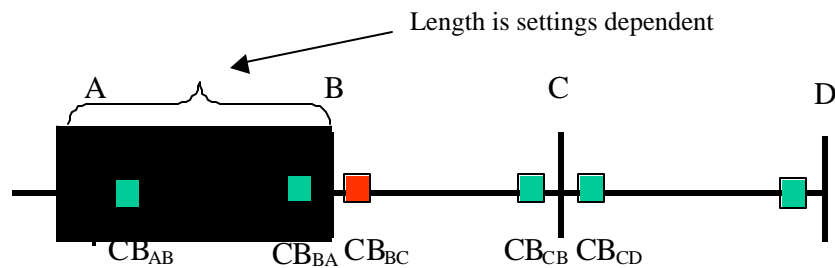


Figure 13: Region of Vulnerability Type 1, Reverse Local Bus.

As its name indicates, the type 1 region of vulnerability—reverse local bus—relates to the closest bus to the circuit breaker CB_{BC} . The Region of Vulnerability extends over the transmission line AB and any other line connected to bus B (not shown in the figure). The particular length depends on the relay settings related to the previously mentioned hidden failure modes, rows 1, 2, 4, 6, and 8.

Figure 14 shows the second type of Region of Vulnerability to be presented: reverse remote bus. In the presence of a particular PEFD and an electrical fault occurring inside the shaded area, the circuit breaker CB_{BC} will trip the B-side of the transmission line BC incorrectly. From Table 5, the hidden failure modes associated to this Region of Vulnerability type 2 are rows: 3, 5, 7 and 9.

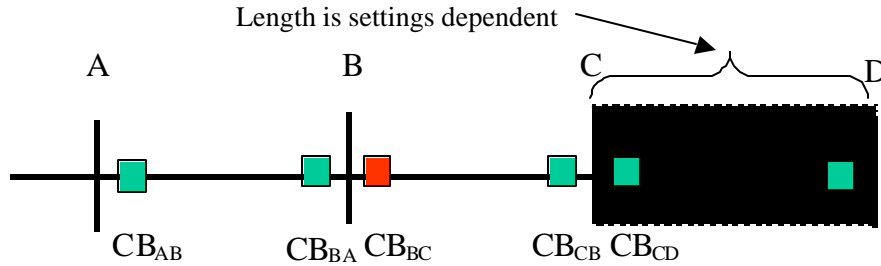


Figure 14: Region of Vulnerability Type 2, Reverse Remote Bus.

As its name indicates, type 2 region of vulnerability—reverse remote bus—relates to the far bus in the forward direction to the circuit breaker CB_{BC} . The Region of Vulnerability is located over the transmission line CD and any other line connected to bus C (not shown in the figure). The particular length depends on the relay settings related to the previously mentioned hidden failure modes, rows 3, 5, 7 and 9.

Figure 15 presents the third type of region of vulnerability: Zone 2. This Region of Vulnerability is similar to the type 2: reverse remote bus. In the presence of a particular PEFD and an electrical fault occurring inside the shaded area, the circuit breaker CB_{BC} will trip the B-side of the transmission line BC incorrectly. From Table 5, the hidden failure mode associated to this Region of Vulnerability type 3 is row 16.

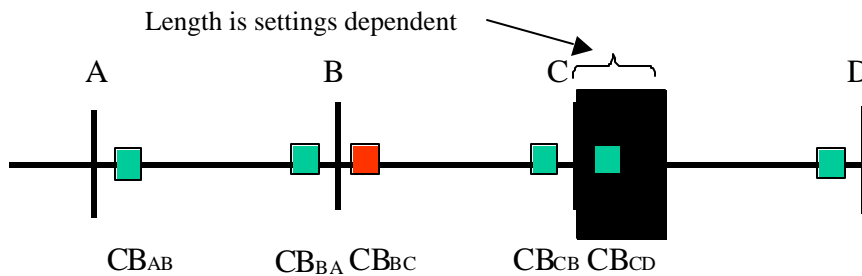


Figure 15: Region of Vulnerability Type 3, Zone 2.

The Region of Vulnerability extends a segment of the transmission line CD and any other line connected to bus C (not shown in the figure). The particular length depends on the relay settings related to the previously mentioned hidden failure mode, row 16.

Figure 16 presents the fourth type of region of vulnerability: Zone 3. This Region of Vulnerability is similar to the type 3: Zone 2. In the presence of a particular PEFD and an electrical fault occurring inside the shaded area, the circuit breaker CB_{BC} will trip the B-side of the transmission line BC incorrectly. From Table 5, the hidden failure mode associated to this Region of Vulnerability type 4 is row 19.

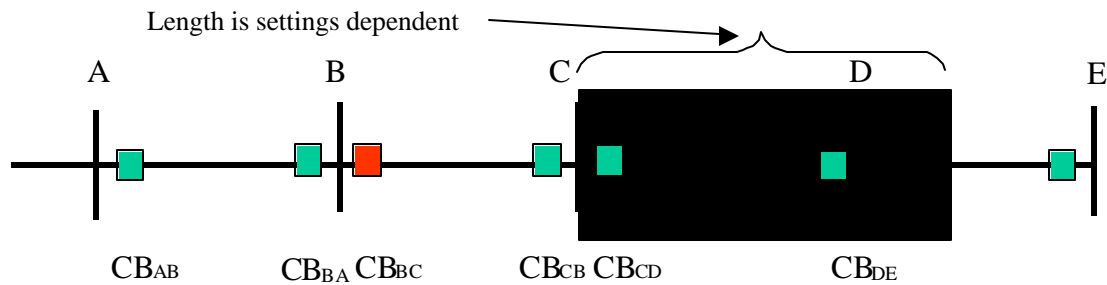


Figure 16: Region of Vulnerability Type 4, Zone 3.

The Region of Vulnerability extends over the transmission line CD, a section of transmission line DE, and any other line connected to bus C (not shown in the figure). The particular length depends on the relay settings related to the previously mentioned hidden failure mode, row 19.

Regions of Vulnerability for Generators, Transformers and Buses

The Region of Vulnerability for generators, transformers and buses can be developed following a procedure similar to the one described in Section 2.2. This dissertation focuses on transmission lines because 1) this power system element presents higher susceptibility to faults, the “another condition” presented in the hidden failure sequence of events; and 2) we are interested in determining the Regions of Vulnerability as physical areas.

Even though the Region of Vulnerability for buses, transformers and generators could be developed, the complete methodology could not be evaluated due to the limitations that are described in Chapter Chapter 3, which deals with the relay models that were used during the simulations.

Chapter 3. Protection System Design

This chapter analyzes and implements protection schemes for power system elements and wide area protection schemes using the relay models available in a transient stability program (ETMSP). The dynamic behavior of the relays and the impact of its operation are considered in the sequence of events of the cases to simulate in Chapter 5.

3.1 Protection System Design: Scope and Limitations

For the cases to simulate in Chapter 5, the contingency to be applied is a three phase fault and the permanent disconnection of two transmission lines. The first disconnection (N-1) is caused by the permanent fault and the second (N-2) is caused by a Hidden Failure. After this point, we are assuming that there are not more faults and no more hidden failures in the relays. The main goal of including a protection system in the simulation process is to detect the N-3, N-4 ... N-K contingency due to relay operations. In other words, we are interested in the response of the modeled relays to the double contingency.

We know that a basic protection system design is composed of protection schemes for transmission lines, transformers, buses, and generators, and each of these power system components imposes specific needs and challenges. Each setting is a compromise [8] and is certainly the result of multiple simulations, extensive power system elements information, and the most important ingredient: engineering judgment.

It is important, however, to recognize the limitations of the relaying infrastructure that is developed here in. The limitations are originated from two sources: 1) the relay models that are available in the transient stability program (ETMSP) and 2) the system in which the relays are

applied. Since the available relay models is limited and the system we are working with is not fully representative of a real system¹, it is not the objective of this dissertation's relaying infrastructure to emulate the complicated and extensive network of relays and special protection schemes that lay in a practical power system. Rather, it is our objective to show and evaluate the methodology of Regions of Vulnerability, Areas of Consequence, and Index of Severity in which the relaying infrastructure dynamics is important. The relays implemented are monitored during the contingency and its operations are considered in the evaluation of the above mentioned methodology.

The relay models available in ETMSP are described below and the task of implementing these models for the protection of transmission lines, generators, transformers, and buses is described. We limited the scope of the present protection system design to these four elements; shunt equipment (reactors and capacitors) and equipment alike is not considered.

The main system in which we are testing the methodology is depicted in Figure 17. The basic information of the system is presented in Table 6 and its details are included in Appendix A. This system is a derivation of a simplified and reduced equivalent of the WSCC in the USA. For the data shown in Table 6, the load and generation has been essentially conserved in magnitude whereas the network transmission lines and buses have been drastically reduced; the relaying infrastructure is adapted to this system conditions.

¹ This system was significantly reduced in transmission lines and buses, while keeping essentially the same load and generation amounts.

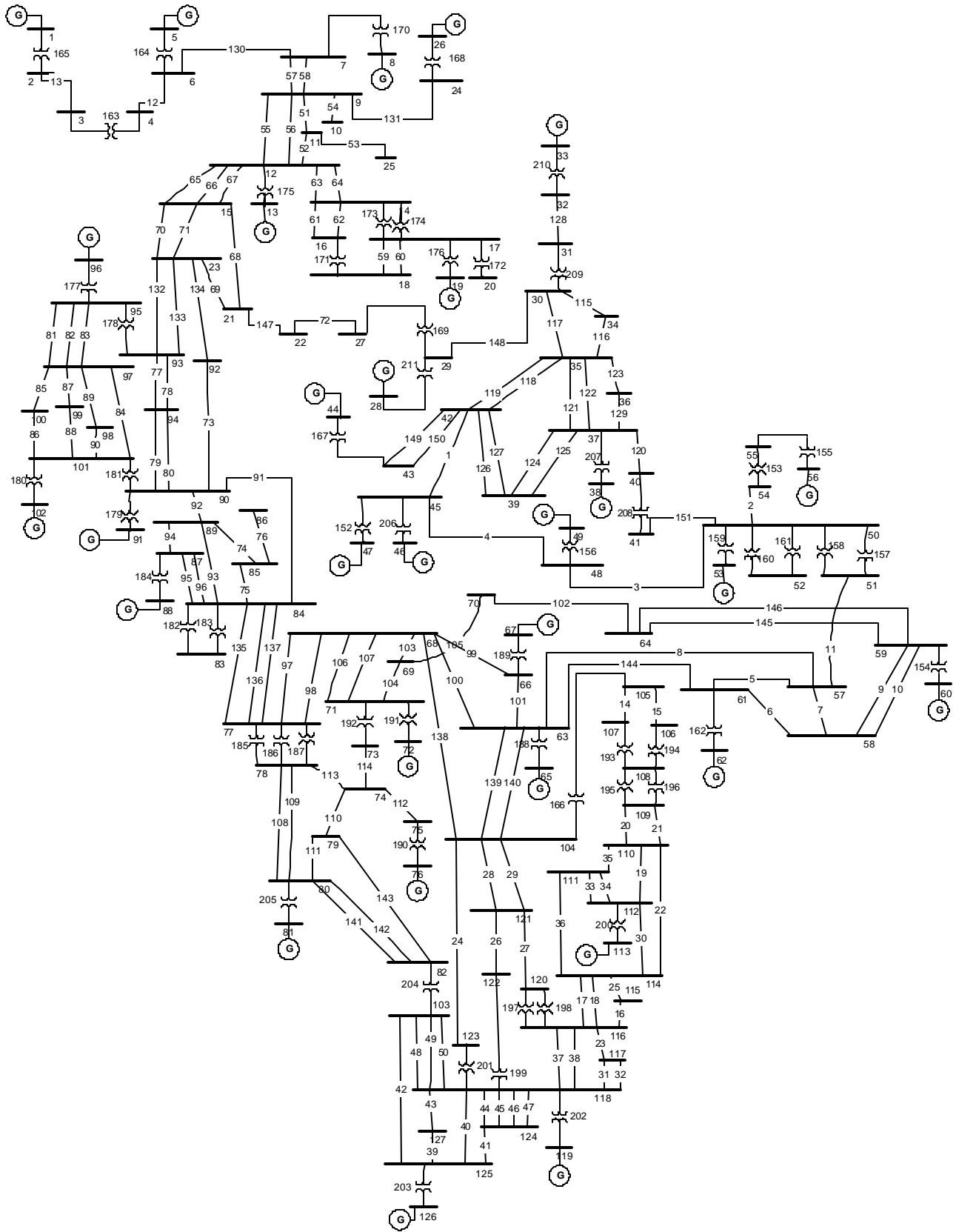


Figure 17: Single Line Diagram of the 127 Bus Sample System.

Table 6: Basic Information of the 127 Bus Sample System.

Number of Branches	211
Number of Buses	127
Load Active Power (MW)	60,785
Load Reactive Power (MVAR)	15,351
Active Generation (MW)	61,411
Reactive Generation (MVAR)	12,332

3.2 Protection Schemes for Power System Components

The relay models available to design the protection system in ETMSP are shown in Table 7.

Table 7 : Relay Models available in ETMSP

Ref	Relay Model	Name	Functionality
1	UFVD	Load Shedding	Shed-Restore load in response to frequency or voltage deviations
2	UFLS	Under Frequency Load Shedding	Shed load in response to frequency deviations
3	VDLD	Voltage Difference Load Shedding	Shed load in response to voltage deviations
4	GUFRR	Generator Under Frequency	Trip a generator if frequency is below a threshold
5	UFLT	Under Frequency Line Tripping	Trip a line if frequency is below a threshold
6	DIST	Distance	Trip a line in response of the apparent impedance
7	RCPR	Rate of Change of Power	Trip a line based on Power Rate of Change
8	SCGR	Series Capacitor Gap	Short Circuit bypasses the Series Capacitor
9	DPDA	Change of Power Change of Angle	Trip a line in response of power / angle changes

From the table above, we can see that the first three relays are related to load shedding in response to frequency or voltage variations. Relays four and five are under-frequency element protection for generators and lines respectively. Relay number six is a distance relay model which reacts to the apparent impedance. Relay seven trips a line based on the rate of change of power in the line. Relay eight is used for series compensated lines, and relay nine was particularly designed to meet the requirements of the Bonneville Power Authority, a sponsor in the development of ETMSP [9].

Table 8 presents the remote commands that ETMSP permits the user to perform in concert with the local relays. These are transfer trips originated upon the operation of a specific local relay. Then, the relay operation may have a combination of local and/or remote operations as defined by the user.

Table 8 : Remote Operation Commands available in ETMSP

Application	Command Description	Code
Network Change	Disconnect a Transmission Line	DLI
	Reconnect a Transmission Line	RLI
	Disconnect a Transmission Line with reclosing	DLR
Network Change	Disconnect a Transformer	DTR
	Reconnect a Transformer	RTR
Generator Change	Disconnect a Generator	GR
	Reduce Generation	GM
	Reduce Mechanical Power of a Generator	GFD
Load Change	Shed Load	SLD
	Restore Load	RLD

Table 7 and Table 8 showed the relay models and remote operation commands available in ETMSP. Next we present the basic protection requirements for power system components and the power system itself (wide area protection) and the scope of the protection system design to be developed.

3.2.1. Protection Schemes for Generators, Buses, and Transformers

Generators

The basic protection requirements for generators are presented in Table 9 which is based on [10] and [6]. For each of the required protections listed in Table 9 we will assess the feasibility of its incorporation in our simulation in ETMSP.

Table 9: General Protection Requirements for Generators.

Ref	Protection Requirement
1	Stator short-circuits
2	Stator ground faults
3	Negative sequence
4	Over-speed
5	Over excitation
6	Loss of excitation
7	Field ground protection
8	Loss of Synchronism
9	Motoring
10	Over Voltage
11	Abnormal Frequencies

From the table above, the protection requirements that are not possible to implement due to lack of relay models are: 1, 2, 3, 5, 6, 7 and 10. With respect to generator over speed, ETMSP has a customizable function that is related to this protection, but is not selective, however. This means that ETMSP halts the complete simulation in the event that a generator speed exceeds a certain speed threshold; unfortunately it does not have the functionality to disconnect that specific generation of the system and continue the simulation.

The protection of generators against loss of synchronism has been applied with different relay designs such as concentric scheme, single-blinder scheme, double lens, double blinder, among others [10]. The relay model “DIST” of ETMSP, includes a concentric scheme that could be implemented against loss of synchronism. The principle of detecting out of step conditions using the concentric scheme is simple; the application, however, is quite complicated since they seldom work as expected, and it is hard to accomplish a complete protection against loss of synchronism with it [8]. To set a relay against a system is not as problematic as to set the relays that detect loss of synchronism conditions between zones in the power system. Because of the lack of other models in the program, and the difficulty of effectively protect a system against loss of synchronism using the concentric scheme relays in the field, we will not implement this protection. In fact, [10] does not mention the concentric scheme as an option to protect a system or generator against loss of synchronism.

Generator motoring occurs when the energy supply to the prime mover is removed, while the generator is still online and it is defined as the flow of real power into the generator acting as a motor [10]. Normally motoring protection is applied using power reverse relays, and its precision depends on the load (prime mover) that the motor has to handle. Motoring protection is normally applied with a time delay; generally 30 to 60 seconds so that it can prevent operations during transient swings, then it is not applicable for our 10 seconds simulation time.

In the protection of generators against abnormal frequencies the primary under frequency protection of steam and gas turbines is applied by using an Under Frequency Load Shedding program. Back-up protection for under frequency conditions is applied using under frequency relays on each generator terminals [10]. Then, under frequency conditions in the first instance are

alleviated by shedding load in the power system. Our relaying infrastructure includes an Under Frequency Load Shedding Program; therefore, the primary protection of the generator under frequency conditions is covered. Inside the simulation environment the primary protection for generators provided by the Under Frequency Load Shedding program (UFLS) suffice the purpose and the back-up protection is not required. This was proved with the results of our simulations, where the UFLS program effectively brought back the frequency to nominal or slightly above nominal conditions.

With respect to over frequency conditions there is no relay model to implement it in ETMSP.

Buses and Transformers

The protection requirements for buses are internal phase or ground faults [6]. Normally differential protection is applied and ETMSP has no models of such kind of relay.

Transformers protection requirements to be considered are: internal phase or ground faults, phase over-current, and over excitation. There are not relay models available in ETMSP to implement these kinds of protection.

3.2.2. Protection Schemes for Transmission Lines

The protection of transmission lines is of main importance in the relaying infrastructure and the ETMSP model that we will use is “DIST,” numbered 6, in Table 7. The protection schemes that we will develop are the Directional Comparison Blocking and stepped distance relays. We have selected these schemes because of its wide application and use; the Directional Comparison Blocking is perhaps the pilot relaying system most used in the USA [7].

Before getting into the details of the settings of the two schemes, the phenomena known as “infeed effect” will be presented; this may have implications in the relay settings as well as in the evaluation of the Regions of Vulnerability as we will see in Chapter Chapter 4.

Infeed Effect: the currents caused by Intermediate Generation Sources

[11] defines “infeed” as a source of fault current between a relay location and a fault location. Figure 18 depicts a part of our test system that was chosen to show the “infeed effect.” As we can see in the figure, between the relay “R” on line 1 and the fault on the line 2 there is a generation station that will contribute to the fault current.

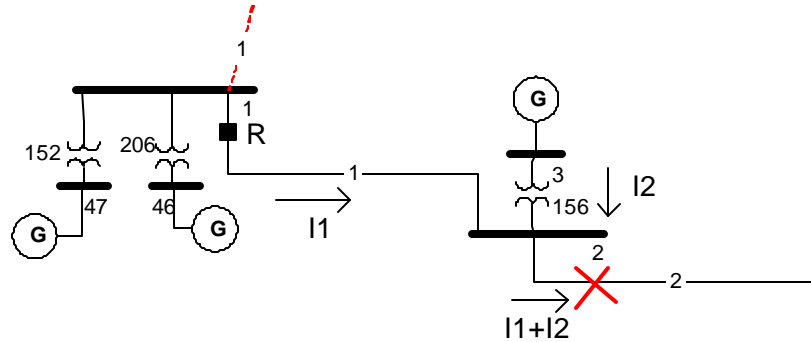


Figure 18: Part of Our Test System used to Describe the Infeed Effect.

This is the nomenclature to be used in the following equations:

- I_1 : Fault Current Contribution of Bus 1 to the Fault; the fault current that is measured by relay “R”
- I_2 : Fault Current Contribution of Bus 2 to the Fault
- R: Distance Relay located on Line 1, Bus 1 side
- V_1 : Voltage during the fault sensed by relay “R”
- Z_1 : Impedance of Line 1
- Z_f : Impedance to the fault in Line 2, measured from Bus 2

Recalling that distance relays react to the apparent impedance which results from its voltage and current inputs, we can express the apparent impedance that the relay “sees” as:

$$Z_{app} = \frac{V_1}{I_1} \tag{1}$$

Analyzing the faulted circuit, we can express the voltage during the fault that the relay “R” will measure from bus 1 as:

$$V_1 = Z_1 I_1 + Z_f (I_1 + I_2) \tag{2}$$

Substituting (2) into (1) we calculate the apparent impedance, and after some simplification we have:

$$Z_{app} = Z_1 + Z_f \left(1 + \frac{I_2}{I_1} \right) \quad (3)$$

Analyzing the circuit of Figure 18 we can see that the impedance to the fault (as measured from the relay location) is $Z_1 + Z_f$ and observing the equation above we can see that the Z_{app} has an additional factor:

$$Z_{infeed} = Z_f \left(\frac{I_2}{I_1} \right) \quad (4)$$

From the equation above we can see that Z_{infeed} depends on:

Z_f : the impedance between the location of the generator and the fault;

$\left(\frac{I_2}{I_1} \right)$: the ratio of the fault current contributions from bus 2 and bus 1 respectively.

Then the apparent impedance that the relay detects from its current and voltage inputs will be different than the real impedance from the relay to the fault location. This has an implication; given an overreaching relay, say Z2 distance relay, which is set following the traditional rule of 120 % its line impedance, the infeed effect will cause the relay to underreach for all faults past the point where infeed occurs [11]. Whether this implication causes a change in the relay settings methodology or not depends on a variety of issues related to the protection scheme under consideration, as we will see next.

Directional Comparison Blocking.

In the Directional Comparison Blocking the relays that define the Region of Vulnerability (the ones that react to the “another condition”) and whose settings will be computed are D_A and D_B ;

see Figure 19. We know that D_B and D_A 's objective is to be able to detect a fault anywhere on the transmission line, and common practices indicate to be set between 120-150 % of the line impedance [7]. [11] states this clearly as: "tripping functions must be set to reach beyond the remote terminal line with a margin, so that they will be able to detect a fault anywhere in the transmission line." Given these guidelines, the directional relays D_B and D_A are set to overreach the protected line by a factor of K_f equals to 0.2. Then, for each of the transmission lines in the sample system, the setting of the relay D_B and D_A is 1.2 times the impedance of the respective line.

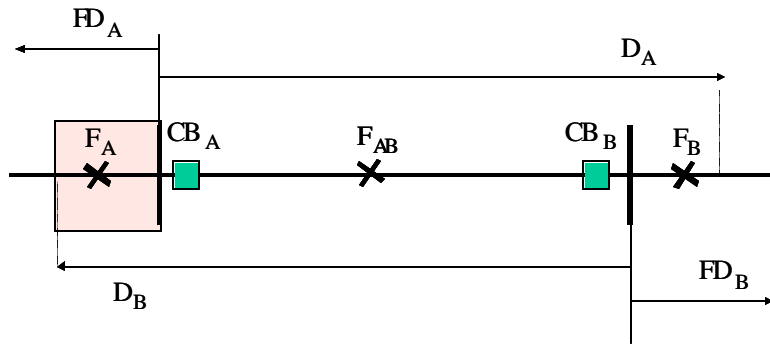


Figure 19: Directional Comparison Blocking, Single Line Diagram

Analyzing Figure 19 we see that there are no generation stations at any bus. In our sample system, however, there are a number of cases with generation stations at the buses where the infeed effect can cause a distance relay to under-reach, consequently reducing the 20% security margin. In any case (with or without infeed effect present) our objective is to cover the 100 % of the line and the infeed effect may be neglected for the setting of this relay considering its role in this particular protection system [8]. Then, for this case, the infeed effect has no implication on the relay settings; we have neglected the possible reduction of security in the protection system design and we have obtained a consistent setting method for the relays. This enables us to obtain a fair comparison of the Regions of Vulnerability in the system.

We will see in Chapter Chapter 4 how the infeed effect has a remarkable implication in the evaluation of the Regions of Vulnerability. Since the infeed effect reduces the security margin, then it reduces the reach of the relay that defines the Region of Vulnerability, D_B and D_A .

Stepped Distance Relays.

A particular characteristic of ETMSP program is that during fault simulations in transmission lines it disconnects the line at the exact moment of the fault inception. This issue was proved with extensive simulations and was confirmed by conversations with the ETMSP program support personnel [12]. The user has no access to the fault current, and therefore the apparent impedance that is seen by the relays that are located in the faulted line. This program characteristic makes impossible for relays to operate for internal faults. Then the Zone 1 function of the stepped distance relay can not be applied, since the program automatically opens the line, and virtually do the job that the relay should be doing [13].

The objective of a Zone 2 distance relay in a stepped distance scheme applied as primary protection is the same as the D_B and D_A in the Directional Comparison Blocking: to protect 100% of the line. Because of this fact, and considering that in both schemes we are using distance relays, we will use the same procedure to set the relays. Then for Z2 distance relays the infeed effect does not have an implication in the relay settings, but affects the evaluation of the Region of Vulnerability as we will see in Chapter Chapter 4.

The implementation of Zone 3 distance relays as remote back up protection has caused controversy among the relaying community. [14] argues that the operation of a Zone 3 relay due to load encroachment was a contributing factor to the degradation of the disturbance on the July 2nd Outage [6] and [15]. Additionally, since the Zone 3 distance relay's reach is much longer than the Zone 2, the simulation could be somehow "biased." The relay settings need to consider the infeed effect and the only way to assure complete coverage is to place faults on each of the remote buses and set the relay according to the apparent impedance as seen from the relay location. Since the infeed effect is considered the relay settings are increased, and consequently the Region of Vulnerability. Meetings were held in order decide upon whether to implement Zone 3 relays or not, and the recommendation was in favor of not to include them for this study [8].

Implementing “DIST” Relay Model in the Test System

The format of the ETMSP relay model “DIST” is presented in Table 10.

Table 10: ETMSP Card for Relay Model “DIST”

DIST					
Bus 1	Bus 2	Cid	Rflag	Rtype	
DT1	DT2	DT3	DT4		
DT5	DT6	DT7	DT8		TRC
Remote Operation Commands					
<p>Nomenclature:</p> <p>DIST: Keyword</p> <p>Bus 1: From Bus Number</p> <p>Bus 2: To Bus Number</p> <p>Cid: Circuit ID</p> <p>Rflag: “C” for Remote Tripping Only, and “ ” for Local and Remote Trip</p> <p>Rtype: “C” for Impedance Relay and “D” for Default Distance Relay</p> <p>DT1: R/X ratio of the line in question</p> <p>DT2: Zone 1 Reach</p> <p>DT3: Zone 2 Reach</p> <p>DT4: Minimum Torque Angle that activates the relay logic, in degrees, Default = 60</p> <p>DT5: Maximum Torque Angle in degrees, Default = 70</p> <p>DT6: Blank</p> <p>DT7: Blank</p> <p>DT8: Relay Time Delay in Cycles</p> <p>TRC: Time Delay for line Reclosing in Cycles.</p>					

The format filled in with the information of relay 3-2 of our sample system is shown in Table 11.

Table 11: Filled in Sample of ETMSP Card for Relay Model “DIST”

DIST					
Bus 1	Bus 2	Cid	Rflag	Rtype	
3	2	1		D	
DT1	DT2	DT3	DT4		
.1	.8	1.2	60		
DT5	DT6	DT7	DT8		TRC
85			28		0

A brief explanation regarding how we filled in the card slots for the relays implemented is presented next. The card slots can be divided as fixed entries and variable entries; the fixed entries are presented in Table 12.

Table 12: Fixed Entries of ETMSP Card for Relay Model “DIST”

Card Slot	Assigned Value
DIST: Keyword	Keyword (ETMSP Required Input)
Rflag: “C” for Remote Tripping Only, and “ ” for local and remote Trip	We used “ ” in order to trip the line if the apparent impedance falls inside the relay operating zone
Rtype: “C” for Impedance Relay and “D” for Default distance Relay	“D,” we used a default distance relay, mho type
DT2: Zone 1 Reach	Zone 1 is not implemented, as previously explained
DT3: Zone 2 Reach	Zone 2 was set to reach 120 % of the line
DT4: Minimum Torque Angle that activates the relay logic, in degrees.	Minimum Torque was set to 60 degrees
DT5: Maximum Torque Angle in degrees	Maximum torque was set to 85 degrees
DT6: Blank	Default Blank slot
DT7: Blank	Default Blank slot
TRC: Time delay for line Reclosing in cycles	Reclosing was not considered ²

The variable slots of the card are presented in Table 13.

Table 13: Variable Entries of ETMSP Card for Relay Model “DIST”

Card Slot	Assigned Value
Bus 1: From Bus Number	The Bus number of the “From” end of the line is filled according to the line of the relay in question
Bus 2: To Bus Number	The Bus number of the “To” end of the line is filled according to the line of the relay in question
Cid: Circuit ID	The Circuit ID is filled according to the line in question.
DT1: R/X ratio	The R/X is filled for each line in question
DT8: Relay Time Delay in Cycles	Zone 2 time delay was set to 28 cycles, (.3 seconds) ³

When implementing the relay settings in the power system, we may encounter problems related to the different impedances of the lines that are located on each side of the bus. Figure 20 shows a simple 3-bus system to explain the problem. The physical length of the lines depicted in the figure below is proportional to the electrical impedance of each of the lines, then it can be seen in the figure that following the relays setting rule (1.2 times the impedance of the line) may result in problems of miss-coordination. The zone 2 setting of the relay 1-2 (shadow area in Figure 20)

² The reclosing operations for the bulk transmission systems are normally time delayed and supervised by power control center personnel [17], then transmission line reclosing does not apply in our simulation.

³ For this time we have taken into account the relay and breaker operating time, and the coordination time of the Zone 2 relay. The 28 cycles correspond to 18 cycles of Z2 delay plus 10 cycles of relay plus breaker time.

overreach the line 2-3, and by doing that it falls under the same operating zone than the zone 2 of the 2-3 relay (arrows in Figure 20). Miss-coordination takes place and may result in two breakers opening for the same fault. Reference [11] states this very clearly: “Zone 2 settings should never over reach any zone 1 relay on a line beyond the remote terminal.”

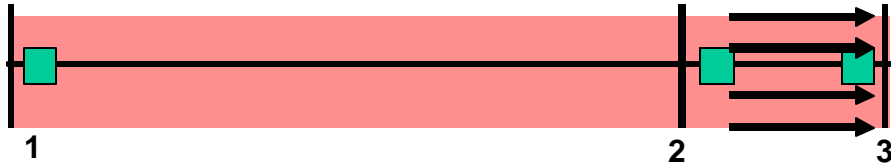


Figure 20: Miss-coordination Problems of Z2 Relays due to Network Characteristics.

Two approaches are suggested to overcome the problem of miss-coordination according to [11]. The first one is to elude zone 2 and incorporate pilot relays utilizing communication channels, and the second is to add additional time delay to the zone 2 that is overreaching. We have selected and implemented the second solution. In our system there are cases in which miss-coordination takes place and additional time delay is required. The additional time delay was chosen as 28 cycles; this time delay was set for coordination purposes and for any actual application it should be verified if this time delay is small enough for the network characteristics regarding critical clearing times.

Table 14 shows the relays that have a higher time delay so that can coordinate with the adjacent lines.

Table 14 : Lines coordinated with additional time delay.

From Bus	To Bus
45	48
58	61
112	110
123	104
122	121
120	121
112	111
112	111
12	14
12	14
37	35
37	35
24	9
21	22
45	42
51	57
112	114
125	127
125	118
125	103
11	12
9	12
9	12
15	12
15	12
90	84
63	68
79	80
63	104
63	104
41	50

Going back to Figure 20, it would be important to mention that in the case there is generation in bus 2 of that figure, the infeed effect will have an impact on the reach of the relay 1-2 and “help” reduce the problem of coordination, i.e., the relay would under-reach. However, the only way to verify the coordination is to place faults and observe if the relay 1-2 can “see” the fault. We have opted to increase the time delay to all the overreaching zones in order to attain coordination among relays.

Our system consists of 151 transmission lines, and implementing two relays per line, we end up with 302 relays. Once the relay formats were ready, we ran a number of simulations in order to validate the relay reaction. We placed faults on lines and verify the apparent impedance seen by

the relay. The relay formats (Input files of ETMSP) are shown in Appendix C. The ETMSP output files were also validated in order to assure that the Input files were read and understood in its totality.

3.3 Wide Area Protection

This section relates to the protection schemes that are designed to protect the power system. We will implement the ETMSP relay model, number 5, “UFLT” of Table 7 to design an under frequency load shedding program. This program is based on [16], which presents general guidelines to be applied in the WSCC system.

3.3.1. Under Frequency Load Shedding

According to [16], the time frame in which an UFLS program operates is around 0.3 to 10 seconds, then it is appropriate for the implementation during the 10 seconds duration of our simulations in ETMSP. During this time frame (0 to 10 seconds) the control systems of the generators governors will not operate (in appreciable levels) and the frequency will change in accordance with the system dynamics.

The methodology to develop a UFLS program suggested by [16] includes a simple and a full network model. In the simple model, the transitory variations on the voltage and its effect on the load are neglected and the frequency is affected solely by the unbalance between load and generation. The full network model uses a transient stability program and takes into account the effect of voltage variations on the load and losses and includes that in the frequency calculation.

The UFLS program development consists in using the simple model and then validating the results in a full detailed model. The validation process depends on specific objectives and it's often the result of a set of simulations in a transient stability program. In this dissertation we have applied the general conclusions and recommendations of [16] to our system. Since the information of the system is not inclusive (there is no information of the load composition and the load criticality), there are not attempts to optimize the design; rather it is a general under

frequency program whose accuracy meet the objective of showing the methodology of Regions of Vulnerability, Areas of Consequence and Index of Severity.

The UFLS program proposed in [16] is presented in Table 15. The program includes 6 under frequency load shedding blocks, indicates the percent of load to shed, the frequency setting at which the load shedding starts, and the tripping time (no intentional time delay).

Table 15 : Characteristics of the Under Frequency Load Shedding Program

Load Shedding Block	% of Customer Load Dropped	Pickup Setting (Hz)	Tripping Time
1	5.06	59.3	None
2	5.62	59.1	None
3	6.18	58.9	None
4	5.9	58.7	None
5	5.6	58.5	None
6	5.3	58.3	None

Reference [16] includes a number of assumptions considered during the program development, among these are: 1) the minimum and maximum permissible dynamic frequency range to be 57.9-61.0 Hz, 2) the minimum separation between frequency steps to be 0.1 Hz, and 3) the maximum operating time of frequency relay and breaker to be 14 cycles. Similarly the main recommendations for the implementation of the program are: a) post disturbance frequencies settle to be above 60 Hz ⁴, b) automatic restoration shall begin no sooner than thirty minutes after the frequency has been restored to levels of 59.95 Hz, and c) to use under frequency relays with definite time characteristic which enable for voltages $\geq .8$ pu.

An important part of the implementation of any UFLS program is the selection of the loads to be shed. Since there is no information regarding load priorities, we will consider the same criticality for all loads. Buses with positive real power will be included (negative is generation) and the

⁴ Governors will operate to adjust the off nominal frequency. If frequency settles above 60 Hz (but less than 60.5 Hz), the reestablishment is easier to implement than if frequency settles below 60 Hz (but above 59.5).

criterion to select the buses to be included in the program is that its MVA value must be larger than 200 MVA.

The system has 104 load buses and the classification of the load according to its representation is shown in Table 16. If a load bus meets the above stated criterion it will be included into the UFLS program and its dynamic behavior as a function of the power system parameter excursions is dictated by the model used to represent the load. The system data contains also load represented as shunt elements and they have been included in the UFLS program.

Table 16 : Classification of the Load According to its Representation.

Load Representation	Number of Buses
Constant Current	62
Constant MVA	22
Constant Impedance	20

Implementation of “UFLT” Relay Model in the Sample System

The format card required by ETMSP for the “UFLT” relay model is presented in Table 17.

Table 17 : ETMSP Card for Relay Model “UFLT.”

UFLT					
Bus 1	Bus 2	Cid	Rflag		
FS	TD	TCB		TRC	
SLD	Bus	Ishunt	%P	%Q	Tdelay
Nomenclature: UFLT: Keyword Bus 1: From Bus Number Bus 2: To Bus Number Cid: Circuit ID Rflag: “C” for Remote Tripping Only, and “ ” for Local and Remote Trip FS: Frequency setting in Hz. Relay operates if frequency remains below the setting for a period specified by TD TD: Time delay in seconds TCB: Relay and Circuit Breaker operation time in cycles TRC: Time delay for line Reclosing in cycles. Remote Operation Commands: SLD: Keyword Bus: Bus to shed load from Ishunt: “1” to shed shunt elements with the load, “0” to leave shunt elements connected (shed only load) %P: Percentage of Real Load to be shed %Q: Percentage of Reactive Load to be shed Tdelay: Time delay to shed the load.					

The format filled in with the data of the relay 2-3 of our test system is shown in Table 18.

Table 18 : Filled in Sample of ETMSP Card for Relay Model “UFLT”

UFLT					
Bus 1	Bus 2	Cid	Rflag		
2	3	1	C		
ES	TD	TCB		TRC	
49.6 ⁵	0.0	14.0		0.0	
Remote Operation Commands:					
SLD	Bus	Ishunt	%P	%Q	Tdelay
SLD	2	1	5	5	0

The “UFLT” relay model is designed to protect power system components against under-frequency. We have not used the local functions of the relay (trip the transmission line), but the remote operation commands (shed load). For a bus that meets the criterion, we select a line that connects it and implement the “UFLT” in that line. The operation of the “UFLT” relay executes the remote operation and the load is shed if the frequency is below a threshold.

A brief explanation regarding how we filled in the card slots for the relays implemented is presented next. The card slots can be divided as fixed and variable entries; the fixed entries are presented in Table 19.

Table 19 : Fixed Entries of ETMSP Card for Relay Model “UFLT.”

Card Slot	Assigned Value
UFLT: Keyword	Keyword (ETMSP Required Input)
Rflag: “C” for Remote Tripping Only, and “ ” for local and remote Trip	C, since we are using Remote Tripping Operation
TD: Time delay in seconds	Time delay is zero
TCB: Relay and Circuit Breaker operation time in cycles	Time for relay and Circuit breaker operation is 14 cycles
TRC: Time delay for line Reclosing in cycles	Reclosing was not considered

⁵ This number is related to the frequency setting and it is the result of multiple simulations in which the under frequency relays were tested; it represents the first frequency setting, 59.3 Hz.

The variable entries of the “UFLT” relay model card are presented in Table 20.

Table 20 : Variable Entries of ETMSP Card for Relay Model “UFLT.”

Card Slot	Assigned Value
Bus 1: From Bus Number	The Bus number of the “From” end of the line is filled according to the line in question.
Bus 2: To Bus Number	The Bus number of the “To” end of the line is filled according to the line in question
Cid: Circuit ID	The Circuit ID is filled according to the line in question
FS: Frequency setting in Hz.	Three steps were implemented and the frequency settings, According to Table 15 are: 59.3 59.1 58.9

For the remote operation commands, all card entries are presented in Table 21.

Table 21 : Remote Command Entries of ETMSP Card for Relay Model “UFLT”

Fixed Entries	
SLD	Keyword (ETMSP required input)
Ishunt	Ishunt was filled with “1,” since the shunt elements are being shed with the load.
%P	5 % is the real load to be shed each step
%Q	5 % is the reactive load to be shed each step
Tdelay	No time delay was added to shed the load.
Variable Entries	
Bus :	The specific bus in which the load is being shed

Once the relay formats were ready, we ran a number of simulations in order to validate the relay reaction. We simulate cases affecting the load/generation balance and assure that the under-frequency relays were responding appropriate and tripping only if the frequency went below the setting threshold.

The relay formats (Input files of ETMSP) are shown in Appendix C. The ETMSP output files were also validated in order to assure that the Input files were read and understood in its totality. Forty three under-frequency relays were set on each frequency step and the buses in which the load is shed are shown in Figure 21.

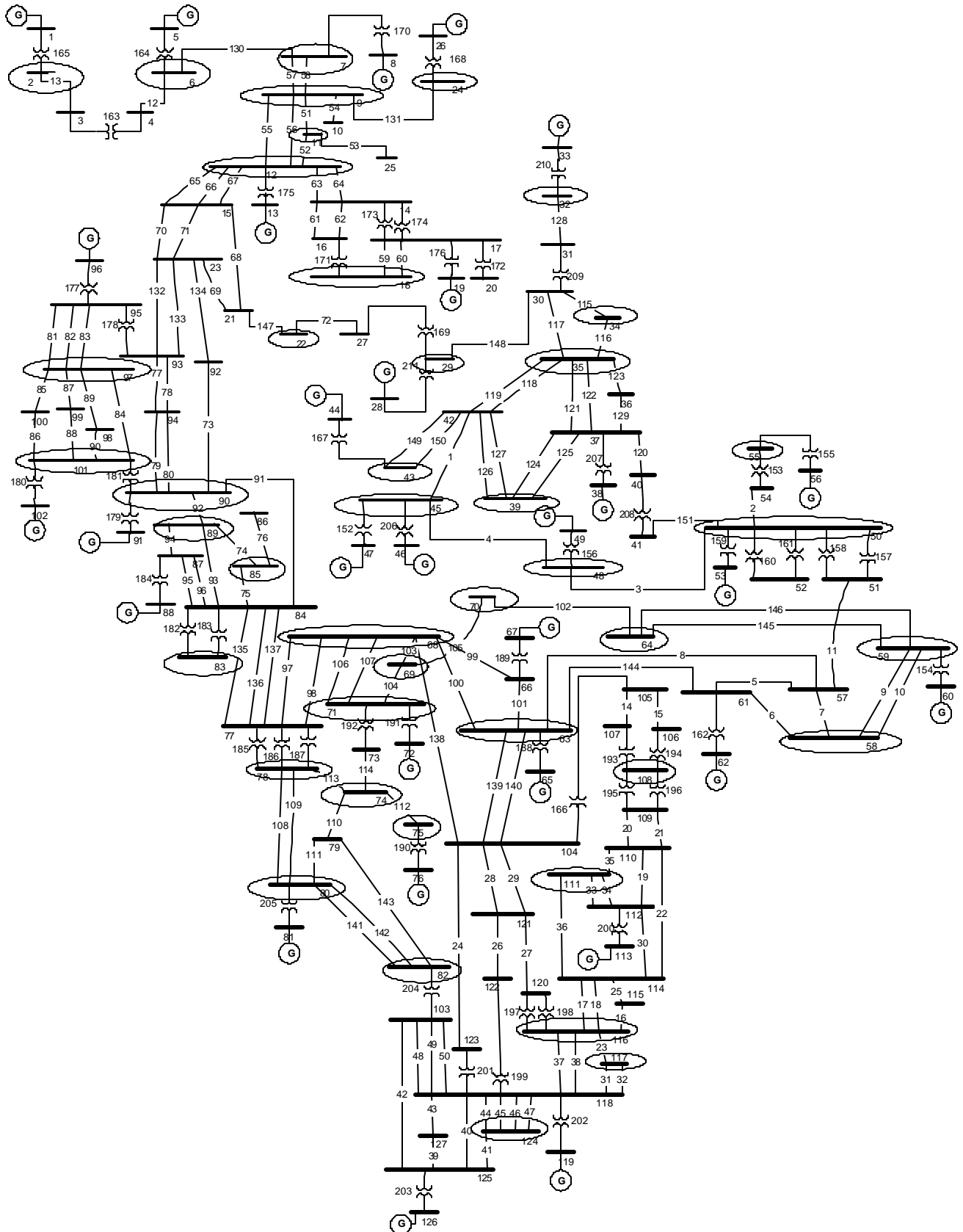


Figure 21: UFLS Relays Localization in the Test System

3.3.2. Under Voltage Load Shedding and Generation Rejection

Under Voltage Load Shedding has been used as a remedy to attack the voltage collapse problem in power systems. The phenomena of voltage collapse is substantially different in nature when compare to frequency. It is well know that frequency has the characteristic of being essentially the same over wide geographical areas; on the other hand, voltage is a local parameter and its profile varies among geographical regions. Reference [17] states that the development of an UVLS scheme should include time delays in order to prevent tripping the load under transient variations of the voltage. This time delays are from 3 to 10 seconds, and due to the fact that the duration of our simulation is 10 seconds, an UVLS will not be developed herein.

We have implemented generation rejection schemes in our simulations in order to keep the stability of the system. This implementation was performed for faults applied near generation stations in which because of the contingency, the machine loses the capacity to deliver power to the system. Generation rejection was considered in the computation of the Index of Severity. In cases in which, due to relaying actions, a generation station is left without transmission capacity, the generation lost is also considered.

Chapter 4. Quantitative Evaluation of Regions of Vulnerability

This chapter refines the methodology for the evaluation of the Region of Vulnerability. The modifications in the dimension of the Region of Vulnerability have “per unit” as the reference. The first change is to bring the Region of Vulnerability from per unit to ohms; subsequently, the dimension of the Region of Vulnerability is modified from ohms to kilometers. The benefits obtained from these changes in dimension are demonstrated.

The representation of the Region of Vulnerability in the power system is then analyzed. The novel concept of *Validation of the Region of Vulnerability* is introduced and the assurance of the operation of the relay is a fundamental issue in this validation. The strong impact of the infeed currents is highlighted. The Regions of Vulnerability for the five simulation cases to be presented in chapter 5 are evaluated based on the refined methodology.

It is important to mention that the results that are obtained are applicable for this system; a different outcome may result if the methodology developed in this chapter is applied to another system.

4.1 Refinement of the Methodology: Dimension of the Region of Vulnerability

This section presents the evaluation of the Regions of Vulnerability in different dimensions: per unit, ohms, and kilometers. The benefits from the changes in dimension are demonstrated.

4.1.1. Evaluation of the Region of Vulnerability in Per Unit

This section presents the quantitative evaluation of the Regions of Vulnerability for the directional comparison blocking scheme. The settings developed in Chapter Chapter 3 are employed and the IEEE-39 bus sample system serves as framework for this development (see Figure 22). The details of the IEEE-39 bus system are included in Appendix C.

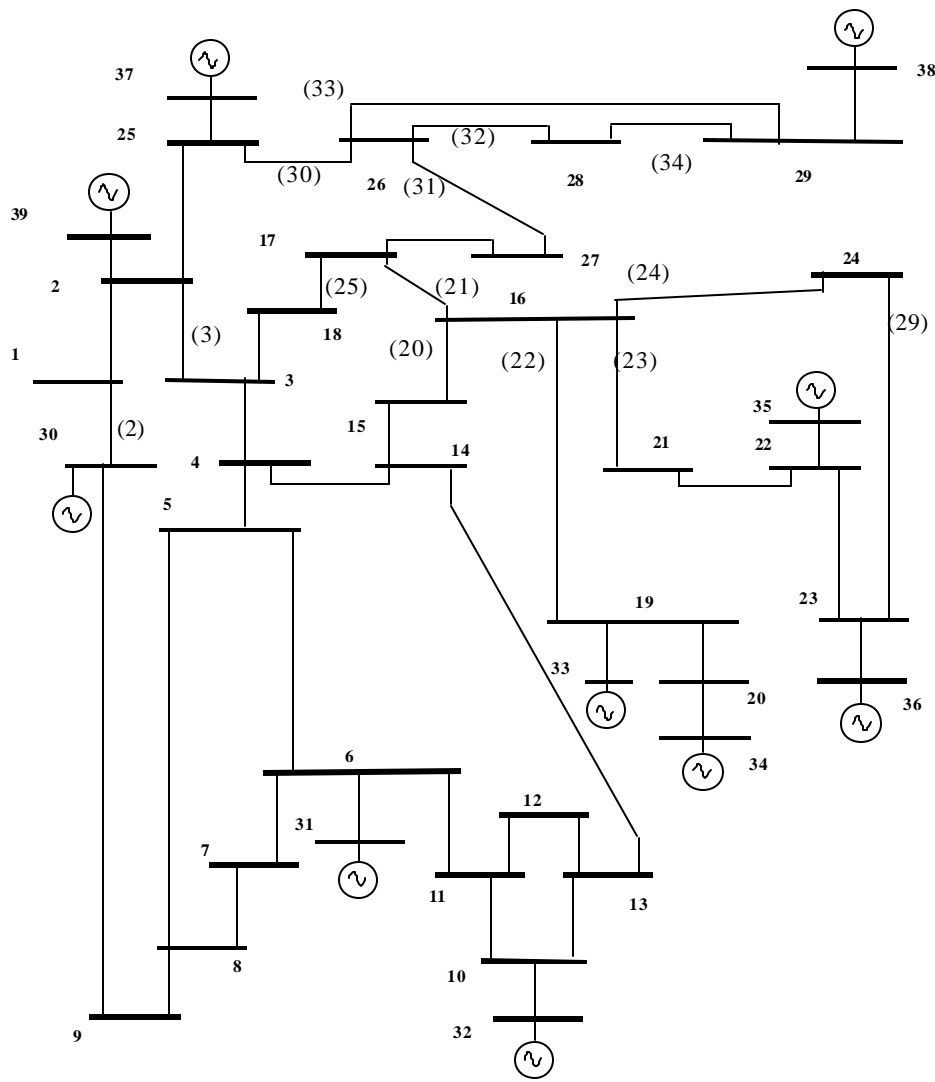


Figure 22: Single Line Diagram of the IEEE-39 Bus System.

Due to the similarities of the hidden failure modes of the Directional Comparison Blocking with the Zone 2 distance relay, the results presented in this chapter apply to the Z2 distance relay as well. The hidden failure modes were presented in Table 5; for the directional comparison blocking is number 1 and for the Z2 distance relay is number 16.

The equation to compute the Region of Vulnerability in per unit is:

$$RV_{PerUnit} = (Z_{Line} * Kf) * (Bus_{Density} - 1)$$

(5)

Where:

$RV_{PerUnit}$	Region of Vulnerability, in Per Unit
Z_{Line}	Impedance of Line, in Per Unit
K_f	$K_f = 0.2$, as defined in Chapter Chapter 3
$BusDensity$	Number of Transmission Lines or Transformers at the bus in which the relay that defines the Region of Vulnerability (the one that reacts to the “another condition”) is pointing to. See Figure 23.

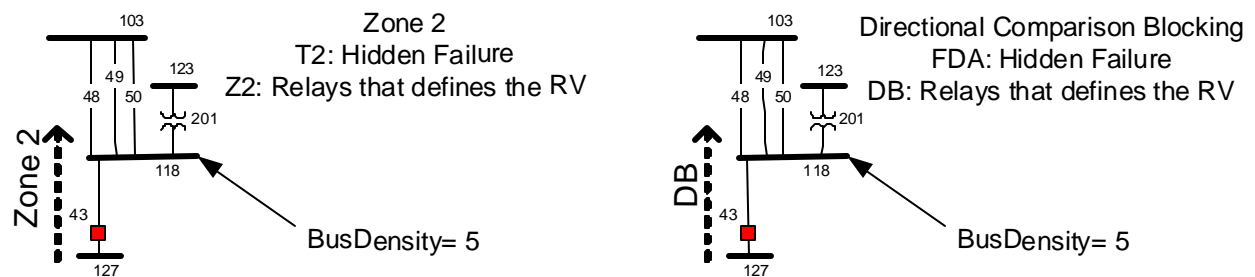


Figure 23: The term Bus Density applied in a segment of the power system for the Directional Comparison Blocking and the Z2 distance relay.

As we can see in Figure 23, the bus density is related to the number of power system elements that are connected to the bus in which the relay that defines the Region of Vulnerability (the one that reacts to the “another condition”) is pointing to. The Directional Comparison Blocking and the Z2 distance relay are presented in the figure above and in this case the bus density is five.

From equation (5) we can see that the factors that affect the evaluation of the Region of Vulnerability are the impedance of the line in per unit, the value of “ K_f ” which is related to the relay settings, and finally the Bus Density. See in equation (5) that the Bus Density is adjusted to (Bus Density - 1) to avoid including the line whose Region of Vulnerability is being calculated.

Equation (5) is subject to a restriction which is presented with Figure 24. The restriction is related to the ratio of the impedance of the protected line with respect to the impedance of the transmission lines or transformers connected to each bus of the protected line. Applying this statement to the relay “I” of Figure 24, the restriction is related to the ratio of the impedance of the line 1 (Z1) with respect to the impedance of the line 2 (Z2). Similarly, for relay “J” the ratio of Z1 with respect to Z3.

There are specific cases in the power system in which the value of the transmission line impedance multiplied by the factor “ K_f ” is larger than the impedance of the adjacent transmission line or transformer. This means that the setting of the relay and therefore the magnitude of the Region of Vulnerability to be distributed overreaches the adjacent line or transformer and extends to other elements connected downstream.

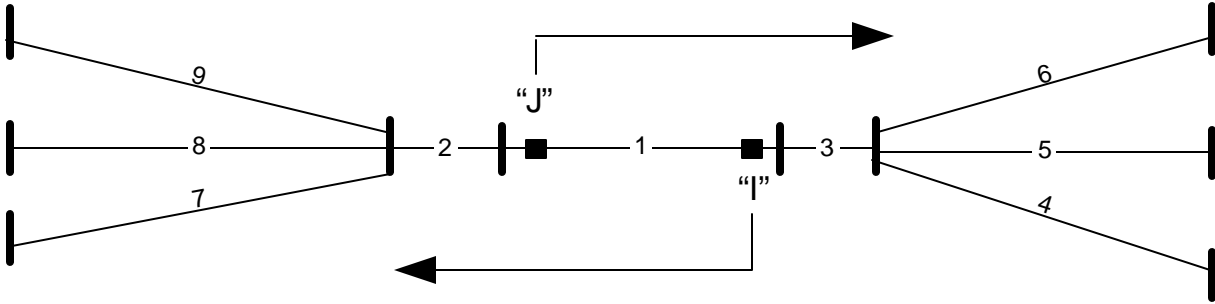


Figure 24: The Restriction applied in a simple transmission system.

Applying this to Figure 24 for the relay “I”, the Region of Vulnerability would extend over element 2 and elements “7”, “8”, and “9;” similarly, for the relay “J,” the Region of Vulnerability covers completely over element “3” and over elements “4”, “5”, and “6.” The Region of Vulnerability expands until the point the value $(Z_1 * K_f)$ is distributed along the elements connected downstream.

Based on this for relay “I” in Figure 24 the Region of Vulnerability covers elements “7”, “8”, and “9” if $K_f * Z_1 > Z_2$. Similarly, for the “J” relay this occurs if $K_f * Z_1 > Z_3$.

Then if we define:

Z_a as the impedance of the line whose Region of Vulnerability is being evaluated, in per unit, and Z_b as the impedance of the adjacent line, in per unit,

Equation (5) is restricted to the following:

$$K_f * Z_a \leq Z_b$$

(6)

Equation (5) is accurate enough and it can be used to compute the Region of Vulnerability in per unit for the lines that do not violate the restriction. The restriction applies to both ends of each line. For the cases in which the restriction is violated, the Region of Vulnerability must be re-computed and include the elements or portions of elements until the value $Z_a * K_f$ is represented along the downstream elements. Clearly, all of this is a function of the K_f that it was used in the protection system, and the network topology of the system.

As we have mentioned, Figure 24 applies for transmission lines and transformers. The inclusion of the transformers in the calculation of the Region of Vulnerability is conceptually correct. If there is a fault inside the transformer within the reach of the D_B or Z_2 , the transformer breakers should operate by its differential protection and the line with the hidden failure would be incorrectly disconnected. This also applies to generators; however, the generators would enter in the evaluation of the Region of Vulnerability only if the transformer is overreached.

Figure 25 shows the evaluation of the Regions of Vulnerability of the directional comparison blocking scheme for the thirty-four transmission lines applied in the IEEE-39 bus sample system. The “I” and “J” letters are used to differentiate the two Regions of Vulnerability of each transmission line. The numbers shown in the horizontal axis are the transmission line numbers of the IEEE-39 bus sample system one-line diagram, which is included in Figure 22. At a glance, it can be seen that the Region of Vulnerability magnitude of a particular line depends on the D_B and D_A relay settings, which are calculated based on the transmission line impedance. The magnitude of the biggest Region of Vulnerability is 0.0376 per unit, which is derived from the transmission line 33. This line has the largest impedance, with a value of 0.0627 per unit.

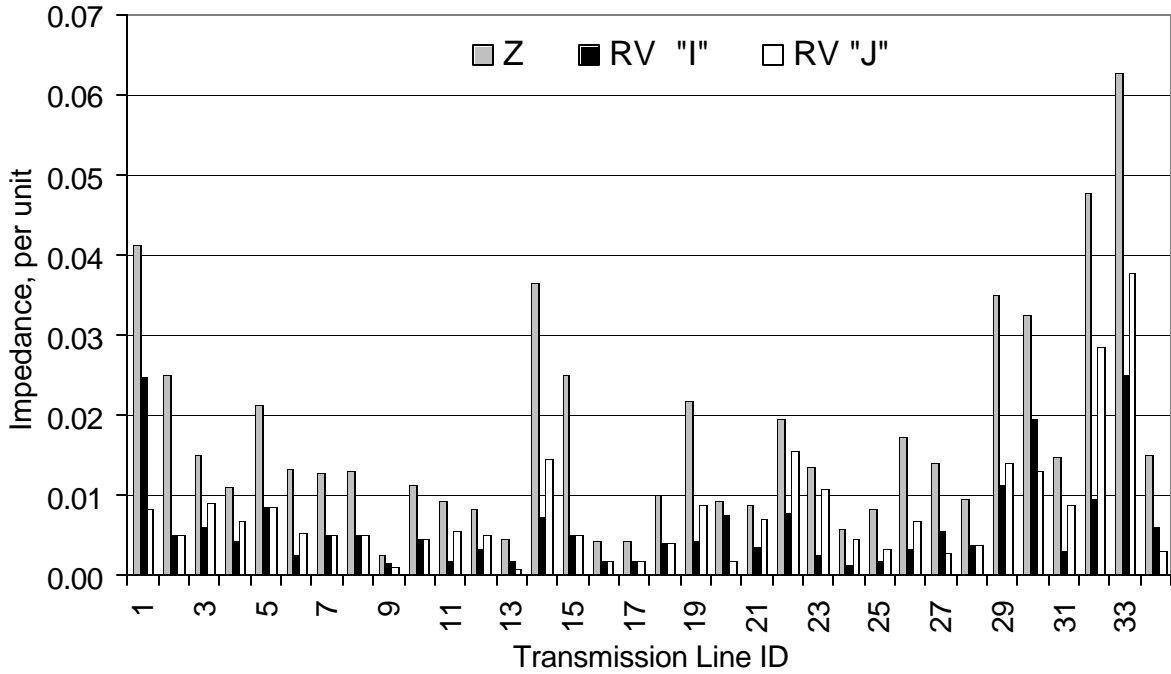


Figure 25: Transmission Lines and Their Respective Region of Vulnerability.

The factors different from the transmission line D_A and D_B relay settings, which also influence the Region of Vulnerability evaluation, can be derived from Figure 26. This figure presents for a number of transmission lines, the ratio of the Regions of Vulnerability over their respective impedance.

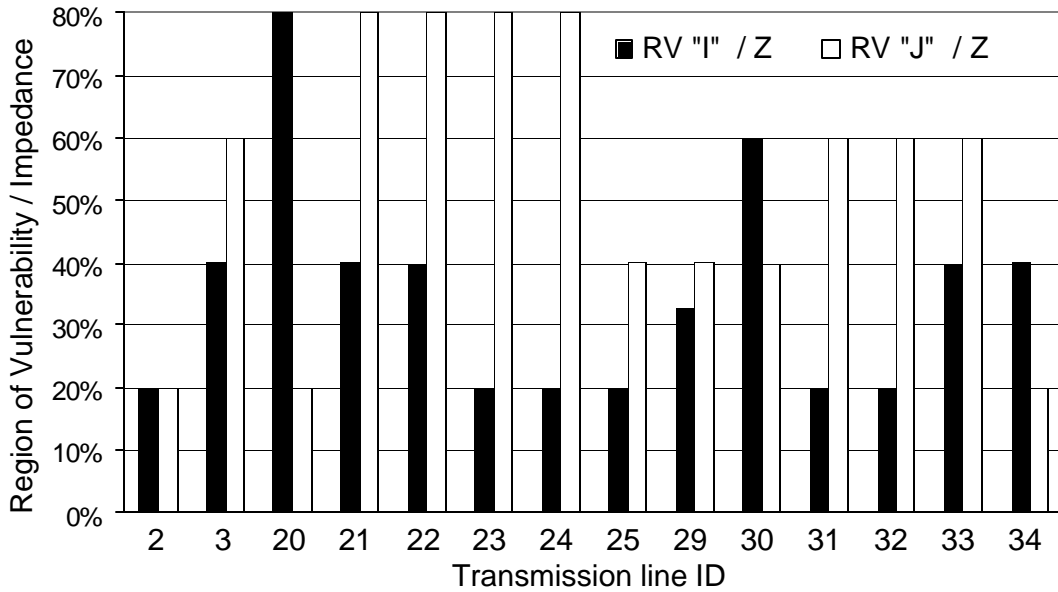


Figure 26: Ratio of Region of Vulnerability Over Transmission Line Impedance.

As mentioned earlier, one of the factors that influence the evaluation of the Region of Vulnerability for a specific transmission line is the Bus Density. Figure 26 shows that the Region of Vulnerability-impedance ratios varies from 0.2 up to 0.8. These values are related to the number of lines or transformers connected to the bus at each end of the transmission line, previously defined as Bus Density.

The minimum ratio shown in Figure 26 is 0.2 and indicates that the bus to which the transmission line is connected has a bus density equal to 2, i.e., two power system elements, either transmission lines or transformers connected to that bus. The Region of Vulnerability-impedance ratio equal to 0.2 comes from the previous assumption of the value “ K_f ”, and indicates that the Region of Vulnerability has only one path to get distributed, which could be either a transmission line or a transformer. In Figure 26, the transmission line with ID number 2 is an example of a line with a Region of Vulnerability-impedance ratio equal to 0.2. This transmission line and its bus density at each end can be seen in Figure 22.

In a similar analysis, there are transmission lines that have a Region of Vulnerability-impedance ratio that is a multiple of 0.2. This means that at least in one of the transmission line ends, the Region of Vulnerability has more than one path to get distributed; therefore, the bus density of at least one of the buses is greater than 2. For the IEEE-39 bus sample system, the maximum bus density is equal to 5, meaning that the Region of Vulnerability finds four paths to get distributed and the Region of Vulnerability-impedance ratio is equal to 0.8. Transmission lines with ID numbers 20, 21, 22, 23, and 24 are examples of this case. Figure 26 shows other lines whose Region of Vulnerability-impedance ratio falls in another multiple of the value 0.2, and smaller than 0.8. These lines may be identified in Figure 22.

The restriction presented in equation (6) and Figure 24 was considered in the Region of Vulnerability evaluation and Figure 26 shows the transmission line 29 as an example of this case. As can be seen in the figure, the Region of Vulnerability-impedance ratios of transmission line 29 are 0.40 and 0.33. The value of 0.33 is the result of a Region of Vulnerability that overreached a transmission line, in this case line 24. The fact that the value of 0.33 is not a multiple of K_f (0.2) confirms that the evaluation of this Region of Vulnerability included

fractions of other transmission lines downstream, in this case lines 20, 21, 22, and 23. See Figure 22.

4.1.2. Evaluation of the Region of Vulnerability in Electrical Quantities

The 127 bus sample system presented in Figure 27 serves as framework for this development.

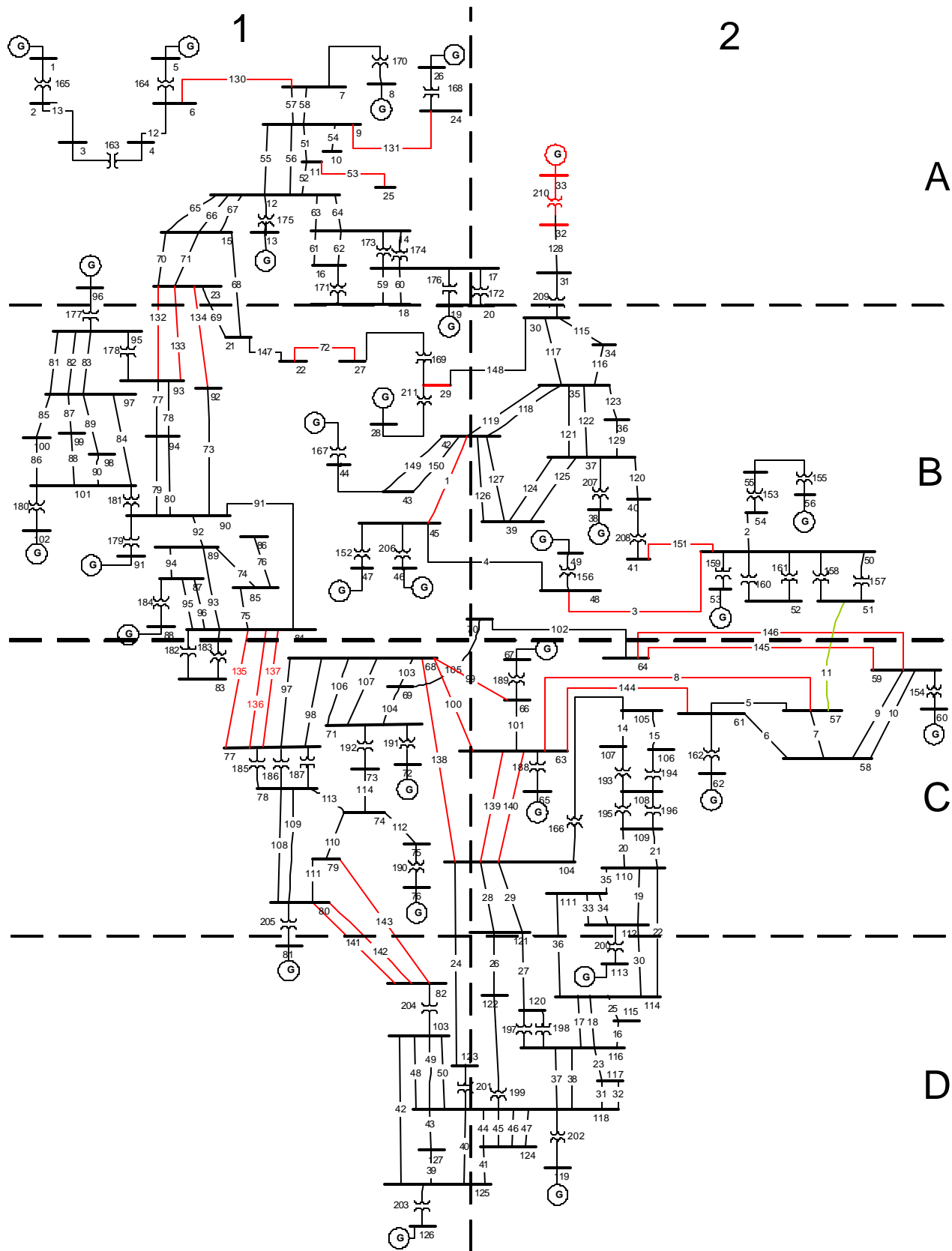


Figure 27: Single Line Diagram of the 127 Sample System.

The equation to compute the Regions of Vulnerability in per unit is presented once again:

$$RV_{PerUnit} = (Z_{Line} * Kf) * (Bus_{Density} - 1) \quad (5)$$

Setting aside for the moment the restriction to this equation, i.e., assuming a network topology that complies with the $Kf * Z_a \leq Z_b$ inequality for the transmission lines, we can re-analyze equation (5) with a deeper look at the Z_{ine} variable. Z_{ine} is the impedance of the line and it is expressed in per unit; we will refer Z_{ine} as Z_{pu} and it can be expressed as:

$$Z_{pu} = \frac{Z_{Ohms}}{Z_{Base}} \quad (7)$$

Where:

Z_{Ohms} Impedance of the line in Ohms
 Z_{Base} Impedance Base

Z_{Base} is expressed as:

$$Z_{Base} = \frac{kV_{Base}^2}{MVA_{Base}} \quad (8)$$

Where:

MVA_{Base} Base MVA
 kV_{Base} Base Voltage

Substituting (8) into (7) we obtain:

$$Z_{pu} = \frac{Z_{Ohms}}{(kV_{Base}^2 / MVA_{Base})} \quad (9)$$

Equation (9) deserves further analysis. Considering the normal practice of setting MVA_{Base} to a constant value of 100 MVA, the remaining variables in the equation are Z_{Ohms} , and kV_{Base} .

Directly from equation (9) we can see that the impedance calculation in per unit depends on the base voltage. The $(kV_{Base}^2 / MVA_{Base})$ factor for the different voltage levels of our sample system are shown in Table 22.

Table 22 : Factors $(kV_{Base}^2 / MVA_{Base})$ for the different Voltage Levels of the Sample Power System

Nominal Voltage (kV)	$(kV_{Base}^2 / MVA_{Base})$ Factor
200	400
230	529
287	824
345	1190
500	2500

Clearly, from Table 22 we can observe that the $(kV_{Base}^2 / MVA_{Base})$ factors are substantially different for each voltage level. Then by using equation (9) we could obtain smaller per unit impedance values for larger transmission line nominal voltages. Recalling that the impedance of the line is an important factor in the evaluation of the Region of Vulnerability (as we saw in Figure 25), then we could obtain smaller Region of Vulnerability for larger transmission line voltages.

When comparing the Regions of Vulnerability that are represented in parts of the power system with different voltages, we face a problem of not providing a fair comparison given the fact that the Z_{Ohms} is affected by the $(kV_{Base}^2 / MVA_{Base})$ and this is dependent of the voltage base in question. In addition to this, the Region of Vulnerability expressed in per unit it has an inverse relationship with the transmission line criticality. A number of factors related to the line criticality are: voltage level, line length, proximity to generation sources, among others [11]; critical transmission lines are in general built having larger voltages.

In order to verify the above mentioned statement in the 127 bus sample system, Table 23 presents the transmission lines with the twenty greatest impedances in *per unit*.

Table 23: Transmission Lines with the Twenty Greatest Impedances in *Per Unit*

kV_{BASE}	Z_{pu}	Rank
200	0.2768	1
200	0.2069	2
200	0.1712	3
200	0.1626	4
345	0.1371	5
200	0.1150	6
345	0.1104	7
200	0.1021	8
230	0.0971	9
200	0.0937	10
345	0.0883	11
287	0.0798	12
287	0.0798	13
500	0.0740	14
230	0.0708	15
500	0.0701	16
200	0.0677	17
345	0.0676	18
200	0.0673	19
200	0.0662	20

Out of the twenty transmission lines listed in Table 23, Table 24 shows the classification of those transmission lines according to its voltage level. As we can see, the majority of the transmission lines are of 230 kV or below (60%); there are ten transmission lines of 200 kV, four transmission lines of 345 kV, and only *two* 500 kV transmission lines (10%).

Table 24: Classification of the Twenty Greatest Transmission Lines According to its Voltage level; Impedances in Per Unit

BasekV	Number of Transmission Lines	Presence Percentage
200	10	50%
230	2	10%
287	2	10%
345	4	20%
500	2	10%

Converting all transmission lines impedances in the sample power system to its ohmic value, we present now in Table 25 the transmission lines that have the twenty greatest impedances in *Ohms*.

Table 25: Transmission Lines with the Twenty Greatest Impedances in *Ohms*

kV_{BASE}	Z_{Ohms}	Rank
500	185.0083	1
500	175.2186	2
345	163.2309	3
345	131.4429	4
200	110.7182	5
345	105.1268	6
500	94.31570	7
500	94.02338	8
200	82.74906	9
500	82.74521	10
500	80.92521	11
345	80.44303	12
500	77.64543	13
500	74.45708	14
500	74.45708	15
345	71.91987	16
500	69.64235	17
200	68.47553	18
500	67.38220	19
287	65.70647	20

Doing a similar analysis, Table 26 shows the classification of the transmission lines impedances in Ohms according to its voltage level. As we can see, the majority of the transmission lines are now of 500 kV, having 11 transmission lines of this voltage level. There are five transmission lines of 345 kV and only three 200 kV transmission lines.

Table 26: Classification of the Twenty Greatest Transmission Lines According to its Voltage level; Impedances in Ohms

BasekV	Number of Transmission Lines	Presence Percentage
500	11	55%
345	5	25%
287	1	5%
200	3	15%

The results of the tables are a proof of the previous statement in which we mentioned that the use of equation (9) may have a tendency to obtain smaller per unit impedance values for larger transmission line nominal voltages. The comparison of the results of Table 24 and Table 26 clearly shows that by changing the impedance from *per unit to ohms*, produces that the majority of first twenty greatest impedances in the system are 500 kV, where as with the values in *per unit*, we had the majority of 230 kV and below.

Given the previous statement and having seen the results that back it up, *we propose to use the impedance in ohms rather than in per unit*. The equation to compute the Region of Vulnerability in Ohms is expressed as:

$$RV_{Ohms} = (Z_{Line} * Kf) * (Bus_{Density} - 1) * (Z_{Base}) \quad (10)$$

Where:

RV_{Ohms}	Region of Vulnerability, in Ohms
Z_{Line}	Impedance of Line, in Per Unit
Kf	$Kf = 0.2$
$Bus_{Density}$	Number of Transmission Lines or Transformers at the bus in which the relay that defines the Region of Vulnerability is pointing to.
Z_{Base}	Impedance Base

In equation (10) we multiply by Z_{base} in order to use the impedance of the line in ohms.

The same restriction, $Kf * Z_a \leq Z_b$ applies to this equation.

A number of examples that show the improvement in calculating the Region of Vulnerability in Ohms rather than in per unit will be shown later in section 4.1.4.

4.1.3. Evaluation of the Region of Vulnerability in Physical Quantities

Previous section showed that by changing the dimension of the Region of Vulnerability to Ohms, the problem of impedances in per unit was corrected. The equation of the Region of Vulnerability in Ohms is presented once again as:

$$RV_{Ohms} = (Z_{Line} * K_f) * (Bus_{Density} - 1) * (Z_{Base}) \quad (10)$$

This section describes the representation of the Regions of Vulnerability in different segments of the power system. Analyzing equation (10), we can see that it still presents problems when comparing the Region of Vulnerability in transmission lines with different voltage levels. To leave the Region of Vulnerability in ohms, would erroneously assume that the ohms per unit of length are a constant value regardless of the nominal voltage. Typical values of ohms per kilometer for different voltage levels are shown in Table 27 [18]. As we can see, the Ohms per kilometer, “OKM_{factor},” diminishes with increments in the voltage level; then there is the need of a modification to equation (10) to take in consideration the different values of Ohms per unit of length that each voltage level presents.

Table 27: Typical Values for Resistance and Reactance in Ohms/Km for Different Voltage Levels

Parameter	Nominal Voltage 230 kV	Nominal Voltage 345 kV	Nominal Voltage 500 kV
Resistance (Ohms/km)	.050	.037	.028
Reactance (Ohms/km)	.488	.367	.325
OKM _{factor} = $\sqrt{R^2 + X^2}$.490	.369	.326

In order to calculate the Regions of Vulnerability in Kilometers, i.e., the physical areas, we have used typical values of ohms per unit of length for the transmission line voltage. Furthermore, we have assumed that all lines of the same voltage level connected to the bus have the same ohms per unit of length. This is an approximation and a more accurate computation could be obtained with the specific data of the line parameters according to its design.

When representing the Regions of Vulnerability in Kilometers a particular consideration with respect to transformers and generators must be taken into account. As we described previously, the inclusion of generators and transformers in the evaluation of the Region of Vulnerability is conceptually correct. The problem lays, however, in the representation of the physical area. Unlike transmission lines, the representation of the Region of Vulnerability in transformers would be confined in the substation switchyard. Practically, the physical area would be the whole transformer bank or a part of the transformer windings, and this could be negligible when compared with the area in which the Region of Vulnerability is represented over transmission lines. We are primarily interested in the representation of the Region of Vulnerability in kilometers of transmission lines. The exclusion of transformers has minimal impact in this calculation and therefore we have excluded the transformers or generators in the computation of the Region of Vulnerability in Kilometers.

The equation to compute the Region of Vulnerability in Kilometers is expressed as:

$$RV_{Km} = (Z_{Line} * Kf) * (BUS_{Density-TxsOff} - 1) * (Z_{Base}) * (OKM_{factor}^{-1}) \quad (11)$$

Where:

RV_{Km}	Region of Vulnerability, in Kilometers
Z_{Line}	Impedance of Line, in Per Unit
Kf	$Kf = 0.2$
$BUS_{Density-TxsOff}$	Bus Density excluding transformers
Z_{Base}	Impedance Base
OKM_{factor}	Ohms per Kilometer Factor

The same restriction, $Kf * Z_a \leq Z_b$ applies to this equation.

We multiply by (OKM_{factor}^{-1}) in order to represent the impedance as a physical area in Kilometers, and therefore represent the Region of Vulnerability in Kilometers. Note that in the new factor $\{BUS_{Density-TxsOff}\}$ the transformers have been eliminated leaving only transmission lines.

When representing the Regions of Vulnerability along the system having different transmission lines voltages, the best dimension for the Region of Vulnerability is *Kilometers*. A number of examples that show the improvement in calculating the Region of Vulnerability in Kilometers rather than in Ohms is shown next.

4.1.4. Comparison of the Regions of Vulnerability in Different Dimensions

The next examples compute the Region of Vulnerability in the different dimensions and show the improvements caused by changing from per unit to Ohms and from Ohms to Kilometers. The cases presented next do not violate the restriction equation (6).

Figure 28 shows the representation of the Region of Vulnerability of the directional comparison blocking scheme applied to the transmission line number 73. The single line diagram of the sample power system was included in Figure 27 and this portion of the system is located in the B-1 section. The D_B relay is shown in the figure with the square and it is set to 120 % the impedance of the line, as mentioned in Chapter Chapter 3. The power system elements in which the Region of Vulnerability is represented are marked with a circle, as shown in the figure.

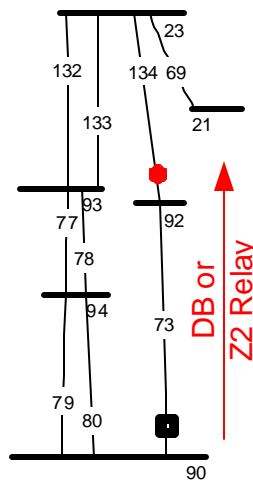


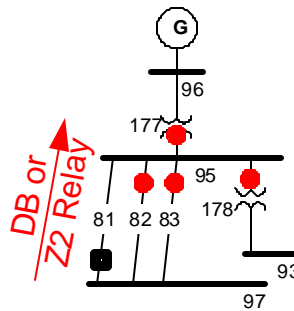
Figure 28: Representation of the Region of Vulnerability, Case Line 73

The Region of Vulnerability expressed in Per Unit, Ohms, and Kilometers is shown in Table 28.

Table 28 : Magnitude of the Region of Vulnerability, Case Line 73, in Per Unit, Ohms, and Kilometers.

Relay Setting	$Z(73)*1.2 = 0.0135$
Bus Density	2
Region of Vulnerability Per Unit	$Z(73)*.2 = 0.0022$
Region of Vulnerability Ohms	5.60 Ohms
Region of Vulnerability Km	17.18 Km

Figure 29 shows the representation of the Region of Vulnerability of the directional comparison blocking scheme applied to the transmission line number 81. This portion of the system is located in the B-1 coordinates (see Figure 27). The D_B relay is shown in the figure with the square and is set to 120 % the impedance of the line. The power system elements in which the Region of Vulnerability is represented are marked with a circle, as shown in the figure. As we can see, in this case the power system elements include transmission lines as well as transformers.

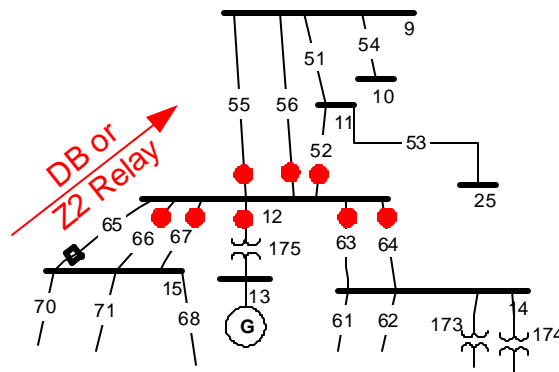
**Figure 29: Representation of the Region of Vulnerability, Case Line 81**

The Region of Vulnerability expressed in Per Unit, Ohms, and Kilometers is shown in Table 29. As previously mentioned, in this case a problem exists with the representation of the physical area when transformers are present. The Region of Vulnerability expressed in Km has been calculated for the transmission lines only.

Table 29: Magnitude of the Region of Vulnerability, Case Line 81, in Per Unit, Ohms, and Kilometers.

Relay Setting	$Z(81) * 1.2 = 0.0812$
Bus Density	5
Region of Vulnerability Per Unit	$Z(81) * .2 * 4 = 0.0542$
Region of Vulnerability Ohms	21.66
Region of Vulnerability Km	22.08 Km

Figure 30 shows the representation of the Region of Vulnerability of the directional comparison blocking scheme applied to the transmission line number 65. This portion of the system is located in the A-1 coordinates (see Figure 27).

**Figure 30: Representation of the Region of Vulnerability, Case Line 65**

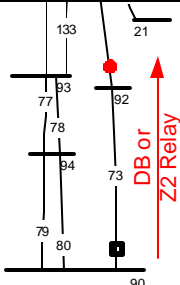
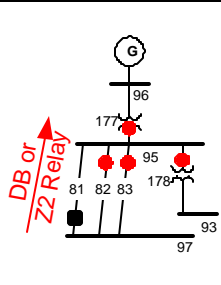
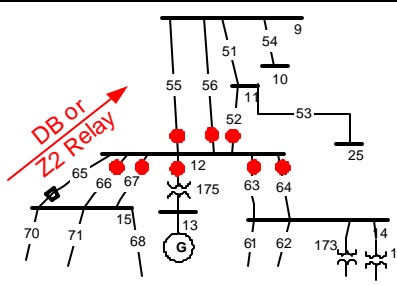
The Region of Vulnerability expressed in Per Unit, Ohms, and Kilometers is shown in Table 30. Since transformers are present, the Region of Vulnerability expressed in Km has been calculated for the transmission lines only.

Table 30 : Magnitude of the Region of Vulnerability, Case Line 65, in Per Unit, Ohms, and Kilometers.

Relay Setting	$Z(65)*1.2 = 0.0170$
Bus Density	9
Region of Vulnerability Per Unit	$Z(65)*.2 *8 = 0.0226$
Region of Vulnerability Ohms	56.53
Region of Vulnerability Km	151.65 Km

Table 31 shows the results of the three cases previously presented. In order to compare the cases, we have taken out the transformers for the Region of Vulnerability evaluation in Ohms and Per Unit.

Table 31: Comparison of the Region of Vulnerability in Different Dimensions

	Case Line 73	Case Line 81	Case Line 65
			
Base Kv	500	200	500
Relay Setting	0.0135	0.0812	0.0170
Bus Density	2	5	9
Region of Vulnerability Per Unit	0.0022	0.0270	0.0196
Region of Vulnerability Ohms	5.60 Ohms	10.8322	49.46
Region of Vulnerability Km	17.18 Km	22.08 Km	151.65 Km

Taking the results of each case in per unit dimension and sort them out, we can classify the Regions of Vulnerability in descending order as shown in Table 32.

Table 32: Region of Vulnerability in Per Unit for Cases 81, 65, and 73 (Sorted in Descending Order).

Rank	Case #	Region of Vulnerability (Per Unit)
1	81	0.027
2	65	0.019
3	73	0.002

As we can see in the table above, the results indicate that the largest Region of Vulnerability is the Case 81. Analyzing the single line diagram of each case shown in Table 31 we realized that case 65 has seven lines with a “circle” and case 81 has only two. So, even though case 65 has seven lines in which the Region of Vulnerability can be distributed, case 81 with only two present a greater Region of Vulnerability in per unit. We can see that line 65 is 500 kV and line 81 is 200 kV, then we can deduce that the factor $(kV_{Base}^2 / MVA_{Base})$ has an impact. This is shown as the relay setting in per unit of line 81 is larger than the relay setting in per unit of line 65. *This is a typical case of the biased results of the calculation of the Region of Vulnerability in Per Unit.*

Taking the results of each case in Ohms and Kilometers dimensions and sort them out, we can classify the Regions of Vulnerability in descending order, as shown in Table 33.

Table 33: Region of Vulnerability in Ohms and Kilometers for Cases 81, 65, and 73 (Sorted in Descending Order).

Rank	Case #	Region of Vulnerability (Ohms)	Region of Vulnerability (Km)
1	65	49.46	151.65
2	81	10.83	22.08
3	73	5.60	17.18

From the table above, we can clearly observe that the rank has changed and now the biggest Region of Vulnerability is case 65. By changing the impedance to ohms, we computed the Region of Vulnerability in this dimension and obtained better results; we correct the effect of voltage level. Taking the results of Table 33 for each case and relate them with the single line diagram we can see that 49.46 ohms for case 65, 10.83 ohms for case 81 and 5.6 ohms for case

73 are numbers that associate more appropriately and accurately the relationship of the magnitude of the Region of Vulnerability with the single line diagram: the representation of the Region of Vulnerability.

Finally, the results of each case in Kilometers have, in this occasion, not change the rank as they included the Ohms per Kilometer ratio; they provide the final dimension for the Region of Vulnerability.

4.2 Refinement of the Methodology: Physical Representation of the RV in the System

This section presents the novel concept of *Validation of the Region of Vulnerability* in which the assurance of the operation of the relay is a fundamental issue. The strong impact of the infeed currents is highlighted. The Regions of Vulnerability for the five simulation cases to be presented in Chapter 5 are evaluated based on the refined methodology.

4.2.1. Region of Vulnerability distributed along Power System Elements

The previous section showed a number of examples of calculation of Regions of Vulnerability in different dimensions but did not emphasize how the Regions of Vulnerability spread inside the power system as a function of the different transmission line configurations. A number of the most representative Regions of Vulnerability are presented in the next two figures.

For Figure 31 and Figure 32 the symbols to use are described next.



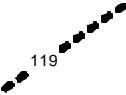
Symbol	Represents
 Square	Relay
 Arrow	Direction in which the relay Setting is pointing to
 Dotted Power System Element	The dotted element <i>completely</i> covered implies that the power system element is overreached by the relay setting.

Figure 31 shows a number of the Regions of Vulnerability that get confined within the nearby power system elements. For all the cases presented in the figure, the restriction equation $Kf * Z_a \leq Z_b$ was not violated. Cases 2 and 5 are examples in which the Region of Vulnerability expands on the unique downstream element, a transmission line. Cases 3 and 4 have one and two elements, respectively, but in this case are transformers; its Region of Vulnerability is confined inside the transformers. Finally, case 1 presents the Region of Vulnerability which is represented in two power system elements, a transformer and a transmission line.

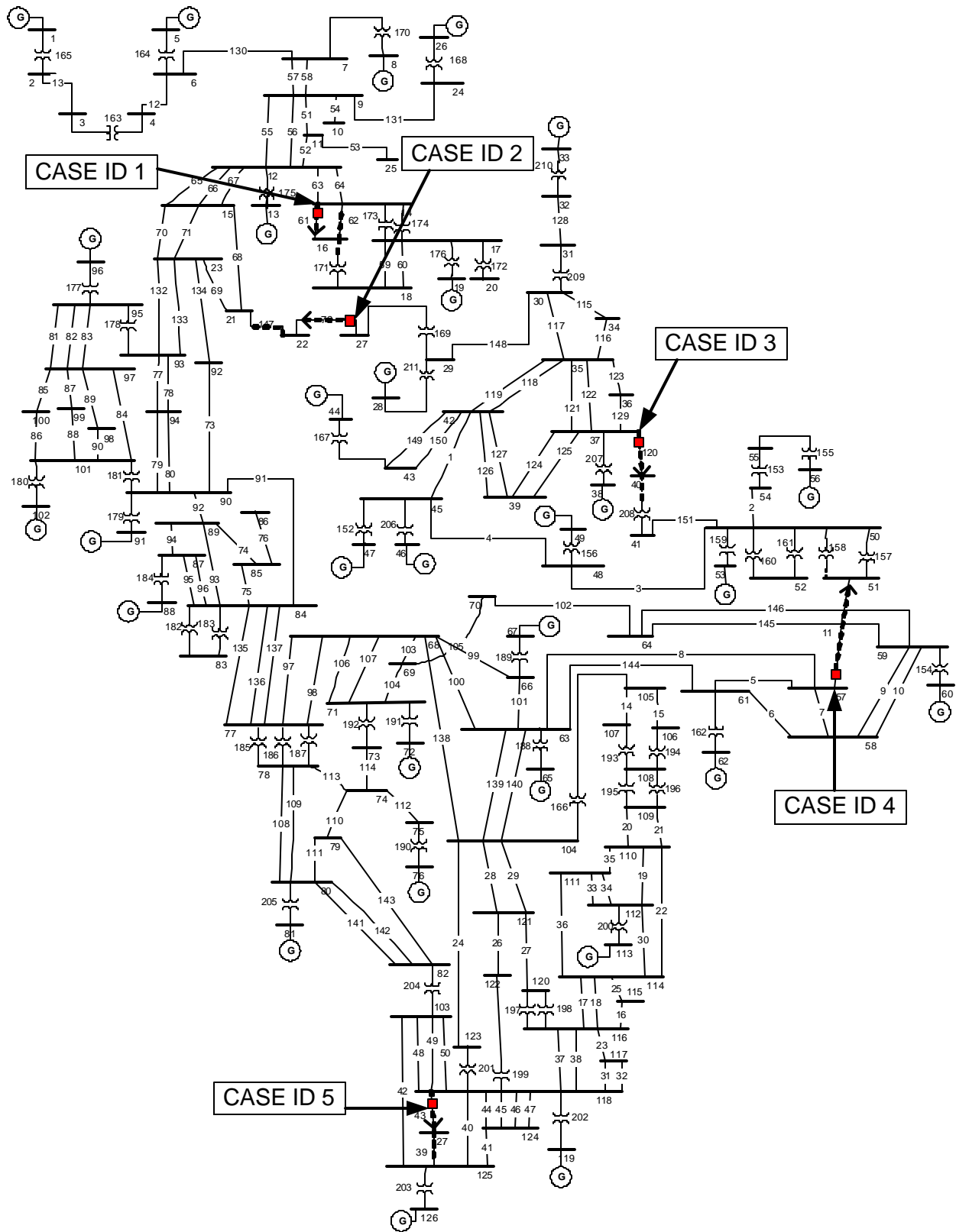


Figure 31: Representation of Regions of Vulnerability that are confined within the Nearby Power System Elements. None of the cases presented violate the restriction equation.

Figure 32 shows a number of the Regions of Vulnerability that get distributed and extended along several power system elements. Four of the five cases presented in the figure do violate the restriction equation $Kf * Z_a \leq Z_b$ and provide a path in which the Region of Vulnerability covers over other power system elements.

The Region of Vulnerability of case 1 extends over seven transmission lines and one transformer. Line numbers 57 and 58 are completely overreached and serve as a path in which the Region of Vulnerability is extended furthermore. Case 2 does not violate the restriction equation and the Region of Vulnerability is distributed in the six transmission lines as depicted in the figure below. The Region of Vulnerability of case 3 extends over ten transmission lines and two transformers. Line number 93 is completely overreached and serves as path in which the Region of Vulnerability is extended furthermore. For case 4, the Region of Vulnerability extends over eleven transmission lines and one transformer. Line numbers 118, 119, 149, and 150 are completely overreached and serve as a path in which the Region of Vulnerability is extended furthermore. The Region of Vulnerability of case 5 extends over twelve transmission lines and no transformers. Line number 138 is completely overreached and serves as a path in which the Region of Vulnerability is extended furthermore.

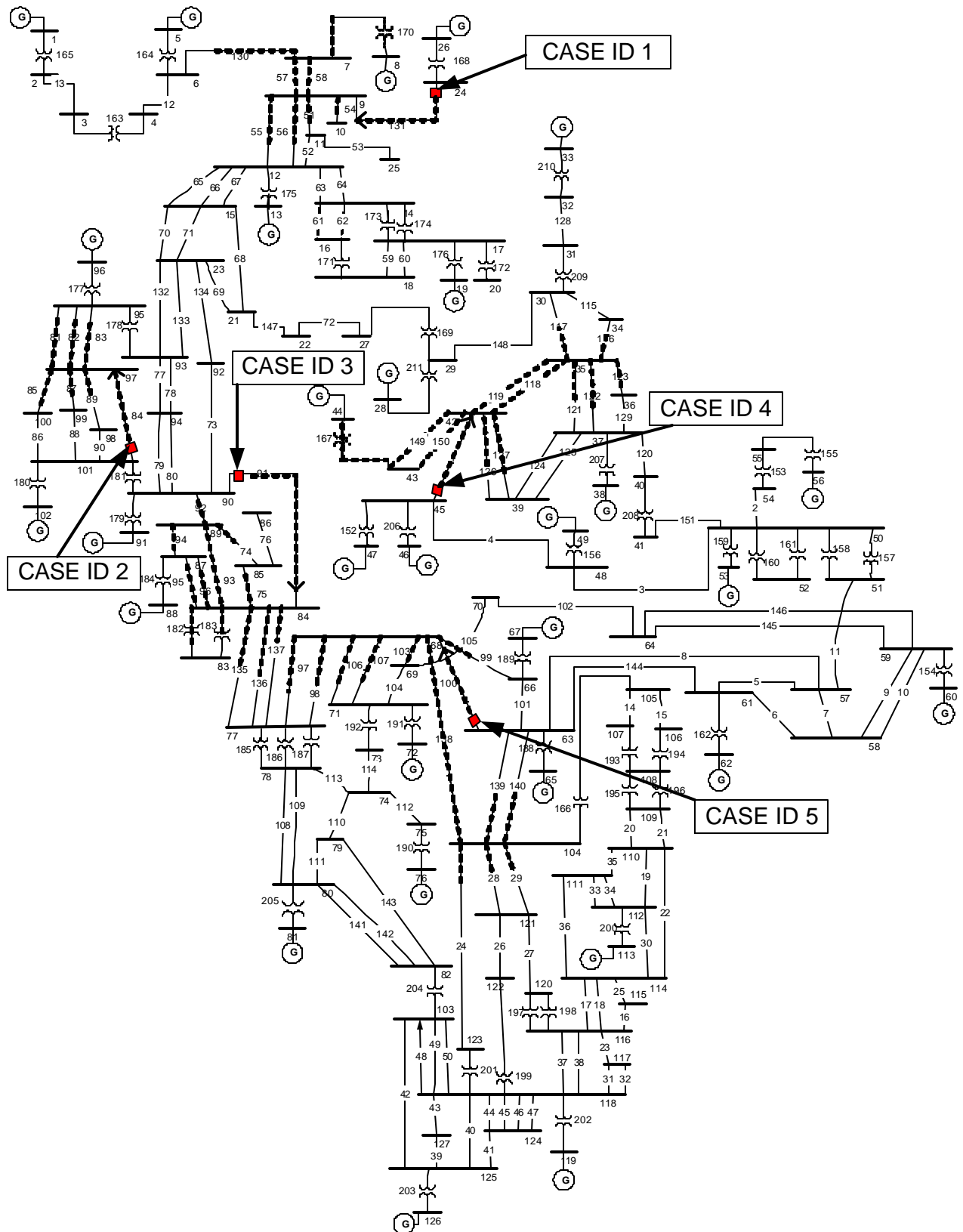


Figure 32: Representation of Regions of Vulnerability that are distributed along the Power System Elements. Four of the Five Cases presented do violate the Restriction Equation.

4.2.2. Region of Vulnerability that overreaches Transmission lines

Figure 24 showed a fictitious bus network in order to explain the restriction to which all the equations that calculate the Region of Vulnerability are limited to. For the system we are studying there are 63 cases in which the setting of a transmission line relay overreaches at least one power system element that is connected downstream (i.e., 63 cases that violate the restriction equation (6)). The elements overreached can be transmission lines, transformers, or generators. Table 34 shows these 63 cases along with the number of power system elements that are overreached for each case. The cases are sorted in descending order of overreached power system elements, “Number of Elements” in the table.

Table 34: 63 Cases in which the Setting of a Transmission Line Relay Overreaches at Least one Power System Element

Case ID	From Bus	To Bus	Overreached Elements				Number Of Elements	
38	125	118	48	49	50	199	43	5
31	45	42	118	119	149	150		4
39	125	103	204	48	49	50		4
40	11	12	175	63	64			3
41	9	12	175	63	64			3
43	15	12	175	63	64			3
44	15	12	175	63	64			3
51	79	80	141	142	205			3
57	63	104	29	138	28			3
58	63	104	29	138	28			3
1	42	45	152	206				2
2	45	48	156	3				2
3	58	61	5	162				2
8	123	104	28	29				2
9	122	121	28	29				2
10	120	121	28	29				2
11	112	111	35	36				2
12	112	111	35	36				2
13	12	14	61	62				2
14	12	14	61	62				2
27	24	9	57	58				2
32	48	45	152	206				2
36	112	114	25	36				2

Case ID	From Bus	To Bus	Overreached Elements	Number Of Elements
45	97	101	181 180	2
46	100	101	181 180	2
47	99	101	181 180	2
48	98	101	181 180	2
62	30	29	211 169	2
63	41	50	3 159	2
4	4	6	164	1
5	105	107	193	1
6	105	106	194	1
7	112	110	35	1
15	84	90	179	1
16	89	90	179	1
17	66	68	138	1
18	74	73	192	1
19	40	37	207	1
20	37	35	116	1
21	37	35	116	1
22	39	37	207	1
23	39	37	207	1
24	32	31	209	1
25	36	37	207	1
26	7	6	164	1
28	64	59	154	1
29	64	59	154	1
30	21	22	72	1
33	51	57	5	1
34	6	4	163	1
35	3	2	165	1
37	125	127	43	1
42	9	12	175	1
49	90	84	93	1
50	63	68	138	1
52	35	37	207	1
53	35	37	207	1
54	31	32	210	1
55	6	7	170	1
56	9	24	168	1
59	80	82	204	1
60	80	82	204	1
61	79	82	204	1

The 63 cases shown in Table 34 are sorted in order to appreciate the problem in the appropriate perspective. We will start with the cases in which the overreached power system elements are transmission lines, and these are shown in Table 35. A specific case may have transmission lines and transformers as overreached elements; these elements show an asterisk “*” on the “Case ID” and only the transmission lines are shown in Table 35; transformers will be treated separately.

Table 35: 31 Cases in which the Setting of a Transmission Line Relay overreaches only Transmission Lines.

Case ID	From Bus	To Bus	Overreached Elements	Number Of Elements
2*	45	48	3	1
3*	58	61	5	1
7	112	110	35	1
8	123	104	28 29	2
9	122	121	28 29	2
10	120	121	28 29	2
11	112	111	35 36	2
12	112	111	35 36	2
13	12	14	61 62	2
14	12	14	61 62	2
17	66	68	138	1
20	37	35	116	1
21	37	35	116	1
27	24	9	57 58	2
30	21	22	72	1
31	45	42	118 119 149 150	4
33	51	57	5	1
36	112	114	25 36	2
37	125	127	43	1
38*	125	118	48 49 50 43	4
39*	125	103	50 48 49	3
40*	11	12	63 64	2
41*	9	12	63 64	2
43*	15	12	63 64	2
44*	15	12	63 64	2
49	90	84	93	1
50	63	68	138	1
51*	79	80	141 142	2
57	63	104	29 138 28	3
58	63	104	29 138 28	3
63*	41	50	3	1

Out of the 31 cases shown in Table 35, the total number of transmission lines overreached is 57. Figure 33 shows the representation of the case numbers 27, 31, 49, and 50 and how eight transmission lines (the lines completely covered with the dotted format: 57, 58, 118, 119, 149, 150, 93, and 138) provide a path in which the Region of Vulnerability expands over the power system. Analyzing case ID 31 in the figure, the transmission lines 118 and 119 provide a path in which the transmission lines 117, 116, 121, 122, and 123 constitute also part of the Region of Vulnerability. This expansion over the overreached transmission lines is of particular importance because the magnitude of the Region of Vulnerability is increased as it finds more transmission lines downstream. The representation of the Region of Vulnerability as depicted in the figure below would imply that the relay with the hidden failure (relay 45-42, case ID 31) would be able to operate for faults located far away from its location, such as faults in transmission lines 116, 117, 121, 122, and 123 which are part of the Region of Vulnerability.

The fundamental question is: For the region of vulnerability, as depicted below, does the relay respond to the fault?

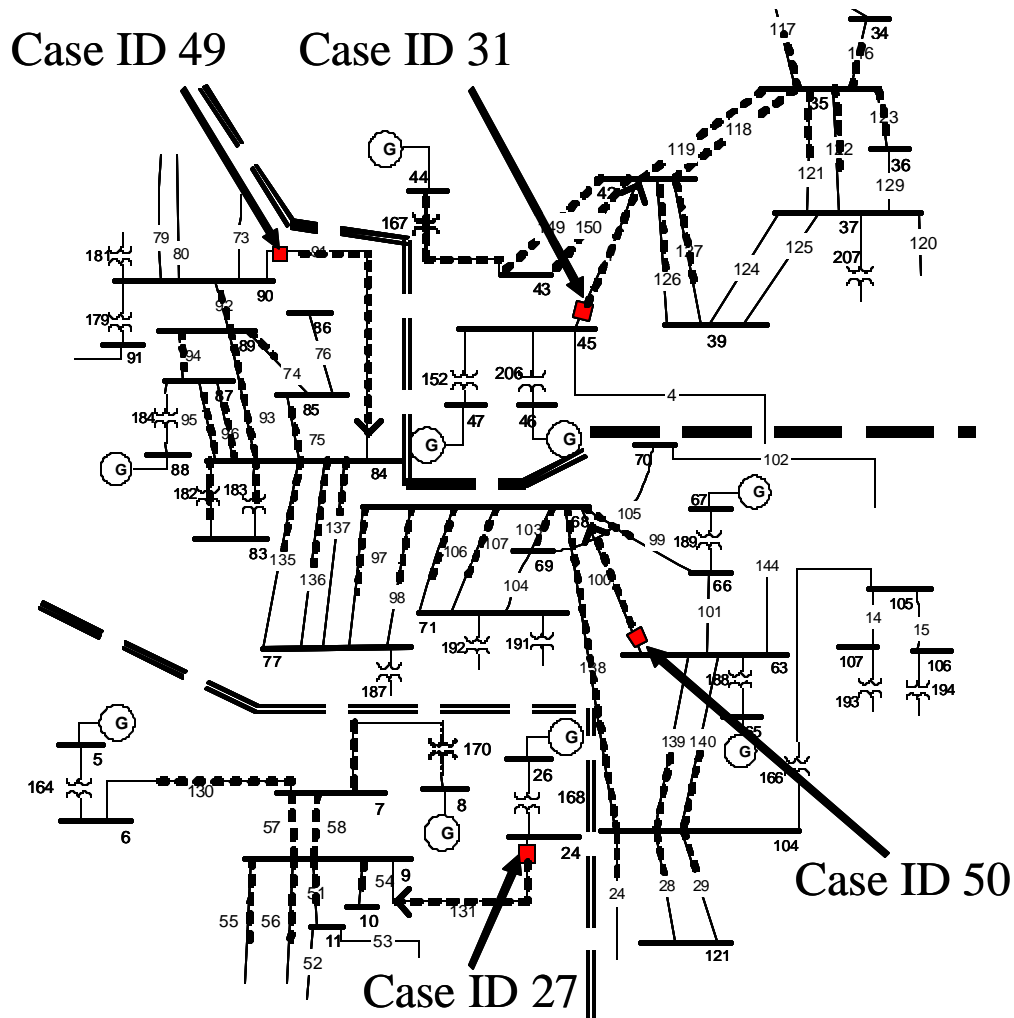


Figure 33: Representation of Cases 27, 31, 49 and 50.

This is an important question and its answer uncovers a fundamental contribution of this dissertation: the *Validation of the Region of Vulnerability*. Figure 34 depicts the process in the evaluation of the Region of Vulnerability. Number “1” in this figure is related to the relay settings which were defined in Chapter Chapter 3. Number “2” is related to equation (5), equation (10), and equation (11), with its respective restriction in order to compute the Region of Vulnerability in the different dimensions. Number “3” is the stage in the process in which the important question is raised: *For the Region of Vulnerability as depicted in Figure 33, does the relay respond to the fault?*

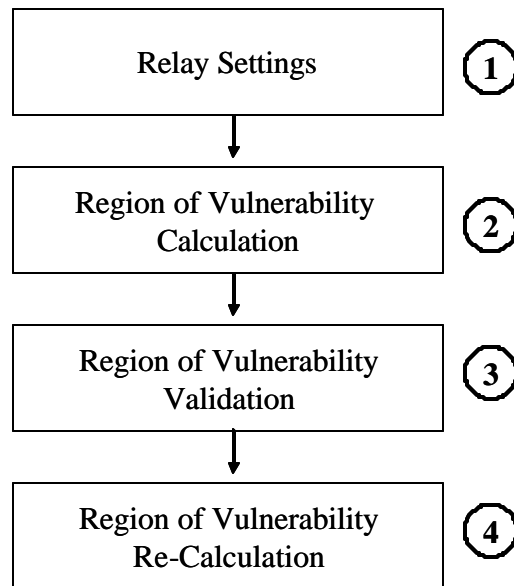


Figure 34: Process in the Calculation of the Region of Vulnerability.

As we mentioned in Chapter Chapter 3 we do monitor the distance relays in order to detect any relay operation after the second contingency. A fundamental step that has to be considered *before* this is related to what really produces the second contingency: *the operation of the relay that defines the Region of Vulnerability, the one that reacts to the “another condition.”*

We have to assure that the relay operates and disconnects the line for the fault which is located inside the Region of Vulnerability. The operation of the relay is a fundamental “break or make” step in this process and this is verified by monitoring the apparent impedance as seen from the relay terminals.

Applying this previous statement to the Case ID 31 we have to simulate faults along the lines that are part of the Region of Vulnerability (118, 119, 149, 150, 126, 127, 116, 117, 121, 122, and 123) and determine if the relay operates by monitoring the apparent impedance seen by the relay terminals. This process is defined as *Validation of the Region of Vulnerability*.

The 31 cases (57 transmission lines) included in Table 35 have been submitted to the process of *Validation of the Region of Vulnerability*. The presence of intermediate generation between the fault and the relay location produce infeed currents and the relay may underreach. Table 36 shows the simulation results on its last column. There are only two outputs: “Valid” and “Not

Valid.” The “Valid” result implies that for the faults placed along the transmission line, the apparent impedance fall *inside* the relay operating region. On the other hand, “Not Valid” means that the apparent impedance *did not* fall inside the operating zone; therefore the relay *does not operate*. Since the relay does not operate, there is no second disconnection and therefore no double contingency.

Clearly each case presents its own particular characteristics and we placed faults along the transmission lines with a specific bus as reference, which is bus 42 for the case shown in Figure 35. For the cases found as “Non Valid” faults were applied between 1% and 90 % of the line; most of the cases were found as “Not Valid” when faults were applied between 1 and 50 % of the line. The determination of whether the fault is or is not inside the relay operating zone is made through a graphical test.

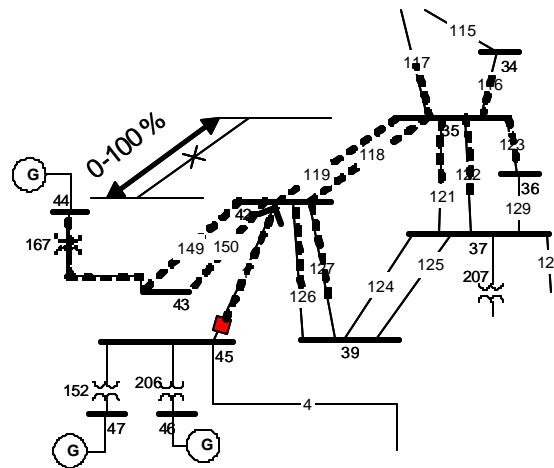


Figure 35: Reference for the Fault Placement during the Validation of the Region of Vulnerability for Cases in Table 36.

Table 36: Validation of the Region of Vulnerability, Simulation Results for Transmission lines: Valid and Not Valid Cases.

Case ID	From Bus	To Bus	Overreached Elements				Simulation Results
2*	45	48	3				Not Valid
3*	58	61	5				Not Valid
7	112	110	35				Not Valid
8	123	104	28	29			Not Valid
9	122	121	28	29			Not Valid
10	120	121	28	29			Not Valid
11	112	111	35	36			Not Valid
12	112	111	35	36			Not Valid
17	66	68	138				Not Valid
20	37	35	116				Not Valid
21	37	35	116				Not Valid
27	24	9	57	58			Not Valid
31	45	42	118	119	149	150	Not Valid
33	51	57	5				Not Valid
36	112	114	25	36			Not Valid
38*	125	118	48	49	50	43	Not Valid
39*	125	103	50	48	49		Not Valid
40*	11	12	63	64			Not Valid
41*	9	12	63	64			Not Valid
43*	15	12	63	64			Not Valid
44*	15	12	63	64			Not Valid
49	90	84	93				Not Valid
50	63	68	138				Not Valid
51*	79	80	141	142			Not Valid
63*	41	50	3				Not Valid
57	63	104	29	138	28		Not Valid
58	63	104	29	138	28		Not Valid
13	12	14	61	62			Valid
14	12	14	61	62			Valid
30	21	22	72				Valid
37	125	127	43				Valid

The results in Table 36 speak for themselves and show the strong impact of the infeed currents on the spread of the Region of Vulnerability along the power system. Out of the 57 overreached transmission lines, 51 of them were proved to be “Not Valid.” *The infeed currents make the relay to underreach, restraining the Region of Vulnerability from spreading along the power system elements.*

Out of the four cases in which the Region of Vulnerability was found “Valid” (see Table 36), two of them are related to network configurations in which there is no intermediate generation source, and therefore not infeed current. Figure 36 shows the cases and its location in the sample system.

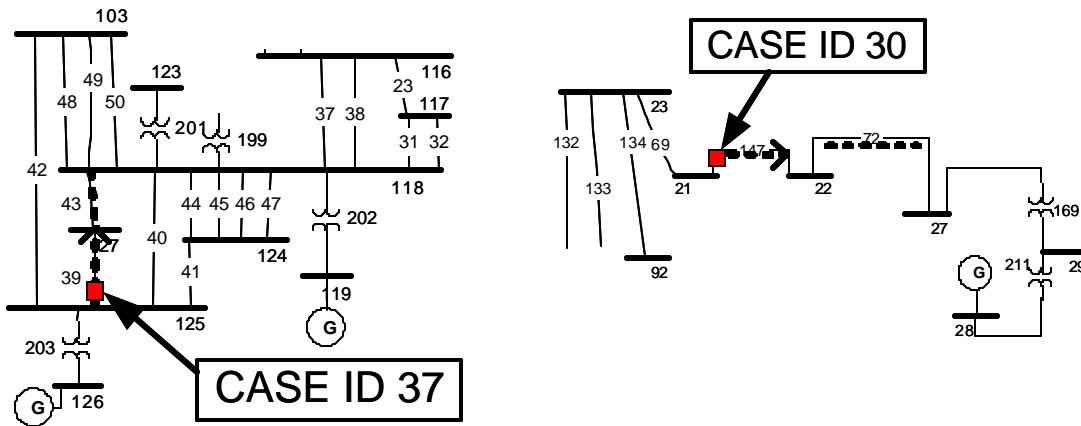


Figure 36: “Valid Cases”, Cases that do not present Infeed Currents due to Network Topology.

The other two cases in which the Region of Vulnerability was found “Valid” have specific network characteristics: they are parallel circuits. Figure 37 shows the cases and its location in the sample system.

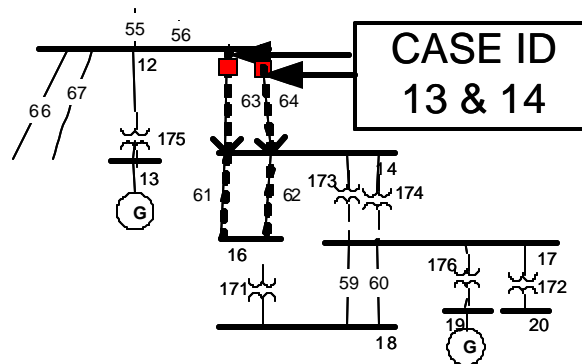


Figure 37: “Valid: Case,” that have Specific Network Characteristic: Parallel Lines.

4.2.3. Region of Vulnerability that overreaches Transformers

Out of the 63 cases shown in Table 34, the cases related to overreached transmission lines were presented in Table 35. Table 37 presents the remaining elements, the transformers, and they have been sorted by transformer types: Generator Step-up and Network transformers. The asterisk “*” was used with the same purpose than in Table 35. In the table below, “G” stands for Generator Step-up transformer and “N” for Network transformer.

Table 37: Cases in which the Setting of a Transmission Line overreaches Transformers.

Case ID	From Bus	To Bus	Overreached Elements	Number Of Elements	Transformer Classification
1	42	45	152 206	2	G
2*	45	48	156	1	G
3*	58	61	162	1	G
4	4	6	164	1	G
15	84	90	179	1	G
16	89	90	179	1	G
19	40	37	207	1	G
22	39	37	207	1	G
23	39	37	207	1	G
25	36	37	207	1	G
26	7	6	164	1	G
28	64	59	154	1	G
29	64	59	154	1	G
32	48	45	152 206	2	G
35	3	2	165	1	G
40*	11	12	175	1	G
41*	9	12	175	1	G
42	9	12	175	1	G
43*	15	12	175	1	G
44*	15	12	175	1	G
45*	97	101	180	1	G
46*	100	101	180	1	G
47*	99	101	180	1	G
48*	98	101	180	1	G
51*	79	80	205	1	G
52	35	37	207	1	G
53	35	37	207	1	G
54	31	32	210	1	G
55	6	7	170	1	G

Case ID	From Bus	To Bus	Overreached Elements	Number Of Elements	Transformer Classification
56	9	24	168	1	G
62	30	29	211	1	G
63*	41	50	159	1	G
5	105	107	193	1	N
6	105	106	194	1	N
18	74	73	192	1	N
24	32	31	209	1	N
34	6	4	163	1	N
38*	125	118	199	1	N
39*	125	103	204	1	N
45*	97	101	181	1	N
46*	100	101	181	1	N
47*	99	101	181	1	N
48*	98	101	181	1	N
59	80	82	204	1	N
60	80	82	204	1	N
61	79	82	204	1	N
62	30	29	169	1	N

Continuing with a similar analysis than the one we performed when the overreached elements by the relay settings were transmission lines, we would have to simulate faults in order to evaluate the infeed effect on the expansion on the Region of Vulnerability. Considering the differences in transformers and transmission lines, we are interested in finding if a fault located in a transmission line passing the overreached transformer would make the relay to operate. The procedure to test this is to apply a fault at 5 % of the transmission line and keep track of the apparent impedance seen by the relay, as depicted in Figure 38. If the apparent impedance falls inside the relays operating region, then we have validated the Region of Vulnerability.

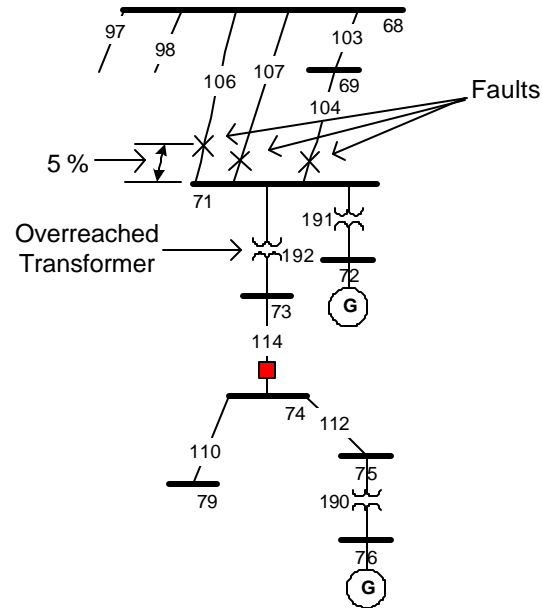


Figure 38: Overreached Transformer and the Faults Located in the Downstream Transmission Lines.

The cases in which the overreached power system element is a Generator Step-up transformer require special consideration since this equipment is critical and it is often equipped with special protection systems. Faults on GSU normally involve actions like generation rejection and other switching maneuvers in order to keep the stability of the system. Then, due to the specific network structure (there are not transmission lines to apply faults) and its characteristics we have decided not to perform this study for cases that involve Generator Step-up transformers.

The Network transformers that are overreached by relay settings are shown in Table 38.

Table 38: Network Transformers that are overreached by Relay Settings.

Case ID	From Bus	To Bus	Overreached Elements
5	105	107	193
6	105	106	194
18	74	73	192
24	32	31	209
34	6	4	163
38*	125	118	199
39*	125	103	204
45*	97	101	181
46*	100	101	181
47*	99	101	181
48*	98	101	181
59	80	82	204
60	80	82	204
61	79	82	204
62	30	29	169

Faults were applied on the transmission lines that are connected downstream the overreached transformer cases of Table 38 and the results are shown in Table 39. In this table the first two cases are particular since the next element after the transformer is another transformer. Setting these cases aside, out of the 13 overreached transformers, 12 were found as “Non Valid”. These results present a similar scenario than the cases of overreached transmission lines: the infeed effect is strong and it restrains the Region of Vulnerability from spreading along power system elements. The same “Valid” and “Non Valid” nomenclature was used in the table below. The results show only one case in which a fault makes the relay to operate and therefore validating the Region of Vulnerability and this case will be presented in Chapter Chapter 5.

Table 39: Cases in which the Setting of a Transmission Line Overreaches Network Transformers.

Case ID	From Bus	To Bus	Overreached Elements	Simulation Results
5	105	107	193	Non Valid
6	105	106	194	Non Valid
18	74	73	192	Valid
24	32	31	209	Non Valid
34	6	4	163	Non Valid
38*	125	118	199	Non Valid
39*	125	103	204	Non Valid
45*	97	101	181	Non Valid
46*	100	101	181	Non Valid
47*	99	101	181	Non Valid
48*	98	101	181	Non Valid
59	80	82	204	Non Valid
60	80	82	204	Non Valid
61	79	82	204	Non Valid
62	30	29	169	Non Valid

It would be important to note that in case of transformers, internal faults could also apply. However, as we mentioned previously, we are mainly interested in faults in transmission lines and determining the Region of Vulnerability in kilometers of transmission lines.

4.2.4. Final Procedure to Compute the Regions of Vulnerability

The previous results validated the Regions of Vulnerability for overreached transmission lines and transformers. The final procedure to compute the Regions of Vulnerability is presented next; it is related to number 4 in Figure 34.

An important contribution to the methodology of evaluation of the Region of Vulnerability is to map the faults along the transmission line into the R-X diagram. This allows us to determine the “Valid” region of vulnerability, for which the relay operates and disconnects the transmission line.

Figure 39 presents a simple transmission line with its relay and three points along the line: A, B, and C. The evaluation of the Region of Vulnerability starts on the point C, which is a value of

impedance measured from point A. This value corresponds to the impedance of the line (27-22) times the K^f constant (0.2).

Once point C is found, faults are applied along the transmission line starting at this point towards point A with the objective of finding the location of the point B. Point B is the place in the transmission line in which the fault, when mapped in the R-X diagram, falls on the relay operating region umbrae as we can see in the figure below.

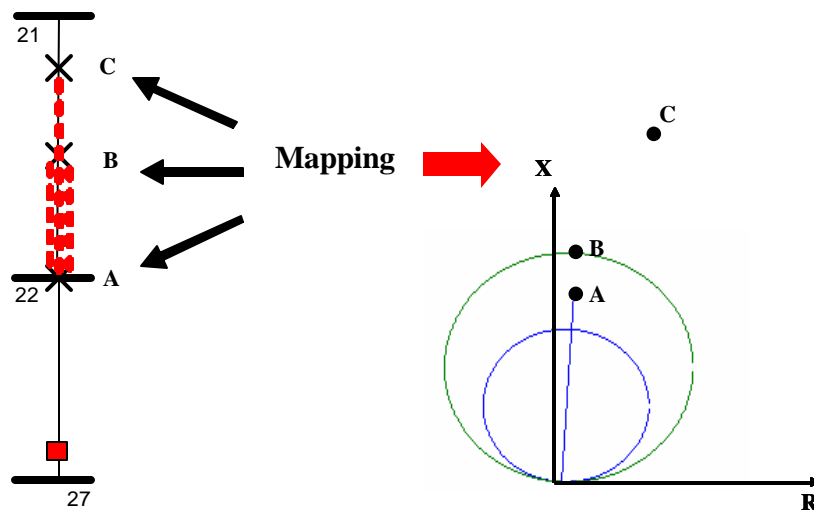


Figure 39: The Mapping of the R-X diagram with the Single Line Diagram in order to determine the Valid Region of Vulnerability for a Single line Case.

Point A is the origin of the transmission line; exactly at this point there is no Region of Vulnerability because is a fault on the bus; this point is used as the reference. Once the point B has been found, the Region of Vulnerability is determined as the impedance from the point B to the point A. In Figure 39 a triple line has been used to differentiate this “Valid” Region of Vulnerability. The value of impedance that exists between points B and A is then changed from per unit to ohms, and then from ohms to kilometers, as it was explained in Section 4.1. At the end, we obtain a physical area in kilometers of transmission line.

In Figure 39 the point C in the transmission line is mapped *outside* of the relay operating zone. The vast majority of the results have shown this behavior; clearly this is not the rule that apply for all cases and for any system. Particular network considerations may present the point C and

the point B very close together; the infeed currents determine the separation distance between the points B and C.

Figure 40 shows a case with multiple lines. The procedure is essentially the same and the important issue is to find the point B at each line.

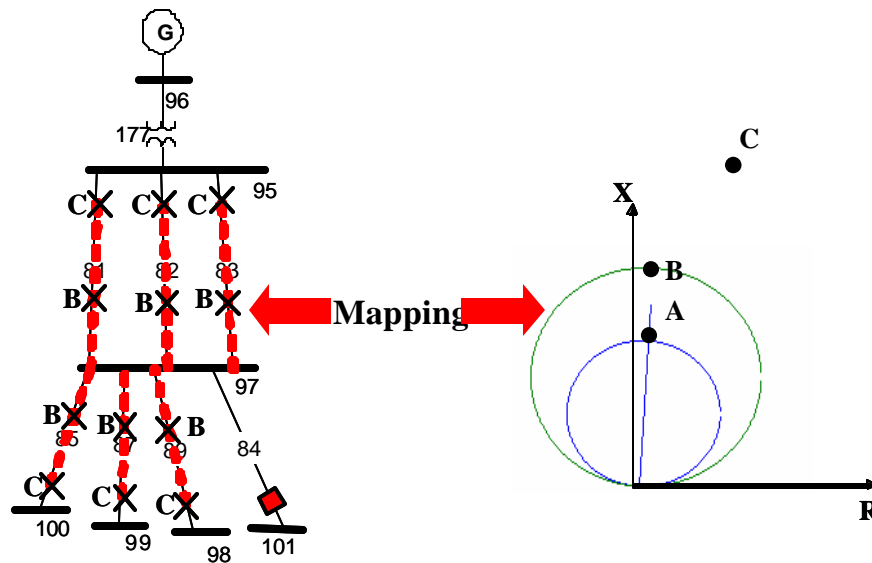


Figure 40: The Mapping of the R-X Diagram with the Single Line Diagram in order to Determine the Valid Region of Vulnerability for a Multiple Line Case.

Once the point B is found for each of the transmission lines, the Region of Vulnerability is computed as:

$$RV_{Km} = \sum_{i=1}^{i=NI} Z_{B-A(i)}$$

(12)

Where:

RV_{Km}	Region of Vulnerability, in Km
NI	Number of Lines
Z_{B-A}	Value of the Impedance of each line, converted from per unit to ohms, and then to Kilometers.

Table 40 shows the stages in the procedure to calculate the Region of Vulnerability, as we described above.

Table 40: Stages in the procedure for the Evaluation of the Region of Vulnerability.

Stage Number	Description
1	Find point C, which is the value of the impedance of the line times the K_f constant.
2	Determine the point "B," the place in the transmission line for which the apparent impedance falls in the relay operating umbrae.
3	Convert the impedance from point B to A, from per unit to Ohms, and finally from Ohms to Kilometers.
4	Add the physical distances on each line in the case of multiple lines.

Table 41 presents the calculation of the Region of Vulnerability for the cases of section 5.2.2 using the procedure described above. The table presents: 1) the transmission lines in which the faults are applied with the objective of finding the point "B;" 2) the location of point B along the line included as a percentage, measured from the reference bus; 3) the value of the impedance Z_{B-A} in per unit, ohms, and kilometers; and 4) the Region of Vulnerability in kilometers.

Table 41: Calculation of the Regions of Vulnerability for the cases presented in Chapter Chapter 5.

Relay Case	Transmission Lines to Apply Faults	Point "B" Location (%)	Z_{B-A} (per unit)	Z_{B-A} (Ohms)	Z_{B-A} (Km)	Region of Vulnerability (Km)
101 -97	83	0.07	0.0047	1.8853	3.8432	20.15
	82	0.07	0.0046	1.8547	3.7807	
	81	0.07	0.0047	1.8956	3.8643	
	89	0.03	0.0035	1.3803	2.8138	
	87	0.04	0.0037	1.4993	3.0563	
	85	0.02	0.0034	1.3695	2.7918	
84-90	92	0.01	0.0003	0.6439	1.9740	9.79
	73	0.03	0.0003	0.8410	2.5781	
	79	0.03	0.0003	0.7797	2.3903	
	80	0.03	0.0004	0.9295	2.8495	
63-104	28	0.78	0.0012	3.1005	9.5048	41.30
	29	0.78	0.0012	3.1005	9.5048	
	24	0.04	0.0008	1.8858	5.7811	
	138	0.34	0.0014	3.4891	10.6962	
	140	0.03	0.0008	1.8978	5.8177	
74-73	104	0.05	0.0002	0.5719	1.7531	4.05
	106	0.02	0.0002	0.3768	1.1550	
	107	0.02	0.0002	0.3754	1.1508	
89-85	76	0.12	0.0016	3.8942	11.9381	40.25512
	75	0.25	0.0037	9.2371	28.3170	

Chapter 5. Areas of Consequence and Index of Severity

This chapter defines the terms of areas of consequence and index of severity. It includes a literature review of the index of severity and its use in power system security, specifically for static and dynamic security assessment. The differences of the index of severity found in the literature review and the developed index of severity are described.

The effects of the unwanted disconnections caused by Hidden Failures in a power system are simulated and assessed through cases performed in a transient stability program. Five simulations are developed and detailed explained. The index of severity for the five simulation cases is computed.

5.1 Definition of Areas of Consequence and Index of Severity Development

This section defines the terms Areas of Consequence and Index of Severity. It includes a literature review of the index of severity and its use in power system security, specifically for static and dynamic security assessment. The differences of the index of severity found in the literature review and the developed index of severity are described.

5.1.1. Definition of Areas of Consequence

As we presented in Chapter Chapter 2, the hidden failure modes are the ways in which particular protection systems may have defects, which remain undetected within the protection system logic, and are triggered by the occurrence of another condition in the power system. The Regions of Vulnerability provide a representation of those defects in the power system, and make possible to visualize zones in which the occurrence of another condition triggers the unwanted disconnection caused by hidden failures. The quantitative evaluation of the Regions of Vulnerability of a particular protection system in a specific power system brings the ability to observe the largest vulnerable zones. The impact or consequences of the unwanted disconnection

of power system elements caused by hidden failures in the power system is critical and must be considered in the methodology.

If the magnitude of a Region of Vulnerability of a transmission line end is larger than the other end, then the exposure to the occurrence of other conditions—such as electrical faults—is greater, and then the Region of Vulnerability magnitude must be taken into account. The consequences of unwanted disconnections caused by hidden failures in the power system must also be considered, since the unwanted trip of a key transmission line in the backbone of the system transmission network would be more important than the unwanted trip of a radial transmission line.

Areas of consequence are related to the effect of the unwanted disconnections caused by hidden failures and in this chapter we measure the affected area by the disturbance as it spans within the power system. As we would expect, the consequence depends on many factors related to the line criticality.

The consequence of unwanted disconnections caused by hidden failures may be relatively small, in which the post-disturbance system conditions are close to the pre-disturbance, and in terms of physical areas, the consequence is confined within the disturbance surroundings. For these cases, relatively small changes in the neighboring transmission lines power flows and small or negligible voltage variations in the neighboring buses take place. On the other hand, the unwanted disconnections caused by hidden failures in some other lines may have areas of consequence that literally affect a major part of the power system. Due to the interconnected characteristic of the power systems, it is well known that a disturbance in one location may expand and affect a big part of the power system. The consequences of these critical unwanted disconnections caused by hidden failures may be relatively large changes in the transmission line power flows, transient stability, under frequency conditions, and voltage depression, among others. All of these excursions of the primary power system parameters, voltage, current, and frequency, may produce the operation of protection systems, augmenting even more the dynamics of the already in stress and in motion power system.

Areas of consequence by definition are a qualitative measure related to the affected physical area. The areas of consequence are good indicators of the effects of the disturbance and they may be expressed as the number of power system elements which suffer a major change in operation conditions. To visualize the qualitative nature of the areas of consequence, a quantitative indication of the consequence of unwanted disconnections caused by hidden failures is computed: the index of severity. The term index of severity has been developed and used by a number of researchers in different applications mainly related to power system security. Power system security is related to the actions of monitoring, assessing, and enhancing the degree in which the system will continue to perform its main mission of providing electric power to all loads, subject to the potential occurrence of losing power system elements. Within the jargon of power system security, failed power system elements are related as contingencies.

5.1.2. Index of Severity for Static and Dynamic Security Assessment

The following definitions related to power system security will place our methodology in the appropriate perspective [19]:

Power System Security: an instantaneous, time varying condition reflecting the robustness of the power system relative to imminent disturbances; the complement of the risk of disruption of unimpaired system performance.

Security Monitoring: the one-line measurement of system and environmental variables that affect the system security; provides base case conditions for analysis of the effects of contingencies (security assessment).

Security Assessment: the evaluation of data, provided by the security monitoring, to estimate the relative robustness (security level) of the system in its present state. (i.e., determination of whether the system is in the Normal or Alert operating state).

Security Enhancement: Specific operations taken on-line to improve the system robustness, i.e., to raise the performance level of system security. Includes or is also referred to variously in the literature as security dispatch, security control, corrective rescheduling, preventive action, etc.

The North American Electric Reliability Council defines security as: “prevention of cascading outages when the power system is subjected to severe disturbances” [20]. In order to prevent cascading outages from occurring, power systems are planned and operated such that the following conditions are met at all times: (1) no equipment or transmission circuits are overloaded; (2) buses voltage magnitudes are kept within the permissible limits (usually 5%); and (3) when any contingency occurs, acceptable steady state conditions will result following the transient, i.e., no instability will occur. The power system security is analyzed in order to make certain that the above conditions are satisfied [19]. The first two conditions, no equipment or transmission circuit overload, and no voltage limits violations require of steady state analysis in which the dynamics of the system from pre to post disturbance are ignored and assumed to be harmless for the system. The last condition, the result of acceptable steady state conditions following the transient caused by the disturbance requires of dynamic analysis. Due to the nature of the problem and the technique characteristics involved with each, the analysis of power security has been divided in static security analysis and dynamic security analysis.

Static security analysis is related to assess the power system conditions after losing a power system element. In other words, this question is raised and answered: “what would be the power system condition if this contingency occurs in terms of over loads in transmission lines and equipment, and voltage limit violations?” A number of the techniques related to static security assessment in which the index of severity has been used are presented next.

A contingency in its simplest form is related to the loss of a certain single component, such as generators, buses, transformers, or transmission lines. More complex contingencies may take the form of double contingencies. Double contingency is defined in [19] as “the overlapping occurrence of two independent contingency events. In other words, a contingency takes place in the system, and while this outage is still in effect, a second totally independent event causes a second outage.”

An important task in static security analysis is the contingency analysis problem. This is related to the definition of the list of contingencies that should be run and the effects in the power system analyzed. Historically the task related to the construction of the contingency list has been the point of interest of several researchers. The main objective in this effort is to find a systematic way to select the list of contingencies, upon the implication that a vast majority of the contingencies do not cause overloads or voltage violations in the power system. Contingency Analysis is a software application that runs in the Energy Management System (EMS), and its main objective is to provide the system operators an indication of what would happen in the event of an unplanned equipment outage, i.e., a contingency [19]. The contingency analysis program is run in the EMS by the system operators at frequent time intervals in order to assess the current security condition of the power system.

The different methodologies to select the important cases from the complete contingency list may be divided as: fixed list, indirect methods, direct methods, and fast contingency screening methods. In the fixed list approach, the contingencies to run are selected based on the operator intuition and experience. The indirect methods are fast calculations based on approximated algorithms with the goal of obtaining an index that reflects the entire system loading. The direct methods construct severity indices based on the individual monitoring quantities, using full detailed algorithms. Finally the fast screening methods build the list upon ranking the contingencies with a severity index, calculated with a fast or approximated calculation, and then selects the list of contingencies based on the ranking [19].

In the context of static security assessment, the term index of severity has been defined as a number related to the post fault condition of overloads in transmission lines and voltage violations in bus voltages.

A number of the techniques related to on-line dynamic security assessment in which the index of severity has been used are presented next. Dynamic security assessment, as we mentioned above, requires the use of a dynamic study in which the change between the pre and post disturbance conditions is of main interest. The contingencies are not considered only in terms of post-contingency conditions, but in terms of total disturbance [19]. Dynamic security analysis

comprises all types of stabilities in the power system, i.e., rotor angle stability, voltage stability, and frequency stability [21]. Historically, rotor angle stability has been the main stability problem in power systems. Voltage stability has come into the play as the systems become more loaded and a number of wide area disturbances happened and degraded as a result of voltage collapse [14]. The term frequency stability is related to the post contingency balance between load and generation, and has not been yet considered as on-line assessment requirement [21].

A number of the techniques employed in static security analysis have been adopted and applied in dynamic security analysis. Researchers have developed analysis techniques for contingency analysis in the form of contingency screening. As with static security analysis, the basic implication is that from the full list of the possible contingencies in a power system, only a small fraction is going to create a post disturbance condition that affects the power system integrity.

A technique to rank contingencies based on severity indices in dynamic security analysis using simplified and fast calculations is proposed in [22]. Five single performance indices (PI) are computed: PI1 based on coherency of generator rotor angles, PI2 based on transient energy conversion, and PI3 to PI5 based on dot products of the Transient Energy Function. Since experience has shown that some indices work better than others for particular power systems and that combination of indices usually work better than a single index, the five single performance indices are used to calculate a composite index. This composite index is a weighted average of the normalized performance indices.

Another technique has been developed for contingency screening in [23]. Contingency screening is related to the process of ranking the large list of contingencies *and* selecting a small number of severe cases from the large list. Once the list with the small number of severe cases has been defined, the effect of these contingencies in the power system is evaluated with full algorithms and time domain simulations. The task of ranking is done by the use of severity indices, which are capable of detecting the dynamic state of the system in the post-disturbance configuration. Whereas in static contingency screening the index has the capability of detecting the severity of limit violations, the indices of severity in dynamic security analysis are to capture the change in a number of state variables as a consequence of the disturbance [23].

A number of indices related to specific state variables were developed in this research work and are enumerated next:

- Change in generator rotor angles with respect to the center of inertia
- Change in bus voltages
- Change in rotor speed of generators
- Change rate in transient energy of generators
- Acceleration of generators

In addition to the above cited indices, others measures have been proposed as:

- Maximum difference between rotor angles
- Maximum difference of rotor speeds
- Maximum difference of the rate of change in generator transient energy.

The indices developed in this research work were computed using conventional time domain simulations which lasted a few steps after the fault clearing time. Each individual index is intended to capture a different aspect in the power system and the computation of a composite index is used to rank contingencies. Contingency selection involves the use of artificial intelligence and has the purpose of separating the cases that need further analysis. Pattern recognition techniques are utilized that indicate stability or instability for each case.

Another technique has been developed for contingency screening in dynamic security assessment related to rotor angle stability [21]. In this reference stability indices are computed using the Extended Equal Area Criterion (EEAC) in a fast contingency screening algorithm, giving an indication of the relative severity of the contingencies. Once the critical contingencies have been selected, conventional time domain simulations are run in a detailed analysis. In this analysis, a transient stability index is calculated using the EEAC and time domain simulations which measure the proximity of the system to instability due to loss of synchronism [24].

In the context of dynamic security assessment, the term severity index has been defined and used to select stable from unstable contingencies. Similarly, but with different nomenclature, the term stability index has been used to rank and separate stable from unstable contingencies.

5.1.3. Index of Severity for this Dissertation

The previous section presented a literature review of the index of severity as it has been applied by a number of researchers within the field of power system security for static and dynamic security assessment. Since there is previous research work and experience with the methodology on the development of indices of severity, this methodology is considered in the computation of the index of severity of this dissertation. The index of severity developed herein, however, is applied to a distinct problem, and a number of differences with respect to the index found in the literature review are shown in Table 42.

Table 42: Characteristics and Differences of the Index of Severity in Static and Dynamic Security Analysis compared with the Index of Severity developed in this Dissertation

Characteristic	Index of Severity for Static and Dynamic Security Analysis	Index of Severity Developed in this Dissertation
1.- Objective	Rank Contingencies	Rank Protection Systems
2.- Contingency Type	Single Contingency	Double Contingency
3.- Scope	Rotor Angle Stability	Broader Scope, due to the Inclusion of Protection System Dynamics
4.- Computation Method	Fast and Simplified Calculations	Time Domain Simulation

The index of severity to be developed herein has the objective of identifying the critical protection systems, whose unwanted operations would disconnect power system elements affecting considerably the power system integrity and its capacity to deliver energy. The differences among the two indices are described next:

1. Rank protection systems versus contingencies

The purpose of the index of severity to be developed here in is to identify the critical protection systems, where as the index of severity found in the literature review is concerned with ranking contingencies. Clearly those critical protection systems have contingencies associated with them; however, still differences exist as we will see in the next point.

2. Double Contingency versus Single Contingency.

A fundamental concept of this dissertation is the one related to unwanted disconnections caused by Hidden Failures. As it was seen in Chapter Chapter 2, there are two equipment disconnections

(double contingency) occurring nearly at the same time and a particular characteristic of these disconnections is that the events are mutually dependent. The characteristics of the double contingencies related to unwanted disconnections caused by hidden failures differs from the one defined in [19] at least in one important issue: the mutually dependency of the events. This characteristic is important in the double contingency as found in [6] and the effects in the power system tend to be more severe due to the closeness of the physical location of the disconnections. As we saw in the previous point, the index of severity found on the literature review is used to rank single contingencies, i.e., the disconnection of one power system element.

3. Broader scope of the index: the dynamics of the protection system

An excerpt from [19] states: “In dynamic security analysis, there is a significantly different way of looking at contingencies where the post- contingency outages are determined by the dynamics of the system, including the *protection system*.”

An important feature of the index of severity to be developed herein is that it is capable of capturing the dynamics of the protection system and quantifies the consequence in terms of total disturbance. Following the disconnection of the two power system elements we are interested in the effect of the post contingency conditions on the protection system. The addition of models of protective relays and special protection systems has been claimed as a requirement by a number of utilities as Ontario Hydro [25] and has been implemented and considered in the computation of our index of severity. The addition of the protection schemes in the time domain simulation allows observing the system response to the double contingency in a more realistic way since part of the protection and control of the system has been modeled. An insight of the mechanisms of the disturbances is gained upon the identification of the protection schemes that may suffer from frequent operations as a consequence of the dynamics related to the double contingency. The mechanisms may show, for instance, that the outages were exacerbated by the operation of distance relays, or due to loss of synchronism [19].

The developed index of severity could detect stability problems but it is not the intention and has not been designed with that objective. Its scope is broader since it is able to track, for instance, the lost load due to under frequency conditions detected by the modeled relays as we will see in

Section 5.2. The index of severity developed in the literature review does not model the protection system [26].

4. Computation method: 10 seconds of time domain simulation

The developed index of severity is computed based on the results of 10 seconds-long time domain simulation, which is required to observe the reaction of the protection schemes. There are different methods of computation of the indices of severity of the literature review and most of them use a few steps after the fault inception in order to include the transients. This short time is justified by the absence of the protection system models [26].

Index of Severity and its role within Power System Security

Part of the research results of [6] are the mechanisms of the Hidden Failures and the characteristics of its occurrence in wide-area disturbances. As mentioned in Chapter Chapter 1, it was found that the unwanted disconnections caused by hidden failures are particularly harmful and these disconnections have been found as key players in the disturbance sequence of events. In order to justify the need of additional interest and attention to the unwanted disconnections caused by hidden failures, a “third party” excerpt of [19] is presented:

“An overload itself can damage transmission and generation equipment if it is severe and if it persists long enough. However, virtually all equipment in a power system is protected against a fault with fast acting relays. Therefore, an overload which persists long enough on a piece of transmission or generation equipment usually is disconnected once it fails. However the outage of a *second piece* of equipment due to *relay action* usually results in yet more readjusted power flows and bus voltages that can in turn cause more overloads and cause further removals of equipment. This can cause an uncontrollable cascading series of overloads and equipment removals resulting in shutting down of a large part of the system.”

From the paragraph above, it is important to emphasize the importance that is given to the consequences of the disconnection of a *second piece* of equipment. It is this second and incorrect disconnection the one that may cause the uncontrollable cascading series of overloads and

further removal of equipment: a cascading outage and eventually a wide-area disturbance or blackout.

A core problem of dynamic security assessment, specifically in the contingency screening techniques lies on the extensive number of possible contingencies. For a power system with a few thousands buses, the number of single contingencies is around 5000 [19]. The attempt to consider double contingencies makes this list prohibited [27]. For the development of the contingency list, it has become common to include all the single contingencies and a careful selection of multiple outages [19]. There is a conflict in developing a systematic procedure that determines the “credible contingencies” due to the intrinsically subjective characteristics of the problem.

Considering the problem of defining which contingencies will be considered as “credible,” the attempts to convince system operators to include unwanted disconnections caused by hidden failures would be a hard task. Furthermore, even in the case we could convince them the problem does not finish at that point. As it mentioned in [19], if the current condition of the power system for a imminent contingency is found to be insecure, security control must be applied to bring the power system security level back to an acceptable number. The task of security control is complex in nature since applying controls to improve power system security can increase operating costs, increase duty on equipment, and burden additional work to the dispatcher; control actions normally require finding an optimal point among security, economy and other operational issues [19]. Based on the intrinsic nature of unwanted disconnections caused by hidden failures, the impact on the power system tends to be more severe than single contingencies. Then, considering the complex tasks of security control involved with single contingencies, the complexity level of security control for unwanted disconnections caused by hidden failures tends to be higher.

As it is shown in Figure 41 the problem of unwanted disconnections caused by Hidden Failures under a power system security point of view has two main parts: 1) to include the unwanted disconnections caused by hidden failures in the catalogue of “credible contingencies” and 2) to apply security control for the cases found to leave the system below an acceptable security level.

Since these two parts are not feasible under a pragmatic point of view, the approach proposed in this dissertation is to increase the power system dynamic security by adding a *local monitoring and control system* in order to *avoid* the occurrence of unwanted disconnections caused by Hidden Failures. Considering the nature of the problem of unwanted disconnections caused by Hidden Failures (low probability), the feasible solution is to avoid its occurrence, rather than to change and adjust the power system operation as a preventive measure of its occurrence.

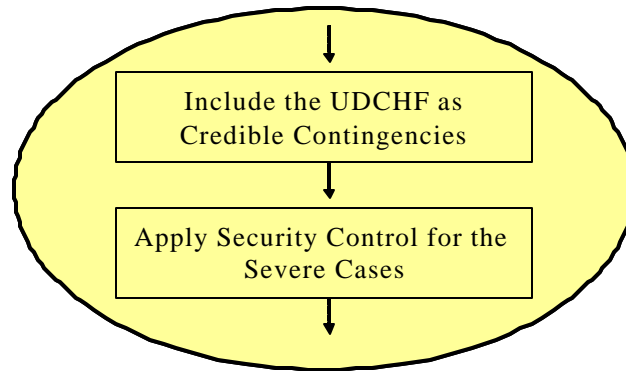


Figure 41: Power System Security Stages for Unwanted Disconnections Caused by Hidden Failures.

The three definitions used to place our methodology in the appropriate perspective were: Security Monitoring, Security Assessment, and Security Enhancement. The use of the index of severity in the power system security context is to rank contingencies within security assessment stage. The final goal is to put the system back into an acceptable security level if any contingency was found to leave the system in an insecure operation. In this dissertation, the index of severity is used to rank protection schemes and *we do not intend to incorporate our index of severity into the power system security methodology*. The solution to the problem is sketched in Figure 42 in which a part of the test system is presented. We intend to increase the power system security by avoiding unwanted disconnections caused by Hidden Failures. The Hidden Failure Monitoring and Control System (HFMCs) have the sole purpose of avoiding the occurrence of the double contingency. As we mentioned previously the index of severity should be able to detect the more severe protection schemes, and these systems are the first candidates to the implementation of the HFMCs.

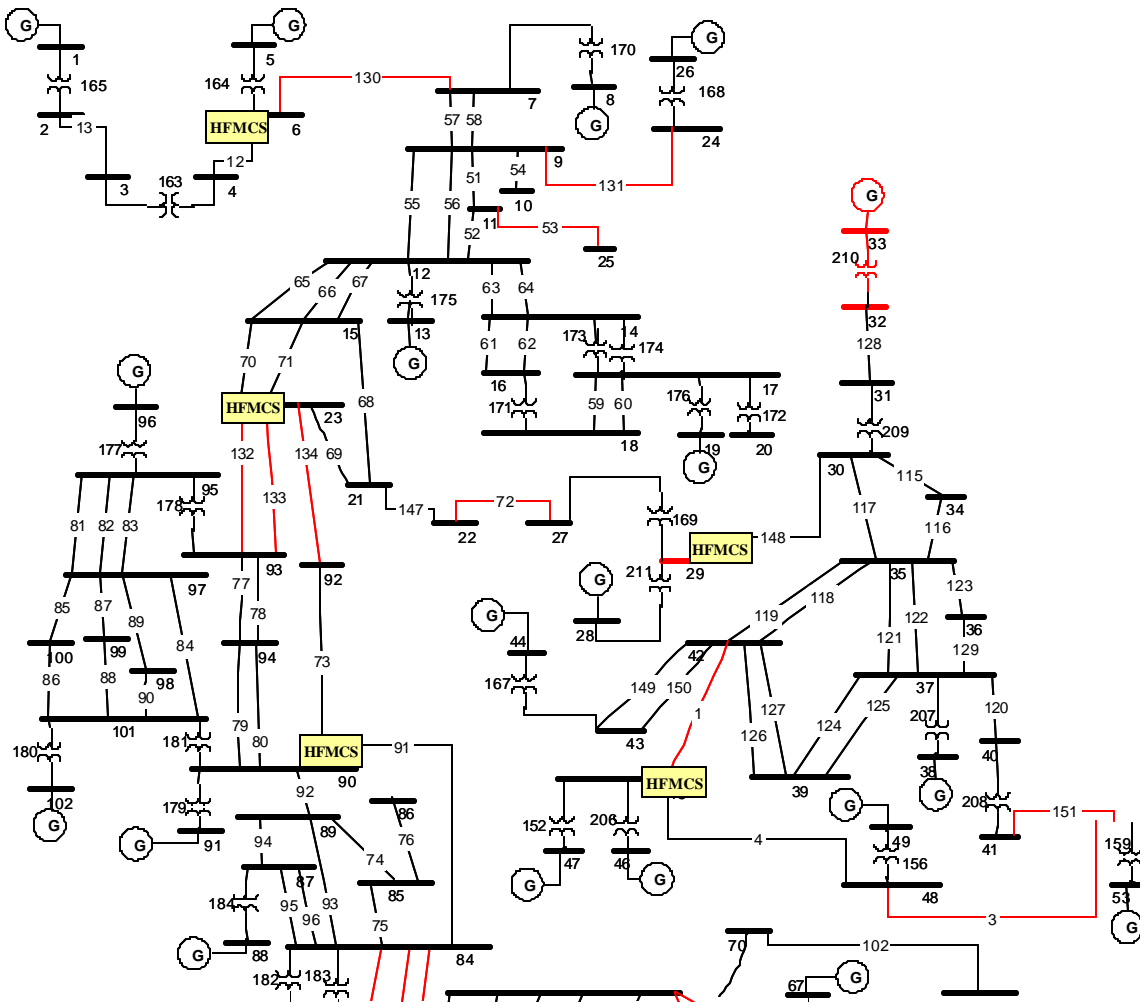


Figure 42: Solution Proposed to the Unwanted Disconnections Caused by Hidden Failures: HFMCs

Individual Indices that conform the Composite Index of Severity

The composite index of severity will be composed by the following individual indices as shown in Table 43.

Table 43: Individual Indices that Conform the Composite Index of Severity

Index ID	Index Description
1	Area in Km of the Region of Vulnerability of the Protection Scheme
2	MW lost due to the operation of Load Shedding Program
3	MW lost due to the operation of Generation Rejection Schemes or relaying action.

The magnitude of the Region of Vulnerability computed in kilometers is captured by index 1. The response of the under frequency load shedding program in terms of total MW lost is captured by index 2. The total lost generation in MW due to the generation rejection schemes or relaying action is captured by index 3.

In addition to the computation of the three above mentioned indices, an assessment of overloads in the remaining equipment and transmission lines is performed for the cases in which the post-contingency condition is found to be stable. Though these overloads are not included in the composite index of severity, if the post-disturbance condition results in overloads, these are displayed as alarm flags that required the operator intervention.

The procedure to compute the loading condition of the post-disturbance equipment is based on a full load flow, which is run without the removed elements due to the contingency. The load flow program that was used was IPFLOW. The equipment and transmission lines thermal rates were computed and an overload factor was determined for the base case. This base case is taken as a reference in order to assess the overload condition of the case that is being evaluated.

The base case equipment rates and loading factors for a number of equipment and transmission lines are included in Table 44. The full list of loading factors is included in the Appendix D. The equipment that is subject to overload assessment is composed of all the transmission lines and the Network transformers. For the Generator Step Up transformers it is assumed that the power flow supplied by the generator will never exceed the transformer capacity due to design considerations.

Table 44: A number of Base Case Transmission Line Loading Factors

Line ID	From Bus	To Bus	Line Thermal Rate	Line Loading Factor
57	7	9	3600	0.76834
58	7	9	3600	0.76834
72	22	27	3000	0.72724
204	103	82	2500	0.71644
153	55	54	1500	0.70006
172	17	20	250	0.65531
69	23	21	2000	0.64444
163	4	3	1210	0.63465
134	23	92	1800	0.63405
77	93	94	1800	0.61743
78	93	94	1800	0.61743
169	27	29	1500	0.60365
171	16	18	2500	0.59507
138	68	104	3000	0.57258
11	51	57	1800	0.57042
8	57	63	1800	0.55631
132	23	93	1800	0.54529
133	23	93	1800	0.53967
2	54	50	2000	0.53099
144	61	63	1630	0.52102
53	11	25	3000	0.50356
73	92	90	2667	0.49526
170	7	8	20000	0.49341
145	59	64	1800	0.48654
146	59	64	1800	0.48654
79	94	90	2450	0.48262
64	14	12	2175	0.46886
63	14	12	2175	0.46353
193	107	108	340	0.43762
194	106	108	340	0.43762
183	83	84	1120	0.43026
178	95	93	840	0.40528
80	94	90	2450	0.40485
182	83	84	840	0.39234
13	3	2	2000	0.38728
71	15	23	2000	0.38425
56	9	12	3000	0.37698
131	9	24	3000	0.36847
185	77	78	1120	0.36273
186	77	78	1120	0.36273

5.2 Simulation Cases of the effects of Hidden Failures in a Power System

This section presents the procedure developed for the simulation cases, the five simulation cases detailed explained, and the computation of the index of severity. The cases presented with its respective index of severity are not comprehensive and we will not present all the possible cases of the test system; rather we will use human expertise in order to select and present only the interesting ones. These cases are selected to show the methodology itself as well as to prove a number of the conjectures that the research group had since the beginning of this work.

5.2.1. Procedure for the Simulation Cases

Figure 43 shows the first part of the algorithm to be followed for each case. The number “1” in the figure is related to the display of the fault location and the relay with the Hidden Failure (HF relay). Every case starts by showing the part of the power system in which the protection scheme belongs, the fault location with respect to the HF relay, and the Region of Vulnerability represented over the line in question.

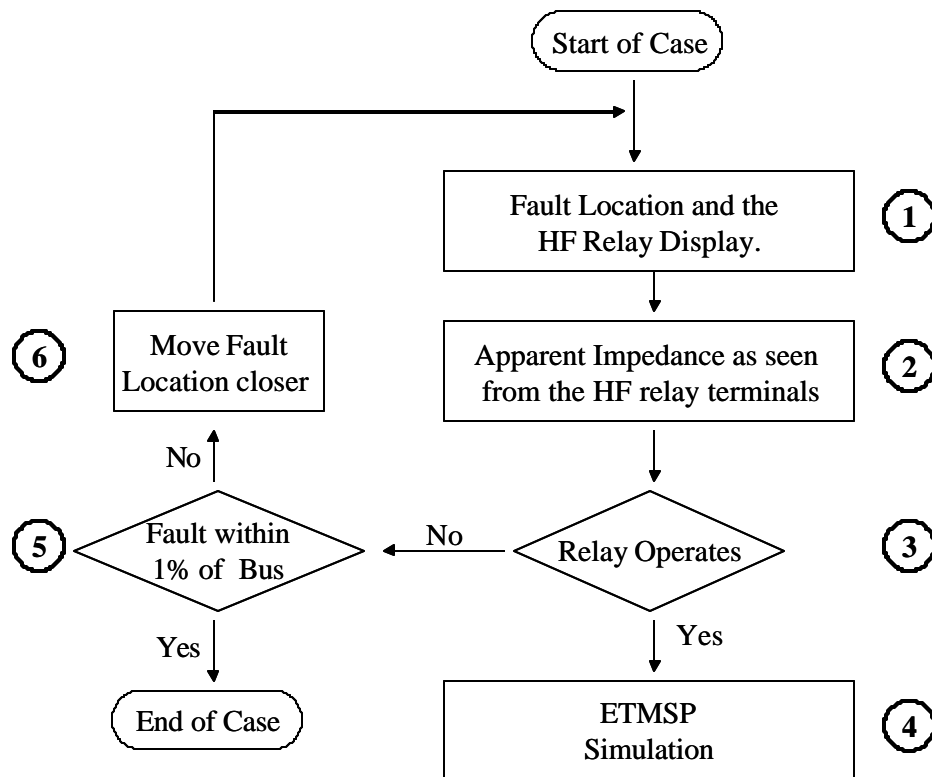


Figure 43: First Part of the Algorithm for the Simulation Cases.

Figure 44 shows a sample of the power system segment that will be shown at the beginning of each case. The HF relay is represented by a square, the fault location with an “X,” and the Region of Vulnerability with dashed and bold lines. The HF relay that is being represented is related to the schemes Zone 2 and directional comparison blocking as explained in Chapter Chapter 4. The HF relay is “looking” in the direction in which the Region of Vulnerability is represented. The dashed lines terminating as shown in the figure indicate the extension of the Region of Vulnerability over the transmission line in question, i.e., it does not cover the entire but a fraction of the transmission line.

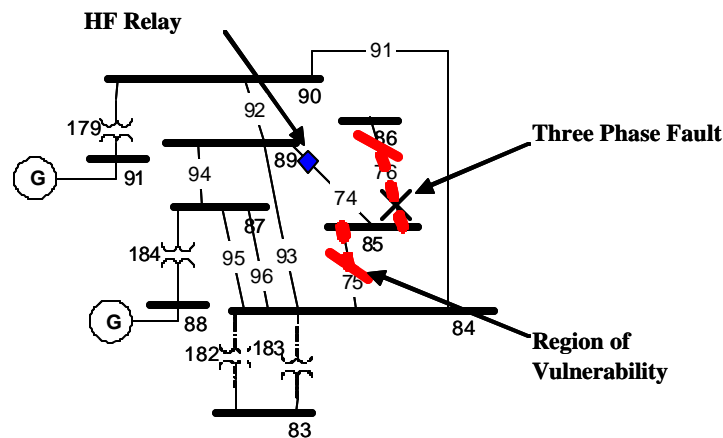


Figure 44: A Sample of the Representation of the Fault Location, HF Relay, and the Region of Vulnerability.

The number “2” in Figure 43 is related to the apparent impedance as “seen” by the relay that defines the Region of Vulnerability for the fault location in question.

Figure 45 shows a sample of the plots to be presented in the cases in order to validate the Region of Vulnerability. The part “a” of the figure shows the apparent impedance as seen by the relay falling inside the relay operating zone; therefore the Region of Vulnerability is Valid.” On the other hand, the part “b” of the figure shows that due to the infeed effect, the apparent impedance falls outside of the relay operating zone and the Region of Vulnerability is “Not Valid.” The plots shown in Figure 45 are the result of monitoring the real and imaginary components of the apparent impedance and were obtained using a simulation in ETMSP during the time the fault is applied.

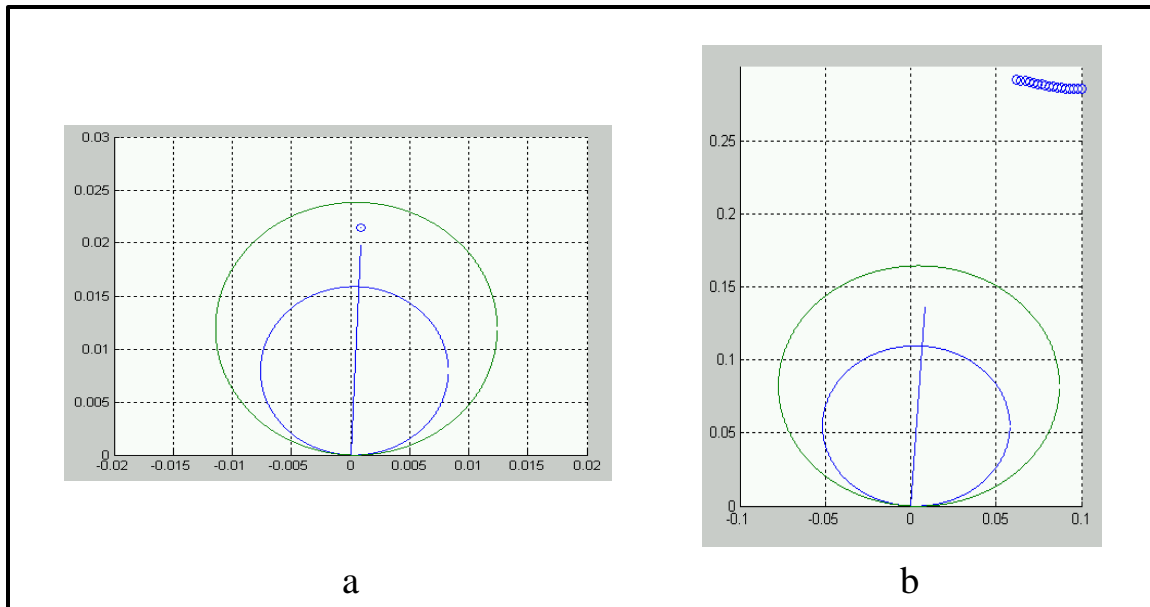


Figure 45: Monitoring the operation of the Relay and the Validation of the Region of Vulnerability

As shown in number “3” of Figure 43, the simulation methodology has a decision point which is related to the operation of the relay. If the relay does “see” the fault the procedure is directed to number “4” of Figure 43, in which the time domain simulation is run. If the relay does not “see” the fault the procedure is directed to number “5” of Figure 43, in which the fault location is adjusted in the search for a valid region of vulnerability. There is a limit in this search and it has been decided to stop the search for a valid Region of Vulnerability when the fault location is within 1 % of the bus.

Figure 46 shows a part of the power system in which the infeed is strong and the Region of Vulnerability was not valid for faults located at 1% from the relay remote bus (bus 42 in the figure). In this situation, the case is terminated since the limit was reached and the Region of Vulnerability was not found to be valid, as shown in Figure 43.

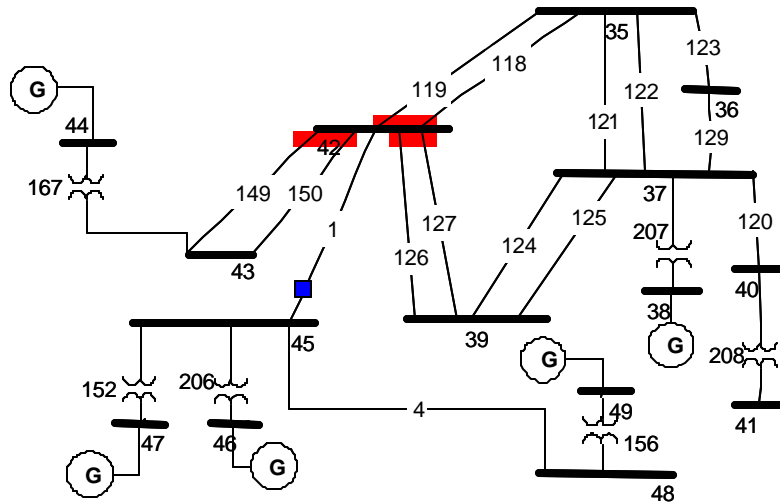


Figure 46: The limit in the Search for a Valid Region of Vulnerability, 1% around the bus in question.

Figure 47 shows the second part of the algorithm for the simulation cases which start with “ETMSP Simulation,” number 7.

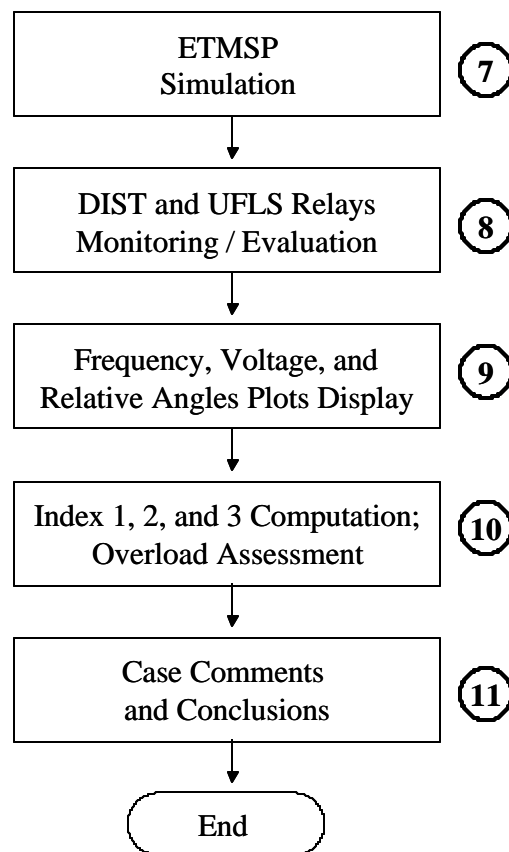


Figure 47: Second Part of the Algorithm for the Simulation Cases

Once the Region of Vulnerability has found to be valid, the time domain simulation is run and the double contingency is applied. The simulation time is 10 seconds and the first contingency is a permanent three phase fault occurring at 1.5 seconds. We are simulating a permanent three phase fault, such as a tower collapse, caused by natural forces or even human forces⁶. The sequence of events of the double contingency is better explained by following Figure 48. At time 1.5 seconds the permanent three phase fault is applied as it is shown with the “X” in the figure. The fault duration is 100 ms, and at 1.6 seconds the circuit breakers of line 83 (number “1” in figure below) have opened both ends to remove the fault. This is the first contingency, the opening of the line 83 in order to isolate the faulted segment of the power system. *Because of the fact the fault has fallen inside the Region of Vulnerability of the HF relay shown, number “2” in the figure*, the second disconnection takes place. This is the unwanted disconnection caused by Hidden Failures, occurs at 1.6 seconds, and opens the breaker of line 84 as shown in Figure 48. Then we have a double contingency, two lines being disconnected of the power system. The permanent characteristics of the fault make the three opened breakers shown in the figure to remain in that condition since reclosing is not applicable. The dynamics of the power system caused by the fault and the switching activities are captured by the transient stability program ETMSP for further analysis and assessment of the consequence.

⁶ At present times the “not credible” events have happened even here at the United States.

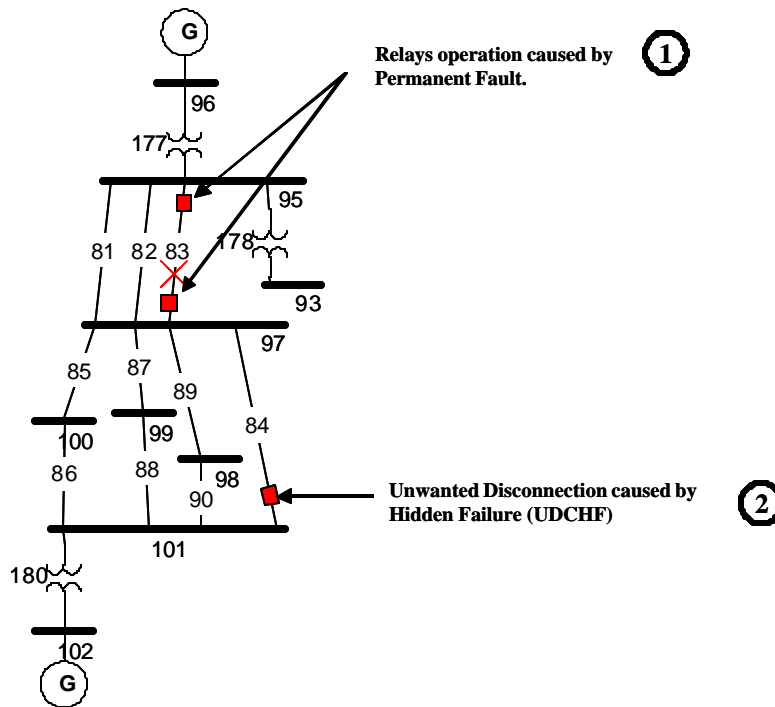


Figure 48: Sequence of Events of the Double Contingency.

Table 45 shows a sample of the contingency description to be presented in each case. The bus numbers correspond to the figure above and the fault was applied at 5% from the Bus 97.

Table 45: A sample of the Contingency Description to be presented in the Cases.

Time (s)	Event Description	From Bus	To Bus	Cid	% From Bus
1.5	Three phase fault on line	97	95	1	5
1.6	Fault Removal	97	95	1	
1.6	Remove Line	97	101	1	

The number “8” in Figure 47 is related to the distance and under frequency relays whose settings were discussed in Chapter Chapter 3. The operation of distance and under frequency relays is monitored by reading an output file from ETMSP. A matlab-based program was designed to read the ETMSP output file and identifies for the distance and underfrequency relays two events: 1) the relay that operated, and 2) the time in which the operation took place. The operation of the distance relays is caused by the voltage and current excursions due to the double contingency and the impact of its operation is taken into account since another element is lost during the simulation. Every time is found that a distance relay has operated, the apparent impedance as “seen” from the relay terminals is monitored in order to validate the result of the ETMSP file. A

sample of the plots used to validate the operation of the distance relays is shown in Figure 49. The operation of the underfrequency relays is utilized to compute the individual index # 2: lost load. The summation of the individual load shed at the buses is computed and attached to this index.

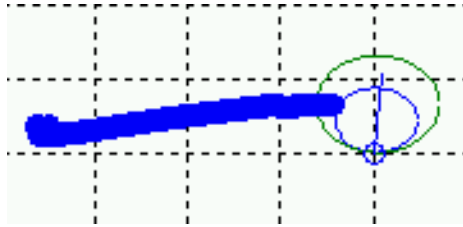


Figure 49: A Sample of the Monitoring of a Distance Relay Operation.

The number “9” in Figure 47 is related to the frequency, voltage, and generator relative angles plots. The ETMSP program handles a list of “input” and “output” files with specific characteristics and purposes, and a number of these files are included in Appendix E. The program capability in terms of output variables is extensive and only the output variables of interest will be shown in Table 46.

Table 46: Selected Output Variables in the Time Domain Simulation.

Element	Variables	Usage
Generators	Terminal Voltage	Visual Inspection, Selected Cases
	Active Generation	Visual Inspection, Selected Cases
	Reactive Generation	Visual Inspection, Selected Cases
	Absolute Generator Angle	Visual Inspection, All Cases
	Speed Deviation	Visual Inspection, All Cases
Buses	Terminal Voltage	Visual Inspection, All Cases
	Voltage Phase Angle	Visual Inspection, Selected Cases
Transmission Lines and Transformers	Active Flow	Visual Inspection, Selected Cases
	Reactive Flow	Visual Inspection, Selected Cases
	Real Apparent Impedance	Visual Inspection, All Cases
	Imaginary Apparent Impedance	Visual Inspection, All Cases

Table 46 shows the output variables that are used in order to analyze the post-disturbance condition of the system. A number of mathematical manipulations are performed and the variables are mainly utilized for the purpose of determining the post-disturbance condition in terms of stability: rotor angle, voltage, and frequency. In the “Usage” column in Table 46 the

variables with the “Visual Inspection, All Cases” are the parameters that are monitored for all the cases regardless the consequence or impact of the double contingency. On the other hand, the “Visual Inspection, Selected Cases” are the parameters that are only used on special cases, usually the ones that end up in a system-wide consequence in the power system.

As it is known, the results of a time domain simulation require of human expertise in the sense of interpreting the simulation results. For each case, the relative angles and the speed deviation of each of the machines in the test system are displayed in plots so the simulation results may be visually evaluated. These plots provide a general view of the case rotor angle stability. For the relative angle computation, the machine taken as a reference is Bus number 13. For the speed deviation or frequency plots, the machine frequencies that result *after* the operation of the Under Frequency Load Shedding Scheme (if it actually happens) are displayed. The frequency on the buses without generation is not available as an output variable in ETMSP, and then we are monitoring frequency on all the machine buses. With respect to voltage stability, only buses with relative large excursions in the voltage magnitude are displayed in the voltage related plots.

The number “10” in Figure 47 is related to the computation of the index of severity. As it was mentioned earlier, the magnitude of the Region of Vulnerability, the lost load, and the lost generation are the individual indices to evaluate the composite index of severity. After these calculations and for the cases in which the post-disturbance does not result in instability, the overload condition of the remaining power system is assessed. The last step in the algorithm for the simulation cases is a series of comments and conclusions related to the case in question, as the number “11” of Figure 47 illustrates.

5.2.2. Simulation Cases

This section presents the cases in which the unwanted disconnections caused by hidden failures are simulated in ETMSP according to the procedure previously described.

5.2.2.1. Case Relay 101-97

The protection scheme to evaluate in this case is the relay 101-97. Figure 50 shows the segment of the power system in which the protection scheme belongs, the region of vulnerability, and the fault location. As we can see in the figure, the Region of Vulnerability expands over the lines 81, 82, 83, 85, 87, and 89, covering a fraction of each of these lines. The ratio of the relay setting with respect to the impedance of line 83 is .822; therefore the Region of Vulnerability is represented as it is shown in Figure 50.

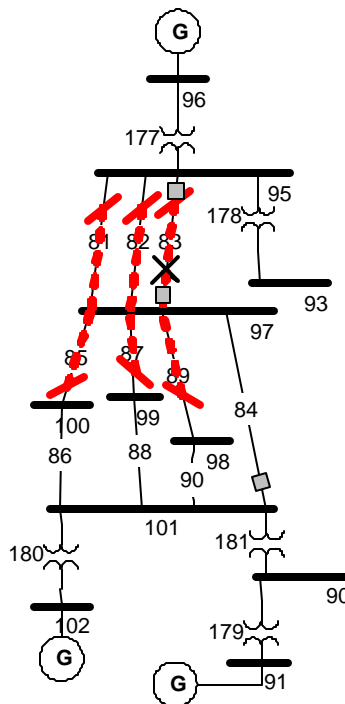


Figure 50: Protection Scheme 101-97, its Region of Vulnerability, and the Fault Location.

Table 47 shows the representation of the Region of Vulnerability over the line 83 in three different dimensions before the validation process; this is the point C of the procedure of section 4.2.4. We can see that the Region of Vulnerability expands over the line 83 up to 45.14 Km measured from bus 97 and this is the starting point for the validation process. In this case the

fault was placed at an impedance of .0034 per unit from Bus 97, which when referred to the kilometers value results in a fault location over the line 83 at 2.75 kilometers from bus 97.

Table 47: Representation of the Region of Vulnerability and Location of the Fault, Relay 101-97.

Description	Per Unit	Ohms	Km
Region of Vulnerability represented in Line 83 before the validation process	0.0554	22.14	45.14
Impedance to the Fault, from bus 97	0.0034	1.35	2.75

Table 48 shows the contingency description for the relay 101-97. As the table describes, the fault is located over line 83, at 5% from bus 97, and at time 1.6 seconds the system has been exposed to a double contingency.

Table 48: Contingency Description for the Relay 101-97.

Time (s)	Event Description	From Bus	To Bus	Cid	% From Bus
1.5	Three phase fault on line	97	95	1	5
1.6	Fault Removal	97	95	1	
1.6	Remove Line	97	101	1	

Figure 51 shows the apparent impedance seen by the relay for the fault location previously described. As we can see in the figure, the impedance falls inside the relay operating zone and then the Region of Vulnerability is “Valid.”

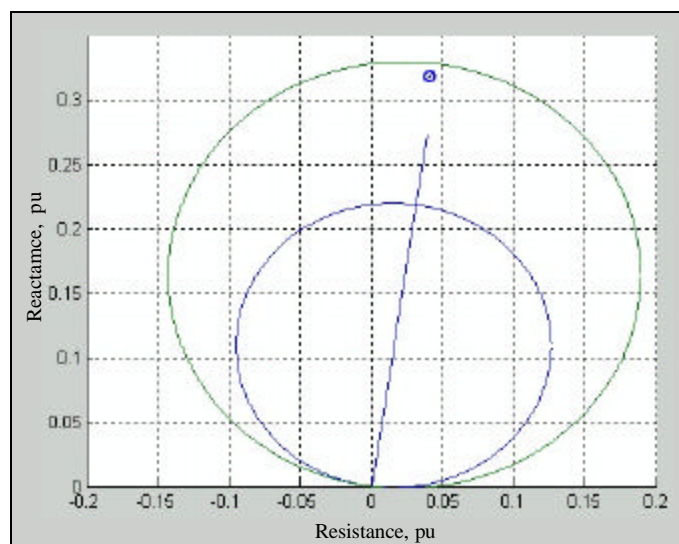


Figure 51: Apparent Impedance seen by the Relay 101-97 during the fault period.

Table 49 shows that there are none distance relay operations during the 10 seconds simulation time.

Table 49: Distance Relays Operated during the Relay 101-97 Case.

Time (s)	Bus ID
None	None

Figure 52 shows that the frequency deviations are not severe and the frequency trend along the time axis presents damped oscillations. The generator with the biggest change in frequency is 96, which is electrically closer to the fault as we can see in Figure 50.

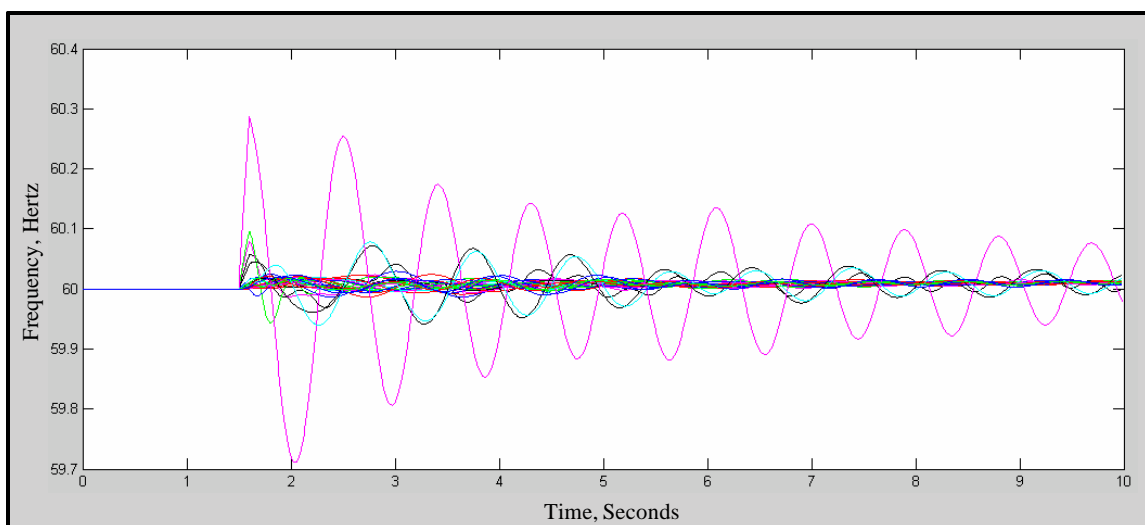


Figure 52: Generators Frequency Response for the Relay 101-97 Case.

Table 50 shows that there are none under frequency relay operations during the 10 seconds simulation time.

Table 50: Under Frequency Relays Operated during the Relay 101-97 Case.

Time (s)	Bus ID
None	None

Figure 53 shows that the relative angle variation is quite small, and the machine relative angles get damped over time. The machine with the biggest change in relative angle is generator number 96, which is electrically closer to the fault. A new steady state condition is reached, and instability is not an issue in this case.

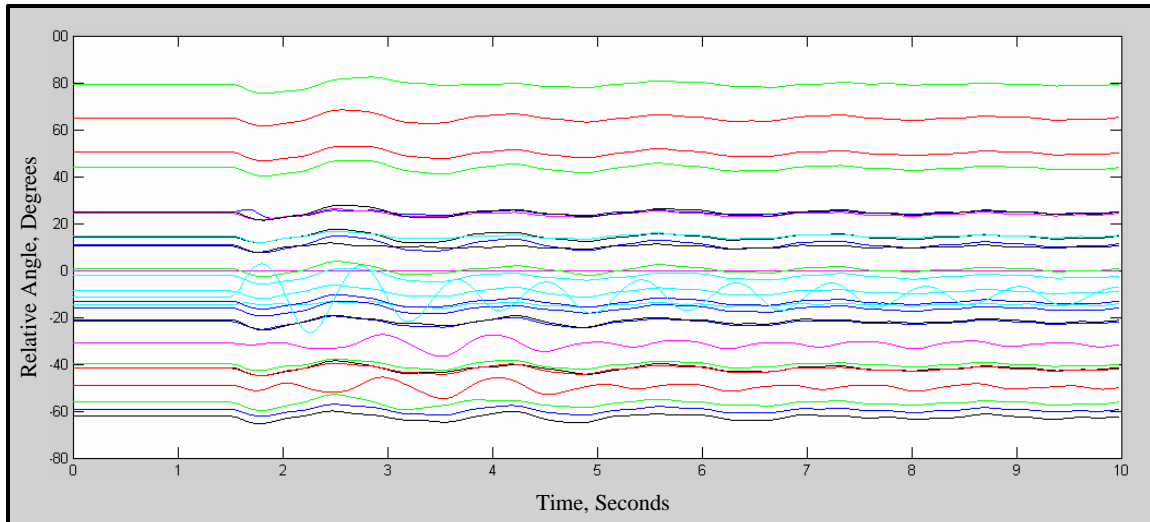


Figure 53: Generator Relative Angles Response for the Relay 101-97 Case.

Figure 54 shows the voltage magnitude of the most affected buses in the system: buses 73 to 108. The buses shown are the closest to the fault, and some voltage magnitudes show a considerable transient depression (values of .1 pu). Bus 97 is the most affected during the time the fault is applied (1.5 to 1.6 seconds).

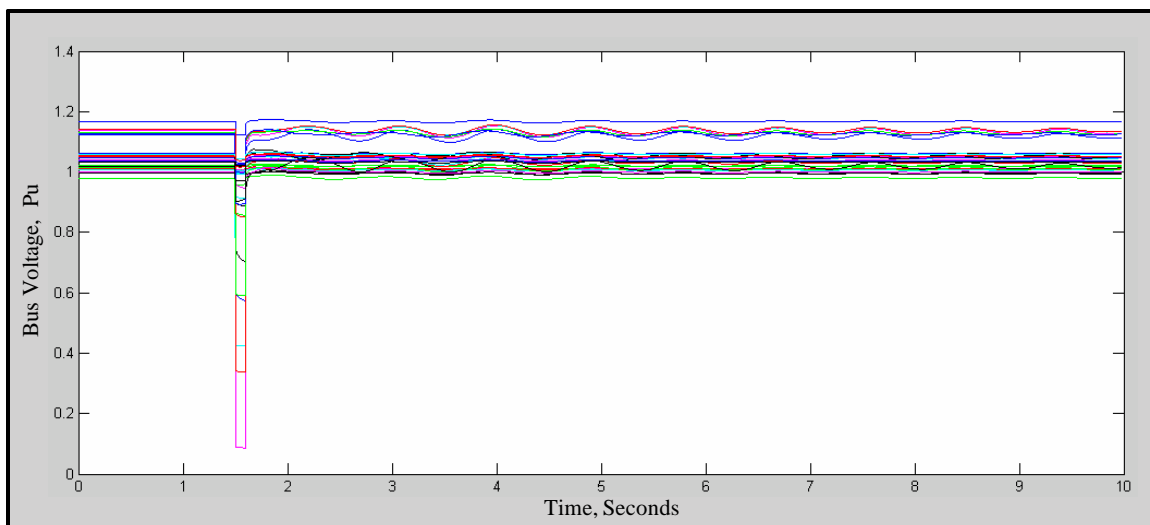


Figure 54: More Affected Bus Magnitudes for the Relay 101-97 Case.

Figure 55 shows the voltage magnitude of the least affected buses in the system: buses 109 to 127. The buses shown are relatively far from the fault and the voltage magnitude variations are practically negligible.

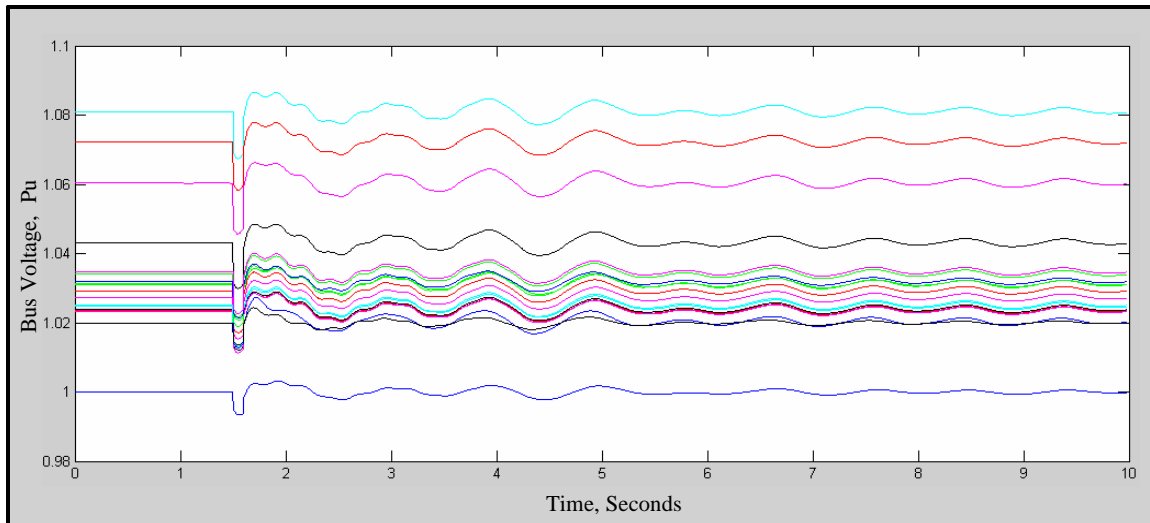


Figure 55: Less Affected Bus Magnitudes for the Relay 101-97 Case.

The assessment of the post-contingency state of the power system with respect to the overload condition using the procedure described in Appendix D is presented in Table 51. As we can see in the table, there is no consequence in the form of overloads in transmission lines or transformers since the maximum loading factor remains in the same line for the pre and post contingency power system topologies.

Table 51: Overload Assessment for the Relay 101-97 Case.

Pre Contingency Maximum Overload Factor	Post Contingency Maximum Overload Factor
0.768	0.768

Table 52 shows the overall evaluation of Relay 101-97 case. As it is shown, there is no load lost, there is no generation lost, and the static overload status was found without any problems.

Table 52: Overall evaluation for the Relay 101-97 Case.

Case Number	Region of Vulnerability (Km)	Lost Load (MW)	Lost Generation (MW)	Post Contingency Overload Status
Relay 101-97	20.15	0	0	Not Overload

The index of severity of this case will be evaluated in section 5.2.3.

5.2.2.2. Case Relay 84-90

The protection scheme to evaluate in this case is the relay 84-90. Figure 56 shows the segment of the power system in which the protection scheme belongs, the region of vulnerability, and the fault location. As we can see in the figure, the Region of Vulnerability expands over the lines 79, 80, 73, and 92, covering a fraction of each of these lines. The ratio of the relay setting with respect to the impedance of line 92 is 0.2920; therefore the Region of Vulnerability is represented as it is shown in Figure 56.

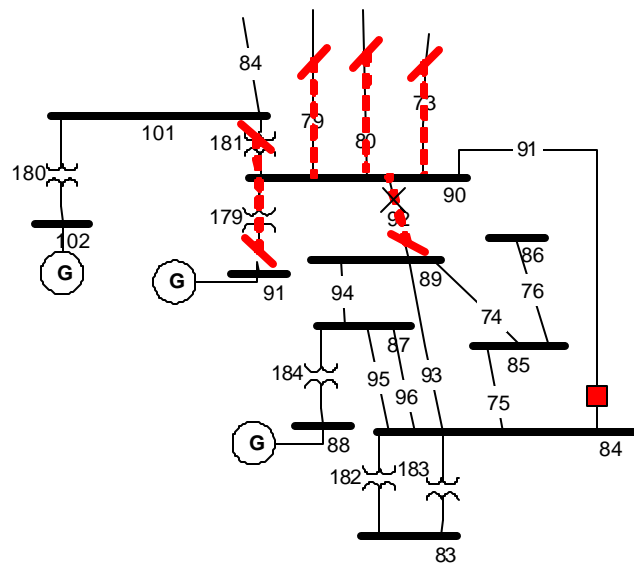


Figure 56: Protection Scheme 84-90, its Region of Vulnerability, and the Fault Location.

Table 53 shows the representation of the Region of Vulnerability over the line 92 in three different dimensions before the validation process. We can see that the Region of Vulnerability expands over the line 92 up to 57.647 Km measured from bus 90 and this is the starting point for the validation process. In this case the fault was placed at an impedance of 0.00026 per unit from Bus 90, which when referred to the kilometers value results in a fault location over the line 92 at 1.974 kilometers from bus 90.

Table 53: Representation of the Region of Vulnerability and Location of the Fault, Relay 84-90.

Description	Per Unit	Ohms	Km
Region of Vulnerability represented in Line 92 before the validation process	0.0075	18.8047	57.647
Impedance to the Fault, from bus 90	0.00026	0.64394	1.974

Table 54 shows the contingency description for the relay 84-90. As the table describes, the fault is located over line 92, at 1% from bus 90, and at time 1.6 seconds the system has been exposed to a double contingency.

Table 54: Contingency Description for the Relay 84-90.

Time (s)	Event Description	From Bus	To Bus	Cid	% From Bus
1.5	Three phase fault on line	90	89	1	1
1.6	Fault Removal	90	89	1	
1.6	Remove Line	90	84	1	

Figure 57 shows the apparent impedance seen by the relay for the fault location previously described. As we can see in the figure, the impedance falls inside the relay operating zone and then the Region of Vulnerability is “Valid.”

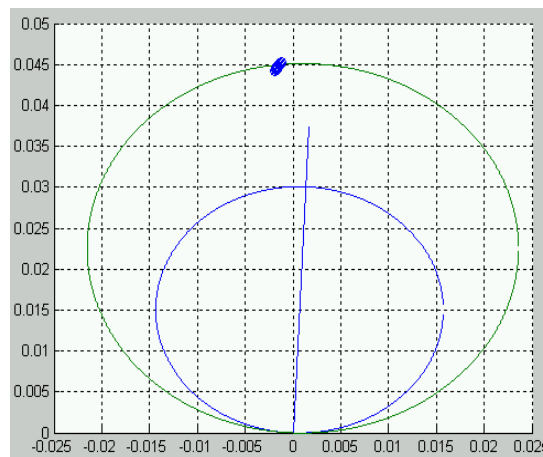


Figure 57: Apparent Impedance seen by the Relay 84-90 during the fault period.

Table 55 shows that there are three distance relay operations during the 10 seconds simulation time.

Table 55: Distance Relays Operated during the Relay 84-90 Case.

Time (s)	From Bus	To Bus
5.76	48	45
6.04	37	40
7.69	45	42

Figure 58 shows the localization of the distance relays that operated due to the power system parameters excursions.

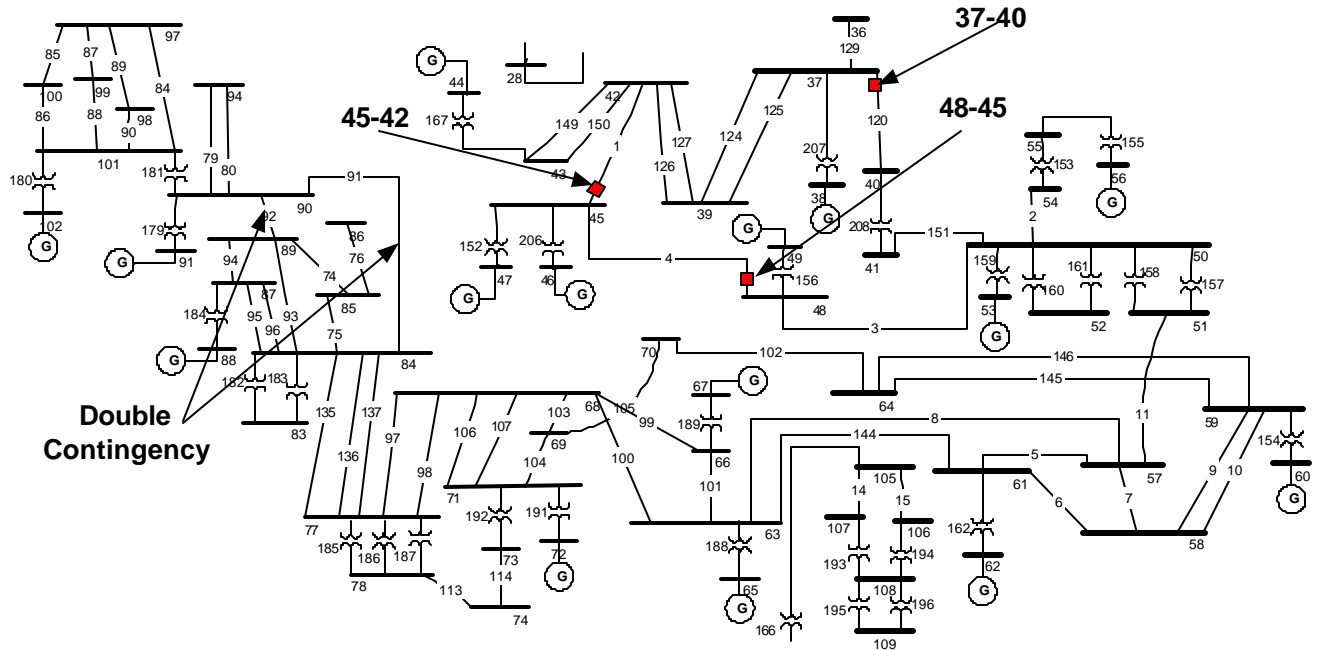


Figure 58: Localization of the Distance Relays that operated in the Sample System for Relay 84-90 Case.

Figure 59 shows the travel of the apparent impedance as seen by the relay terminals as a function of the simulation time. The two disconnections in the power system caused a redistribution of the power flows that affect directly the lines whose distance relays operated.

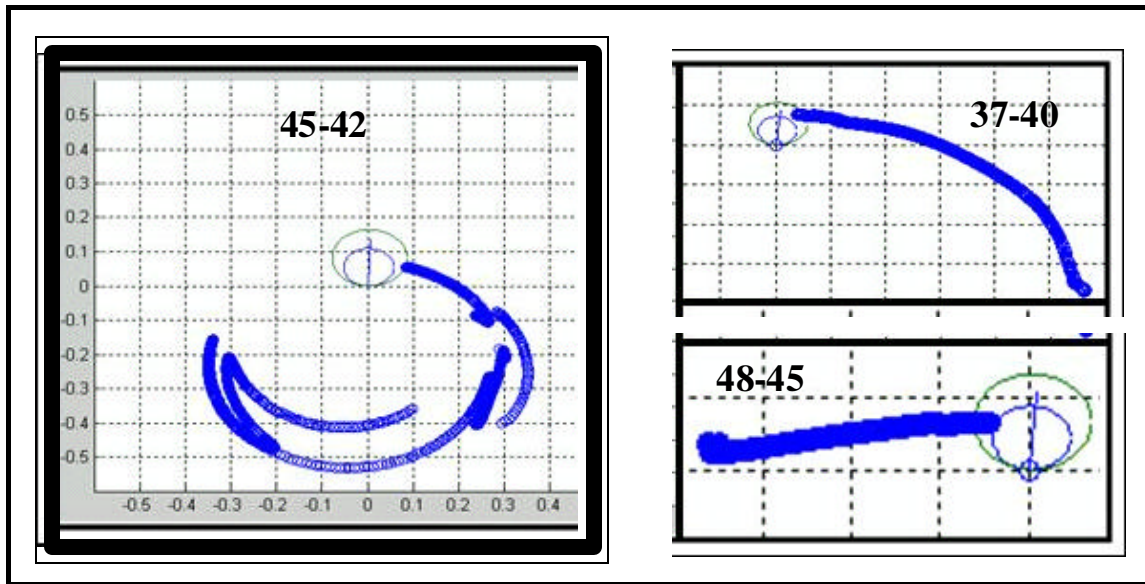


Figure 59: Apparent Impedance as seen by the distance relays that operated due to the excursion of the power system parameters.

The first relay that operated was relay 48-45 at a time of 5.76 seconds. The real power of the line 48-45 is shown in Figure 60. As we can see in the figure, the real power increased drastically during the 2 to 5.5 seconds time frame until it reached the point in which the operating conditions encroached the relay zone.

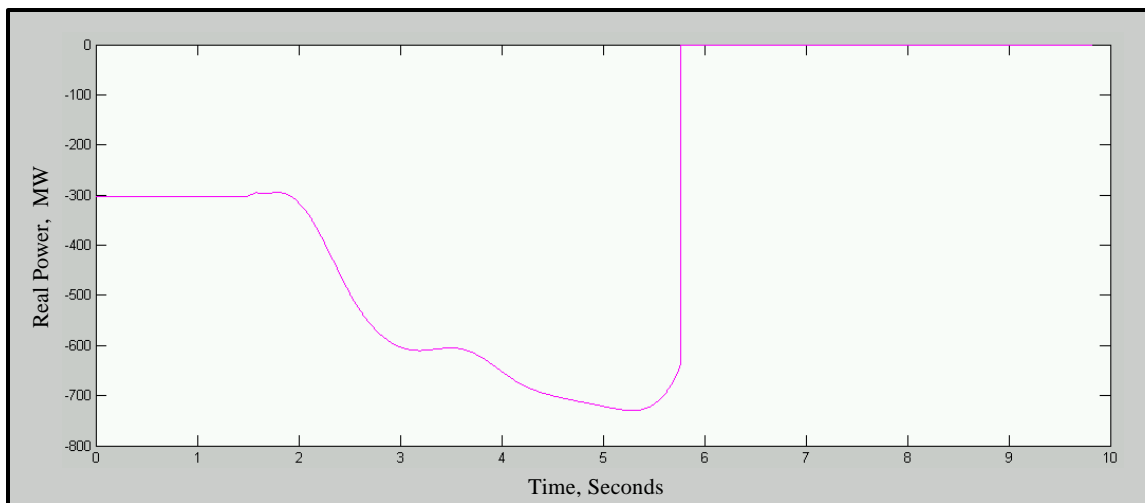


Figure 60: Real Power of the Line 48-45 that was switched open due to the operation of the relay 48-45.

Figure 61 shows the real power in the lines that were disconnected by the operation of the distance relays. The time in which each line was disconnected is presented as can be used to identify each transmission line.

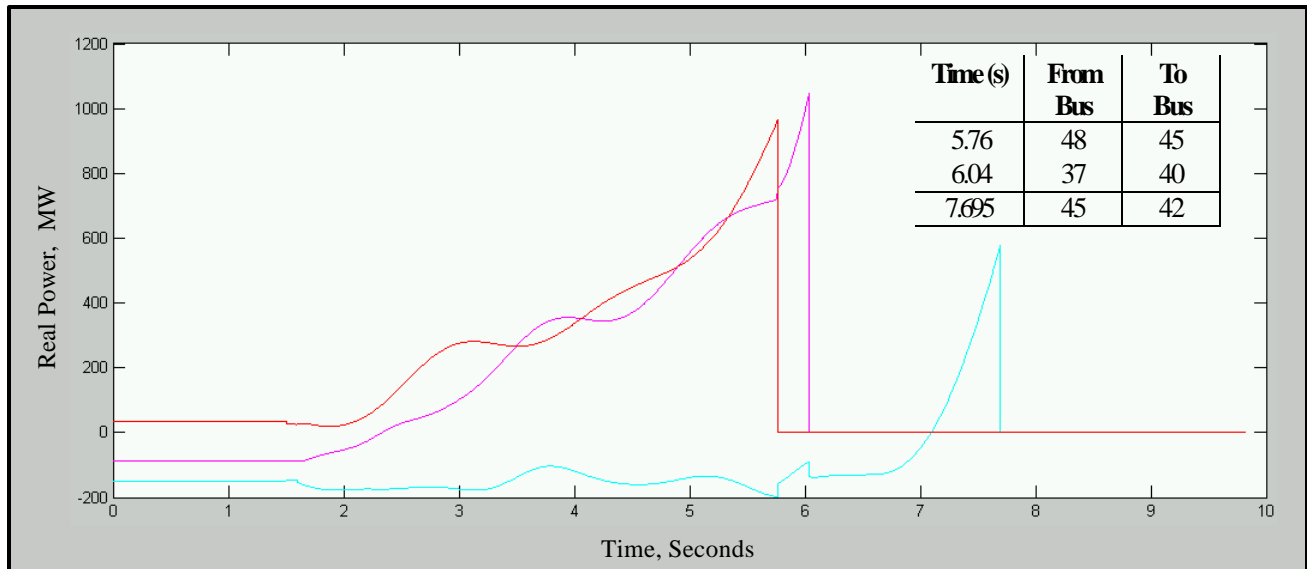


Figure 61: Real Power of the Lines that were switched open due to the operation of Distance Relays.

Figure 62 shows the frequency of the machines for this case. Clearly from the figure we can see three main generator clusters: 1) the group whose frequencies are left above nominal; 2) the group whose frequencies are left below nominal; and 3) the group whose frequencies are increasing steadily.

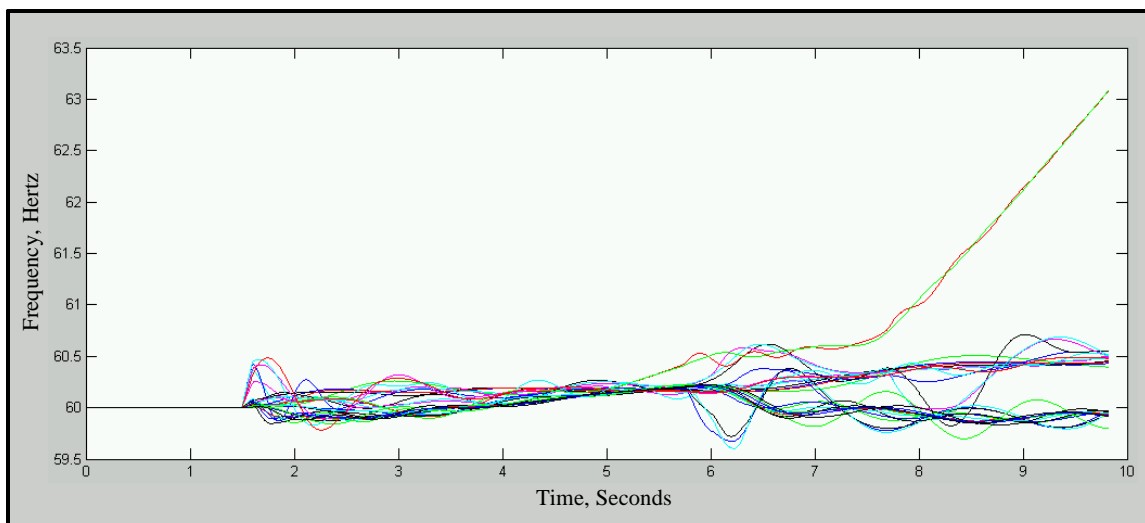


Figure 62: Generators Frequency Response for the Relay 84-90 Case.

The identification of the generator clusters are shown in Table 56.

Table 56: Identification of the Generator Clusters for Relay Case 84-90.

Group Number	Generators ID	Remarks
1	1, 5, 8, 13, 19, 26, 28, 33, 38, 44, 91, 96 and 102	Machines that are located in the North, the area of Generation Surplus
2	49, 53, 56, 60, 62, 65, 67, 72, 76, 81, 88, 113, 119 and 126	Machines that are located in the South, the area of Generation Deficit
3	46, 47	Generation stations that were left without any transmission capacity and therefore are running out of step.

Table 57 shows the operation of the under frequency relays during 10 seconds simulation time. The relays operated thirty three times and there are buses in which the three under frequency load shedding steps were reached.

Table 57: Under Frequency Relays that operated for the Relay 84-90 Case.

Bus ID	Time (s)
89	1.97
83	1.975
85	1.975
80	1.985
75	2.39
74	2.45
75	2.535
82	2.73
124	2.745
117	2.745
111	2.755
116	2.755
48	6.2
50	6.225
55	6.23
48	6.245
55	6.265
50	6.275
48	6.285
50	6.285
55	6.285
75	8.4301
74	8.4351
78	8.4751
108	8.5151

Bus ID	Time (s)
74	8.5151
71	8.5601
68	8.5701
69	8.6101
59	9.0901
58	9.1001
63	9.1301
64	9.1701

Figure 63 shows the localization of the buses in which the under frequency relays operated.

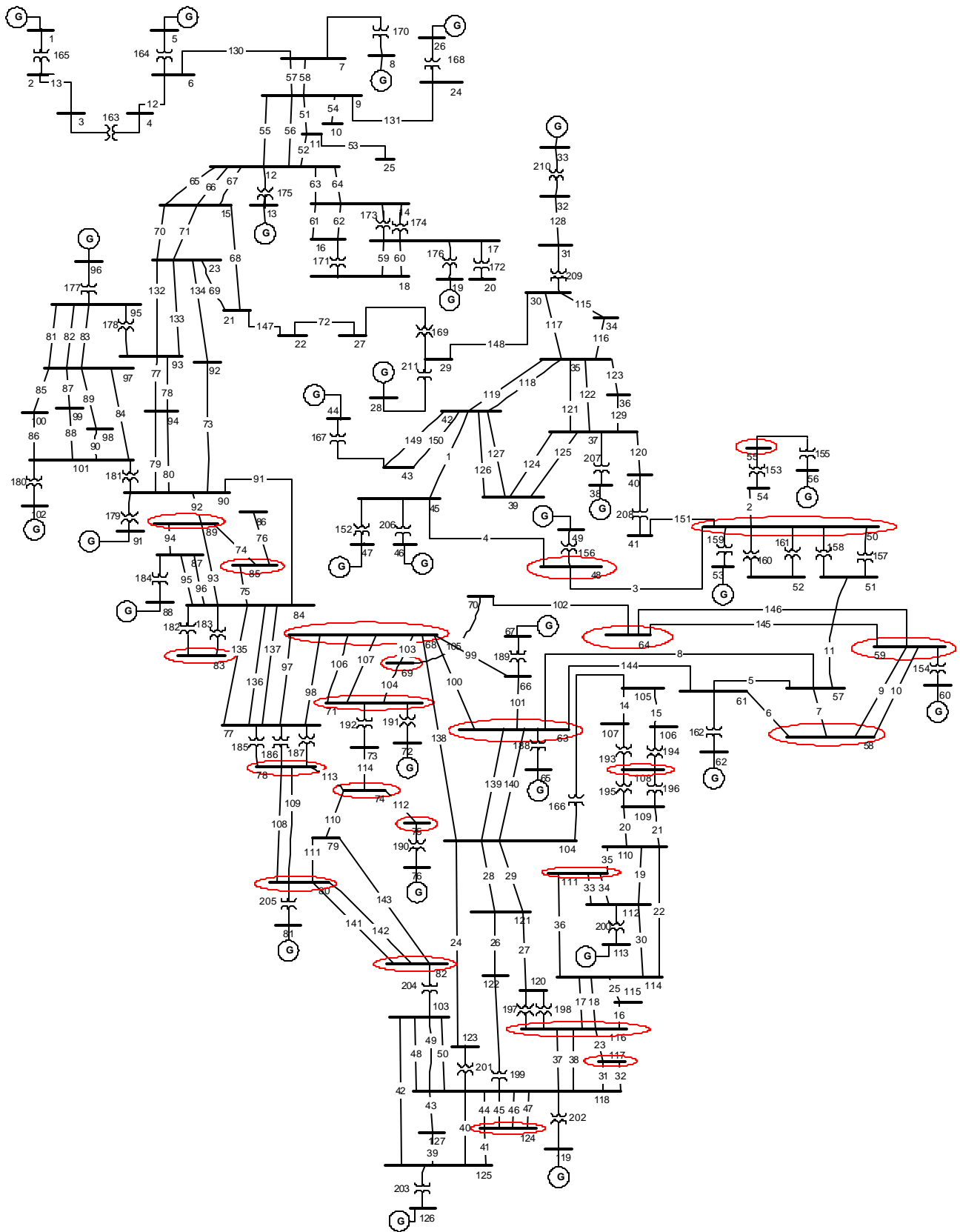


Figure 63: Localization of buses in which the Under Frequency Relays Operated for case 84-90.

Figure 64 shows the generator relative angles in which the three main groups of generators are clearly identified. The system separation starts around 1.8 seconds and within the 6 to 7 seconds time frame two machines have lost the transmission capacity and are drastically pulled into out of step conditions.

This case is a particular example in which the credibility of the results is based on the extent of the models used. The angles of the machines in the figure below show drastic and unrealistic deviations. Other not modeled protection and controls such out of step relays would have operated to separate the system given the contingency. The credibility of these results would be enhanced as we increase the accuracy of the models.

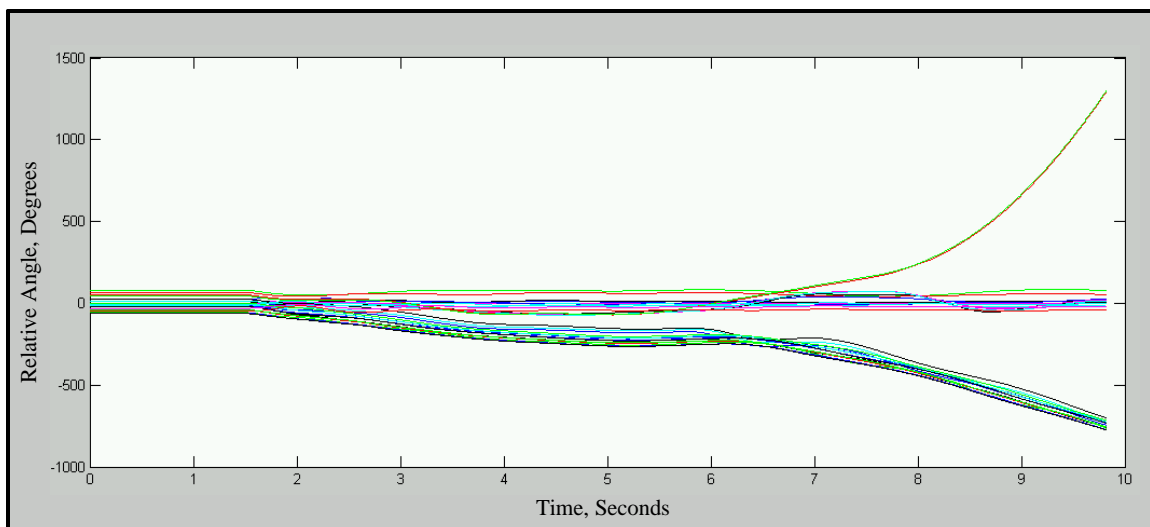


Figure 64: Generator Relative Angles Response for the Relay 84-90 Case.

The redistribution of power flows after the second contingency affected drastically a number of transmission lines in the sample system and these elements are presented in Figure 65.

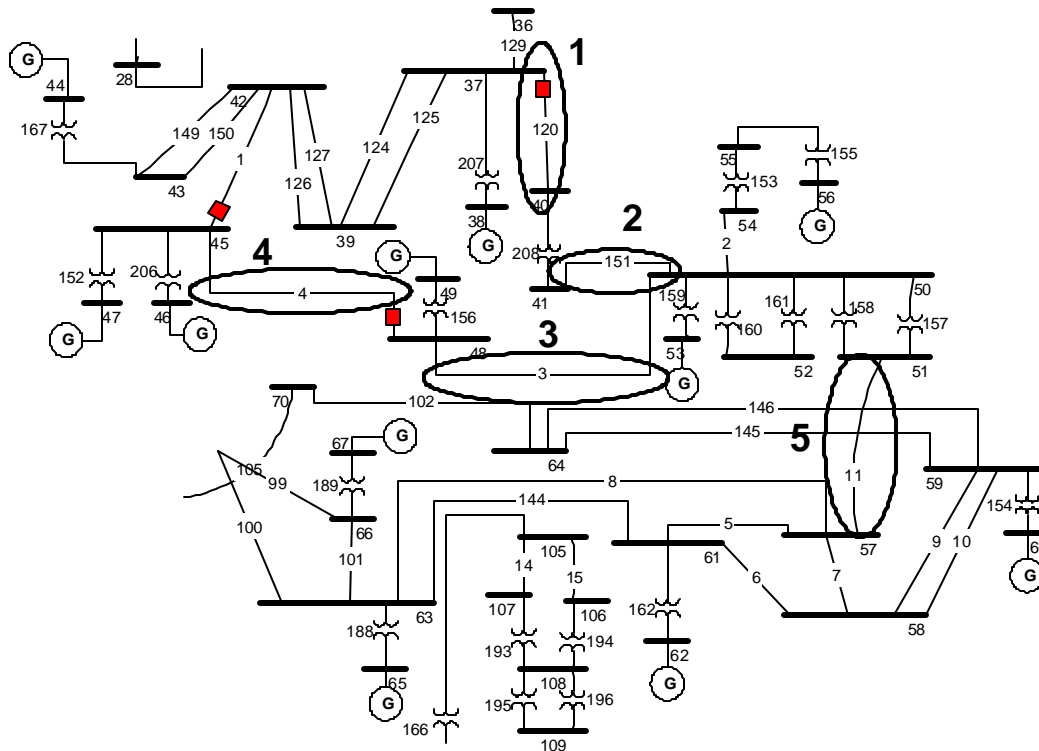


Figure 65: Power System Elements affected by the re-distribution of power flows after the second contingency.

Figure 66 shows the voltage magnitude of the buses 36 to 73. The transient voltage depression caused by the fault is not considerable in these buses. The voltage profile of the buses 40 and 41 presents a drastic reduction which is alleviated by the operation of the distance relay 37-40. Buses 40 and 41 were marked with an ellipse and the number “1” in the Figure 65.

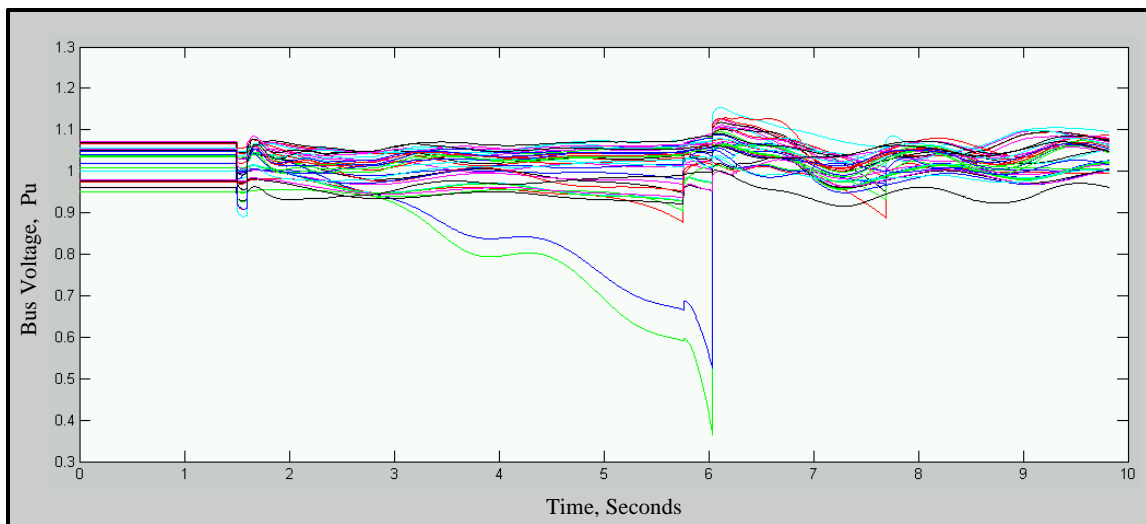


Figure 66: Voltage Magnitude of the Buses 36 to 73, Relay 84-90 Case.

Figure 67 shows the voltage profile of the buses 40 and 41 and the power in the line 37-40 (see Figure 65, number “1”). As we can see in the figure the real power increased steadily from 1.5 to 4 seconds. The rate of increase of power is relatively high; at a voltage level of .9 pu (a relatively acceptable voltage level during transients) the arrow in Figure 67 shows that the power in the transmission line has increased from 150 to 550 MW.

Clearly, the voltage conditions shown in Figure 67 after 3.15 seconds are not operable conditions and “other controls” would probably have operated before the voltage was depressed that much to make operate the distance relays. The thermal capacity of the line and the reaction of the load to the voltage depression are issues that, if modeled, would most probably change the output results.

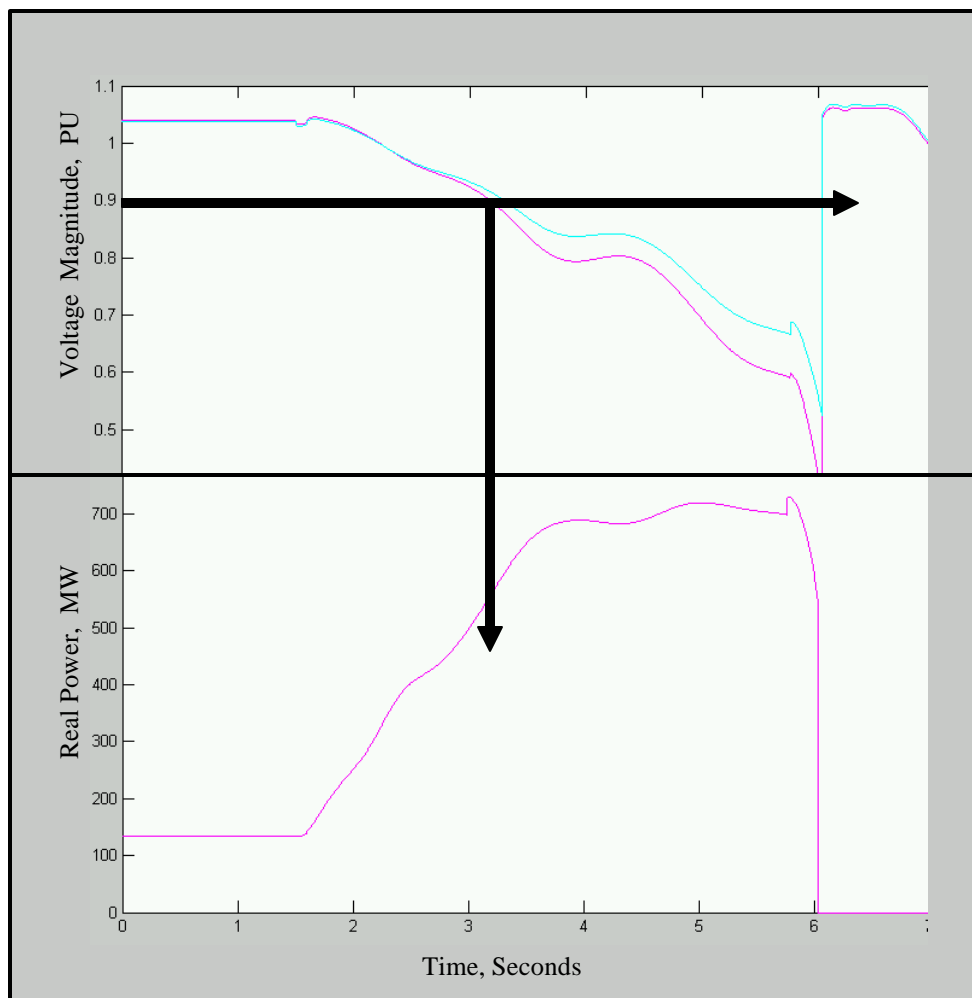


Figure 67: Voltage Profile in the Bus 40 and 41 and its relationship with Real Power through the line 37-40, for the Relay 84-90 Case.

Figure 68 shows the real and reactive power in the line 37-40. The profile on the reactive power in the line is particular since it actually reverses the direction as a consequence of the switching events. From 1.6 seconds to 6 seconds the reactive power changed from a minus 100 MVAR to a plus 1000 MVAR. Once again, these conditions could have been prevented by other, no modeled controls. Part of these controls could be the reactive power limits of the near by generators.

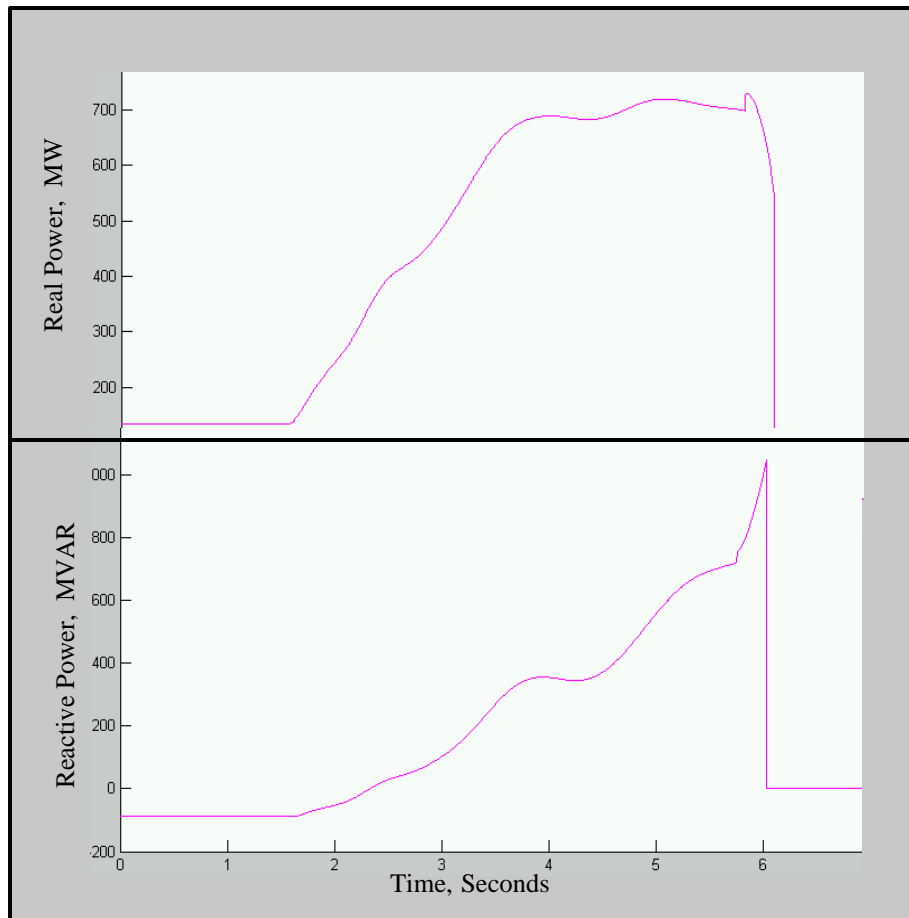


Figure 68: Real and Reactive Power Profile in the Line 37-40 for the Relay 84-90 Case.

Figure 69 shows the real power profile of the line 11 which is marked in Figure 65, number “5.” As we can see in the figure the real power increased steadily from 1.6 to 3 seconds, and the maximum power was around 2000 MW until the relay at bus 37-40 operates (6 seconds), causing power oscillations and reversal of power.

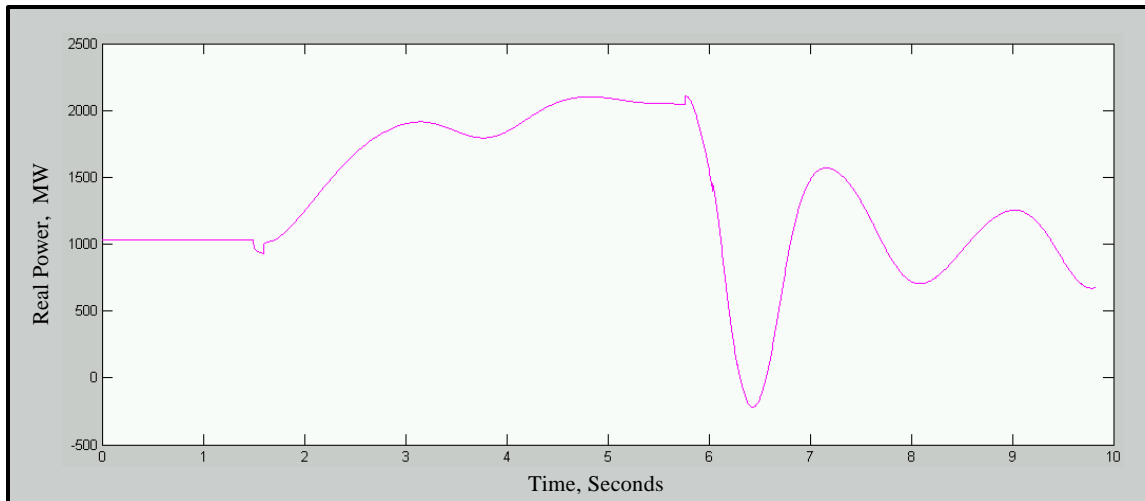


Figure 69: Real Power Profile in the Line 11, see Figure 65, number “5,” Relay 84-90 Case.

Table 58 shows the overall evaluation of Relay 84-90 case. As it is shown, there is lost load, generation lost, and the static overload evaluation does not apply in this case.

Table 58: Overall evaluation for the Relay 84-90 Case.

Case Number	Region of Vulnerability (Km)	Lost Load (MW)	Lost Generation (MW)	Post Contingency Overload Status
Relay 84-90	9.79	1717	3098	System Separation

The index of severity of this case will be evaluated in section 5.2.3

5.2.2.3. Case Relay 89-85

The protection scheme to evaluate in this case is the relay 89-85. Figure 70 shows the segment of the power system in which the protection scheme belongs, the region of vulnerability, and the fault location. As we can see in the figure, the Region of Vulnerability expands over the lines 75 and 76, covering a fraction of each of these lines. The ratio of the relay setting with respect to the impedance of line 76 is 0.3061; therefore the Region of Vulnerability is represented as it is shown in Figure 70.

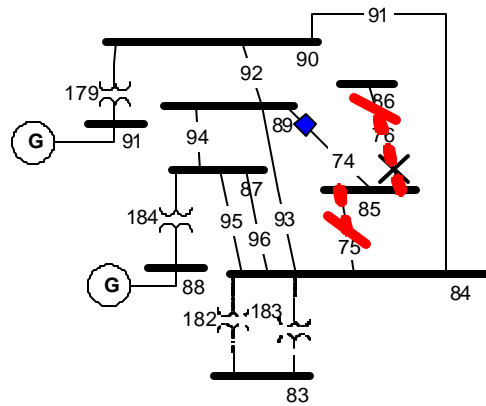


Figure 70: Protection Scheme 89-85, its Region of Vulnerability, and the Fault Location.

Table 59 shows the representation of the Region of Vulnerability over the line 76 in three different dimensions before the validation process. We can see that the Region of Vulnerability expands over the line 76 up to 30.45 Km measured from bus 85 and this is the starting point for the validation process. In this case the fault was placed at an impedance of 0.0006 per unit from bus 85, which when referred to the kilometers value results in a fault location over the line 76 at 4.974 kilometers from bus 85.

Table 59: Representation of the Region of Vulnerability and Location of the Fault, Relay 89-85.

Description	Per Unit	Ohms	Km
Region of Vulnerability represented in Line 76 before the validation process	0.0040	9.9337	30.452
Impedance to the Fault, from bus 85	0.0006	1.6226	4.974

Table 60 shows the contingency description for the relay 89-85. As the table describes, the fault is located over line 76, at 5% from bus 85, and at time 1.6 seconds the system has been exposed to a double contingency.

Table 60: Contingency Description for the Relay 89-85.

Time (s)	Event Description	From Bus	To Bus	Cid	% From Bus
1.5	Three phase fault on line	86	85	1	95
1.6	Fault Removal	86	85	1	
1.6	Remove Line	85	89	1	

Figure 71 shows the apparent impedance seen by the relay for the fault location previously described. As we can see in the figure, the impedance falls inside the relay operating zone and then the Region of Vulnerability is “Valid.”

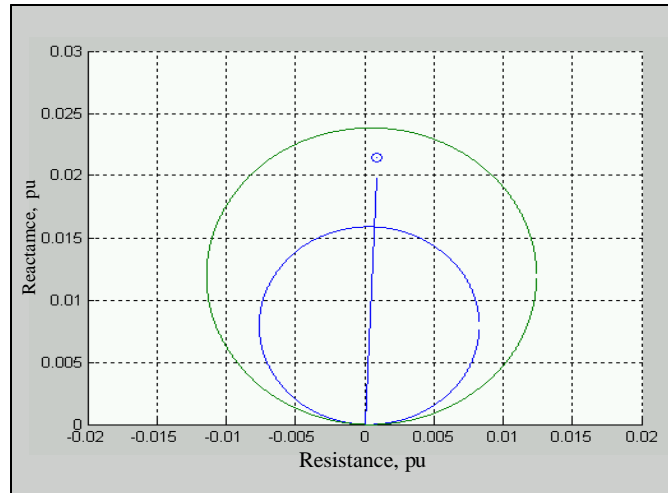


Figure 71: Apparent Impedance seen by the Relay 89-85 during the fault period.

Table 61 shows that there are none distance relay operations during the 10 seconds simulation time.

Table 61: Distance Relays Operated during the Relay 89-85 Case.

Time (s)	Bus ID
None	None

Figure 72 shows that the frequency deviations are not severe and the frequency trend along the time axis presents damped oscillations. The frequency tends to settle to a slightly higher nominal value due to the load lost of bus 86 which was de-energized.

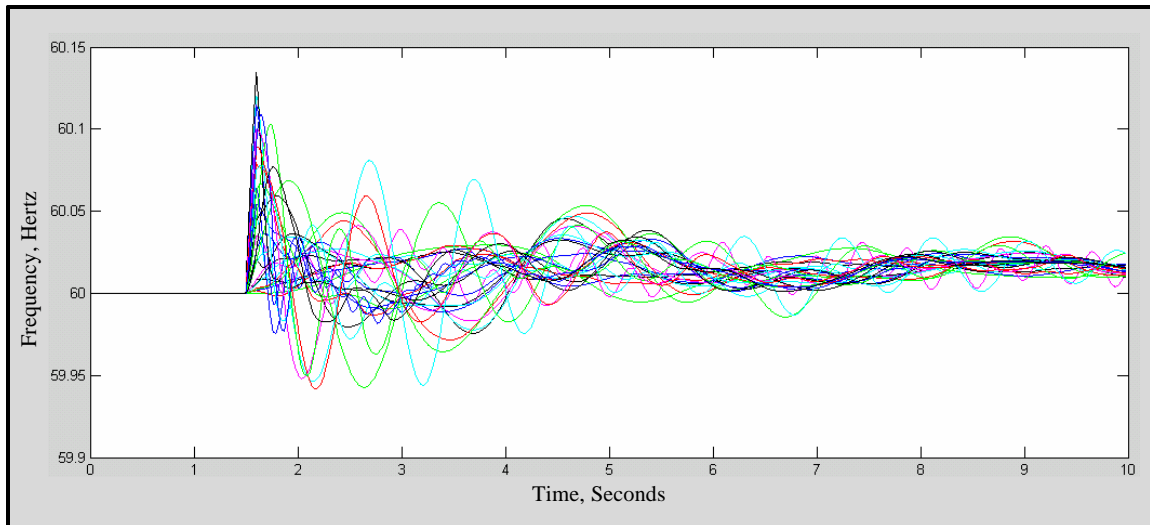


Figure 72: Generators Frequency Response for the Relay 89-85 Case.

Table 62 shows that there are none under frequency relay operations during the 10 seconds simulation time.

Table 62: Under Frequency Relays Operated during the Relay 89-85 Case.

Time (s)	Bus ID
None	None

Figure 73 shows that the relative angle variation is quite small, and the machine relative angles get damped over time. A new steady state condition is reached and instability is not an issue in this case.

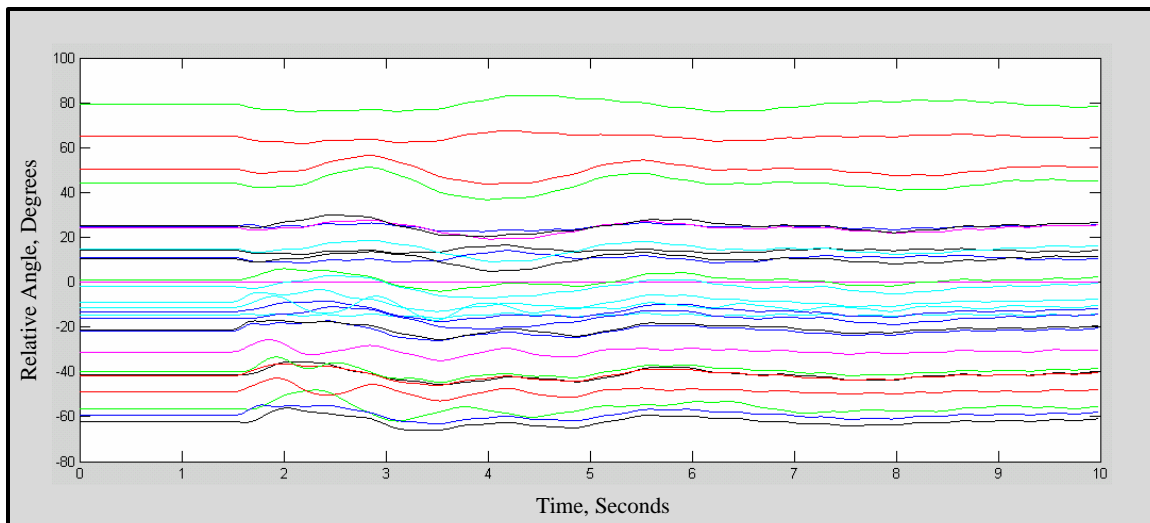


Figure 73: Generator Relative Angles Response for the Relay 89-85 Case.

Figure 74 shows the voltage magnitude of the most affected buses in the system: buses 73 to 108. In addition to the transient voltage depression of the buses closest to the fault, the voltage at bus 86 becomes zero due to the line 76 disconnection.

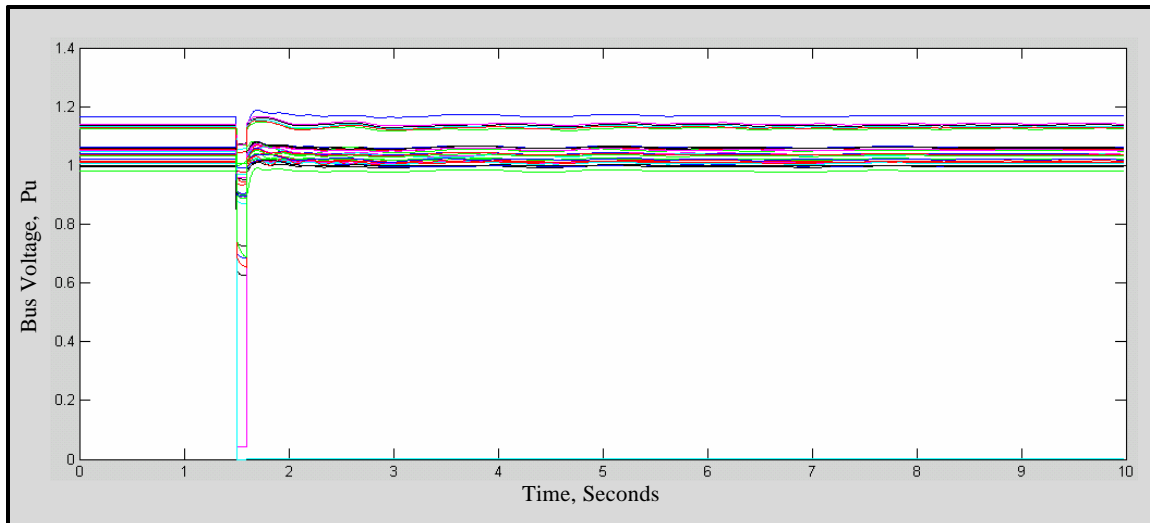


Figure 74: More Affected Bus Magnitudes for the Relay 89-85 Case.

Figure 75 presents the voltage profile for buses 85 and 86. The voltage at bus 85 is recovered after the fault whereas the bus 86 is not; the load lost is shown in Table 64.

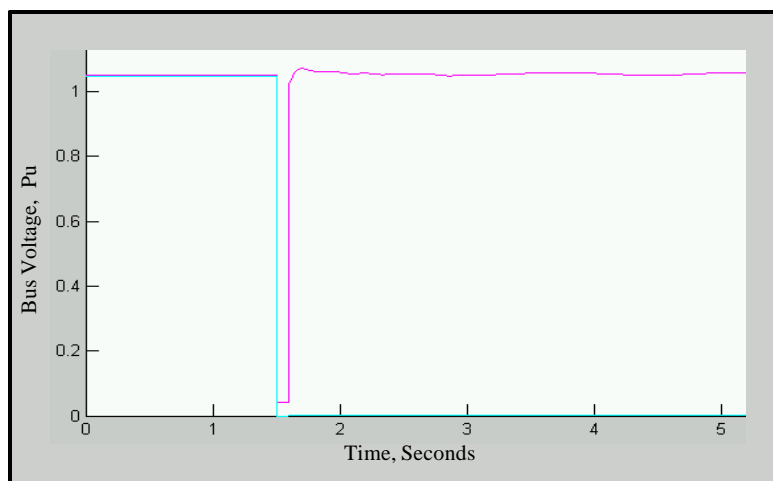


Figure 75: Zoom at the Voltage profiles of Buses 85 and 86, Case Relay 89-85.

Figure 76 shows the voltage magnitude of the least affected buses in the system: buses 109 to 127. The buses shown are relatively far from the fault and the voltage magnitude variations are practically negligible.

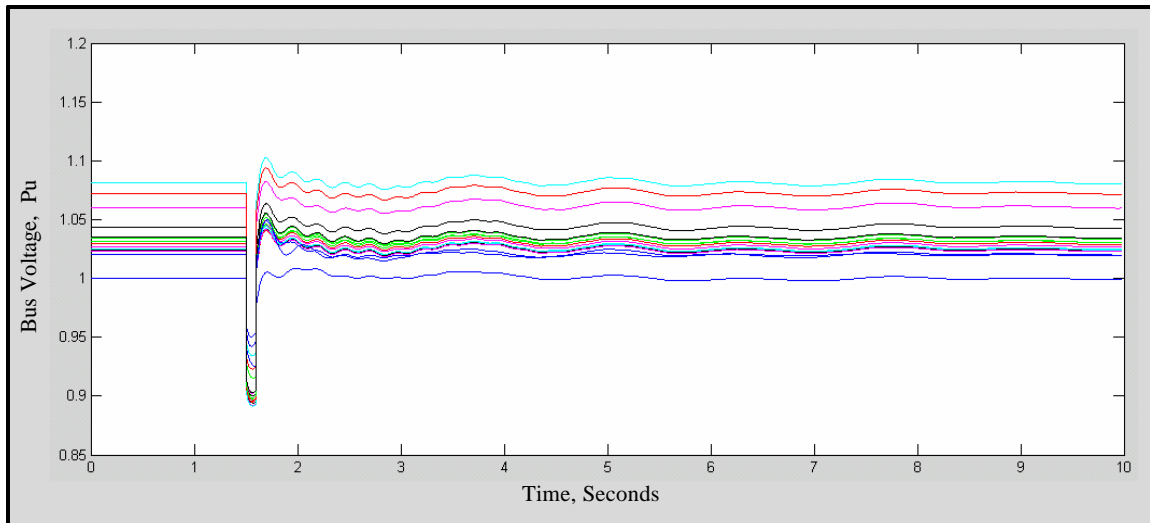


Figure 76: Less Affected Bus Magnitudes for the Relay 89-85 Case.

The assessment of the post-contingency state of the power system with respect to the overload condition is presented in Table 63. As we can see in the table, there is no consequence in the form of overloads in transmission lines or transformers since the maximum loading factor remains in the same line for the pre and post contingency power system topologies.

Table 63: Overload Assessment for the Relay 89-85 Case.

Pre Contingency Maximum Overload Factor	Post Contingency Maximum Overload Factor
0.7683	0.7683

Table 64 shows the overall evaluation of Relay 89-85 case. As it is shown, there is lost load due to the bus isolation, there is no generation lost, and the static overload status was found without any problems.

Table 64: Overall evaluation for the Relay 89-85 Case.

Case Number	Region of Vulnerability (Km)	Lost Load (MW)	Lost Generation (MW)	Post Contingency Overload Status
Relay 89-85	40.25	40	0	Not Overload.

The index of severity of this case will be evaluated in section 5.2.3

5.2.2.4. Case Relay 74-73

This is the case in which the Region of Vulnerability that overreached a transformer was found valid (Table 39). The protection scheme to evaluate in this case is the relay 74-73. Figure 77 shows the segment of the power system in which the protection scheme belongs, the region of vulnerability, and the fault location. As we can see in the figure, the Region of Vulnerability overreaches the transformer 192 and it expands over the lines 106, 107 and 104, covering a fraction of each of these lines.

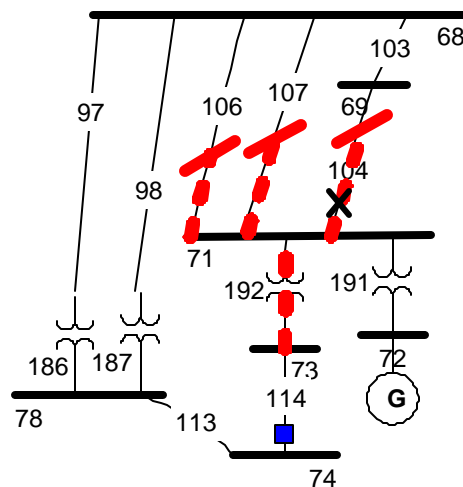


Figure 77: Protection Scheme 74-73, its Region of Vulnerability, and the Fault Location. In this case the relay setting overreaches the transformer and it expands over the lines 106, 107 and 104.

Table 65 shows the representation of the Region of Vulnerability over the line 104 in three different dimensions before the validation process. We can see that the Region of Vulnerability expands over the line 104 up to 44.46 Km measured from bus 71 and this is the starting point for the validation process. In this case the fault was placed at an impedance of 0.00023 per unit from

Bus 71, which when referred to the kilometers value results in a fault location over the line 104 at 1.75 kilometers from bus 71.

Table 65: Representation of the Region of Vulnerability and Location of the Fault, Relay 74-73.

Description	Per Unit	Ohms	Km
Region of Vulnerability represented in <i>Transformer and Line 104</i> before the validation process. *Calculated @ 230 kV.	0.0108	5.714*	11.68*
Region of Vulnerability represented in Line 104 **Calculated @ 500 kV	0.0058	14.503 **	44.46**
Impedance to the Fault, from bus 71	0.00023	0.5718	1.75

Table 66 shows the contingency description for the relay 74-73. As the table describes, the fault is located over line 104, at 5% from bus 71, and at time 1.6 seconds the system has been exposed to a double contingency.

Table 66: Contingency Description for the Relay 74-73.

Time (s)	Event Description	From Bus	To Bus	Cid	% From Bus
1.5	Three phase fault on line	71	69	1	5
1.6	Fault Removal	71	69	1	
1.6	Remove Line	73	74	1	

Figure 78 shows the apparent impedance seen by the relay for the fault location previously described. As we can see in the figure, the impedance falls within the relay operation umbrae and then the Region of Vulnerability is “Valid.”

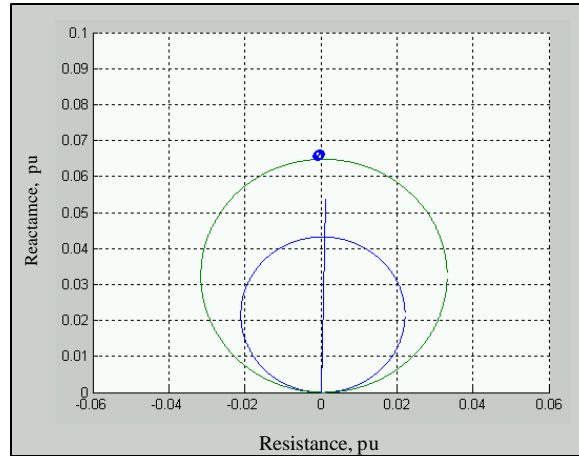


Figure 78: Apparent Impedance seen by the Relay 74-73 during the fault period.

Table 67 shows that there are none distance relay operations during the 10 seconds simulation time.

Table 67: Distance Relays Operated during the Relay 74-73 Case.

Time (s)	Bus ID
None	None

Figure 79 shows that the frequency changes to a value above nominal (around 60.15 Hz). This is caused by the operation of the under frequency relays as described in Table 68.

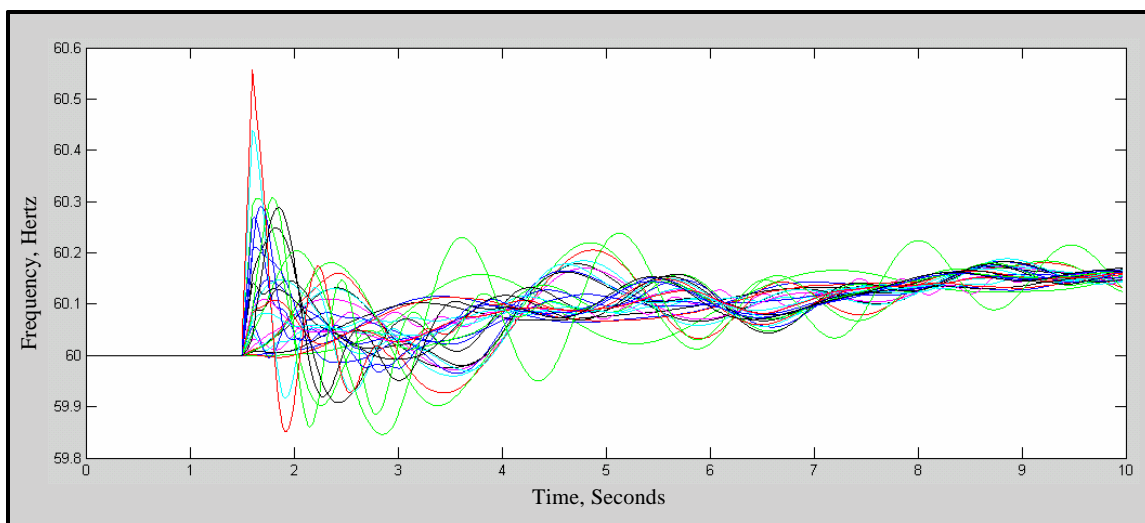


Figure 79: Generators Frequency Response for the Relay 74-73 Case.

Table 68 shows the operation of the under frequency relays installed at buses 71 and 75. The three steps of the under frequency program were reached for bus 71 where as for bus 75 only the first step operated. The amount of load represented at those buses is relatively large, with a value of 3191 and 3098 MW for the bus 75 and 71, respectively. Figure 80 shows the localization of these buses in the sample system.

Table 68: Under Frequency Relays Operated during the Relay 74-73 Case.

Time (s)	Bus ID
1.845	71
1.845	71
1.845	71
2.945	75

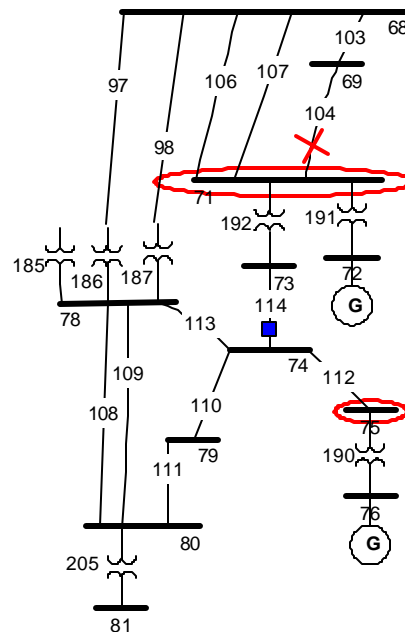


Figure 80: Localization of the Buses in which the Under Frequency Relays Operated, Case 74-73.

Figure 81 shows the relative angles of the generators. As we can see in the figure there are considerable variations in the angles, particularly during the 1.8 to 3 seconds period. The variations get damped with time and a new steady state is reached.

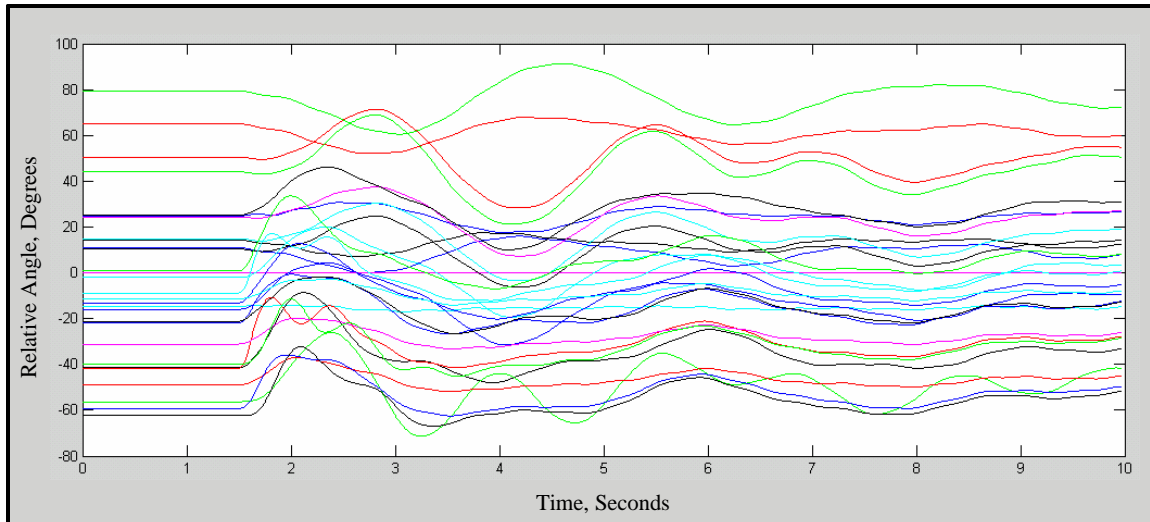


Figure 81: Generator Relative Angles Response for the Relay 74-73 Case.

Figure 82 shows the voltage magnitude of the most affected buses in the system: buses 37 to 72. The transient voltage depression of the buses closest to the fault is appreciated.

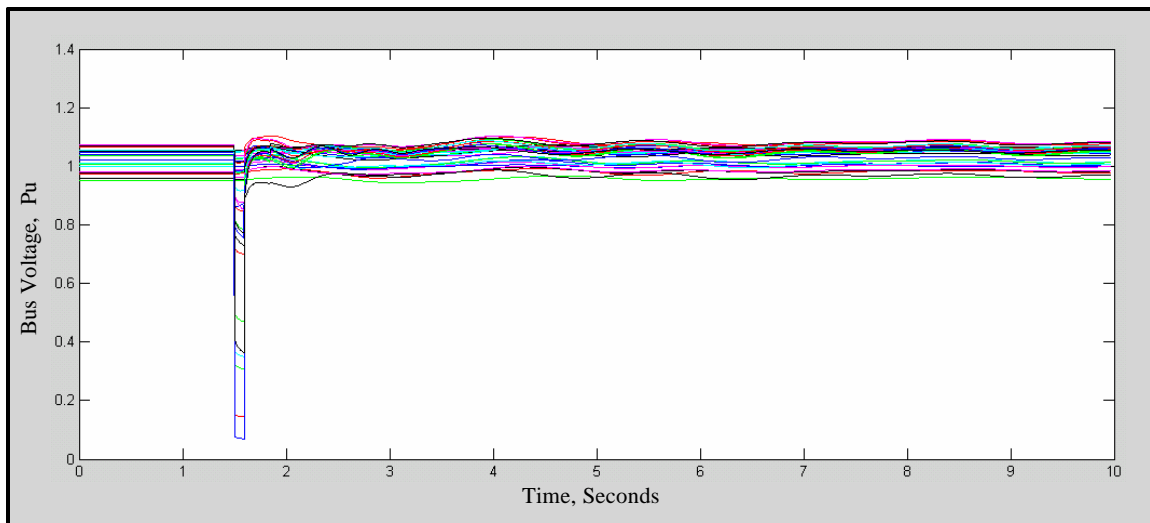


Figure 82: More Affected Bus Magnitudes for the Relay 74-73 Case.

Figure 83 shows the voltage magnitude of the buses 1 to 36. We can see that there is ripple in the voltage waveform of most of the buses and buses 1, 2, 3, 4, and 5 present voltage oscillations of lower frequency.

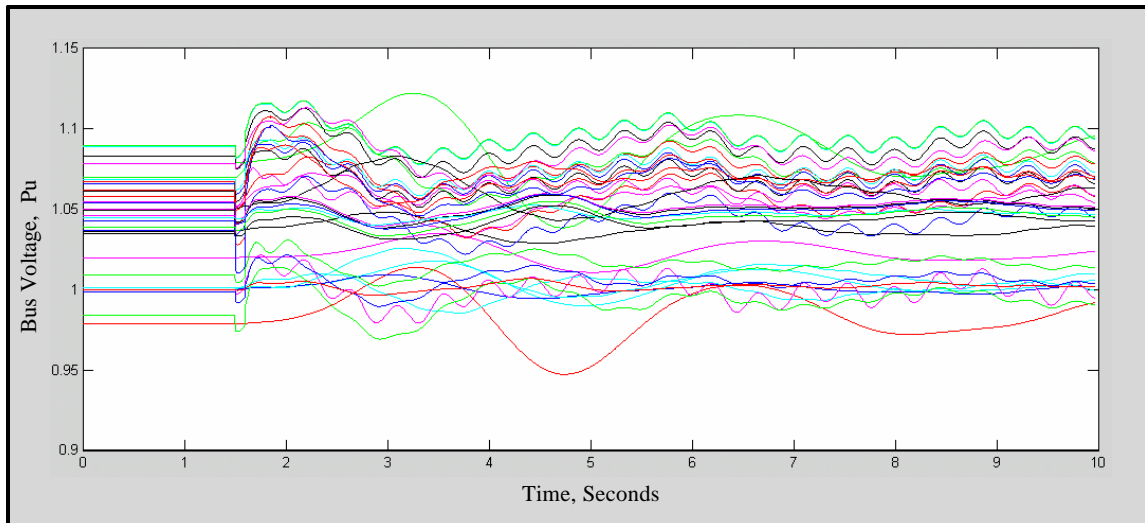


Figure 83: Less Affected Bus Magnitudes for the Relay 74-73 Case.

The assessment of the post-contingency state of the power system is presented in Table 69. As we can see, there is no consequence in the form of overloads in transmission lines or transformers since the maximum loading factor remains in the same line for the pre and post contingency power system topologies.

Table 69: Overload Assessment for the Relay 74-73 Case.

Pre Contingency Maximum Overload Factor	Post Contingency Maximum Overload Factor
0.76834	0.76834

Table 70 shows the overall evaluation of Relay 74-73 case. As it is shown, there is lost load due to the operation of under frequency relays, there is no generation lost, and the static overload status was found without any problems.

Table 70: Overall evaluation for the Relay 74-73 Case.

Case Number	Region of Vulnerability (Km)	Lost Load (MW)	Lost Generation (MW)	Post Contingency Overload Status
Relay 74-73	4.058	601.4	0	Not Overloaded

The index of severity of this case will be evaluated in section 5.2.3.

5.2.2.5. Case Relay 63-104

The protection scheme to evaluate in this case is the relay 63-104. Figure 84 shows the segment of the power system in which the protection scheme belongs, the region of vulnerability, and the fault location. As we can see in the figure, the Region of Vulnerability expands over the lines 140, 28, 29, 24, and 138. The ratio of the relay setting with respect to the impedance of line 28 is 3.1828; then the restriction equation (6) is violated and the point C of the procedure of section 4.2.4 is found beyond bus 121, over lines 26 and 27.

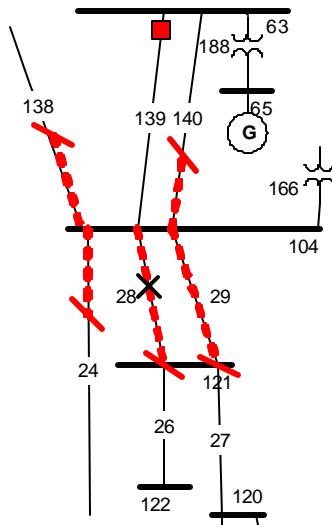


Figure 84: Protection Scheme 63-104, its Region of Vulnerability, and the Fault Location.

Table 71 shows the representation of the Region of Vulnerability over the line 28 in three different dimensions before the validation process. Since this case violates the restriction equation the Region of Vulnerability overreaches the line 28 and could be spread up to 38.78 Km measured from bus 104. This is the starting point for the validation process. In this case the fault was placed at an impedance of .000795 per unit from bus 104, which when referred to the kilometers value results in a fault location over the line 28 at 6.09 kilometers from bus 104.

Table 71: Representation of the Region of Vulnerability and Location of the Fault, Relay 63-104.

Description	Per Unit	Ohms	Km
Region of Vulnerability represented in Line 28 before the validation process	0.0051	12.65	38.78
Impedance to the Fault, from bus 104	.000795	1.987	6.09

Table 72 shows the contingency description for the relay 63-104. As the table describes, the fault is located over line 28, at 50% from bus 104, and at time 1.6 seconds the system has been exposed to a double contingency.

Table 72: Contingency Description for the Relay 63-104.

Time (s)	Event Description	From Bus	To Bus	Cid	% From Bus
1.5	Three phase fault on line	121	104	1	50
1.6	Fault Removal	121	104	1	
1.6	Remove Line	63	104	1	

Figure 85 shows the apparent impedance seen by the relay for the fault location previously described. As we can see in the figure, the impedance falls inside the relay operating zone and then the Region of Vulnerability is “Valid”.

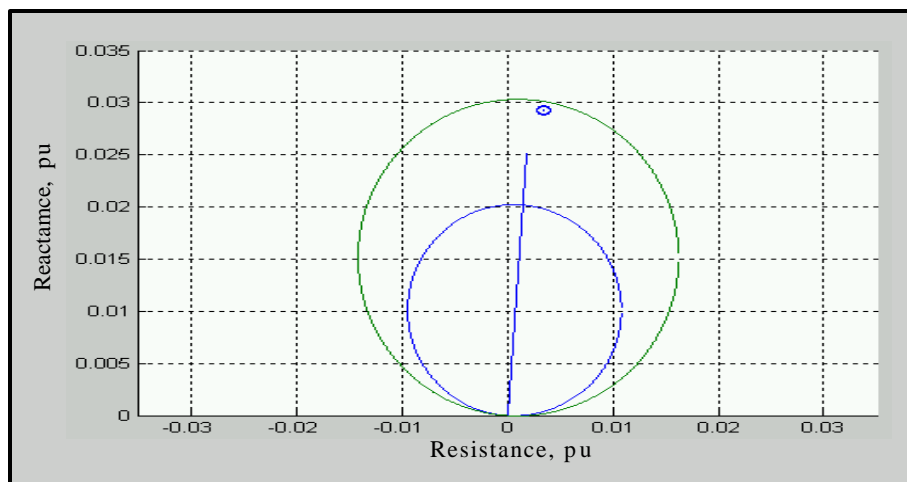


Figure 85: Apparent Impedance seen by the Relay 63-104 during the fault period.

Table 73 shows that there are none distance relay operations during the 10 seconds simulation time.

Table 73: Distance Relays Operated during the Relay 63-104 Case.

Time (s)	Bus ID
None	None

Figure 86 shows that the frequency changes to a value above nominal (around 60.1 Hz). This is caused by the operation of the under frequency relays as we will describe in Table 74.

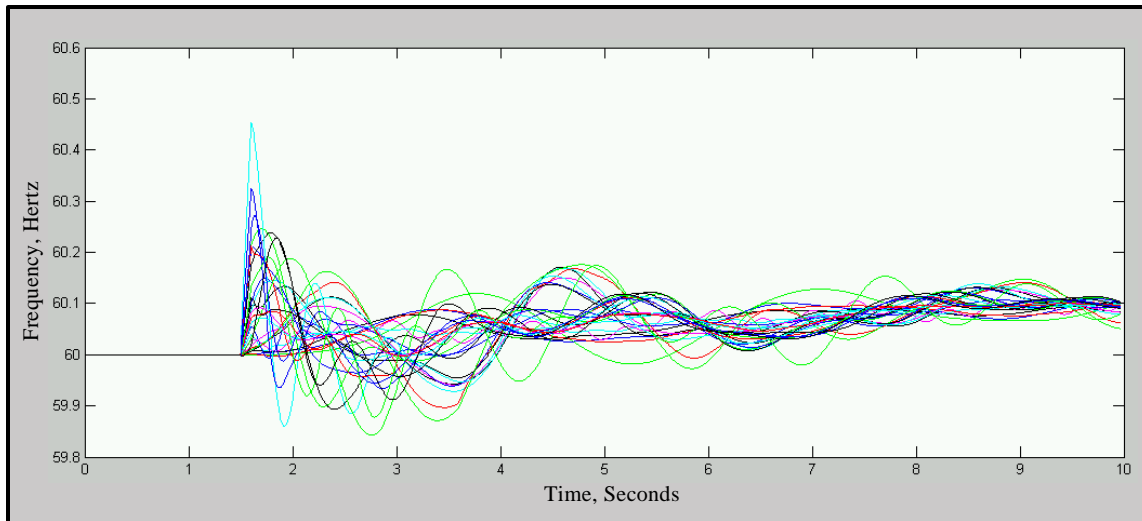


Figure 86: Generators Frequency Response for the Relay 63-104 Case.

Table 74 shows that there are two under frequency relay operations during the 10 seconds simulation time. Figure 87 shows the localization of these buses in the sample system.

Table 74: Under Frequency Relays Operated during the Relay 63-104 Case.

Time (s)	Bus ID
2.84	75
3.59	45

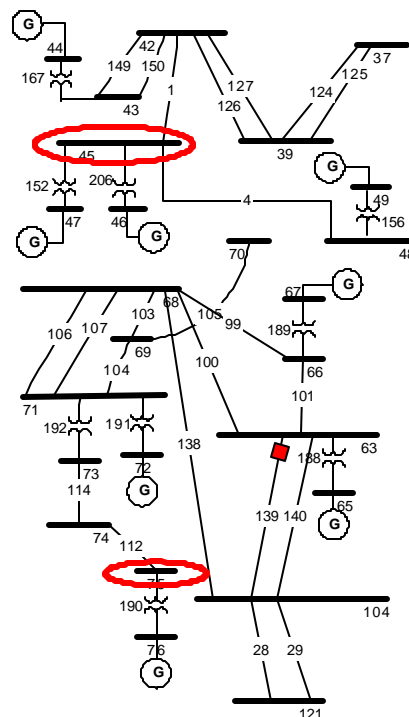


Figure 87: Localization of the buses in which the under frequency relays operated, Case 63-104.

Figure 88 shows the relative angles of the generators. As we can see in the figure there are considerable variations in the angles, particularly during the 1.8 to 3 seconds period. The variations get damped with time and a new steady state is reached.

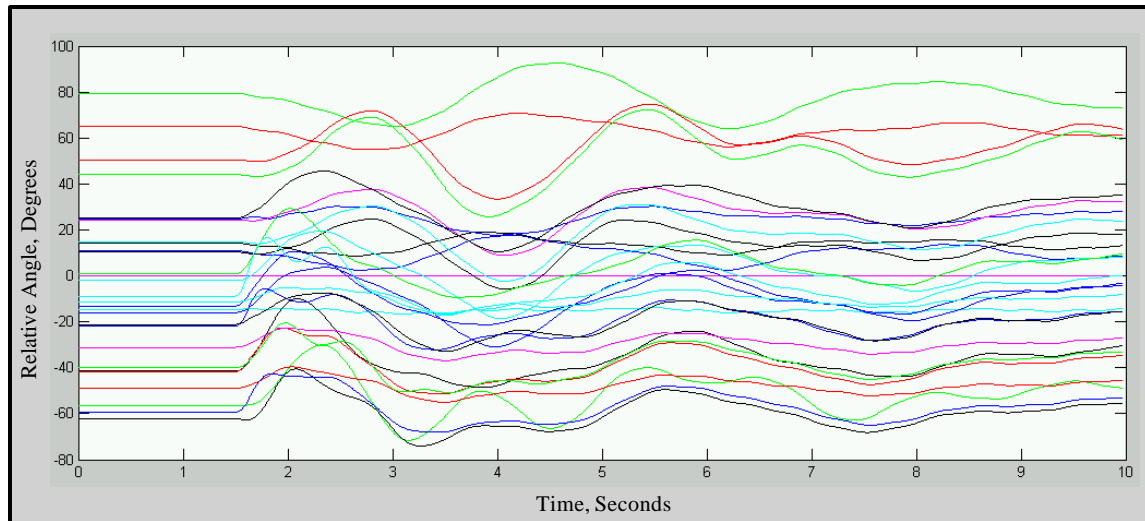


Figure 88: Generator Relative Angles Response for the Relay 63-104 Case.

Figure 89 shows the voltage magnitude of the most affected buses in the system: buses 73 to 108. The transient voltage depression of the buses closest to the fault is appreciated.

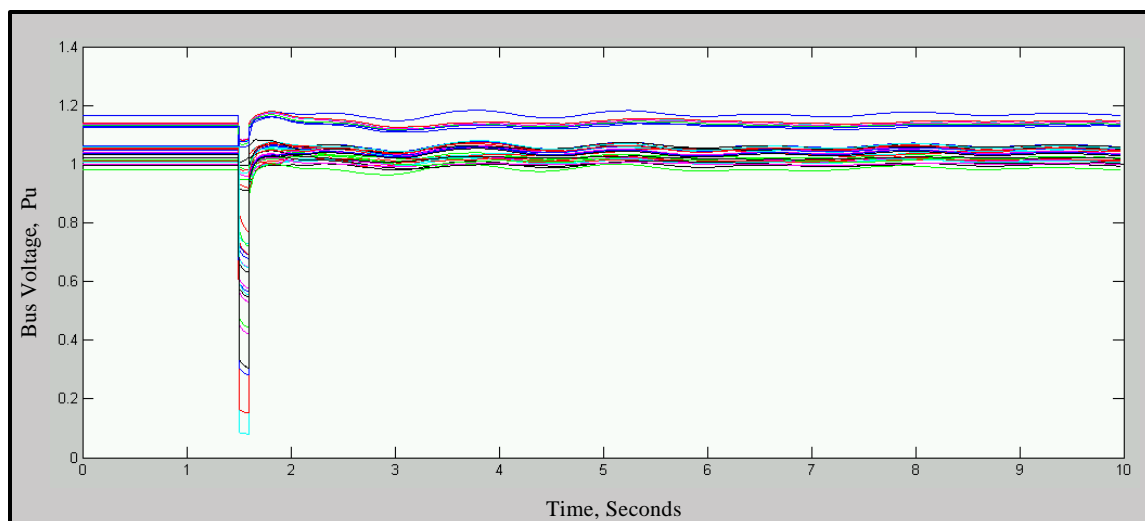


Figure 89: More Affected Bus Magnitudes for the Relay 63-104 Case.

Figure 90 shows the voltage magnitude of the least affected buses in the system: buses 1 to 36. The buses shown are relatively far from the fault and the voltage magnitudes variations (ripple) are kept within limits.

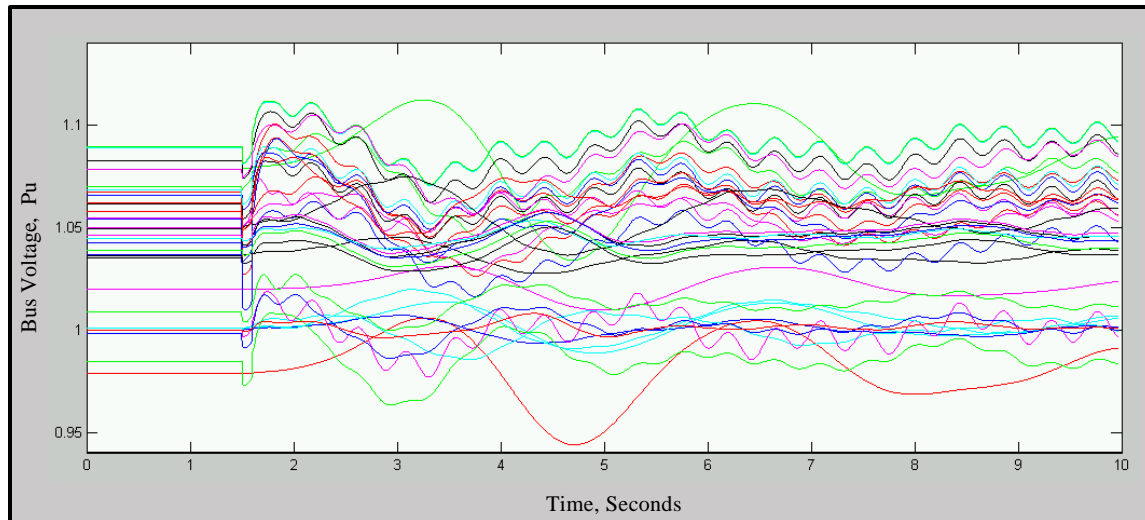


Figure 90: Less Affected Bus Magnitudes for the Relay 63-104 Case.

The assessment of the post-contingency state of the power system is presented in Table 75. As we can see in the table, there is no consequence in the form of overloads in transmission lines or transformers since the maximum loading factor remains in the same line for the pre and post contingency power system topologies.

Table 75: Overload Assessment for the Relay 63-104 Case.

Pre Contingency Maximum Overload Factor	Post Contingency Maximum Overload Factor
.7683	.7683

Table 76 shows the overall evaluation of Relay 63-104 case. As it is shown, there is lost load due to the operation of the under frequency relays, there is no generation lost, and the static overload status was found without any problems.

Table 76: Overall evaluation for the Relay 63-104 Case.

Case Number	Region of Vulnerability (Km)	Lost Load (MW)	Lost Generation (MW)	Post Contingency Overload Status
Relay 63-104	41.30	277.05	0	Not Overloaded

The index of severity of this case will be evaluated in section 5.2.3

5.2.3. Critical Protection Schemes: The Ranking of the Index of Severity

The indexes of severity to be derived are valid under the following assumptions:

- for the current system in which we are applying the methodology
- for the current system operating condition: the base case load flow
- for the specific scope and settings of the protection systems
- for the specific scope and degree of detail of the equipment models

Recalling our definition, the index of severity is a number used to identify the critical protection systems, whose unwanted operations would disconnect power system elements affecting considerably the power system integrity and its capacity to deliver energy. The index is a relative number which indicate the criticality of each case with respect to the simulated cases.

The indexes of severity for the cases presented in section 5.2.2 are calculated next. Table 77 shows the individual indexes that are used to compute the composite index of severity: 1) the magnitude of the Region of Vulnerability in Km, 2) the lost load in MW, and 3) the lost generation in MW.

Table 77: Individual Indexes for the Five Cases Presented.

Relay Case	Region of Vulnerability (Km)	Lost Load (MW)	Lost Generation (MW)
101 -97	20.15	0	0
84-90	9.79	1717	3098
63-104	41.30	277.05	0
74-73	4.05	601.4	0
89-85	40.25	40	0

Given the individual indexes above, the first stage in the procedure is to find the maximum value for each individual index as shown in Table 78.

Table 78: Maximum Value for each Individual Index for the Five Cases Presented.

Relay Case	Maximum Region of Vulnerability (Km)	Maximum Lost Load (MW)	Maximum Lost Generation (MW)
84-90	--	1717	3098
63-104	41.30	--	--

The second stage in the procedure is to divide each individual index by the maximum value in order to obtain the normalized individual indexes as shown in Table 79.

Table 79: Normalized Individual Indexes for the Five Cases Presented.

Relay Case	Region of Vulnerability	Lost Load	Lost Generation
101 -97	0.48784	0	0
84-90	0.23706	1	1
63-104	1	0.161357	0
74-73	0.09826	0.350262	0
89-85	0.97459	0.023296	0

Finally, the index of severity is obtained by adding each of the normalized individual indexes for each case, as shown in Table 80. The final index of severity shown in the last column of the table below is the normalized value with respect to the maximum index, case 84-90. The cases are sorted in descending order according to its index of severity.

Table 80: Index of Severity for the Five Cases Presented, Sorted By Descending Order.

Relay Case	Region of Vulnerability	Lost Load	Lost Generation	Index of Severity	Final Index of Severity
84-90	0.23706	1	1	2.23706	1
63-104	1	0.161357	0	1.16135	0.5191
89-85	0.97459	0.023296	0	0.99788	0.4460
101 -97	0.48784	0	0	0.48784	0.2180
74-73	0.09826	0.350262	0	0.44852	0.2004

As we mentioned previously, we intend to increase the power system security by avoiding unwanted disconnections caused by Hidden Failures. Table 80 prioritizes the protection systems that are suited for the implementation of the Hidden Failure Monitoring and Control System (HFMCs).

Chapter 6. Conclusions and Future Work

This dissertation presented a methodology to assess and rank the effects of unwanted disconnections caused by hidden failures based on Regions of Vulnerability and index of severity in the protection schemes. The objectives and goals of this research have been accomplished. This section starts with a summary of the main findings of this work and finalizes with the recommended direction for future work.

The methodology for the evaluation of the Region of Vulnerability was improved. Firstly, the dimension of the Region of Vulnerability was modified from per unit to ohms and from ohms to kilometers. The benefits from the changes in dimension were demonstrated and we found that the indicator that most accurately reflects the relationship of the Region of Vulnerability with the single line diagram is kilometers. Then, with respect to the representation of the Region of Vulnerability in the power system we defined the novel concept of *Validation of the Region of Vulnerability*. In this procedure, we found segments in the transmission line in which the occurrence of faults do make the relay to operate, producing the unwanted disconnection caused by hidden failure. The results in this system showed that the infeed currents restrain the Region of Vulnerability from spreading along power system elements.

Finally the methodology to compute the index of severity was developed. The index considers the dynamics of the protection schemes and was computed based on the magnitude of the Region of Vulnerability in kilometers, the lost load in MW, the lost generation in MW, and the static overload assessment. The index had the objective of ranking the protection schemes according to the severity and the overall consequences in the power system.

Future Work and Recommendations.

Protection System Design

The protection system design developed in this dissertation was limited by the system data and by the relay models that were available in the transient stability program (ETMSP). The protection system design could be expanded if the methodology is tested in a more realistic system that contains more detailed information. To continue this research with the collaboration of a utility is strongly recommended; the common interest among the universities and the utilities regarding this topic could be exploited and deployed in a research project in which the theory developed in this dissertation and the relaying practices generated through experience are combined in a common objective.

A considerable amount of time was invested working with the transient stability program (ETMSP). During the time in which we contacted utilities and the program vendor, we found that a decreasing minority of utilities uses the program. To continue this research using a tool that is more powerful and is well known/used in the power industry is recommended [28].

Index of Severity

The index of severity was developed considering the factors of Region of Vulnerability, load lost, generation lost, and static overload assessment. A number of different individual indicators could be added in order to enhance the reliability and scope of the composite index of severity. These could be: the excursions in the voltage magnitudes, the coherency of the relative machine angles, and the frequency excursions. In addition, the probability of occurrence or susceptibility of the relay's hidden failure could be explored. In the development of the index, not attempts were made to assign weights to the individual indexes of severity; to perform research around this task is recommended.

Hidden Failure Monitoring and Control System (HFMCS)

Based on the research results obtained, the intent to develop a system to prevent the occurrence of hidden failures is a quite difficult task. Then, the development of a system that is capable of preventing the effect of hidden failures in the power system is the viable alternative to solve the problem. The ultimate goal of this system would be to prevent the unwanted disconnection caused by hidden failures.

This dissertation justified the application and development of the HFMCS under a power system security point of view (contingency analysis) in order to increase the security of the power system.

The HFMCS presents the most important recommendation of future work. To continue this research with the collaboration of a relays manufacturer company is highly recommended. In fact, similar efforts have been developed focused on the specific problem of unwanted disconnections caused by hidden failures. Reference [29] describes the design, development, and field experience of a product with a sole purpose: avoiding these unwanted trips.

It is interesting to note that the starting point of this dissertation [5] was included as supporting evidence in the work of [29]. Extensive phone conversations with the utility and the relay manufacturer related that the utility had suffered from the problem and took the initiative to work with the relay manufacturer. The timing in which they found the initial work of Virginia Tech [5] and the one in which they were developing their project was coincidental.

The work developed in [29] is evidence that the problem of unwanted disconnections caused by hidden failure is real, is critical, and it requires a solution. A methodology for the solution was described in this dissertation.

The results regarding the Regions of Vulnerability culminated in a good appreciation of the problem and a methodology for its evaluation and representation as a physical area. The concept of Region of Vulnerability was presented as an “additional factor” to be considered in assessing the potential severity of a double contingency and it could provide additional insight at the

moment of assessing the severity of a given contingency. Further research towards the application of the methodology to other hidden failure modes and the development of its particular Regions of Vulnerability could be possible. However, we believe that the direction for further research should go towards the design, development, and application of the HFMCS.

Part of this research work was presented in a number of conferences and it was very well received. The issue of “re-think” on the philosophy of the protection schemes and adapt them to the current state of the technology was a major point of discussion. Applying this ideas we select the protection scheme that is most used in the United States, the Directional Comparison Blocking. If we analyze it, we recall that the scheme is biased towards dependability, and there are cases in which the no signal means no blocking, and therefore a trip. Sometimes, this trip may be an unwanted trip and it may be related to a Hidden Failure. The overall philosophy in the design is justified because it considered the current state of the communications technology... fifty years ago. The current advancements in communication and computer technology could be applied in the Power system. We believe that the developed methodology could be applied and through the HFMCS important contributions could emerge.

References

1. Massoud Amin, "Toward Self-Healing Energy Infrastructure Systems," IEEE Computer Applications in Power, January 2001, pp. 20-28.
2. Sugarman Robert, "New York City's Blackout: A 350 Million Drain," IEEE Spectrum, November 1978, pp. 20-28.
3. WSCC, "Disturbance Report for the Power System Outages that occurred on the Western Interconnection on July 2 1996 1424 MAST and July 3 1996 1403 MAST" (approved by the WSCC Operations Committee on September 19, 1996).
4. WSCC, "Disturbance Report for the Power System Outage that occurred on the Western Interconnection on August 10 1996 1548 PAST" (approved by the WSCC Operations Committee on October 18, 1996).
5. Surachet Tamronglak, "Analysis of Power System Disturbances due to Relay Hidden Failures," Ph.D. Dissertation, Virginia Polytechnic and State University, Blacksburg, Virginia, March 1994.
6. David C. Elizondo, "Hidden Failures in Protection Systems and Its Impact on Wide-Area Disturbances," MSEE Thesis, Virginia Polytechnic and State University, Blacksburg, Virginia, April 2000.
7. Stanley H. Horowitz and Arun G. Phadke "Power System Relaying", second edition. Research Studies Press Ltd., England, and John Wiley and Sons Inc. New York, 1995.
8. Conclusions of Meetings with Project Consultant, Stanley Horowitz. Meeting took place on the Power System Laboratory of Virginia Tech during the year 2002.
9. Conclusions of Phone Conversations with Wang Lei, Powertech Labs Inc. Conversations and written correspondence took place during the year 2002.
10. IEEE Guide for Alternate Current Generator Protection. IEEE Std C37.102-1995.
11. IEEE Guide for Protection Relay Applications to Transmission Lines, IEEE Std C37-113-1999.
12. Conclusions of conversations with Support Entity for ETMSP Program, Kant Lee. Conversations and written correspondence took place during the year 2002.
13. Conclusions of conversations with ETMSP Program Consultant, Peter Hirsch. Conversations and written correspondence took place during the year 2002.
14. Carson W. Taylor, Dennis C. Erickson, "Recording and Analyzing the July 2 Cascading Outage," IEEE Computer Applications in Power, January 1997.
15. David C. Elizondo, J. De La Ree, Arun G. Phadke, Stan Horowitz, "Hidden Failures in Protection Systems and Their Impact on Wide-Area Disturbances," IEEE PES Winter Meeting Proceedings, Columbus, OH. 2001.

16. WSCC, "Coordinated Off-Nominal Frequency Load Shedding and Restoration Plan," Final Report. Prepared by the Underfrequency Issues Work Group, Technical Studies Subcommittee, November 25, 1997.
17. WSCC, "Under Voltage Load Shedding Guidelines," Final Report. Prepared by the Undervoltage Load Shedding Task Force, Technical Studies Subcommittee, July 1999.
18. Prabha Kundur, "Power System Stability and Control," Electric Power Research Institute, Power System Engineering Series. McGraw-Hill Inc. 1994, Page 922.
19. "On-Line Power System Security Analysis," IEEE Special Report, Proceedings of the IEEE, Vol 80, No 2, February, 1992.
20. North American Reliability Council, Glossary of Terms. Prepared by the Glossary of Terms Task Force, August 1996.
21. Morison, K.; Hamadanizadeh, H.; Lei Wang, "Dynamic Security Assessment Tools," Power Engineering Society Summer Meeting, 1999. IEEE, Volume: 1, 1999, pages: 282-286.
22. Chengjun Fu, Anjan Bose, "Contingency Ranking Based on Severity Indices in Dynamic Security Analysis," IEEE Transactions in Power Systems, Vol. 14, No 3, August 1999.
23. V. Brandwajn, A.B.R Kumar, A. Ipakchi, Anjan Bose, Steve D. Kuo, "Severity Indices for Contingency Screening in Dynamic Security Assessment," IEEE Transactions in Power Systems, Vol. 12, No 3, August 1997.
24. Kundur, P.; Morison, G.K.; Wang, L, "Techniques for on-line transient stability assessment and control," Power Engineering Society Winter Meeting, 2000.
25. C.K.Tang, C.E. Graham, M. El-Kady, R.T.H. Alden, "Transient Stability Index from Conventional Time Domain Simulation," IEEE Transactions in Power Systems, Vol. 9, No 3, August 1994.
26. Conclusions of conversations with Lei Wang, Powertech Labs. Conversations and written correspondence took place during the year 2002.
27. Conclusions of conversations with AEP and Southern Company. Conversations and written correspondence took place during the year 2002
28. <http://www.pti-us.com/pti/software/psse/>
29. Dick Curtner, David Burns, David Kidd, "Development, Application and Field Experience of a Trip Security System for Transmission Line Protective Relays," 25th Annual Western Protective Relay Conference, Spokane, Washington, October, 15, 1998.

Appendices

Appendix A 127-Bus Sample System Data

The data of the 127-bus sample system is presented next. The appendix is divided in:

- Bus Data.
- Load Data.
- Generation Data
- Branch Data

Bus Data.

Table A- 1 represents the bus data. The nomenclature for the table headings is:

Bus Number	Number of the Bus (1 to 127)
Bus Name	Alphabetic identifier for each bus
Bus BaskV	Bus Base Voltage, in Kv
Bus Type	Bus Type code: (1) Load Bus, PQ bus (2) Generator Bus, PV bus (3) Swing Bus
Bus GL	Real component of shunt admittance to ground; entered in MW
Bus BL	Reactive component of shunt admittance to ground; entered in MVAR
Bus Voltage	Voltage Magnitude, in per unit
Bus Angle	Voltage angle, in degrees

Table A- 1: 127-Bus Sample System: Bus Data

Bus Number	Bus Name	Bus BaskV	Bus Type	Bus GL	Bus BL	Bus Voltage (pu)	Bus Angle
1	'CMAIN GM'	20	2	0	0	1.02	67.7952
2	'CA230 '	230	1	0	0	1.0011	62.874
3	'CA230TO '	230	1	0	0	0.9785	53.8251
4	'CANALB '	500	1	0	0	1.0786	49.2362
5	'CANAD G1'	20	2	0	0	1	24.7373
6	'CANADA '	500	1	0	0	1.0363	20.9467
7	'NORTH '	500	1	0	12	1.0499	12.108
8	'NORTH G3'	20	2	0	0	1	26.5866
9	'HANFORD '	500	1	0	5.5	1.0495	0.2255
10	'COULEE '	500	1	0	0	1.07	0.1643
11	'GARRISON'	500	1	0	0	1.0371	-12.1586
12	'JOHN DAY'	500	1	0	10.1935	1.0828	-11.123
13	'JOHN DAY'	13.8	3	0	0	1	0

Bus Number	Bus Name	Bus BaskV	Bus Type	Bus GL	Bus BL	Bus Voltage (pu)	Bus Angle
14	'BIG EDDY'	500	1	0	0	1.0892	-13.3097
15	'GRIZZLY '	500	1	-0.0929	-5.6029	1.0674	-17.1477
16	'CELILOCA'	500	1	0	4.62	1.0896	-13.4178
17	'BIG EDDY'	230	1	0	5.7685	1.0659	-14.5698
18	'CELILO '	230	1	0	7.92	1.0616	-15.076
19	'DALLES21'	13.8	2	0	0	1.055	-7.94
20	'BIG EDDY'	115	1	0	0	1.0686	-16.9325
21	'SUMMER L'	500	1	0.0028	1.1638	1.0582	-18.2347
22	'BURNS2 '	500	1	11.5674	-23.7541	0.9844	-6.6864
23	'MALIN '	500	1	0.0799	-0.8631	1.0543	-23.3444
24	'MONTANA '	500	1	0	0	1.0493	48.2014
25	'COLSTRP '	500	1	0	0	1.0784	-1.3598
26	'MONTA G1'	20	2	0	0	1	56.5938
27	'MIDPOINT'	500	1	-10.9334	-2.2	1.0619	-5.2003
28	'BRIDGER2'	22	2	0	0	1.009	2.4592
29	'MIDPOINT'	345	1	0	-8.7	0.9984	-1.573
30	'BENLOMND'	345	1	0	0	1.0446	-3.3956
31	'BENLOMND'	230	1	0	0	1.0462	-3.9612
32	'NAUGHTON'	230	1	0	0	1.0445	0.6116
33	'NAUGHT '	20	2	0	0	1	3.4113
34	'TERMINAL'	345	1	0	0	1.0391	-3.4235
35	'CAMP WIL'	345	1	0	-0.6	1.0429	-2.4189
36	'SPAN FRK'	345	1	0	0	1.0351	-1.0948
37	'EMERY '	345	1	0	-2.2	1.0371	4.8869
38	'EMERY '	20	2	0	0	1.05	9.6023
39	'SIGURD '	345	1	0	-0.5	1.0519	-0.5484
40	'PINTO '	345	1	0	-0.18	1.0404	-1.4059
41	'PINTO PS'	345	1	0	0	1.0368	-2.4446
42	'MONA '	345	1	0	0	1.056	-2.0101
43	'INTERMT '	345	1	0	4.3	1.0526	-4.3689
44	'INTERM1G'	26	2	0	0	1.05	0.2783
45	'CRAIG '	345	1	0	0	0.9752	16.2723
46	'CRAIG '	22	2	0	0	0.95	23.5503
47	'HAYDEN '	20	2	0	0	1	33.7267
48	'SAN JUAN'	345	1	0	3.9	1.0356	-3.8778
49	'SJUAN G4'	22	2	0	0	1	-0.8905
50	'FOURCORN'	345	1	0	-1.55	1.0091	-4.6908
51	'FOURCORN'	500	1	0.0058	-1.13	1.0681	-7.9073
52	'FOURCORN'	230	1	0	0	1.0073	-5.2342
53	'FCNGN4CC'	22	2	0	0	1	2.2266
54	'CHOLLA '	345	1	0	0	0.9774	-16.9637
55	'CORONADO'	500	1	0	0	0.9795	-26.1779
56	'CORONADO'	20	2	0	0	1.04	-19.6623

Bus Number	Bus Name	Bus Bask V	Bus Type	Bus GL	Bus BL	Bus Voltage (pu)	Bus Angle
57	'MOENKOPI'	500	1	-0.0058	-3.707	1.0673	-24.8563
58	'WESTWING'	500	1	0	-4.27	1.0559	-29.5933
59	'PALOVRDE'	500	1	0	-1.46	1.0486	-29.643
60	'PALOVRD2'	24	2	0	0	0.96	-21.7162
61	'NAVAJO '	500	1	0	-1.9	1.0721	-23.9375
62	'NAVAJO 2'	26	2	0	0	1	-17.8136
63	'ELDORADO'	500	1	0	-3.19	1.0512	-33.0975
64	'DEVERS '	500	1	0	0	1.0354	-43.5237
65	'ELDORADO'	20	2	0	0	1.02	-25.976
66	'MOHAVE '	500	1	0	-1.96	1.07	-29.3631
67	'MOHAVICC'	22	2	0	0	1.05	-21.0426
68	'LUGO '	500	1	0	0	1.055	-46.092
69	'SERRANO '	500	1	0	0	1.0413	-50.0801
70	'VALLEY '	500	1	0	0	1.0369	-47.7633
71	'MIRALOMA'	500	1	0	4	1.0409	-49.6816
72	'MIRALOMA'	20	2	0	0	1.05	-45.4441
73	'MIRALOMA'	230	1	0	0	1.0382	-50.1274
74	'MESA CAL'	230	1	0	0	1.0071	-55.0621
75	'LITEHIPE'	230	1	0	0	1.0119	-55.7768
76	'LITEHIPE'	20	2	0	0	1.02	-49.6273
77	'VINCENT '	500	1	0.0179	0	1.0612	-48.9478
78	'VINCENT '	230	1	0	-1.9	0.9949	-51.6351
79	'EAGLROCK'	230	1	0	0	1.0101	-52.7625
80	'PARDEE '	230	1	0	0	1.006	-51.6845
81	'PARDEE '	20	2	0	0	1.01	-39.6021
82	'SYLMAR S'	230	1	0	0	1.0207	-48.258
83	'MIDWAY '	200	1	0	-1.3	1.1671	-51.4458
84	'MIDWAY '	500	1	-0.1346	-2.6639	1.0593	-48.6079
85	'LOSBANOS'	500	1	0	0	1.0493	-49.5302
86	'MOSSLAND'	500	1	0	0	1.0464	-49.7949
87	'DIABLO '	500	1	0	0	1.053	-46.1289
88	'DIABLO1 '	25	2	0	0	0.98	-42.3267
89	'GATES '	500	1	0.1196	-2.6538	1.0471	-47.6849
90	'TEVATR '	500	1	0.0321	15.5844	0.9982	-38.9959
91	'TEVATR2 '	20	2	0	0	1	-30.7837
92	'OLINDA '	500	1	-0.0096	0.1388	1.0372	-31.0691
93	'ROUND MT'	500	1	-0.1281	0.4316	1.0346	-27.9327
94	'TABLE MT'	500	1	0.1196	-0.4221	1.0134	-32.0706
95	'ROUND MT'	200	1	0	-1.28	1.1239	-25.1416
96	'ROUND MT'	20	2	0	0	1.02	-15.0807
97	'COTWDPGE'	200	1	0	0	1.1361	-30.4898
98	'LOGAN CR'	200	1	0	0	1.1402	-34.5853
99	'GLENN '	200	1	0	0	1.1409	-34.2002
100	'CORTINA '	200	1	0	0	1.131	-34.9759

Bus Number	Bus Name	Bus Bask V	Bus Type	Bus GL	Bus BL	Bus Voltage (pu)	Bus Angle
101	'TEVATR '	200	1	0	-0.32	1.1274	-39.6352
102	'TEVATR '	20	2	0	0	1.05	-35.6869
103	'SYLMARLA'	230	1	0	21.46	1.0383	-47.1515
104	'VICTORVL'	500	1	0	0	1.0587	-42.4778
105	'VICTORVL'	287	1	0	-1.08	1.0521	-44.4952
106	'STA B2 '	287	1	0	0	1.0366	-50.7194
107	'STA B1 '	287	1	0	0	1.0366	-50.7194
108	'STA B '	138	1	0	0	1.0326	-51.903
109	'STA BLD '	230	1	0	0	1.0273	-52.1113
110	'STA F '	230	1	0	0	1.0248	-51.8816
111	'RIVER '	230	1	0	0	1.0236	-51.8466
112	'HAYNES '	230	1	0	0	1.0313	-50.6547
113	'HAYNES3G'	18	2	0	0	1	-47.3515
114	'STA G '	230	1	0	0	1.0239	-51.1767
115	'GLENDALE '	230	1	0	0	1.0234	-50.9251
116	'STA E '	230	1	0	0	1.0252	-50.0595
117	'VALLEY '	230	1	0	0	1.0293	-49.0331
118	'RINALDI '	230	1	0	0	1.034	-47.8414
119	'OWENS G '	11.5	2	0	0	1.02	-47.2709
120	'STA E '	500	1	0	0	1.043	-47.666
121	'ADELANTO'	500	1	0	9.12	1.0603	-42.1581
122	'ADELAN&1'	500	1	0	0	1.0809	-46.2283
123	'RINALDI '	500	1	0	-0.8	1.0721	-45.4838
124	'STA J '	230	1	0	0	1.0311	-48.9161
125	'CASTAIC '	230	1	0	0	1.032	-47.2928
126	'CASTAI4G'	18	2	0	0	1.02	-45.983
127	'OLIVE '	230	1	0	0	1.0348	-47.6317

Load Data.

Table A- 2 represents the load data. The nomenclature for the table headings is:

Bus Number Number of the Bus
 PL Real component of the load, entered in MW
 QL Reactive component of the load, entered in MVAR

Table A- 2: 127-Bus Sample System: Load Data

Bus Number	PL (MW)	PQ (MVAR)
1	100	0
2	3600	700
5	100	0
6	4400	1000
7	5000	400
8	100	0
9	3500	500
11	2584	394
12	3200	1100
13	100	0
14	-44.2	22
15	-66.6	-97
17	-67.5	160
18	3137	1681
19	100	0
20	160	31.25
23	-339	-119
24	1700	300
25	-1525	-50
26	100	0
28	100	0
29	610	-414
30	33.9	11.9
31	148	-7.9
32	255	100
33	100	0
34	185	78.5
35	457.7	81.7
36	141.2	71.4
37	116.1	38.4
38	100	0
39	379	-43
40	31.6	11.5
42	-62	12.8

Bus Number	PL (MW)	PQ (MVAR)
43	2053	907.1
44	100	0
45	2350	-127
46	100	0
47	100	0
48	840	5
49	100	0
50	239	-56
52	139.7	23.8
53	100	0
55	1750	-56
56	100	0
58	617	-69
59	793.4	207
60	100	0
61	90	70
62	100	0
63	902.3	-11.4
64	856	19.6
65	100	0
67	100	0
68	204.2	-28.2
69	1230	72.8
70	406	41
71	3098	1189
72	100	0
74	377.4	64.5
75	3191	630
76	100	0
78	1066	-10.8
79	175	18
80	3118	78
81	100	0
82	401	80.6
83	777.6	32.6
84	55.6	-329
85	265	14
86	40	21.5
87	50	25
88	100	0
89	305	-7.6
90	5661	3491
91	100	0
92	-189	61.5

Bus Number	PL (MW)	PQ (MVAR)
94	-0.7	118.5
95	148	0
96	100	0
97	210.4	-77
98	8.01	0
99	27.5	-0.1
100	-43.3	20
101	884	54.8
102	100	0
103	-2771	1654
105	-129	32.2
108	237.2	-63.2
109	138	28
110	117	24
111	320	65
113	100	0
114	121	25
115	135	27
116	807.8	132.1
117	205.2	17.6
118	121	25
119	100	0
121	-1862	971
124	887.7	-6.2
126	100	0
127	-72.8	-17

Generation Data

Table A- 3 represents the generation data. The nomenclature for the table headings is:

Bus Number	Number of the Bus
PG	Generator Real Power Output, in MW
PQ	Generator Reactive Power Output, in MVAR
Qmax	Maximum Generator Reactive Power Output, In MVAR
Qmin	Minimum Generator Reactive Power Output, In MVAR

Table A- 3: 127-Bus Sample System: Generation Data

Bus Number	PG	PQ	Gen Qmax	Gen Qmin
1	44.8	11.5017	5320	-3500
5	44.5	10.1105	4000	-4000
8	99.5	18.5397	5780	-2000
13	51.7477	8.5522	2649	-1850
19	13.01	4.3147	692	-711
26	29.1	9.5328	1500	-1000
28	16.4	2.8566	600	-525
33	4.45	0.9173	9999	-9999
38	16.65	-0.3137	9999	-9999
44	17.8	5.3459	850	-440
46	10.48	-1.3291	400	-400
47	20.5	4.6483	900	-900
49	9.62	1.4878	300	-300
53	21.6	-0.3047	700	-500
56	8	1.2304	300	-300
60	26.4	3.7808	1300	-900
62	16.9	1.9554	700	-280
65	9.827	-1.2876	300	-300
67	16.8	4.4663	700	-300
72	16.9	5.9382	900	-400
76	31.95	10.325	2000	-900
81	22	3.9372	600	-600
88	7.65	-2.0624	330	-310
91	34.67	16.5455	2500	-1000
96	10.57	0.2561	400	-400
102	5.94	1.9236	300	-300
113	3.25	0.6827	300	-220
119	1.1	0.2908	100	-100
126	2	-0.5216	268	-134

Branch Data

Table A-4 represents the branch (transmission lines and transformers) data. The nomenclature for the table headings is:

Number	Number of the Branch
From Bus	Branch Starting bus number
To Bus	Branch Finishing bus number
Resistance (pu)	Branch Resistance, in per unit
Reactance (pu)	Branch Reactance, in per unit
Susceptance (B)	Total Branch Charging susceptance, in per unit
Branch Tap	Transformer off-nominal turns ratio

Table A-4: 127-Bus Sample System: Branch Data

Number	From Bus	To Bus	Resistance (pu)	Reactance (pu)	Suceptance (B)	Branch Tap
1	45	42	0.0081	0.1369	2.4348	1
2	54	50	0.0018	0.0199	2.576	1
3	50	48	0.0005	0.0053	0.0882	1
4	48	45	0.0098	0.11	2	1
5	61	57	0.0008	0.0055	1.3922	1
6	61	58	0.0026	0.0376	4.7289	1
7	57	58	0.0018	0.0269	3.3453	1
8	57	63	0.0022	0.016	3.8163	1
9	59	58	0.0004	0.0096	0.9038	1
10	59	58	0.0004	0.0096	0.9038	1
11	51	57	0.0018	0.0323	3.1129	1
12	6	4	0.0035	0.07	4.606	1
13	3	2	0.002	0.02	0.8	1
14	107	105	0.0107	0.079	0.3667	1
15	106	105	0.0107	0.079	0.3667	1
16	116	115	0.0005	0.0072	0.0162	1
17	116	114	0.0012	0.0124	0.028	1
18	116	114	0.0012	0.0124	0.028	1
19	110	112	0.002	0.0307	0.0689	1
20	110	109	0.0007	0.0103	0.0256	1
21	110	109	0.0007	0.0103	0.0256	1
22	110	114	0.0011	0.0119	0.0251	1
23	117	116	0.0013	0.0098	0.0212	1
24	104	123	0.0008	0.0188	1.6667	1
25	115	114	0.0004	0.0054	0.012	1
26	121	122	0.0007	0.0186	1.4026	1
27	121	120	0.0008	0.0167	1.188	1
28	121	104	0	0.0016	0.12	1
29	121	104	0	0.0016	0.12	1

Number	From Bus	To Bus	Resistance (pu)	Reactance (pu)	Suceptance (B)	Branch Tap
30	112	114	0.0028	0.043	0.0965	1
31	118	117	0.0014	0.0112	0.0247	1
32	118	117	0.0014	0.0112	0.0247	1
33	111	112	0.0022	0.0342	0.0772	1
34	111	112	0.0024	0.0367	0.0828	1
35	111	110	0.0004	0.0037	0.0083	1
36	111	114	0.0006	0.0059	0.0125	1
37	118	116	0.0023	0.0158	0.0306	1
38	118	116	0.0023	0.0158	0.0306	1
39	125	127	0.0022	0.0335	0.0734	1
40	125	118	0.0029	0.038	0.0824	1
41	125	124	0.0031	0.0468	0.1008	1
42	125	103	0.0023	0.0342	0.0751	1
43	118	127	0.0003	0.0043	0.0095	1
44	118	124	0.0014	0.0097	0.0194	1
45	118	124	0.0014	0.0097	0.0194	1
46	118	124	0.0016	0.0097	0.0193	1
47	118	124	0.0016	0.0097	0.0193	1
48	118	103	0.0003	0.0039	0.0092	1
49	118	103	0.0003	0.0039	0.0092	1
50	118	103	0.0003	0.0039	0.0092	1
51	11	9	0.0014	0.0226	1.88	1
52	11	12	0.002	0.033	1.88	1
53	11	25	0.0018	0.0141	3.68	1
54	9	10	0.0011	0.0207	1.8553	1
55	9	12	0.0012	0.0232	1.7152	1
56	9	12	0.0003	0.02	3.6	1
57	7	9	0.0002	0.0082	1.3	1
58	7	9	0.0002	0.0082	1.3	1
59	17	18	0.0001	0.0013	0.0038	1
60	17	18	0.0001	0.0012	0.0033	1
61	14	16	0	0.0003	0.0143	1
62	14	16	0	0.0003	0.0184	1
63	14	12	0.0002	0.0045	0.3332	1
64	14	12	0.0002	0.0045	0.305	1
65	15	12	0.0006	0.0141	1.0976	1
66	15	12	0.0011	0.0241	1.5554	1
67	15	12	0.0011	0.0241	1.5535	1
68	15	21	0.001	0.0051	1.0513	1
69	23	21	0.0008	0.0077	0.3273	1
70	15	23	0.0021	0.0166	2.9358	1
71	15	23	0.0021	0.0158	2.9538	1
72	22	27	0.0029	0.0025	23.9151	1
73	92	90	0.0016	0.0111	3.6348	1

Number	From Bus	To Bus	Resistance (pu)	Reactance (pu)	Suceptance (B)	Branch Tap
74	85	89	0.0008	0.0199	0	1
75	85	84	0.0015	0.0147	0	1
76	86	85	0.0005	0.013	0	1
77	93	94	0.0014	0.0069	0.7944	1
78	93	94	0.0014	0.0069	0.7944	1
79	94	90	0.001	0.0104	0.9312	1
80	94	90	0.0016	0.0123	2.2819	1
81	97	95	0.0111	0.0668	0.0729	1
82	97	95	0.0105	0.0654	0.0686	1
83	97	95	0.0111	0.0664	0.0716	1
84	97	101	0.039	0.274	0.3107	1
85	97	100	0.0248	0.1694	0.2023	1
86	100	101	0.0148	0.101	0.1207	1
87	97	99	0.0138	0.0927	0.1106	1
88	99	101	0.0306	0.2046	0.2447	1
89	97	98	0.0167	0.1138	0.1361	1
90	98	101	0.0223	0.1611	0.1834	1
91	90	84	0.0017	0.0376	2.0789	1
92	90	89	0.001	0.0257	0.7976	1
93	89	84	0.0007	0.0061	2.824	1
94	89	87	0.0008	0.0194	1.3285	1
95	87	84	0.0009	0.0209	1.4571	1
96	87	84	0.0009	0.0209	1.4571	1
97	68	77	0.0004	0.0113	0.8292	1
98	68	77	0.0004	0.0113	0.8292	1
99	68	66	0.0019	0.031	4.1402	1
100	63	68	0.0019	0.0278	4.6712	1
101	66	63	0.0006	0.0141	1.0429	1
102	64	70	0.0004	0.0091	0.6679	1
103	68	69	0.0006	0.0128	0.9462	1
104	71	69	0.0002	0.0046	0.3234	1
105	69	70	0.0004	0.0093	0.6856	1
106	68	71	0.0003	0.0075	0.5174	1
107	68	71	0.0004	0.0075	0.5536	1
108	80	78	0.0029	0.0365	0.1266	1
109	80	78	0.0014	0.034	0.1125	1
110	79	74	0.0019	0.0258	0.0984	1
111	79	80	0.0084	0.0703	0.1595	1
112	75	74	0.0011	0.0127	0.048	1
113	78	74	0.0032	0.0395	0.144	1
114	73	74	0.0014	0.054	0.1525	1
115	30	34	0.0016	0.0226	0.381	1
116	35	34	0.0008	0.0106	0.2039	1
117	30	35	0.0024	0.0332	0.5849	1

Number	From Bus	To Bus	Resistance (pu)	Reactance (pu)	Suceptance (B)	Branch Tap
118	35	42	0.0017	0.0225	0.3992	1
119	35	42	0.0021	0.0238	0.3845	1
120	37	40	0.0096	0.0878	1.4265	1
121	35	37	0.0052	0.0602	1.01	1
122	35	37	0.0049	0.0537	0.8843	1
123	35	36	0.0012	0.0172	0.2987	1
124	37	39	0.0034	0.0374	0.6208	1
125	37	39	0.0034	0.0372	0.6182	1
126	42	39	0.0038	0.034	0.5824	1
127	42	39	0.0032	0.0349	0.5722	1
128	31	32	0.0108	0.0965	0.3296	1
129	37	36	0.0034	0.0392	0.6524	1
130	6	7	0.0008	0.0239	3.3	1
131	9	24	0.0007	0.074	4.87	1
132	23	93	0.0011	0.0091	1.2808	1
133	23	93	0.001	0.0092	1.5715	1
134	23	92	0.0011	0.0129	2.7575	1
135	84	77	0.0013	0.0082	1.9687	1
136	84	77	0.0013	0.0081	1.9492	1
137	84	77	0.0011	0.0077	1.6015	1
138	68	104	0.0002	0.0041	0.2962	1
139	63	104	0.0018	0.0252	0.5355	1
140	63	104	0.0018	0.0252	0.5355	1
141	80	82	0.0006	0.0119	0.0467	1
142	80	82	0.0006	0.0119	0.0467	1
143	79	82	0.0014	0.0264	0.102	1
144	61	63	0.0028	0.0211	1.0194	1
145	59	64	0.0026	0.0297	2.153	1
146	59	64	0.0026	0.0297	2.153	1
147	22	21	0.0012	0.0237	2.2071	1
148	30	29	0.0062	0.0673	1.1156	1
149	43	42	0.0018	0.0245	0.4392	1
150	43	42	0.0018	0.0245	0.4392	1
151	41	50	0.0048	0.0436	0.7078	1
152	45	47	0	0.015	0	1
153	55	54	0	0.0146	0	1
154	59	60	0.0001	0.005	0	1.1061
155	55	56	0	0.0173	0	0.9545
156	48	49	0	0.006	0	1.0435
157	51	50	0	0.011	0	1.063
158	51	50	0	0.011	0	1.063
159	50	53	0	0.0059	0	1
160	50	52	0.0003	0.0138	0	1
161	50	52	0.0003	0.0139	0	1

Number	From Bus	To Bus	Resistance (pu)	Reactance (pu)	Suceptance (B)	Branch Tap
162	61	62	0	0.0067	0	1.08
163	4	3	0	0.01	0	1.1
164	6	5	0	0.0015	0	1.05
165	2	1	0	0.002	0	1
166	104	105	0.0002	0.0234	0	0.9789
167	43	44	0	0.0052	0	1.025
168	24	26	0	0.005	0	1.09
169	27	29	0	0.0072	0	1.05
170	7	8	0	0.0025	0	1.066
171	16	18	0	0.0022	0	1.0234
172	17	20	0.0009	0.0299	0	0.9873
173	14	17	0.0002	0.0118	0	1.0238
174	14	17	0.0001	0.0073	0	1.0238
175	12	13	0	0.0037	0	1.0977
176	17	19	0	0.0103	0	1.0455
177	96	95	0	0.0228	0	0.9174
178	95	93	0.0001	0.0174	0	1.119
179	91	90	0	0.0045	0	0.9452
180	102	101	0	0.0181	0	0.9091
181	101	90	0.0002	0.0125	0	1.119
182	83	84	0.0003	0.0174	0	1.119
183	83	84	0.0002	0.0119	0	1.119
184	87	88	0	0.0098	0	1.05
185	77	78	0	0.0115	0	1.0631
186	77	78	0	0.0115	0	1.0631
187	77	78	0	0.0115	0	1.0631
188	65	63	0	0.0151	0	0.996
189	66	67	0	0.0098	0	1.05
190	76	75	0	0.0037	0	0.9787
191	72	71	0	0.0052	0	0.9843
192	71	73	0	0.005	0	1
193	107	108	0.0006	0.0149	0	1.0017
194	106	108	0.0006	0.0149	0	1.0017
195	109	108	0.0003	0.0133	0	1
196	109	108	0.0003	0.0134	0	1
197	120	116	0.0001	0.0139	0	1.0106
198	120	116	0.0001	0.0139	0	1.0106
199	122	118	0.0001	0.0069	0	1.05
200	112	113	0.0006	0.0254	0	1.0491
201	123	118	0.0003	0.0139	0	1.05
202	118	119	0.005	0.1147	0	1.0478
203	125	126	0.0005	0.0238	0	1
204	103	82	0	0.0012	0	1.0133
205	81	80	0	0.0103	0	0.9871

Number	From Bus	To Bus	Resistance (pu)	Reactance (pu)	Suceptance (B)	Branch Tap
206	45	46	0	0.0124	0	1
207	37	38	0.0002	0.0058	0	0.9855
208	40	41	0	0.0195	0	1
209	30	31	0.0003	0.0181	0	1
210	32	33	0.0005	0.0141	0	1.0588
211	29	28	0	0.0046	0	1

Appendix B ETMSP Relay Settings Information

Relay Data Card

This appendix contains the settings for the Under Frequency and Distance relays. The data is shown as it is entered in the ETMSP program. In the file, firstly the 129 Under Frequency relays are shown and the format is presented next.

Line 1	UFLT					
Line 2	Bus 1	Bus 2	Cid	Rflag		
Line 3	FS	TD	TCB		TRC	
Line 4	SLD	Bus	Ishunt	%P	%Q	Tdelay
Line 5	ESC					

Nomenclature:

UFLT: Keyword
 Bus 1: From Bus Number
 Bus 2: To Bus Number
 Cid: Circuit ID
 Rflag: "C" for Remote Tripping Only, and " " for Local and Remote Trip
 FS: Frequency setting in Hz. Relay operates if frequency remains below the setting for a period specified by TD
 TD: Time delay in seconds
 TCB: Relay and Circuit Breaker operation time in cycles
 TRC: Time delay for line Reclosing in cycles.
 ESC: Keyword

After the Under Frequency relay settings information, the 302 distance relays are included in the file. The format is presented next.

Line 1	DIST					
Line 2	Bus 1	Bus 2	Cid	Rflag	Rtype	
Line 3	DT1	DT2	DT3	DT4		
Line 4	DT5	DT6	DT7	DT8		TRC
Line 5	ESC					

Nomenclature:

- DIST: Keyword
- Bus 1: From Bus Number
- Bus 2: To Bus Number
- Cid: Circuit ID
- Rflag: "C" for Remote Tripping Only, and " " for Local and Remote Trip
- Rtype: "C" for Impedance Relay and "D" for Default Distance Relay
- DT1: R/X ratio of the line in question
- DT2: Zone 1 Reach
- DT3: Zone 2 Reach
- DT4: Minimum Torque Angle that activates the relay logic, in degrees, Default = 60
- DT5: Maximum Torque Angle in degrees, Default = 70
- DT6: Blank
- DT7: Blank
- DT8: Relay Time Delay in Cycles
- TRC: Time Delay for line Reclosing in Cycles.
- ESC: Keyword

=====

UFLT	2	31	C				
		53.4		0.0	14.0		0.0
SLD	2	1		5.0	5.0		0.0
ESC							
	6	51	C				
		53.4		0.0	14.0		0.0
SLD	6	1		5.0	5.0		0.0
ESC							
	7	81	C				
		53.4		0.0	14.0		0.0
SLD	7	1		5.0	5.0		0.0
ESC							
	9	241	C				
		53.4		0.0	14.0		0.0
SLD	9	1		5.0	5.0		0.0
ESC							
	11	91	C				
		53.4		0.0	14.0		0.0
SLD	11	1		5.0	5.0		0.0
ESC							
	12	111	C				
		53.4		0.0	14.0		0.0
SLD	12	1		5.0	5.0		0.0
ESC							
	18	171	C				
		53.4		0.0	14.0		0.0
SLD	18	1		5.0	5.0		0.0
ESC							
	24	261	C				
		53.4		0.0	14.0		0.0
SLD	24	1		5.0	5.0		0.0
ESC							
	32	331	C				
		53.4		0.0	14.0		0.0
SLD	32	1		5.0	5.0		0.0
ESC							

34	351	C					
	53.4		0.0	14.0		0.0	
SLD	34	1	5.0	5.0			0.0
ESC							
35	371	C					
	53.4		0.0	14.0		0.0	
SLD	35	1	5.0	5.0			0.0
ESC							
43	441	C					
	53.4		0.0	14.0		0.0	
SLD	43	1	5.0	5.0			0.0
ESC							
48	491	C					
	53.4		0.0	14.0		0.0	
SLD	48	1	5.0	5.0			0.0
ESC							
59	601	C					
	53.4		0.0	14.0		0.0	
SLD	59	1	5.0	5.0			0.0
ESC							
64	591	C					
	53.4		0.0	14.0		0.0	
SLD	64	1	5.0	5.0			0.0
ESC							
69	681	C					
	53.4		0.0	14.0		0.0	
SLD	69	1	5.0	5.0			0.0
ESC							
70	691	C					
	53.4		0.0	14.0		0.0	
SLD	70	1	5.0	5.0			0.0
ESC							
71	721	C					
	53.4		0.0	14.0		0.0	
SLD	71	1	5.0	5.0			0.0
ESC							
74	731	C					
	53.4		0.0	14.0		0.0	
SLD	74	1	5.0	5.0			0.0
ESC							
75	761	C					
	53.4		0.0	14.0		0.0	
SLD	75	1	5.0	5.0			0.0
ESC							
80	811	C					
	53.4		0.0	14.0		0.0	
SLD	80	1	5.0	5.0			0.0
ESC							
82	1031	C					
	53.4		0.0	14.0		0.0	
SLD	82	1	5.0	5.0			0.0
ESC							
83	841	C					
	53.4		0.0	14.0		0.0	
SLD	83	1	5.0	5.0			0.0
ESC							
85	861	C					
	53.4		0.0	14.0		0.0	
SLD	85	1	5.0	5.0			0.0
ESC							
90	891	C					
	53.4		0.0	14.0		0.0	
SLD	90	1	5.0	5.0			0.0
ESC							
22	271	C					
	53.4		0.0	14.0		0.0	
SLD	22	1	5.0	5.0			0.0
ESC							
29	301	C					
	53.4		0.0	14.0		0.0	
SLD	29	1	5.0	5.0			0.0

ESC							
39	421	C					
	53.4		0.0	14.0	0.0		
SLD	39	1	5.0	5.0			0.0
ESC							
45	421	C					
	53.4		0.0	14.0	0.0		
SLD	45	1	5.0	5.0			0.0
ESC							
50	541	C					
	53.4		0.0	14.0	0.0		
SLD	50	1	5.0	5.0			0.0
ESC							
55	541	C					
	53.4		0.0	14.0	0.0		
SLD	55	1	5.0	5.0			0.0
ESC							
58	571	C					
	53.4		0.0	14.0	0.0		
SLD	58	1	5.0	5.0			0.0
ESC							
63	681	C					
	53.4		0.0	14.0	0.0		
SLD	63	1	5.0	5.0			0.0
ESC							
68	771	C					
	53.4		0.0	14.0	0.0		
SLD	68	1	5.0	5.0			0.0
ESC							
78	741	C					
	53.4		0.0	14.0	0.0		
SLD	78	1	5.0	5.0			0.0
ESC							
89	871	C					
	53.4		0.0	14.0	0.0		
SLD	89	1	5.0	5.0			0.0
ESC							
97	981	C					
	53.4		0.0	14.0	0.0		
SLD	97	1	5.0	5.0			0.0
ESC							
108	1091	C					
	53.4		0.0	14.0	0.0		
SLD	108	1	5.0	5.0			0.0
ESC							
124	1181	C					
	53.4		0.0	14.0	0.0		
SLD	124	1	5.0	5.0			0.0
ESC							
101	1021	C					
	53.4		0.0	14.0	0.0		
SLD	101	1	5.0	5.0			0.0
ESC							
111	1121	C					
	53.4		0.0	14.0	0.0		
SLD	111	1	5.0	5.0			0.0
ESC							
116	1171	C					
	53.4		0.0	14.0	0.0		
SLD	116	1	5.0	5.0			0.0
ESC							
117	1181	C					
	53.4		0.0	14.0	0.0		
SLD	117	1	5.0	5.0			0.0
ESC							
2	31	C					
	51.5		0.0	14.0	0.0		
SLD	2	1	5.0	5.0			0.0
ESC							
6	51	C					
	51.5		0.0	14.0	0.0		

SLD	6	1	5.0	5.0			0.0
ESC							
	7	81	C				
		51.5		0.0	14.0		0.0
SLD	7	1	5.0	5.0			0.0
ESC							
	9	241	C				
		51.5		0.0	14.0		0.0
SLD	9	1	5.0	5.0			0.0
ESC							
	11	91	C				
		51.5		0.0	14.0		0.0
SLD	11	1	5.0	5.0			0.0
ESC							
	12	111	C				
		51.5		0.0	14.0		0.0
SLD	12	1	5.0	5.0			0.0
ESC							
	18	171	C				
		51.5		0.0	14.0		0.0
SLD	18	1	5.0	5.0			0.0
ESC							
	24	261	C				
		51.5		0.0	14.0		0.0
SLD	24	1	5.0	5.0			0.0
ESC							
	32	331	C				
		51.5		0.0	14.0		0.0
SLD	32	1	5.0	5.0			0.0
ESC							
	34	351	C				
		51.5		0.0	14.0		0.0
SLD	34	1	5.0	5.0			0.0
ESC							
	35	371	C				
		51.5		0.0	14.0		0.0
SLD	35	1	5.0	5.0			0.0
ESC							
	43	441	C				
		51.5		0.0	14.0		0.0
SLD	43	1	5.0	5.0			0.0
ESC							
	48	491	C				
		51.5		0.0	14.0		0.0
SLD	48	1	5.0	5.0			0.0
ESC							
	59	601	C				
		51.5		0.0	14.0		0.0
SLD	59	1	5.0	5.0			0.0
ESC							
	64	591	C				
		51.5		0.0	14.0		0.0
SLD	64	1	5.0	5.0			0.0
ESC							
	69	681	C				
		51.5		0.0	14.0		0.0
SLD	69	1	5.0	5.0			0.0
ESC							
	70	691	C				
		51.5		0.0	14.0		0.0
SLD	70	1	5.0	5.0			0.0
ESC							
	71	721	C				
		51.5		0.0	14.0		0.0
SLD	71	1	5.0	5.0			0.0
ESC							
	74	731	C				
		51.5		0.0	14.0		0.0
SLD	74	1	5.0	5.0			0.0
ESC							
	75	761	C				

	51.5		0.0	14.0	0.0	
SLD	75	1	5.0	5.0		0.0
ESC						
80	811		C			
	51.5		0.0	14.0	0.0	
SLD	80	1	5.0	5.0		0.0
ESC						
82	1031		C			
	51.5		0.0	14.0	0.0	
SLD	82	1	5.0	5.0		0.0
ESC						
83	841		C			
	51.5		0.0	14.0	0.0	
SLD	83	1	5.0	5.0		0.0
ESC						
85	861		C			
	51.5		0.0	14.0	0.0	
SLD	85	1	5.0	5.0		0.0
ESC						
90	891		C			
	51.5		0.0	14.0	0.0	
SLD	90	1	5.0	5.0		0.0
ESC						
22	271		C			
	51.5		0.0	14.0	0.0	
SLD	22	1	5.0	5.0		0.0
ESC						
29	301		C			
	51.5		0.0	14.0	0.0	
SLD	29	1	5.0	5.0		0.0
ESC						
39	421		C			
	51.5		0.0	14.0	0.0	
SLD	39	1	5.0	5.0		0.0
ESC						
45	421		C			
	51.5		0.0	14.0	0.0	
SLD	45	1	5.0	5.0		0.0
ESC						
50	541		C			
	51.5		0.0	14.0	0.0	
SLD	50	1	5.0	5.0		0.0
ESC						
55	541		C			
	51.5		0.0	14.0	0.0	
SLD	55	1	5.0	5.0		0.0
ESC						
58	571		C			
	51.5		0.0	14.0	0.0	
SLD	58	1	5.0	5.0		0.0
ESC						
63	681		C			
	51.5		0.0	14.0	0.0	
SLD	63	1	5.0	5.0		0.0
ESC						
68	771		C			
	51.5		0.0	14.0	0.0	
SLD	68	1	5.0	5.0		0.0
ESC						
78	741		C			
	51.5		0.0	14.0	0.0	
SLD	78	1	5.0	5.0		0.0
ESC						
89	871		C			
	51.5		0.0	14.0	0.0	
SLD	89	1	5.0	5.0		0.0
ESC						
97	981		C			
	51.5		0.0	14.0	0.0	
SLD	97	1	5.0	5.0		0.0
ESC						

108	1091	C				
	51.5		0.0	14.0		
SLD	108	1	5.0	5.0		0.0
ESC						
124	1181	C				
	51.5		0.0	14.0		
SLD	124	1	5.0	5.0		0.0
ESC						
101	1021	C				
	51.5		0.0	14.0		
SLD	101	1	5.0	5.0		0.0
ESC						
111	1121	C				
	51.5		0.0	14.0		
SLD	111	1	5.0	5.0		0.0
ESC						
116	1171	C				
	51.5		0.0	14.0		
SLD	116	1	5.0	5.0		0.0
ESC						
117	1181	C				
	51.5		0.0	14.0		
SLD	117	1	5.0	5.0		0.0
ESC						
2	31	C				
	49.6		0.0	14.0		
SLD	2	1	5.0	5.0		0.0
ESC						
6	51	C				
	49.6		0.0	14.0		
SLD	6	1	5.0	5.0		0.0
ESC						
7	81	C				
	49.6		0.0	14.0		
SLD	7	1	5.0	5.0		0.0
ESC						
9	241	C				
	49.6		0.0	14.0		
SLD	9	1	5.0	5.0		0.0
ESC						
11	91	C				
	49.6		0.0	14.0		
SLD	11	1	5.0	5.0		0.0
ESC						
12	111	C				
	49.6		0.0	14.0		
SLD	12	1	5.0	5.0		0.0
ESC						
18	171	C				
	49.6		0.0	14.0		
SLD	18	1	5.0	5.0		0.0
ESC						
24	261	C				
	49.6		0.0	14.0		
SLD	24	1	5.0	5.0		0.0
ESC						
32	331	C				
	49.6		0.0	14.0		
SLD	32	1	5.0	5.0		0.0
ESC						
34	351	C				
	49.6		0.0	14.0		
SLD	34	1	5.0	5.0		0.0
ESC						
35	371	C				
	49.6		0.0	14.0		
SLD	35	1	5.0	5.0		0.0
ESC						
43	441	C				
	49.6		0.0	14.0		
SLD	43	1	5.0	5.0		0.0

ESC							
48	491	C					
	49.6		0.0	14.0	0.0		
SLD	48	1	5.0	5.0			0.0
ESC							
59	601	C					
	49.6		0.0	14.0	0.0		
SLD	59	1	5.0	5.0			0.0
ESC							
64	591	C					
	49.6		0.0	14.0	0.0		
SLD	64	1	5.0	5.0			0.0
ESC							
69	681	C					
	49.6		0.0	14.0	0.0		
SLD	69	1	5.0	5.0			0.0
ESC							
70	691	C					
	49.6		0.0	14.0	0.0		
SLD	70	1	5.0	5.0			0.0
ESC							
71	721	C					
	49.6		0.0	14.0	0.0		
SLD	71	1	5.0	5.0			0.0
ESC							
74	731	C					
	49.6		0.0	14.0	0.0		
SLD	74	1	5.0	5.0			0.0
ESC							
75	761	C					
	49.6		0.0	14.0	0.0		
SLD	75	1	5.0	5.0			0.0
ESC							
80	811	C					
	49.6		0.0	14.0	0.0		
SLD	80	1	5.0	5.0			0.0
ESC							
82	1031	C					
	49.6		0.0	14.0	0.0		
SLD	82	1	5.0	5.0			0.0
ESC							
83	841	C					
	49.6		0.0	14.0	0.0		
SLD	83	1	5.0	5.0			0.0
ESC							
85	861	C					
	49.6		0.0	14.0	0.0		
SLD	85	1	5.0	5.0			0.0
ESC							
90	891	C					
	49.6		0.0	14.0	0.0		
SLD	90	1	5.0	5.0			0.0
ESC							
22	271	C					
	49.6		0.0	14.0	0.0		
SLD	22	1	5.0	5.0			0.0
ESC							
29	301	C					
	49.6		0.0	14.0	0.0		
SLD	29	1	5.0	5.0			0.0
ESC							
39	421	C					
	49.6		0.0	14.0	0.0		
SLD	39	1	5.0	5.0			0.0
ESC							
45	421	C					
	49.6		0.0	14.0	0.0		
SLD	45	1	5.0	5.0			0.0
ESC							
50	541	C					
	49.6		0.0	14.0	0.0		

SLD	50	1	5.0	5.0		0.0
ESC	55	541	C			
	49.6		0.0	14.0	0.0	
SLD	55	1	5.0	5.0		0.0
ESC	58	571	C			
	49.6		0.0	14.0	0.0	
SLD	58	1	5.0	5.0		0.0
ESC	63	681	C			
	49.6		0.0	14.0	0.0	
SLD	63	1	5.0	5.0		0.0
ESC	68	771	C			
	49.6		0.0	14.0	0.0	
SLD	68	1	5.0	5.0		0.0
ESC	78	741	C			
	49.6		0.0	14.0	0.0	
SLD	78	1	5.0	5.0		0.0
ESC	89	871	C			
	49.6		0.0	14.0	0.0	
SLD	89	1	5.0	5.0		0.0
ESC	97	981	C			
	49.6		0.0	14.0	0.0	
SLD	97	1	5.0	5.0		0.0
ESC	108	1091	C			
	49.6		0.0	14.0	0.0	
SLD	108	1	5.0	5.0		0.0
ESC	124	1181	C			
	49.6		0.0	14.0	0.0	
SLD	124	1	5.0	5.0		0.0
ESC	101	1021	C			
	49.6		0.0	14.0	0.0	
SLD	101	1	5.0	5.0		0.0
ESC	111	1121	C			
	49.6		0.0	14.0	0.0	
SLD	111	1	5.0	5.0		0.0
ESC	116	1171	C			
	49.6		0.0	14.0	0.0	
SLD	116	1	5.0	5.0		0.0
ESC	117	1181	C			
	49.6		0.0	14.0	0.0	
SLD	117	1	5.0	5.0		0.0

EDATA
 ?????????????????? T H I S A R E T H E D I S T A N C E R E L A Y S ??????????????????
 ?????????????????? T H I S A R E T H E D I S T A N C E R E L A Y S ??????????????????
 ?????????????????? T H I S A R E T H E D I S T A N C E R E L A Y S ??????????????????
 ?????????????????? T H I S A R E T H E D I S T A N C E R E L A Y S ??????????????????

DIST	3	21	D			
		0.1	0.8	1.2	60.0	
		85.0			28.0	0.0
ESC	2	31	D			
		0.1	0.8	1.2	60.0	
		85.0			28.0	0.0
ESC	6	41	D			
		0.05	0.8	1.2	60.0	
		85.0			28.0	0.0

ESC	4	61	D				
		0.05	0.8	1.2	60.0		
		85.0			28.0		0.0
ESC	6	71	D				
		0.0347	0.8	1.2	60.0		
		85.0			28.0		0.0
ESC	7	61	D				
		0.0347	0.8	1.2	60.0		
		85.0			28.0		0.0
ESC	7	91	D				
		0.0244	0.8	1.2	60.0		
		85.0			28.0		0.0
ESC	9	71	D				
		0.0244	0.8	1.2	60.0		
		85.0			28.0		0.0
ESC	7	92	D				
		0.0244	0.8	1.2	60.0		
		85.0			28.0		0.0
ESC	9	72	D				
		0.0244	0.8	1.2	60.0		
		85.0			28.0		0.0
ESC	9	101	D				
		0.0546	0.8	1.2	60.0		
		85.0			28.0		0.0
ESC	10	91	D				
		0.0546	0.8	1.2	60.0		
		85.0			28.0		0.0
ESC	9	121	D				
		0.0518	0.8	1.2	60.0		
		85.0			46.0		0.0
ESC	12	91	D				
		0.0518	0.8	1.2	60.0		
		85.0			28.0		0.0
ESC	9	122	D				
		0.015	0.8	1.2	60.0		
		85.0			46.0		0.0
ESC	12	92	D				
		0.015	0.8	1.2	60.0		
		85.0			28.0		0.0
ESC	9	241	D				
		0.0095	0.8	1.2	60.0		
		85.0			28.0		0.0
ESC	24	91	D				
		0.0095	0.8	1.2	60.0		
		85.0			46.0		0.0
ESC	11	91	D				
		0.0629	0.8	1.2	60.0		
		85.0			28.0		0.0
ESC	9	111	D				
		0.0629	0.8	1.2	60.0		
		85.0			28.0		0.0
ESC	11	121	D				
		0.0593	0.8	1.2	60.0		

	85.0			46.0	0.0
ESC	12 111	D			
	0.0593	0.8	1.2	60.0	
	85.0			28.0	0.0
ESC	11 251	D			
	0.1274	0.8	1.2	60.0	
	85.0			28.0	0.0
ESC	25 111	D			
	0.1274	0.8	1.2	60.0	
	85.0			28.0	0.0
ESC	14 121	D			
	0.051	0.8	1.2	60.0	
	85.0			28.0	0.0
ESC	12 141	D			
	0.051	0.8	1.2	60.0	
	85.0			46.0	0.0
ESC	14 122	D			
	0.051	0.8	1.2	60.0	
	85.0			28.0	0.0
ESC	12 142	D			
	0.051	0.8	1.2	60.0	
	85.0			46.0	0.0
ESC	14 161	D			
	0.0333	0.8	1.2	60.0	
	85.0			28.0	0.0
ESC	16 141	D			
	0.0333	0.8	1.2	60.0	
	85.0			28.0	0.0
ESC	14 162	D			
	0.0333	0.8	1.2	60.0	
	85.0			28.0	0.0
ESC	16 142	D			
	0.0333	0.8	1.2	60.0	
	85.0			28.0	0.0
ESC	15 121	D			
	0.0446	0.8	1.2	60.0	
	85.0			46.0	0.0
ESC	12 151	D			
	0.0446	0.8	1.2	60.0	
	85.0			28.0	0.0
ESC	15 122	D			
	0.0453	0.8	1.2	60.0	
	85.0			46.0	0.0
ESC	12 152	D			
	0.0453	0.8	1.2	60.0	
	85.0			28.0	0.0
ESC	15 123	D			
	0.0448	0.8	1.2	60.0	
	85.0			28.0	0.0
ESC	12 153	D			
	0.0448	0.8	1.2	60.0	
	85.0			28.0	0.0
ESC	15 211	D			

	0.1969	0.8	1.2	60.0	
	85.0			28.0	0.0
ESC					
21	151	D			
	0.1969	0.8	1.2	60.0	
	85.0			28.0	0.0
ESC					
15	231	D			
	0.1286	0.8	1.2	60.0	
	85.0			28.0	0.0
ESC					
23	151	D			
	0.1286	0.8	1.2	60.0	
	85.0			28.0	0.0
ESC					
15	232	D			
	0.1338	0.8	1.2	60.0	
	85.0			28.0	0.0
ESC					
23	152	D			
	0.1338	0.8	1.2	60.0	
	85.0			28.0	0.0
ESC					
17	181	D			
	0.0458	0.8	1.2	60.0	
	85.0			28.0	0.0
ESC					
18	171	D			
	0.0458	0.8	1.2	60.0	
	85.0			28.0	0.0
ESC					
17	182	D			
	0.0517	0.8	1.2	60.0	
	85.0			28.0	0.0
ESC					
18	172	D			
	0.0517	0.8	1.2	60.0	
	85.0			28.0	0.0
ESC					
22	211	D			
	0.0514	0.8	1.2	60.0	
	85.0			28.0	0.0
ESC					
21	221	D			
	0.0514	0.8	1.2	60.0	
	85.0			46.0	0.0
ESC					
22	271	D			
	1.1532	0.8	1.2	60.0	
	85.0			28.0	0.0
ESC					
27	221	D			
	1.1532	0.8	1.2	60.0	
	85.0			28.0	0.0
ESC					
23	211	D			
	0.1095	0.8	1.2	60.0	
	85.0			28.0	0.0
ESC					
21	231	D			
	0.1095	0.8	1.2	60.0	
	85.0			28.0	0.0
ESC					
23	921	D			
	0.082	0.8	1.2	60.0	
	85.0			28.0	0.0
ESC					
92	231	D			
	0.082	0.8	1.2	60.0	
	85.0			28.0	0.0
ESC					

23	931	D				
	0.1191	0.8	1.2	60.0		
	85.0			28.0		0.0
ESC						
93	231	D				
	0.1191	0.8	1.2	60.0		
	85.0			28.0		0.0
ESC						
23	932	D				
	0.1134	0.8	1.2	60.0		
	85.0			28.0		0.0
ESC						
93	232	D				
	0.1134	0.8	1.2	60.0		
	85.0			28.0		0.0
ESC						
30	291	D				
	0.0921	0.8	1.2	60.0		
	85.0			28.0		0.0
ESC						
29	301	D				
	0.0921	0.8	1.2	60.0		
	85.0			28.0		0.0
ESC						
30	341	D				
	0.0708	0.8	1.2	60.0		
	85.0			28.0		0.0
ESC						
34	301	D				
	0.0708	0.8	1.2	60.0		
	85.0			28.0		0.0
ESC						
30	351	D				
	0.0723	0.8	1.2	60.0		
	85.0			28.0		0.0
ESC						
35	301	D				
	0.0723	0.8	1.2	60.0		
	85.0			28.0		0.0
ESC						
31	321	D				
	0.1119	0.8	1.2	60.0		
	85.0			28.0		0.0
ESC						
32	311	D				
	0.1119	0.8	1.2	60.0		
	85.0			28.0		0.0
ESC						
35	341	D				
	0.0755	0.8	1.2	60.0		
	85.0			28.0		0.0
ESC						
34	351	D				
	0.0755	0.8	1.2	60.0		
	85.0			28.0		0.0
ESC						
35	361	D				
	0.0698	0.8	1.2	60.0		
	85.0			28.0		0.0
ESC						
36	351	D				
	0.0698	0.8	1.2	60.0		
	85.0			28.0		0.0
ESC						
35	371	D				
	0.0864	0.8	1.2	60.0		
	85.0			28.0		0.0
ESC						
37	351	D				
	0.0864	0.8	1.2	60.0		
	85.0			46.0		0.0

ESC						
35	372	D				
	0.0912	0.8	1.2	60.0		
	85.0			28.0		0.0
ESC						
37	352	D				
	0.0912	0.8	1.2	60.0		
	85.0			46.0		0.0
ESC						
35	421	D				
	0.0756	0.8	1.2	60.0		
	85.0			28.0		0.0
ESC						
42	351	D				
	0.0756	0.8	1.2	60.0		
	85.0			28.0		0.0
ESC						
35	422	D				
	0.0882	0.8	1.2	60.0		
	85.0			28.0		0.0
ESC						
42	352	D				
	0.0882	0.8	1.2	60.0		
	85.0			28.0		0.0
ESC						
37	361	D				
	0.0867	0.8	1.2	60.0		
	85.0			28.0		0.0
ESC						
36	371	D				
	0.0867	0.8	1.2	60.0		
	85.0			28.0		0.0
ESC						
37	391	D				
	0.0909	0.8	1.2	60.0		
	85.0			28.0		0.0
ESC						
39	371	D				
	0.0909	0.8	1.2	60.0		
	85.0			28.0		0.0
ESC						
37	392	D				
	0.0914	0.8	1.2	60.0		
	85.0			28.0		0.0
ESC						
39	372	D				
	0.0914	0.8	1.2	60.0		
	85.0			28.0		0.0
ESC						
37	401	D				
	0.1093	0.8	1.2	60.0		
	85.0			28.0		0.0
ESC						
40	371	D				
	0.1093	0.8	1.2	60.0		
	85.0			28.0		0.0
ESC						
41	501	D				
	0.1101	0.8	1.2	60.0		
	85.0			46.0		0.0
ESC						
50	411	D				
	0.1101	0.8	1.2	60.0		
	85.0			28.0		0.0
ESC						
42	391	D				
	0.1118	0.8	1.2	60.0		
	85.0			28.0		0.0
ESC						
39	421	D				
	0.1118	0.8	1.2	60.0		

	85.0			28.0	0.0
ESC	42 392	D			
	0.0917	0.8	1.2	60.0	
	85.0			28.0	0.0
ESC	39 422	D			
	0.0917	0.8	1.2	60.0	
	85.0			28.0	0.0
ESC	43 421	D			
	0.0735	0.8	1.2	60.0	
	85.0			28.0	0.0
ESC	42 431	D			
	0.0735	0.8	1.2	60.0	
	85.0			28.0	0.0
ESC	43 422	D			
	0.0735	0.8	1.2	60.0	
	85.0			28.0	0.0
ESC	42 432	D			
	0.0735	0.8	1.2	60.0	
	85.0			28.0	0.0
ESC	45 421	D			
	0.0592	0.8	1.2	60.0	
	85.0			46.0	0.0
ESC	42 451	D			
	0.0592	0.8	1.2	60.0	
	85.0			28.0	0.0
ESC	48 451	D			
	0.0888	0.8	1.2	60.0	
	85.0			28.0	0.0
ESC	45 481	D			
	0.0888	0.8	1.2	60.0	
	85.0			46.0	0.0
ESC	50 481	D			
	0.0943	0.8	1.2	60.0	
	85.0			28.0	0.0
ESC	48 501	D			
	0.0943	0.8	1.2	60.0	
	85.0			28.0	0.0
ESC	51 571	D			
	0.0557	0.8	1.2	60.0	
	85.0			46.0	0.0
ESC	57 511	D			
	0.0557	0.8	1.2	60.0	
	85.0			28.0	0.0
ESC	54 501	D			
	0.09	0.8	1.2	60.0	
	85.0			28.0	0.0
ESC	50 541	D			
	0.09	0.8	1.2	60.0	
	85.0			28.0	0.0
ESC	57 581	D			
	0.0684	0.8	1.2	60.0	
	85.0			28.0	0.0
ESC	58 571	D			

	0.0684	0.8	1.2	60.0	
	85.0			28.0	0.0
ESC					
57	631	D			
	0.1388	0.8	1.2	60.0	
	85.0			28.0	0.0
ESC					
63	571	D			
	0.1388	0.8	1.2	60.0	
	85.0			28.0	0.0
ESC					
59	581	D			
	0.0417	0.8	1.2	60.0	
	85.0			28.0	0.0
ESC					
58	591	D			
	0.0417	0.8	1.2	60.0	
	85.0			28.0	0.0
ESC					
59	582	D			
	0.0417	0.8	1.2	60.0	
	85.0			28.0	0.0
ESC					
58	592	D			
	0.0417	0.8	1.2	60.0	
	85.0			28.0	0.0
ESC					
59	641	D			
	0.0873	0.8	1.2	60.0	
	85.0			28.0	0.0
ESC					
64	591	D			
	0.0873	0.8	1.2	60.0	
	85.0			28.0	0.0
ESC					
59	642	D			
	0.0873	0.8	1.2	60.0	
	85.0			28.0	0.0
ESC					
64	592	D			
	0.0873	0.8	1.2	60.0	
	85.0			28.0	0.0
ESC					
61	571	D			
	0.1429	0.8	1.2	60.0	
	85.0			28.0	0.0
ESC					
57	611	D			
	0.1429	0.8	1.2	60.0	
	85.0			28.0	0.0
ESC					
61	581	D			
	0.0677	0.8	1.2	60.0	
	85.0			28.0	0.0
ESC					
58	611	D			
	0.0677	0.8	1.2	60.0	
	85.0			46.0	0.0
ESC					
61	631	D			
	0.1327	0.8	1.2	60.0	
	85.0			28.0	0.0
ESC					
63	611	D			
	0.1327	0.8	1.2	60.0	
	85.0			28.0	0.0
ESC					
63	681	D			
	0.0694	0.8	1.2	60.0	
	85.0			46.0	0.0
ESC					

68	631	D				
	0.0694	0.8	1.2	60.0		
	85.0			28.0		0.0
ESC						
63	1041	D				
	0.0709	0.8	1.2	60.0		
	85.0			46.0		0.0
ESC						
104	631	D				
	0.0709	0.8	1.2	60.0		
	85.0			28.0		0.0
ESC						
63	1042	D				
	0.0709	0.8	1.2	60.0		
	85.0			46.0		0.0
ESC						
104	632	D				
	0.0709	0.8	1.2	60.0		
	85.0			28.0		0.0
ESC						
64	701	D				
	0.0464	0.8	1.2	60.0		
	85.0			28.0		0.0
ESC						
70	641	D				
	0.0464	0.8	1.2	60.0		
	85.0			28.0		0.0
ESC						
66	631	D				
	0.0396	0.8	1.2	60.0		
	85.0			28.0		0.0
ESC						
63	661	D				
	0.0396	0.8	1.2	60.0		
	85.0			28.0		0.0
ESC						
68	661	D				
	0.0613	0.8	1.2	60.0		
	85.0			28.0		0.0
ESC						
66	681	D				
	0.0613	0.8	1.2	60.0		
	85.0			46.0		0.0
ESC						
68	691	D				
	0.0469	0.8	1.2	60.0		
	85.0			28.0		0.0
ESC						
69	681	D				
	0.0469	0.8	1.2	60.0		
	85.0			28.0		0.0
ESC						
68	711	D				
	0.0372	0.8	1.2	60.0		
	85.0			28.0		0.0
ESC						
71	681	D				
	0.0372	0.8	1.2	60.0		
	85.0			28.0		0.0
ESC						
68	712	D				
	0.0467	0.8	1.2	60.0		
	85.0			28.0		0.0
ESC						
71	682	D				
	0.0467	0.8	1.2	60.0		
	85.0			28.0		0.0
ESC						
68	771	D				
	0.0391	0.8	1.2	60.0		
	85.0			28.0		0.0

ESC						
77	681	D				
	0.0391	0.8	1.2	60.0		
	85.0			28.0		0.0
ESC						
68	772	D				
	0.0391	0.8	1.2	60.0		
	85.0			28.0		0.0
ESC						
77	682	D				
	0.0391	0.8	1.2	60.0		
	85.0			28.0		0.0
ESC						
68	1041	D				
	0.0488	0.8	1.2	60.0		
	85.0			28.0		0.0
ESC						
104	681	D				
	0.0488	0.8	1.2	60.0		
	85.0			28.0		0.0
ESC						
69	701	D				
	0.043	0.8	1.2	60.0		
	85.0			28.0		0.0
ESC						
70	691	D				
	0.043	0.8	1.2	60.0		
	85.0			28.0		0.0
ESC						
71	691	D				
	0.046	0.8	1.2	60.0		
	85.0			28.0		0.0
ESC						
69	711	D				
	0.046	0.8	1.2	60.0		
	85.0			28.0		0.0
ESC						
73	741	D				
	0.0256	0.8	1.2	60.0		
	85.0			28.0		0.0
ESC						
74	731	D				
	0.0256	0.8	1.2	60.0		
	85.0			28.0		0.0
ESC						
75	741	D				
	0.0866	0.8	1.2	60.0		
	85.0			28.0		0.0
ESC						
74	751	D				
	0.0866	0.8	1.2	60.0		
	85.0			28.0		0.0
ESC						
78	741	D				
	0.081	0.8	1.2	60.0		
	85.0			28.0		0.0
ESC						
74	781	D				
	0.081	0.8	1.2	60.0		
	85.0			28.0		0.0
ESC						
79	741	D				
	0.0736	0.8	1.2	60.0		
	85.0			28.0		0.0
ESC						
74	791	D				
	0.0736	0.8	1.2	60.0		
	85.0			28.0		0.0
ESC						
79	801	D				
	0.1201	0.8	1.2	60.0		

	85.0			46.0	0.0
ESC	80 791	D			
	0.1201	0.8	1.2	60.0	
	85.0			28.0	0.0
ESC	79 821	D			
	0.053	0.8	1.2	60.0	
	85.0			28.0	0.0
ESC	82 791	D			
	0.053	0.8	1.2	60.0	
	85.0			28.0	0.0
ESC	80 781	D			
	0.0781	0.8	1.2	60.0	
	85.0			28.0	0.0
ESC	78 801	D			
	0.0781	0.8	1.2	60.0	
	85.0			28.0	0.0
ESC	80 782	D			
	0.0406	0.8	1.2	60.0	
	85.0			28.0	0.0
ESC	78 802	D			
	0.0406	0.8	1.2	60.0	
	85.0			28.0	0.0
ESC	80 821	D			
	0.0548	0.8	1.2	60.0	
	85.0			28.0	0.0
ESC	82 801	D			
	0.0548	0.8	1.2	60.0	
	85.0			28.0	0.0
ESC	80 822	D			
	0.0548	0.8	1.2	60.0	
	85.0			28.0	0.0
ESC	82 802	D			
	0.0548	0.8	1.2	60.0	
	85.0			28.0	0.0
ESC	84 771	D			
	0.1523	0.8	1.2	60.0	
	85.0			28.0	0.0
ESC	77 841	D			
	0.1523	0.8	1.2	60.0	
	85.0			28.0	0.0
ESC	84 772	D			
	0.1534	0.8	1.2	60.0	
	85.0			28.0	0.0
ESC	77 842	D			
	0.1534	0.8	1.2	60.0	
	85.0			28.0	0.0
ESC	84 773	D			
	0.1482	0.8	1.2	60.0	
	85.0			28.0	0.0
ESC	77 843	D			
	0.1482	0.8	1.2	60.0	
	85.0			28.0	0.0
ESC	85 841	D			

	0.1041	0.8	1.2	60.0	
	85.0			28.0	0.0
ESC					
84	851	D			
	0.1041	0.8	1.2	60.0	
	85.0			28.0	0.0
ESC					
85	891	D			
	0.0418	0.8	1.2	60.0	
	85.0			28.0	0.0
ESC					
89	851	D			
	0.0418	0.8	1.2	60.0	
	85.0			28.0	0.0
ESC					
86	851	D			
	0.0409	0.8	1.2	60.0	
	85.0			28.0	0.0
ESC					
85	861	D			
	0.0409	0.8	1.2	60.0	
	85.0			28.0	0.0
ESC					
87	841	D			
	0.0417	0.8	1.2	60.0	
	85.0			28.0	0.0
ESC					
84	871	D			
	0.0417	0.8	1.2	60.0	
	85.0			28.0	0.0
ESC					
87	842	D			
	0.0417	0.8	1.2	60.0	
	85.0			28.0	0.0
ESC					
84	872	D			
	0.0417	0.8	1.2	60.0	
	85.0			28.0	0.0
ESC					
89	841	D			
	0.1211	0.8	1.2	60.0	
	85.0			28.0	0.0
ESC					
84	891	D			
	0.1211	0.8	1.2	60.0	
	85.0			28.0	0.0
ESC					
89	871	D			
	0.0408	0.8	1.2	60.0	
	85.0			28.0	0.0
ESC					
87	891	D			
	0.0408	0.8	1.2	60.0	
	85.0			28.0	0.0
ESC					
90	841	D			
	0.0458	0.8	1.2	60.0	
	85.0			46.0	0.0
ESC					
84	901	D			
	0.0458	0.8	1.2	60.0	
	85.0			28.0	0.0
ESC					
90	891	D			
	0.0369	0.8	1.2	60.0	
	85.0			28.0	0.0
ESC					
89	901	D			
	0.0369	0.8	1.2	60.0	
	85.0			28.0	0.0
ESC					

	92	901	D					
		0.1432	0.8	1.2	60.0			
		85.0			28.0		0.0	
ESC								
	90	921	D					
		0.1432	0.8	1.2	60.0			
		85.0			28.0		0.0	
ESC								
	93	941	D					
		0.2092	0.8	1.2	60.0			
		85.0			28.0		0.0	
ESC								
	94	931	D					
		0.2092	0.8	1.2	60.0			
		85.0			28.0		0.0	
ESC								
	93	942	D					
		0.2092	0.8	1.2	60.0			
		85.0			28.0		0.0	
ESC								
	94	932	D					
		0.2092	0.8	1.2	60.0			
		85.0			28.0		0.0	
ESC								
	94	901	D					
		0.0947	0.8	1.2	60.0			
		85.0			28.0		0.0	
ESC								
	90	941	D					
		0.0947	0.8	1.2	60.0			
		85.0			28.0		0.0	
ESC								
	94	902	D					
		0.1302	0.8	1.2	60.0			
		85.0			28.0		0.0	
ESC								
	90	942	D					
		0.1302	0.8	1.2	60.0			
		85.0			28.0		0.0	
ESC								
	97	951	D					
		0.1667	0.8	1.2	60.0			
		85.0			28.0		0.0	
ESC								
	95	971	D					
		0.1667	0.8	1.2	60.0			
		85.0			28.0		0.0	
ESC								
	97	952	D					
		0.1606	0.8	1.2	60.0			
		85.0			28.0		0.0	
ESC								
	95	972	D					
		0.1606	0.8	1.2	60.0			
		85.0			28.0		0.0	
ESC								
	97	953	D					
		0.1664	0.8	1.2	60.0			
		85.0			28.0		0.0	
ESC								
	95	973	D					
		0.1664	0.8	1.2	60.0			
		85.0			28.0		0.0	
ESC								
	97	981	D					
		0.1466	0.8	1.2	60.0			
		85.0			28.0		0.0	
ESC								
	98	971	D					
		0.1466	0.8	1.2	60.0			
		85.0			28.0		0.0	

ESC						
97 991	D					
0.1491	0.8	1.2	60.0			
85.0			28.0			0.0
ESC						
99 971	D					
0.1491	0.8	1.2	60.0			
85.0			28.0			0.0
ESC						
97 1001	D					
0.1465	0.8	1.2	60.0			
85.0			28.0			0.0
ESC						
100 971	D					
0.1465	0.8	1.2	60.0			
85.0			28.0			0.0
ESC						
97 1011	D					
0.1424	0.8	1.2	60.0			
85.0			28.0			0.0
ESC						
101 971	D					
0.1424	0.8	1.2	60.0			
85.0			28.0			0.0
ESC						
98 1011	D					
0.1388	0.8	1.2	60.0			
85.0			28.0			0.0
ESC						
101 981	D					
0.1388	0.8	1.2	60.0			
85.0			28.0			0.0
ESC						
99 1011	D					
0.1495	0.8	1.2	60.0			
85.0			28.0			0.0
ESC						
101 991	D					
0.1495	0.8	1.2	60.0			
85.0			28.0			0.0
ESC						
100 1011	D					
0.1465	0.8	1.2	60.0			
85.0			28.0			0.0
ESC						
101 1001	D					
0.1465	0.8	1.2	60.0			
85.0			28.0			0.0
ESC						
104 1231	D					
0.0441	0.8	1.2	60.0			
85.0			28.0			0.0
ESC						
123 1041	D					
0.0441	0.8	1.2	60.0			
85.0			46.0			0.0
ESC						
106 1051	D					
0.1354	0.8	1.2	60.0			
85.0			28.0			0.0
ESC						
105 1061	D					
0.1354	0.8	1.2	60.0			
85.0			28.0			0.0
ESC						
107 1051	D					
0.1354	0.8	1.2	60.0			
85.0			28.0			0.0
ESC						
105 1071	D					
0.1354	0.8	1.2	60.0			

	85.0			28.0	0.0
ESC	110 1091	D			
	0.0712	0.8	1.2	60.0	
	85.0			28.0	0.0
ESC	109 1101	D			
	0.0712	0.8	1.2	60.0	
	85.0			28.0	0.0
ESC	110 1092	D			
	0.0712	0.8	1.2	60.0	
	85.0			28.0	0.0
ESC	109 1102	D			
	0.0712	0.8	1.2	60.0	
	85.0			28.0	0.0
ESC	110 1121	D			
	0.0654	0.8	1.2	60.0	
	85.0			28.0	0.0
ESC	112 1101	D			
	0.0654	0.8	1.2	60.0	
	85.0			46.0	0.0
ESC	110 1141	D			
	0.0925	0.8	1.2	60.0	
	85.0			28.0	0.0
ESC	114 1101	D			
	0.0925	0.8	1.2	60.0	
	85.0			28.0	0.0
ESC	111 1101	D			
	0.1011	0.8	1.2	60.0	
	85.0			28.0	0.0
ESC	110 1111	D			
	0.1011	0.8	1.2	60.0	
	85.0			28.0	0.0
ESC	111 1121	D			
	0.0643	0.8	1.2	60.0	
	85.0			28.0	0.0
ESC	112 1111	D			
	0.0643	0.8	1.2	60.0	
	85.0			46.0	0.0
ESC	111 1122	D			
	0.0649	0.8	1.2	60.0	
	85.0			28.0	0.0
ESC	112 1112	D			
	0.0649	0.8	1.2	60.0	
	85.0			46.0	0.0
ESC	111 1141	D			
	0.0939	0.8	1.2	60.0	
	85.0			28.0	0.0
ESC	114 1111	D			
	0.0939	0.8	1.2	60.0	
	85.0			28.0	0.0
ESC	112 1141	D			
	0.0654	0.8	1.2	60.0	
	85.0			46.0	0.0
ESC	114 1121	D			

	0.0654	0.8	1.2	60.0	
	85.0			28.0	0.0
ESC					
115	1141	D			
	0.0653	0.8	1.2	60.0	
	85.0			28.0	0.0
ESC					
114	1151	D			
	0.0653	0.8	1.2	60.0	
	85.0			28.0	0.0
ESC					
116	1141	D			
	0.0957	0.8	1.2	60.0	
	85.0			28.0	0.0
ESC					
114	1161	D			
	0.0957	0.8	1.2	60.0	
	85.0			28.0	0.0
ESC					
116	1142	D			
	0.0957	0.8	1.2	60.0	
	85.0			28.0	0.0
ESC					
114	1162	D			
	0.0957	0.8	1.2	60.0	
	85.0			28.0	0.0
ESC					
116	1151	D			
	0.065	0.8	1.2	60.0	
	85.0			28.0	0.0
ESC					
115	1161	D			
	0.065	0.8	1.2	60.0	
	85.0			28.0	0.0
ESC					
117	1161	D			
	0.1307	0.8	1.2	60.0	
	85.0			28.0	0.0
ESC					
116	1171	D			
	0.1307	0.8	1.2	60.0	
	85.0			28.0	0.0
ESC					
118	1031	D			
	0.0687	0.8	1.2	60.0	
	85.0			28.0	0.0
ESC					
103	1181	D			
	0.0687	0.8	1.2	60.0	
	85.0			28.0	0.0
ESC					
118	1032	D			
	0.0687	0.8	1.2	60.0	
	85.0			28.0	0.0
ESC					
103	1182	D			
	0.0687	0.8	1.2	60.0	
	85.0			28.0	0.0
ESC					
118	1033	D			
	0.0687	0.8	1.2	60.0	
	85.0			28.0	0.0
ESC					
103	1183	D			
	0.0687	0.8	1.2	60.0	
	85.0			28.0	0.0
ESC					
118	1161	D			
	0.1447	0.8	1.2	60.0	
	85.0			28.0	0.0
ESC					

116	1181	D				
	0.1447	0.8	1.2	60.0		
	85.0			28.0		0.0
ESC						
118	1162	D				
	0.1447	0.8	1.2	60.0		
	85.0			28.0		0.0
ESC						
116	1182	D				
	0.1447	0.8	1.2	60.0		
	85.0			28.0		0.0
ESC						
118	1171	D				
	0.1237	0.8	1.2	60.0		
	85.0			28.0		0.0
ESC						
117	1181	D				
	0.1237	0.8	1.2	60.0		
	85.0			28.0		0.0
ESC						
118	1172	D				
	0.1237	0.8	1.2	60.0		
	85.0			28.0		0.0
ESC						
117	1182	D				
	0.1237	0.8	1.2	60.0		
	85.0			28.0		0.0
ESC						
118	1241	D				
	0.1458	0.8	1.2	60.0		
	85.0			28.0		0.0
ESC						
124	1181	D				
	0.1458	0.8	1.2	60.0		
	85.0			28.0		0.0
ESC						
118	1242	D				
	0.1458	0.8	1.2	60.0		
	85.0			28.0		0.0
ESC						
124	1182	D				
	0.1458	0.8	1.2	60.0		
	85.0			28.0		0.0
ESC						
118	1243	D				
	0.1658	0.8	1.2	60.0		
	85.0			28.0		0.0
ESC						
124	1183	D				
	0.1658	0.8	1.2	60.0		
	85.0			28.0		0.0
ESC						
118	1244	D				
	0.1658	0.8	1.2	60.0		
	85.0			28.0		0.0
ESC						
124	1184	D				
	0.1658	0.8	1.2	60.0		
	85.0			28.0		0.0
ESC						
118	1271	D				
	0.0668	0.8	1.2	60.0		
	85.0			28.0		0.0
ESC						
127	1181	D				
	0.0668	0.8	1.2	60.0		
	85.0			28.0		0.0
ESC						
121	1041	D				
	0.0	0.8	1.2	60.0		
	85.0			28.0		0.0

```

ESC
  104  1211      D
        0.0      0.8      1.2      60.0
        85.0                      28.0
                                0.0
ESC
  121  1042      D
        0.0      0.8      1.2      60.0
        85.0                      28.0
                                0.0
ESC
  104  1212      D
        0.0      0.8      1.2      60.0
        85.0                      28.0
                                0.0
ESC
  121  1201      D
  0.0492      0.8      1.2      60.0
  85.0                      28.0
                                0.0
ESC
  120  1211      D
  0.0492      0.8      1.2      60.0
  85.0                      46.0
                                0.0
ESC
  121  1221      D
  0.0398      0.8      1.2      60.0
  85.0                      28.0
                                0.0
ESC
  122  1211      D
  0.0398      0.8      1.2      60.0
  85.0                      46.0
                                0.0
ESC
  125  1031      D
  0.066       0.8      1.2      60.0
  85.0                      46.0
                                0.0
ESC
  103  1251      D
  0.066       0.8      1.2      60.0
  85.0                      28.0
                                0.0
ESC
  125  1181      D
  0.0763      0.8      1.2      60.0
  85.0                      46.0
                                0.0
ESC
  118  1251      D
  0.0763      0.8      1.2      60.0
  85.0                      28.0
                                0.0
ESC
  125  1241      D
  0.0661      0.8      1.2      60.0
  85.0                      28.0
                                0.0
ESC
  124  1251      D
  0.0661      0.8      1.2      60.0
  85.0                      28.0
                                0.0
ESC
  125  1271      D
  0.066       0.8      1.2      60.0
  85.0                      46.0
                                0.0
ESC
  127  1251      D
  0.066       0.8      1.2      60.0
  85.0                      28.0
                                0.0
ESC
EDATA
  END

```

```

END
=====
=====

```

Appendix C IEEE-39 Bus Sample System Data

This appendix contains the data of the IEEE 39- bus sample system and it is divided in:

- Bus Data.
- Load Data.
- Generation Data
- Branch Data

The nomenclature for the table headings is the same than Appendix 1.

Bus Data.

Table A- 5: IEEE -39 Bus Sample System: Bus Data

Bus Number	Bus Name	Bus BaskV	Bus Type	Bus GL	Bus BL	Bus Voltage (pu)	Bus Angle
1	'BUS-1 '	345	1	0	0	1.0467	-10.2596
2	'BUS-2 '	345	1	0	0	1.0467	-7.6729
3	'BUS-3 '	345	1	0	0	1.025	-10.5253
4	'BUS-4 '	345	1	0	0	0.9925	-11.3133
5	'BUS-5 '	345	1	0	0	0.9889	-10.0791
6	'BUS-6 '	345	1	0	0	0.9902	-9.3488
7	'BUS-7 '	345	1	0	0	0.9807	-11.6299
8	'BUS-8 '	345	1	0	0	0.9804	-12.1545
9	'BUS-9 '	345	1	0	0	1.0217	-11.9947
10	'BUS-10 '	345	1	0	0	1.0063	-6.9372
11	'BUS-11 '	345	1	0	0	0.9996	-7.7563
12	'BUS-12 '	230	1	0	0	0.9879	-7.7799
13	'BUS-13 '	345	1	0	0	1.0036	-7.6704
14	'BUS-14 '	345	1	0	0	1.0019	-9.3845
15	'BUS-15 '	345	1	0	0	1.0103	-9.836
16	'BUS-16 '	345	1	0	0	1.0287	-8.4331
17	'BUS-17 '	345	1	0	0	1.0302	-9.4398
18	'BUS-18 '	345	1	0	0	1.0269	-10.2846
19	'BUS-19 '	345	1	0	0	1.0487	-3.7977
20	'BUS-20 '	230	1	0	0	0.9902	-5.2135
21	'BUS-21 '	345	1	0	0	1.0296	-6.0172
22	'BUS-22 '	345	1	0	0	1.0487	-1.5574
23	'BUS-23 '	345	1	0	0	1.0436	-1.756
24	'BUS-24 '	345	1	0	0	1.0345	-8.3136
25	'BUS-25 '	345	1	0	0	1.0558	-6.3257
26	'BUS-26 '	345	1	0	0	1.05	-7.5772
27	'BUS-27 '	345	1	0	0	1.035	-9.5911
28	'BUS-28 '	345	1	0	0	1.0491	-4.0593
29	'BUS-29 '	345	1	0	0	1.0492	-1.2969

Bus Number	Bus Name	Bus BaskV	Bus Type	Bus GL	Bus BL	Bus Voltage (pu)	Bus Angle
30	'BUS-30 '	22	2	0	0	1.0475	-5.2484
31	'BUS-31 '	22	3	0	0	0.9386	0
32	'BUS-32 '	22	2	0	0	0.9831	1.1458
33	'BUS-33 '	22	2	0	0	0.9972	1.4223
34	'BUS-34 '	22	2	0	0	1.0123	-0.0217
35	'BUS-35 '	22	2	0	0	1.0493	3.4098
36	'BUS-36 '	22	2	0	0	1.0635	6.1047
37	'BUS-37 '	22	2	0	0	1.0278	0.4677
38	'BUS-38 '	22	2	0	0	1.0265	5.7694
39	'BUS-39 '	345	2	0	0	1.03	-11.8082

Load Data.

Table A-6: IEEE-39-Bus Sample System: Load Data

Bus Number	PL (MW)	PQ (MVAR)
3	322	2.4
4	500	184
7	233.8	84
8	522	176
12	8.5	88
15	320	153
16	329	32.3
18	158	30
20	680	103
21	274	115
23	247.5	84.6
24	308.6	-92.2
25	224	47.2
26	139	17
27	281	75.5
28	206	27.6
29	283.5	26.9
31	9.2	4.6
39	1104	250

Generation Data**Table A- 7: IEEE-39-Bus Sample System: Generation Data**

Bus Number	PG	PQ
30	250	157.73
31	573.61	99.99
32	650	255.57
33	632	117.44
34	508	170.93
35	650	220.66
36	560	105.85
37	540	8.14
38	830	27.55
39	1000	117.67

Branch Data**Table A- 8: IEEE-39-Bus Sample System: Branch Data**

Number	From Bus	To Bus	Resistance (pu)	Reactance (pu)	Suceptance (B)	Branch Tap
1	2	1	0.0035	0.0411	0.6987	1
2	39	1	0.001	0.025	0.75	1
3	3	2	0.0013	0.0151	0.2572	1
4	25	2	0.007	0.0086	0.146	1
5	4	3	0.0013	0.0213	0.2214	1
6	18	3	0.0011	0.0133	0.2138	1
7	5	4	0.0008	0.0128	0.1342	1
8	14	4	0.0008	0.0129	0.1382	1
9	6	5	0.0002	0.0026	0.0434	1
10	8	5	0.0008	0.0112	0.1476	1
11	7	6	0.0006	0.0092	0.113	1
12	11	6	0.0007	0.0082	0.1389	1
13	8	7	0.0004	0.0046	0.078	1
14	9	8	0.0023	0.0363	0.3804	1
15	39	9	0.001	0.025	1.2	1
16	11	10	0.0004	0.0043	0.0729	1
17	13	10	0.0004	0.0043	0.0729	1
18	14	13	0.0009	0.0101	0.1723	1
19	15	14	0.0018	0.0217	0.366	1
20	16	15	0.0009	0.0094	0.171	1
21	17	16	0.0007	0.0089	0.1342	1

Number	From Bus	To Bus	Resistance (pu)	Reactance (pu)	Suceptance (B)	Branch Tap
22	19	16	0.0016	0.0195	0.304	1
23	21	16	0.0008	0.0135	0.2548	1
24	24	16	0.0003	0.0059	0.068	1
25	18	17	0.0007	0.0082	0.1319	1
26	27	17	0.0013	0.0173	0.3216	1
27	22	21	0.0008	0.014	0.2565	1
28	23	22	0.0006	0.0096	0.1846	1
29	24	23	0.0022	0.035	0.361	1
30	26	25	0.0032	0.0323	0.513	1
31	27	26	0.0014	0.0147	0.2396	1
32	28	26	0.0043	0.0474	0.7802	1
33	29	26	0.0057	0.0625	1.029	1
34	29	28	0.0014	0.0151	0.249	1
35	12	11	0.0016	0.0435	0	1.006
36	12	13	0.0016	0.0435	0	1.006
37	6	31	0	0.025	0	1.07
38	10	32	0	0.02	0	1.07
39	19	33	0.0007	0.0142	0	1.07
40	20	34	0.0009	0.018	0	1.009
41	22	35	0	0.0143	0	1.025
42	23	36	0.0005	0.0272	0	1
43	25	37	0.0006	0.0232	0	1.025
44	2	30	0	0.0181	0	1.025
45	29	38	0.0008	0.0156	0	1.025
46	19	20	0.0007	0.0138	0	1.06

Appendix D Transmission Line Overload Factors

The procedure to compute the loading condition of the post-disturbance equipment is based on a full load flow, which is run without the removed elements due to the contingency. The equipment and transmission lines thermal rates were computed and an overload factor was determined for the base case. This base case is taken as a reference in order to assess the overload condition of the case that is being evaluated. The loading factors are shown in Table A- 9.

Table A- 9: Base Case Loading Factors

Line ID	From Bus	To Bus	Thermal Rates	Loading Factor (%)
1	45	42	2000	0.1201
2	54	50	2000	0.53099
3	50	48	2000	0.2896
4	48	45	2000	0.15914
5	61	57	1800	0.19163
6	61	58	1800	0.16604
7	57	58	1800	0.1934
8	57	63	1800	0.55631
9	59	58	3000	0.027002
10	59	58	3000	0.027002
11	51	57	1800	0.57042
12	6	4	3000	0.25275
13	3	2	2000	0.38728
14	107	105	2000	0.074803
15	106	105	2000	0.074803
16	116	115	2000	0.1101
17	116	114	2000	0.082046
18	116	114	2000	0.082046
19	110	112	2000	0.038273
20	110	109	2000	0.02386
21	110	109	2000	0.02386
22	110	114	2000	0.054195
23	117	116	2000	0.098106
24	104	123	3000	0.10811
25	115	114	2000	0.043186
26	121	122	3000	0.15069
27	121	120	3000	0.21492
28	121	104	3000	0.13638
29	121	104	3000	0.13638
30	112	114	2000	0.014194
31	118	117	2000	0.10078

Line ID	From Bus	To Bus	Thermal Rates	Loading Factor (%)
32	118	117	2000	0.10078
33	111	112	2000	0.034014
34	111	112	2000	0.031722
35	111	110	2000	0.01915
36	111	114	2000	0.10413
37	118	116	2000	0.13138
38	118	116	2000	0.13138
39	125	127	2000	0.010358
40	125	118	2000	0.013694
41	125	124	2000	0.032167
42	125	103	2000	0.010339
43	118	127	2000	0.045855
44	118	124	2000	0.10346
45	118	124	2000	0.10346
46	118	124	2000	0.10272
47	118	124	2000	0.10272
48	118	103	2000	0.17352
49	118	103	2000	0.17352
50	118	103	2000	0.17352
51	11	9	3000	0.34443
52	11	12	3000	0.051611
53	11	25	3000	0.50356
54	9	10	3000	0.034389
55	9	12	3000	0.32525
56	9	12	3000	0.37698
57	7	9	3600	0.76834
58	7	9	3600	0.76834
59	17	18	3020	0.27789
60	17	18	3020	0.31374
61	14	16	3450	0.22132
62	14	16	3450	0.22132
63	14	12	2175	0.46353
64	14	12	2175	0.46886
65	15	12	3450	0.25107
66	15	12	3020	0.16816
67	15	12	3020	0.16809
68	15	21	2000	0.22529
69	23	21	2000	0.64444
70	15	23	2400	0.30367
71	15	23	2000	0.38425
72	22	27	3000	0.72724
73	92	90	2667	0.49526
74	85	89	2450	0.072835
75	85	84	1560	0.090256

Line ID	From Bus	To Bus	Thermal Rates	Loading Factor (%)
76	86	85	2450	0.018561
77	93	94	1800	0.61743
78	93	94	1800	0.61743
79	94	90	2450	0.48262
80	94	90	2450	0.40485
81	97	95	752	0.23533
82	97	95	602	0.30046
83	97	95	752	0.23662
84	97	101	747	0.098598
85	97	100	838	0.070184
86	100	101	838	0.12116
87	97	99	747	0.12008
88	99	101	747	0.079462
89	97	98	838	0.096088
90	98	101	838	0.083713
91	90	84	1800	0.27553
92	90	89	2450	0.26217
93	89	84	2450	0.1458
94	89	87	3000	0.05255
95	87	84	3000	0.07771
96	87	84	3000	0.07771
97	68	77	3600	0.13855
98	68	77	3600	0.13855
99	68	66	3600	0.29097
100	63	68	3600	0.24867
101	66	63	3600	0.14885
102	64	70	3600	0.24341
103	68	69	3600	0.1685
104	71	69	3600	0.045855
105	69	70	3600	0.13094
106	68	71	3600	0.25922
107	68	71	3600	0.26016
108	80	78	2320	0.013099
109	80	78	2320	0.014099
110	79	74	2320	0.068196
111	79	80	1160	0.023789
112	75	74	2320	0.046006
113	78	74	2320	0.066461
114	73	74	2320	0.076117
115	30	34	2500	0.010171
116	35	34	2500	0.073005
117	30	35	2500	0.022421
118	35	42	2500	0.027945
119	35	42	2500	0.026391

Line ID	From Bus	To Bus	Thermal Rates	Loading Factor (%)
120	37	40	2500	0.053571
121	35	37	2500	0.091117
122	35	37	2500	0.10211
123	35	36	2500	0.060789
124	37	39	2500	0.11124
125	37	39	2500	0.11184
126	42	39	2500	0.033494
127	42	39	2500	0.032697
128	31	32	2000	0.044871
129	37	36	2500	0.11375
130	6	7	3000	0.23378
131	9	24	3000	0.36847
132	23	93	1800	0.54529
133	23	93	1800	0.53967
134	23	92	1800	0.63405
135	84	77	2134	0.039172
136	84	77	2134	0.039454
137	84	77	2100	0.042533
138	68	104	3000	0.57258
139	63	104	3000	0.23916
140	63	104	3000	0.23916
141	80	82	3070	0.17307
142	80	82	3070	0.17307
143	79	82	3070	0.10065
144	61	63	1630	0.52102
145	59	64	1800	0.48654
146	59	64	1800	0.48654
147	22	21	3600	0.25833
148	30	29	2500	0.033229
149	43	42	2500	0.074714
150	43	42	2500	0.074714
151	41	50	2500	0.045237
152	45	47	20000	0.097842
153	55	54	1500	0.70006
154	59	60	20000	0.12729
155	55	56	20000	0.035243
156	48	49	20000	0.043557
157	51	50	1500	0.34582
158	51	50	1500	0.34582
159	50	53	20000	0.10329
160	50	52	430	0.16553
161	50	52	430	0.16434
162	61	62	20000	0.07969
163	4	3	1210	0.63465

Line ID	From Bus	To Bus	Thermal Rates	Loading Factor (%)
164	6	5	20000	0.22172
165	2	1	20000	0.22412
166	104	105	840	0.25899
167	43	44	20000	0.087109
168	24	26	20000	0.1452
169	27	29	1500	0.60365
170	7	8	20000	0.49341
171	16	18	2500	0.59507
172	17	20	250	0.65531
173	14	17	1008	0.21025
174	14	17	1300	0.26197
175	12	13	20000	0.25437
176	17	19	20000	0.06263
177	96	95	20000	0.047941
178	95	93	840	0.40528
179	91	90	20000	0.18181
180	102	101	20000	0.026175
181	101	90	1120	0.10461
182	83	84	840	0.39234
183	83	84	1120	0.43026
184	87	88	20000	0.035198
185	77	78	1120	0.36273
186	77	78	1120	0.36273
187	77	78	1120	0.36273
188	65	63	20000	0.045105
189	66	67	20000	0.080672
190	76	75	20000	0.16053
191	72	71	20000	0.083777
192	71	73	1210	0.14632
193	107	108	340	0.43762
194	106	108	340	0.43762
195	109	108	250	0.20049
196	109	108	250	0.199
197	120	116	1210	0.26688
198	120	116	1210	0.26688
199	122	118	1210	0.36173
200	112	113	20000	0.011652
201	123	118	1210	0.27082
202	118	119	20000	0.0015125
203	125	126	20000	0.005672
204	103	82	2500	0.71644
205	81	80	20000	0.10534
206	45	46	20000	0.0484
207	37	38	20000	0.078286

Line ID	From Bus	To Bus	Thermal Rates	Loading Factor (%)
208	40	41	430	0.23755
209	30	31	300	0.20106
210	32	33	20000	0.017724
211	29	28	20000	0.077856

Appendix E ETMSP: A Brief Description of the Program

This Appendix includes the formats and batch files used for the development of the simulation cases. The programs that were used are: ETMSP, OAP, and Matlab. Only the most relevant files are included herein.

The Procedure for each simulation case, under a software point of view, is briefly described in the table below.

Table A- 10: Brief Description of the Procedure of the Simulation Cases

Step Number	Description
1	Set up the New Directory to work for the case in question
2	Create the Contingency File
3	Go to ETMSP
4	Run "Control_etmsp" batch file and get ETMSP Output Files
5	Go to OAP
6	Run the "Control_oap_xxx....." to get the data from the ETMSP output files.
7	Go to Matlab
8	Verify if the relay operated (Validation of the Region of Vulnerability)
9	Verify for relay operations (Distance and Under Frequency)
10	Obtain and Visualize graphs of Primary Parameters (Voltages, Frequency and Generator Relative Angles)
11	Get values for individual Indexes of Severity

The appendix is divided in:

- Dynamic Data of the System
- Contingency File
- Control_etmsp
- Outdata_ETMSP
- Outdata_ETMSP_Relay

Dynamic Data of the System.

This file is an input file to the ETMSP program and includes the detailed model of the machines, the exciters, the power system stabilizer, and equipment alike. Below are the parameters of one of the machines which are used to describe the format of this file.

Line	DGEN												
1	19	1	100	100									
2	0	10	30	10	0	0	0	0	0	0	0	0	0
3	0.0040		0.890		0.500	0.240	0.370	0.500	0.287	0.306			
4	4.00		0.00		0.020	0.050							
5	0.90		1.00		1.10	1.20	1.50	4.17					
6	3.00		0.0		0.0	1199.	1.0	60.0	1.0	1.0			
7	19	1											
8	200.		0.160		0.0	0.02	0.026	1.0	0.0	0.02			
9	3.20		-3.20		1.0	0.0	0.1	0.0	0.0				
10	.020		0.0		0.0	0.0	1.0	1.0	0.0	0.0			
11	0.0		0.0		99.0	-99.0							
12	19	1											
13	10.0		0.0		0.0	0.0	3.0	0.15	0.05				
14	0.15		0.05		0.15	0.05	0.05	-0.05	0.0	0.0			

General Parameters. The format for the line 1 is presented with the parameters of the machine “19.”

Line 1	NLF	NUN	IPFA	IQFA
	19	1	100	100

Nomenclature:

- NLF Load flow bus number of represented machine
- NUN Unit identification for the dynamic simulation
- IPFA Active power output as a percentage of the total generation at the bus in the load flow.
- IQFA Reactive power output as a percentage of the total generation at the bus in the load flow.

Machine and Equipment. The format for the line 2 is presented with the parameters of the machine “19.”

Line 2	IGEN	ISAT	IEX	ISTAB	IGV	ITEB	IMEL	IGSTAN	IFLTR	IUAL	MASSN	ICBRN
	0	10	30	10	0	0	0	0	0	0	0	0

Nomenclature:

- IGEN Machine data type: “0” for Generator data in impedance and time constant form
- ISAT Machine Saturation representation code: “10” Saturation data in A_{SAT} and B_{SAT} form and only X_{ad} varies with saturation. The data is in form of points on the saturation curve.
- IEX Exciter Type: “30”
- ISTAB Power System Stabilizer type: “10”
- IGV Governor-Turbine type, Not represented
- ITEB Transient Excitation Booster type, Not represented
- IMEL Over Excitation current limiter type, Not Represented
- IGSTAN Governor stabilizer type, Not
- IFLTR Torsional Filter type, Not represented
- IUAL Under Excitation current limiter type, Not Represented
- MASSN Multimass data representation, Not Represented
- ICBRN Cowbar type, Not Represented

Machine Data in Reactances and Time Constants Form. The format for the line 3 and 4 is presented with the parameters of the machine “19.”

Line 3	R_a	X_d	X_q	X_l	X'_d	X'_q	X''_d	X''_q
	0.0040	0.890	0.500	0.240	0.370	0.500	0.287	0.306

Line 4	T'_{do}	T'_{qo}	T''_{do}	T''_{qo}
	4.00	0.00	0.020	0.050

Nomenclature:

- R_a Armature Resistance (pu)
- X_d Unsaturated direct axis synchronous reactance (pu)
- X_q Unsaturated quadrature axis synchronous reactance (pu)
- X_l Leakage Reactance, pu
- X'_d Unsaturated direct axis transient reactance (pu)
- X'_q Unsaturated quadrature axis transient reactance (pu)
- X''_d Unsaturated direct axis subtransient reactance (pu)
- X''_q Unsaturated quadrature axis subtransient reactance (pu)
- T'_{do} Direct axis transient open circuit time constant (seconds)
- T'_{qo} Quadrature axis transient open circuit time constant (seconds)
- T''_{do} Direct axis subtransient open circuit time constant (seconds)
- T''_{qo} Quadrature axis subtransient open circuit time constant (seconds)

Machine Saturation Data. The format for the line 5 is presented with the parameters of the machine “19.”

Line 5	X1	X2	X3	Xn					ICBRN

The parameters to represent the machine saturation are described in graphical form in which the MMF is plotted against the flux linkage. These parameters are not described here and they can be found in the ETMSP user's manual, Chapter 4.

Inertia and MVA Base Data. The format for the line 6 is presented with the parameters of the machine "19."

Line 6	H	KDAMP	CMTL	BMVA	BVR	BFRQ	SPPSS	SPGOV
	3	0	0	1199	1	60	1	1

Nomenclature:

H	Turbine-Generator inertia time constant, in MW-SEC/MVA
KDAMP	Damping Coefficient in (pu torque)/ (pu speed deviation)
CMTL	CMTL entered is zero.
BMVA	Base MVA of the generator data
BVR	Ratio between base kV of the generator data and base kV of the load flow data for the same bus
BFRQ	Base Frequency
SPPSS	Proportion of generator speed fed to the stabilizer
SPGOV	Proportion of generator speed fed to the governor

Lines 7 to 14 in the file include the parameters for the equipment such as exciter, power system stabilizer, governor, etc. Since the parameters of this equipment depend on the type and manufacturer, these formats are variable and therefore are not included here. These details are described in the ETMSP user's manual, Chapter 4.

After the machines and other equipment have been described, the load representation is included in the file.

Load Data. The format for the unique line is presented with the parameters of the bus "2."

Line	Bus	ICCP	ICCQ	ICPP	ICCQ
	2	100			

Nomenclature:

Bus	Bus Number
ICCP	Percentage of Total Initial Real Load to be modeled as Constant Current
ICCQ	Percentage of Total Initial Reactive Load to be modeled as Constant Current
ICPP	Percentage of Total Initial Real Load to be modeled as Constant Power
ICCQ	Percentage of Total Initial Reactive Load to be modeled as Constant Power

```

=====
=====
BSTA
0
EDATA
DGEN
19 1 100 100
0 10 30 10 0 0 0 0 0 0 0 0
0.0040 0.890 0.500 0.240 0.370 0.500 0.287 0.306
4.00 0.00 0.020 0.050
0.90 1.00 1.10 1.20 1.50 4.17
3.00 0.0 0.0 1199. 1.0 60.0 1.0 1.0
19 1
200. 0.160 0.0 0.02 0.026 1.0 0.0 0.02
3.20 -3.20 1.0 0.0 0.1 0.0 0.0 0.0
.020 0.0 0.0 0.0 1.0 1.0 0.0 0.0
0.0 0.0 99.0 -99.0
19 1
10.0 0.0 0.0 0.0 3.0 0.15 0.05
0.15 0.05 0.15 0.05 0.05 -0.05 0.0 0.0
13 1 100 100
0 10 1 10 0 0 0 0 0 0
0.0036 0.93 0.651 0.240 0.357 0.651 0.248 0.297
8.00 0.00 0.030 0.060
0.90 1.00 1.10 1.20 1.50 4.17
3.67 0.0 0.0 5421. 1.0 60.0 1.0 1.0
13 1
40.0 0.060 0.0 0.130 0.300 0.035 4.50
0.05 1.50 0.0 0.02 3.00 -3.00 0.0 0.10
0.020 0.0 0.0
13 4
-0.04 0.0 0.0 0.0 29.5 1.5 0.15
1.50 0.15 0.0 0.0 0.09 -0.09 0.0 0.02
28 1 100 100
0 20 30 10 0 0 0 0 0 0
0.0047 2.070 1.990 0.155 0.280 0.490 0.215 0.215
4.10 0.56 0.033 0.062
0.90 1.00 1.10 1.20 1.50 6.45
2.32 0.0 0.0 885. 1.0 60.0 1.0 1.0
28 1
200. 0.360 0.0 0.02 0.030 1.0 0.0 0.0
5.73 -5.73 1.0 0.0 0.1 0.0 0.0 0.0
.020 0.0 0.0 0.0 1.0 1.0 0.0 0.0
0.0 0.0 99.0 -99.0
28 1
10.0 0.0 0.0 0.0 3.0 0.15 0.05
0.15 0.05 0.15 0.05 0.05 -0.05 0.0 0.0
28 2 100 100
0 20 30 10 0 0 0 0 0 0
0.0047 2.070 1.990 0.155 0.280 0.490 0.215 0.215
4.10 0.56 0.033 0.062
0.90 1.00 1.10 1.20 1.50 6.45
2.32 0.0 0.0 885. 1.0 60.0 1.0 1.0
28 1
200. 0.360 0.0 0.02 0.030 1.0 0.0 0.0
5.73 -5.73 1.0 0.0 0.1 0.0 0.0 0.0
.020 0.0 0.0 0.0 1.0 1.0 0.0 0.0
0.0 0.0 99.0 -99.0
28 1
10.0 0.0 0.0 0.0 3.0 0.15 0.05
0.15 0.05 0.15 0.05 0.05 -0.05 0.0 0.0
5 1 100 100
0 10 30 10 0 0 0 0 0 0
0.002 0.90 0.60 0.09 0.25 0.60 0.15 0.22
8.0 0.0 0.050 0.080
0.90 1.00 1.10 1.20 1.50 11.0
4.34 0.0 0.0 9004.0 1.0 60.0 1.0 1.0
5 1
145. 0.020 0.0 0.02 0.01 1.5 0.0 0.0
8.85 -8.85 1.0 0.0 0.1 0.0 0.0 0.0
.020 .01 .01 0.0 1.0 1.0 0.0 0.0

```

	0.0	0.0	99.0	-99.0					
5	4								
	-3.50	0.0	0.0	0.0	1.0	0.0	3.0		
	0.08	0.027	0.08	0.027	0.10	-0.10	0.0	0.0	
126	1	100	100						
	0	10	30	10	0	0	0	0	0
	0.0014	0.995	0.568	0.089	0.195	0.568	0.155	0.190	
	10.8	0.00	0.028	0.160					
	0.90	1.00	1.10	1.20	1.50	11.2			
	6.41	0.0	0.0	500.	1.0	60.0	1.0	1.0	
126	1								
	300.	0.160	0.0	0.02	0.010	1.0	0.0	0.02	
	7.00	-5.00	1.0	0.0	0.1	0.0	0.0		
	.020	0.0	0.0	0.0	1.0	1.0	0.0	0.0	
	0.0	0.0	99.0	-99.0					
126	3								
	0.00	0.0	0.0	0.0	15.0	0.0	0.053		
	0.0	0.053	0.0	0.0	0.05	-0.05	0.0	0.02	
1	1	100	100						
	0	20	30	10	0	0	0	0	0
	0.0030	1.825	1.78	0.239	0.291	0.440	0.250	0.250	
	4.6	0.37	0.040	0.100					
	0.90	1.00	1.10	1.20	1.50	4.18			
	2.95	0.0	0.0	1525.	1.0	60.0	1.0	1.0	
1	1								
	200.	0.080	0.0	0.02	0.015	1.0	0.0	0.02	
	7.14	-7.14	1.0	0.0	0.1	0.0	0.0		
	.020	0.0	0.0	0.0	1.0	1.0	0.0	0.0	
	0.0	0.0	99.0	-99.0					
1	1								
	10.00	0.10	0.0	0.0	1.0	0.20	0.010		
	0.0	0.00	0.00	0.00	0.05	-0.05	0.0	0.0	
1	2	100	100						
	0	20	30	10	0	0	0	0	0
	0.0030	1.825	1.78	0.239	0.291	0.440	0.250	0.250	
	4.6	0.37	0.040	0.100					
	0.90	1.00	1.10	1.20	1.50	4.18			
	2.95	0.0	0.0	1525.	1.0	60.0	1.0	1.0	
1	1								
	200.	0.080	0.0	0.02	0.015	1.0	0.0	0.02	
	7.14	-7.14	1.0	0.0	0.1	0.0	0.0		
	.020	0.0	0.0	0.0	1.0	1.0	0.0	0.0	
	0.0	0.0	99.0	-99.0					
1	1								
	10.00	0.10	0.0	0.0	1.0	0.20	0.010		
	0.0	0.00	0.00	0.00	0.05	-0.05	0.0	0.0	
1	3	100	100						
	0	20	30	10	0	0	0	0	0
	0.0030	1.825	1.78	0.239	0.291	0.440	0.250	0.250	
	4.6	0.37	0.040	0.100					
	0.90	1.00	1.10	1.20	1.50	4.18			
	2.95	0.0	0.0	1525.	1.0	60.0	1.0	1.0	
1	1								
	200.	0.080	0.0	0.02	0.015	1.0	0.0	0.02	
	7.14	-7.14	1.0	0.0	0.1	0.0	0.0		
	.020	0.0	0.0	0.0	1.0	1.0	0.0	0.0	
	0.0	0.0	99.0	-99.0					
1	1								
	10.00	0.10	0.0	0.0	1.0	0.20	0.010		
	0.0	0.00	0.00	0.00	0.05	-0.05	0.0	0.0	
1	4	100	100						
	0	20	30	10	0	0	0	0	0
	0.0030	1.825	1.78	0.239	0.291	0.440	0.250	0.250	
	4.6	0.37	0.040	0.100					
	0.90	1.00	1.10	1.20	1.50	4.18			
	2.95	0.0	0.0	1525.	1.0	60.0	1.0	1.0	
1	1								
	200.	0.080	0.0	0.02	0.015	1.0	0.0	0.02	
	7.14	-7.14	1.0	0.0	0.1	0.0	0.0		
	.020	0.0	0.0	0.0	1.0	1.0	0.0	0.0	
	0.0	0.0	99.0	-99.0					

1	1								
	10.00	0.10	0.0	0.0	1.0	0.20	0.010		
	0.0	0.00	0.00	0.00	0.05	-0.05	0.0	0.0	
56	1	100	100						
	0	20	8	10	0	0	0	0	0
	0.0030	1.860	1.780	0.145	0.250	0.453	0.195	0.197	
	3.90	0.54	0.032	0.062					
	0.90	1.00	1.10	1.20	1.50	6.90			
	2.64	0.0	0.0	457.	1.0	60.0	1.0	1.0	
56	1								
	8.00	0.40	200.0	1.00	2.86	0.20	-0.20	1.130	
	0.00	0.02	1.00	5.00	0.00	1.00	0.00	4.48	
	0.020	0.00	0.00	0.0098	0.435	3.67	3.33	99.0	
	-99.0	4.48							
56	1								
	5.0	0.0	0.0	0.0	10.0	0.30	0.03		
	0.30	0.03	0.0	0.0	0.10	-0.10	0.0	0.0	
56	2	100	100						
	0	20	8	10	0	0	0	0	0
	0.0030	1.860	1.780	0.145	0.250	0.453	0.195	0.197	
	3.90	0.54	0.032	0.062					
	0.90	1.00	1.10	1.20	1.50	6.90			
	2.64	0.0	0.0	457.	1.0	60.0	1.0	1.0	
56	1								
	8.00	0.40	200.0	1.00	2.86	0.20	-0.20	1.130	
	0.00	0.02	1.00	5.00	0.00	1.00	0.00	4.48	
	0.020	0.00	0.00	0.0098	0.435	3.67	3.33	99.0	
	-99.0	4.48							
56	1								
	5.0	0.0	0.0	0.0	10.0	0.30	0.03		
	0.30	0.03	0.0	0.0	0.10	-0.10	0.0	0.0	
46	1	100	100						
	0	20	8	10	0	0	0	0	0
	0.0030	1.810	1.730	0.140	0.245	0.510	0.190	0.191	
	4.00	0.52	0.032	0.063					
	0.90	1.00	1.10	1.20	1.50	7.14			
	2.61	0.0	0.0	1488.	1.0	60.0	1.0	1.0	
46	1								
	8.20	0.40	200.0	1.00	5.60	0.20	-0.20	1.265	
	0.00	0.02	1.00	5.00	0.00	1.00	0.00	5.01	
	0.020	0.00	0.00	0.0077	0.335	3.56	3.75	99.0	
	-99.0	5.01							
46	3								
	5.50	0.03	0.0	0.0	10.0	0.40	0.040		
	0.00	0.00	0.0	0.0	0.05	-0.05	0.0	0.02	
88	1	100	100						
	0	20	30	10	0	0	0	0	0
	0.0030	2.129	2.074	0.250	0.467	1.270	0.311	0.309	
	6.12	1.50	0.052	0.144					
	0.90	1.00	1.10	1.20	1.50	4.00			
	3.46	0.0	0.0	1685.	1.0	60.0	1.0	1.0	
88	1								
	400.	0.020	0.02	0.02	0.01	2.00	0.0	0.02	
	7.00	-7.00	1.0	0.0	0.1	0.0	0.0		
	.020	0.0	0.0	0.0	1.0	1.0	0.0	0.0	
	0.0	0.0	99.0	-99.0					
88	1								
	10.0	0.0	0.0	0.0	3.0	0.15	0.05		
	0.15	0.05	0.15	0.05	0.05	-0.05	0.0	0.0	
65	1	100	100						
	0	10	30	10	0	0	0	0	0
	0.0020	0.750	0.530	0.215	0.320	0.530	0.300	0.320	
	7.80	0.00	0.060	0.110					
	0.90	1.00	1.10	1.20	1.50	4.65			
	6.07	0.0	0.0	2104.	1.0	60.0	1.0	1.0	
65	1								
	200.	0.020	0.0	0.02	0.010	1.20	0.0	0.02	
	6.50	-6.50	1.0	0.0	0.1	0.0	0.0		
	.020	0.0	0.0	0.0	1.0	1.0	0.0	0.0	
	0.0	0.0	99.0	-99.0					
65	1								

	10.0	0.0	0.0	0.0	3.0	0.15	0.05	
	0.15	0.05	0.15	0.05	0.05	-0.05	0.0	0.0
38	1	100	100					
0	20	30	10	0	0	0	0	
	0.0040	1.640	1.570	0.130	0.240	0.430	0.185	0.185
	3.90	0.49	0.032	0.062				
	0.90	1.00	1.10	1.20	1.50	7.69		
	2.82	0.0	0.0	2229.	1.0	60.0	1.0	1.0
38	1							
	250.	0.020	1.0	10.0	0.00	.020	0.0	0.02
	3.63	-2.90	1.0	0.0	0.1	0.0	0.0	
	.020	0.0	0.0	0.0	1.0	1.0	0.0	0.0
	0.0	0.0	99.0	-99.0				
38	1							
	8.08	0.03	0.0	0.0	10.0	0.15	0.05	
	0.15	0.05	0.0	0.0	0.05	-0.05	0.0	0.0
53	1	100	100					
0	20	30	10	0	0	0	0	
	0.0036	1.76	1.58	0.155	0.285	0.485	0.205	0.205
	8.4	0.46	0.035	0.070				
	0.90	1.00	1.10	1.20	1.50	6.45		
	3.42	0.0	0.0	2458.	1.0	60.0	1.0	1.0
53	1							
	200.	0.020	0.0	0.02	0.010	1.0	0.0	0.02
	4.91	-4.91	1.0	0.0	0.1	0.0	0.0	
	.020	0.0	0.0	0.0	1.0	1.0	0.0	0.0
	0.0	0.0	99.0	-99.0				
53	1							
	10.0	0.0	0.0	0.0	3.0	0.15	0.05	
	0.15	0.05	0.15	0.05	0.05	-0.05	0.0	0.0
47	1	100	100					
0	20	1	10	0	0	0	0	
	0.0020	1.70	1.650	0.140	0.250	0.500	0.190	0.188
	4.50	0.50	0.040	0.060				
	0.90	1.00	1.10	1.20	1.50	7.14		
	2.45	0.0	0.0	3000.	1.0	60.0	1.0	1.0
47	1							
	200.0	0.050	0.0	0.512	3.048	1.049	5.31	
	0.07	1.80	0.0	0.02	14.00	-14.00	0.0	0.10
	0.020	0.0	0.0					
47	3							
	0.00	0.025	0.0	0.0	0.016	0.26	0.026	
	0.26	0.026	0.0	0.0	0.10	-0.10	0.0	0.02
113	1	100	100					
0	20	1	10	0	0	0	0	
	0.0016	1.70	1.62	0.155	0.256	0.410	0.185	0.185
	4.80	0.50	0.037	0.075				
	0.90	1.00	1.10	1.20	1.50	6.45		
	4.13	0.0	0.0	540.	1.0	60.0	1.0	1.0
113	1							
	40.0	0.200	0.0	0.545	0.410	0.035	4.13	
	0.09	1.00	0.0	0.02	2.00	-2.00	0.0	0.10
	0.020	0.0	0.0					
113	4							
	0.00	0.03	0.0	0.0	1.50	0.375	12.0	
	0.0	0.0	0.0	0.0	0.05	-0.05	0.0	0.0
44	1	100	100					
0	20	8	10	0	0	0	0	
	0.0014	1.990	1.900	0.150	0.245	0.420	0.200	0.200
	4.70	0.67	0.031	0.061				
	0.90	1.00	1.10	1.20	1.50	6.67		
	2.88	0.0	0.0	1982.	1.0	60.0	1.0	1.0
44	1							
	7.20	0.60	200.0	1.00	6.36	0.20	-0.20	1.096
	0.00	0.02	1.00	4.00	0.00	1.00	0.00	8.40
	0.020	0.00	0.00	0.005	0.243	4.35	20.0	99.0
	-99.0	8.40						
44	1							
	3.0	0.0	0.0	0.0	10.0	0.30	0.03	
	0.30	0.03	0.0	0.0	0.10	-0.10	0.0	0.0
76	1	100	100					

	5.21	1.50	0.042	0.042				
	0.90	1.00	1.10	1.20	1.50	5.18		
	3.01	0.0	0.0	832.	1.0	60.0	1.0	1.0
33	1							
	200.	0.100	0.0	0.02	0.012	1.0	0.0	0.02
	8.00	-8.00	1.0	0.0	0.1	0.0	0.0	
	.020	0.0	0.0	0.0	1.0	1.0	0.0	0.0
	0.0	0.0	99.0	-99.0				
33	1							
	1.20	0.03	0.0	0.0	30.0	0.40	0.05	
	0.40	0.05	0.0	0.0	0.04	-0.04	0.0	0.0
62	1	100	100					
0	20	30	10	0	0	0	0	
	0.0019	1.760	1.680	0.130	0.220	0.400	0.175	0.175
	4.20	0.60	0.032	0.066				
	0.90	1.00	1.10	1.20	1.50	7.69		
	3.59	0.0	0.0	3540.	1.0	60.0	1.0	1.0
62	1							
	300.	0.020	1.0	10.0	0.00	0.20	0.0	0.02
	4.58	-3.67	1.0	0.0	0.1	0.0	0.0	
	.020	0.0	0.0	0.0	1.0	1.0	0.0	0.0
	0.0	0.0	99.0	-99.0				
62	1							
	10.0	0.0	0.0	0.0	3.0	0.15	0.05	
	0.15	0.05	0.15	0.05	0.05	-0.05	0.0	0.0
8	1	100	100					
0	10	1	10	0	0	0	0	
	0.0020	0.638	0.424	0.127	0.228	0.424	0.161	0.273
	7.20	0.00	0.043	0.079				
	0.90	1.00	1.10	1.20	1.50	7.87		
	3.46	0.0	0.0	13000.	1.0	60.0	1.0	1.0
8	1							
	40.0	0.100	1.0	0.57	0.30	0.035	4.50	
	0.05	1.20	0.0	0.02	3.00	-3.00	0.0	0.10
	0.020	0.0	0.0					
8	4							
	-0.06	0.0	0.0	0.0	29.5	1.50	0.15	
	1.50	0.15	0.0	0.0	0.09	-0.09	0.0	0.02
119	1	100	100					
0	10	30	10	0	0	0	0	
	0.0037	0.619	0.365	0.140	0.238	0.365	0.150	0.170
	7.40	0.00	0.030	0.160				
	0.90	1.00	1.10	1.20	1.50	7.14		
	3.80	0.0	0.0	113.	1.0	60.0	1.0	1.0
119	1							
	200.	0.160	0.0	0.02	0.015	1.0	0.0	0.02
	5.00	-5.00	1.0	0.0	0.1	0.0	0.0	
	.020	0.0	0.0	0.0	1.0	1.0	0.0	0.0
	0.0	0.0	99.0	-99.0				
119	1							
	10.0	0.0	0.0	0.0	3.0	0.15	0.05	
	0.15	0.05	0.15	0.05	0.05	-0.05	0.0	0.0
60	1	100	100					
0	20	8	10	0	0	0	0	
	0.0035	1.980	1.850	0.225	0.375	0.567	0.285	0.284
	8.20	0.48	0.033	0.055				
	0.90	1.00	1.10	1.20	1.50	4.44		
	3.83	0.0	0.0	1039.	1.0	60.0	1.0	1.0
60	1							
	6.80	0.40	200.0	1.00	6.77	0.20	-0.20	1.015
	0.00	0.02	1.00	5.00	0.00	1.50	0.00	4.52
	0.020	0.00	0.00	0.005	0.124	3.77	0.00	99.0
	-99.0	4.52						
60	1							
	10.0	0.0	0.0	0.0	3.0	0.15	0.05	
	0.15	0.05	0.15	0.05	0.05	-0.05	0.0	0.0
60	2	100	100					
0	20	8	10	0	0	0	0	
	0.0035	1.980	1.850	0.225	0.375	0.567	0.285	0.284
	8.20	0.48	0.033	0.055				
	0.90	1.00	1.10	1.20	1.50	4.44		

	3.83	0.0	0.0	1039.	1.0	60.0	1.0	1.0
60	1							
	6.80	0.40	200.0	1.00	6.77	0.20	-0.20	1.015
	0.00	0.02	1.00	5.00	0.00	1.50	0.00	4.52
	0.020	0.00	0.00	0.005	0.124	3.77	0.00	99.0
	-99.0	4.52						
60	1							
	10.0	0.0	0.0	0.0	3.0	0.15	0.05	
	0.15	0.05	0.15	0.05	0.05	-0.05	0.0	0.0
60	3	100	100					
0	20	8	10	0	0	0	0	0
	0.0035	1.980	1.850	0.225	0.375	0.567	0.285	0.284
	8.20	0.48	0.033	0.055				
	0.90	1.00	1.10	1.20	1.50	4.44		
	3.83	0.0	0.0	1039.	1.0	60.0	1.0	1.0
60	1							
	6.80	0.40	200.0	1.00	6.77	0.20	-0.20	1.015
	0.00	0.02	1.00	5.00	0.00	1.50	0.00	4.52
	0.020	0.00	0.00	0.005	0.124	3.77	0.00	99.0
	-99.0	4.52						
60	1							
	10.0	0.0	0.0	0.0	3.0	0.15	0.05	
	0.15	0.05	0.15	0.05	0.05	-0.05	0.0	0.0
81	1	100	100					
0	20	30	10	0	0	0	0	0
	0.0010	1.790	1.715	0.135	0.220	0.440	0.180	0.180
	4.30	0.430	0.032	0.066				
	0.90	1.00	1.10	1.20	1.50	7.41		
	3.03	0.0	0.0	2500.	1.0	60.0	1.0	1.0
81	1							
	250.	0.200	0.0	0.02	0.035	1.75	0.0	0.02
	4.73	-4.73	1.0	0.0	0.1	0.0	0.0	
	.020	0.0	0.0	0.0	1.0	1.0	0.0	0.0
	0.0	0.0	99.0	-99.0				
81	1							
	10.0	0.0	0.0	0.0	3.0	0.15	0.05	
	0.15	0.05	0.15	0.05	0.05	-0.05	0.0	0.0
96	1	100	100					
0	10	1	10	0	0	0	0	0
	0.0062	1.05	0.67	0.140	0.320	0.670	0.263	0.306
	4.00	0.00	0.051	0.033				
	0.90	1.00	1.10	1.20	1.50	7.14		
	4.39	0.0	0.0	1022.	1.0	60.0	1.0	1.0
96	1							
	183.0	0.060	0.0	0.500	0.540	0.035	3.50	
	0.05	1.00	0.0	0.02	2.00	-2.00	0.0	0.10
	0.020	0.0	0.0					
96	4							
	0.00	0.0	0.0	0.0	29.5	1.5	0.15	
	1.50	0.15	0.0	0.0	0.09	-0.09	0.0	0.02
49	1	100	100					
0	20	1	10	0	0	0	0	0
	0.0020	1.67	0.61	0.145	0.260	0.453	0.205	0.205
	3.80	0.49	0.031	0.058				
	0.90	1.00	1.10	1.20	1.50	6.90		
	2.63	0.0	0.0	2054.	1.0	60.0	1.0	1.0
49	1							
	50.0	0.020	0.0	0.642	0.356	0.045	3.46	
	0.103	0.994	0.0	0.02	3.00	-3.00	0.0	0.10
	0.020	0.0	0.0					
49	3							
	0.0	0.0	0.0	0.0	30.0	0.23	0.025	
	0.23	0.025	0.0	0.0	0.06	-0.06	0.0	0.02
102	1	100	100					
0	10	30	10	0	0	0	0	0
	0.0020	0.750	0.530	0.215	0.320	0.530	0.300	0.320
	7.80	0.00	0.060	0.110				
	0.90	1.00	1.10	1.20	1.50	4.65		
	4.16	0.0	0.0	895.	1.0	60.0	1.0	1.0
102	1							
	200.	0.020	0.0	0.02	0.010	1.20	0.0	0.02

	6.50	-6.50	1.0	0.0	0.1	0.0	0.0	
	.020	0.0	0.0	0.0	1.0	1.0	0.0	0.0
	0.0	0.0	99.0	-99.0				
102	1							
	10.0	0.0	0.0	0.0	3.0	0.15	0.05	
	0.15	0.05	0.15	0.05	0.05	-0.05	0.0	0.0
91	1	100	100					
0	20	1	10	0	0	0	0	0
	0.0020	1.70	1.650	0.140	0.250	0.500	0.190	0.188
	4.50	0.50	0.040	0.060				
	0.90	1.00	1.10	1.20	1.50	7.14		
	3.82	0.0	0.0	6840.	1.0	60.0	1.0	1.0
91	1							
	200.0	0.050	0.0	0.512	3.048	1.049	5.31	
	0.07	1.80	0.0	0.02	14.00	-14.00	0.0	0.10
	0.020	0.0	0.0					
91	4							
	0.00	0.0	0.0	0.0	29.5	1.5	0.15	
	1.50	0.15	0.0	0.0	0.09	-0.09	0.0	0.02
EDATA								
NLBS								
2	100							
6	100							
7	100							
9	100							
14	100							
17	100							
20	100							
13	100							
15	100							
27	100							
23	100							
99	70	15	30	15				
101	70	15	30	15				
98	70	15	30	15				
100	70	15	30	15				
97	70	15	30	15				
94	70	15	30	15				
102	70	15	30	15				
92	70	15	30	15				
87	70	15	30	15				
89	70	15	30	15				
95	70	15	30	15				
84	70	15	30	15				
83	70	15	30	15				
24	100							
108	100							
109	100							
116	100							
110	100							
114	100							
124	100							
115	100							
127	100							
118	100							
111	100							
70	100							
82	100							
104	100							
77	10	10	50	50				
68	10	10	50	50				
65	10	10	50	50				
64	10	10	50	50				
117	10	10	50	50				
69	10	10	50	50				
73	10	10	50	50				
81	10	10	50	50				
79	10	10	50	50				
74	10	10	50	50				
76	10	10	50	50				
58	100							

```

59 100
56 100
48 100
46 100
51 100
50 100
36 100
31 100
34 100
35 100
42 100
40 100
38 100
39 100
30 100
32 100
61 100
EDATA
END
=====

```

Contingency File:

This is the file in which the user indicates the contingency characteristic of the case to simulate.

```

=====
DESCRIPTION 3 PHASE SHORT-CIRCUIT/
?
SIMULATION 2 SECONDS/
STEP SIZE 0.005 SECONDS/
PRINT 1 TIME STEPS/
PLOT 1 TIME STEPS/
INTEGRATION RKG4/
??????
??????
??????
AT TIME 1.50 SECONDS/
THREE PHASE FAULT ON LINE ;104;123;1 4/
?
AT TIME 1.60 SECONDS/
NOFAULT/
NOMORE/
=====

```

Control etmsp

This is a batch file that is used in each case of a simulation in ETMSP

```

=====
?
loa
?SELECT AN ITEM BY THE NUMBER (Q TO ENTER FILE NAME):
4
?ENTER APPROPRIATE CODE NUMBER (Q TO QUIT):
?10
9
?SELECT AN ITEM BY THE NUMBER (Q TO ENTER FILE NAME):
q
wscc_127.psf
?
dyn
DynamicDataCard
?
ldyn
?
reladata
relay
rres
?DO YOU HAVE AN EXISTING OUTPUT SPECIFICATION FILE ? (Y/N)
Y
?OUTPUT_04_26_1
outdata_etmsp
?ENTER MORE OUTPUT QUANTITIES ? (Y/N)
n
?
TADATA

?SELECT AN ITEM BY THE NUMBER (G TO GO TO MENU 2; Q TO QUIT):
18
Q
?
ini
?(NECESSARY FOR MULTIPLE CONTINGENCY SIMULATION)
Y
?(DEFAULT=z:/delizond/september/results/09_18_0.int; HIT THE RETURN KEY FOR DEFAULT)

Y
;13
? ESTA 13 is the ref, John Day ES LA DEL REF GENERATOR!
swit
veneno
?
simulat
?DO YOU WANT THE SIMULATION RESULT FILE ? (Y/N)
Y

?DO YOU WANT A SUMMARY OF THE SIMULATION SPECIFICATIONS ? (Y/N)
Y

?
quit
=====
=====

```

Outdata ETMSP

This the file in which the user indicates to the program which variables to get out for analysis. We selected Generators, Transmission lines and Buses. This file shows the format for a number of buses, and it was truncated for practical purposes.

```

B GEO
  1  1
  1  2
  1  3
  1  4
  5  1
  8  1
 13  1
  .  .
  .  .
  .  .
 47  1
 49  1
 53  1
126  1
EDATA
? --- Bus Data -----
MVBS
?2345
  1
  2
  3
  4
  5
  6
  7
  8
  9
 10
 11
 18
 19
 20
  .
  .
  .
  .
121
122
123
124
125
126
127
EDATA
LINE
  2  1  1  1
  3  2  1  1
  4  3  1  1
  6  4  1  1
  6  5  1  1
  6  7  1  1
  7  8  1  1
  7  9  1  1
  7  9  2  1
  9 10  1  1
  9 12  1  1
  9 12  2  1
  9 24  1  1

```

```
11 9 1 1
11 12 1 1
11 25 1 1
12 13 1 1
14 12 1 1
14 12 2 1
14 16 1 1
14 16 2 1
14 17 1 1
14 17 2 1
15 12 1 1
15 12 2 1
. . . .
. . . .
. . . .
. . . .
. . . .
. . . .
118 124 3 1
118 124 4 1
118 127 1 1
120 116 1 1
120 116 2 1
121 104 1 1
121 104 2 1
121 120 1 1
121 122 1 1
122 118 1 1
123 118 1 1
125 103 1 1
125 118 1 1
125 124 1 1
125 126 1 1
125 127 1 1
EDATA
END
```

```
=====
=====
```


Outdata ETMSP_Relay

This file was used to get the values of the apparent impedance on each of the line ends in order to validate the Region of Vulnerability. The voltage and current of each end of every transmission line were required as output. This file shows the format for a number of transmission lines and it was truncated for practical purposes.

```

LINE
  2   3 1 1
  3   2 1 1
  4   6 1 1
  6   4 1 1
  6   7 1 1
  7   6 1 1
  7   9 1 1
  7   9 2 1
  9   7 1 1
  9   7 2 1
  9  10 1 1
  9  11 1 1
  9  12 1 1
  9  12 2 1
  9  24 1 1
 10   9 1 1
 11   9 1 1
 11  12 1 1
 11  25 1 1
 12   9 1 1
 12   9 2 1
 12  11 1 1
 12  14 1 1
 14  16 1 1
 14  16 2 1
 15  12 1 1
 15  12 2 1
 15  12 3 1
 15  23 1 1
 15  23 2 1
 16  14 1 1
 16  14 2 1
 17  18 1 1
 17  18 2 1
 18  17 1 1
  .   . . .
  .   . . .
  .   . . .
  .   . . .
  .   . . .
  .   . . .
 122 121 1 1
 123 104 1 1
 124 118 1 1
 124 118 2 1
 124 118 3 1
 124 118 4 1
 124 125 1 1
 125 103 1 1
 125 118 1 1
 125 127 1 1
 127 118 1 1
 127 125 1 1
EDATA
END

```

Curriculum Vitae

David C. Elizondo

412 Hunt Club Drive Apt. 1500-G
Blacksburg, VA, 24060.

Tel. 540 9515656. Home
Tel. 540 2317834. Work
E-mail: delizond@vt.edu

Main Skills

- Expertise as a power systems engineer, with emphasis in protection relaying. Knowledge of the protection schemes employed in a power system.
- Experience and ability to learn and adapt to transient-stability and load-flow power system computer software: ETMSP, OAP, and IPFLOW.
- Ability to lead technical and commercial teams with industrial and academic experience; recent leadership activity as president of the Latin American and Iberian Graduate Student Association of Virginia Tech.
- Skilled in the process of mediating diverse opinions through motivation, encouragement, and persuasion, resulting in the attainment of a common objective.

Work Experience

INDUSTRIAL

Research and Applications

Virginia Tech — ABB Summer Project Leader.
Virginia Tech, Blacksburg, VA.

May — August 2001

- Designed, installed, and energized an analog simulator to demonstrate the capabilities of modern computer-based distribution automation systems. Panel models a distribution feeder and includes computer-based relays.

Research and Development Engineer (Internship).

May — August 2000

ABB Electric Systems Technology Institute, Raleigh, NC.

- Developed a technical document related to the protection, control, and automation of distribution feeders, to be used to train customers about distribution automation products.

Training and Development Programs

Trainee Engineer.

May 1996 — December 1996

ABB Power T&D Company Inc., Bland, VA.

- Developed a solid business relationship between Mexican and American companies. Proposed, directed, and implemented a direct marketing system (product pricing catalogue) to reduce quotation time from 10 to 5 days.
- Transferred technical expertise and trained the job partners once back in Mexico. Applied knowledge through intensive product presentations to customers, resulting in an unprecedented number of dry-type transformers contracts.
- Received an intensive, multi-functional training program of medium voltage, dry-type transformers. Visited twelve equipment-manufacturing plants related to nine different business divisions in ABB US.

Work Experience

INDUSTRIAL

Marketing and Sales

Regional Branch Sales Manager. May 1997 — August 1998

ABB Sistemas, S.A. de C.V., Monterrey, NL, Mexico.

- Developed the unexplored industrial market of the northeast part of Mexico.
- Promoted and advised customers with technical specifications for low, medium, and high voltage electrical substations (0.440–400 kV).

Marketing Leader and Product Specialist. January 1996 — May 1997

ABB Sistemas, S.A. de C.V., Tlalnepantla, Edo de Mexico, Mexico.

- Supported the sales force with product presentations and technical specifications for medium and high voltage equipment (6.9–34.5 and 69–400 kV). Contributed market studies, strategies, and proposals for industrial substations. Technical advisor for small power transformers.

Engineering

High Voltage Engineer. March 1995 — December 1995

ABB Sistemas, S.A. de C.V., Tlalnepantla, Edo de Mexico, Mexico.

- Reviewed technical content for large turnkey project proposals, including projects related to high voltage substations and transmission lines for CFE, Mexico's largest utility.
- Worked with substation equipment specification and selection, bill of materials, and single line drawings.

ACADEMIC

Research

Graduate Research Assistant. May 1999 — May 2002

EPRI-DoD project, Virginia Tech, Blacksburg, VA.

- Analyzed wide area disturbances in power systems and identified the role and occurrence of particular protection system miss-operations, specifically hidden failures.
- Developed a methodology to evaluate hidden failure effects based on regions of vulnerability, areas of consequence, and index of severity.

Teaching

Graduate Teaching Assistant. August 1998 — May 1999

Power Engineering Laboratory Instructor, Virginia Tech, Blacksburg, VA.

- Taught laboratory sections for undergraduate students. A number of electrical engineering classes also taught upon faculty request.

Education

DOCTOR OF PHILOSOPHY IN ELECTRICAL ENGINEERING 2000 — April 2003

Virginia Tech, Blacksburg, VA.

Area: Power Systems. Topics: Power System Relaying and Power System Security.

MASTER OF SCIENCE IN ELECTRICAL ENGINEERING 1998—2000

Virginia Tech, Blacksburg, VA.

Area: Power Systems. Topics: Power System Relaying and Wide Area Disturbances.

BACHELOR OF ENGINEERING (MECHANICAL AND ELECTRICAL) 1990—1994

ITESM, Monterrey, Mexico.

ADVANCED SEMINARS 1996—2002

Economics, Finance, and Marketing for High Technology Products and Innovations.

ITESM, Mexico D.F, Mexico; Virginia Tech, Blacksburg, VA.

Language Proficiencies

Spanish, English

Selected Publications and Exhibitions

- J. De La Ree, David C. Elizondo, “*Analysis of Hidden Failures of Protection Schemes in Large Interconnected Power Systems*,” Power Systems and Communication Systems Infrastructures for the Future, Beijing, China. Paper to be presented, September 2002. 2002
- J. De La Ree, David C. Elizondo, Juancarlo Depablos, James Stoupis, “*An Adaptive Protection Scheme for Power Distribution Systems*,” Power Systems and Communication Systems Infrastructures for the Future, Beijing, China. Paper to be presented, September 2002. 2002
- David C. Elizondo, J. De La Ree, Arun G. Phadke, Stan Horowitz, “*A Methodology to Evaluate Hidden Failure Effects Based on Regions of Vulnerability in Protection Schemes of Electric Power Systems*,” NAPS Conference, College Station Texas, Texas A & M University. Paper presentation. 2001
- David C. Elizondo, J. De La Ree, Arun G. Phadke, Stan Horowitz, “*Hidden Failures in Protection Systems and Their Impact on Wide-Area Disturbances*,” IEEE PES Winter Meeting Proceedings, Columbus, OH. Paper presentation. 2001